

# UNCLASSIFIED

AD NUMBER
ADB097092
NEW LIMITATION CHANGE
TO Approved for public release, distribution unlimited
FROM Distribution authorized to U.S. Gov't. agencies only; Test and Evaluation; Apr 1985. Other requests shall be referred to Air Force Wright Aeronautical Laboratories, [AFWAL], Attn: MLTN, Wright-Patterson AFB, OH 45433.
AUTHORITY
WL/MTPN, ASC/PA, WL/MTPN fax, 9 Feb 1995

THIS PAGE IS UNCLASSIFIED

AFWAL-TR-85-4060

MANUFACTURING TECHNOLOGY FOR NONAUTOCLAVE  
FABRICATION OF COMPOSITE STRUCTURES

B. A. BURROUGHS  
R. L. HUNZIKER

JUNE 1985

FINAL REPORT FOR PERIOD OCTOBER 1980 - APRIL 1984

Distribution limited to U.S. government agencies only;  
test and evaluation, April 1985. Other requests for  
this document must be referred to AFWAL/MLTN, WPAFB,  
OHIO 45433.

**SUBJECT TO EXPORT CONTROL LAWS**

This document contains information for manufacturing or using munitions of war. Export of the information contained herein, or release to foreign nationals within the United States, without first obtaining an export license, is a violation of the International Traffic-in-Arms Regulations. Such violation is subject to a penalty of up to 2 years imprisonment and a fine of \$100,000 under 22 USC 2778.

Include this notice with any reproduced portion of this document.

MATERIALS LABORATORY  
AIR FORCE WRIGHT AERONAUTICAL LABORATORIES  
AIR FORCE SYSTEMS COMMAND  
WRIGHT PATTERSON AIR FORCE BASE, OHIO 45433



DTIC  
ELECTE  
DEC 03 1985  
S  
D

85 11 29 010

AD-B097 092

FILE COPY

## **DISCLAIMER NOTICE**

**THIS DOCUMENT IS BEST QUALITY  
PRACTICABLE. THE COPY FURNISHED  
TO DTIC CONTAINED A SIGNIFICANT  
NUMBER OF PAGES WHICH DO NOT  
REPRODUCE LEGIBLY.**

NOTICE

When Government drawings, specifications, or other data are used for any purpose other than in connection with a definitely related Government procurement operation, the United States Government thereby incurs no responsibility nor any obligation whatsoever; and the fact that the government may have formulated, furnished, or in any way supplied the said drawings, specifications, or other data, is not to be regarded by implication or otherwise as in any manner licensing the holder or any other person or corporation, or conveying any rights or permission to manufacture, use, or sell any patented invention that may in any way be related thereto.

This technical report has been reviewed and is approved for publication.

D. Beeler  
D. Beeler  
Project Engineer

FOR THE COMMANDER:

R. C. Tomashot  
R. C. Tomashot  
Chief  
Nonmetals and Composites Branch  
Manufacturing Technology Division

"If your address has changed, if you wish to be removed from our mailing list, or if the addressee is no longer employed by your organization please notify AFWAL/MLTN, W-P AFB, OH 45433 to help maintain a current mailing list".

Copies of this report should not be returned unless return is required by security considerations, contractual obligations, or notice on a specific document.



UNCLASSIFIED

SECURITY CLASSIFICATION OF THIS PAGE (When Data Entered)

REPORT DOCUMENTATION PAGE		READ INSTRUCTIONS BEFORE COMPLETING FORM
1. REPORT NUMBER AFWAL-TR-4060 -85-4060	2. GOVT ACCESSION NO. AD-B094 092h	3. RECIPIENT'S CATALOG NUMBER
4. TITLE (and Subtitle) MANUFACTURING TECHNOLOGY FOR NONAUTOCLAVE <del>COMPOSITE FABRICATION</del> Fabrication of Composite Structures		5. TYPE OF REPORT & PERIOD COVERED Final Report 1 Oct. 1980 to 1 April 1984
7. AUTHOR(s) B. A. Burroughs, R. L. Hunziker, T. McGann, G. Hanneman, J. Rosenthal		6. PERFORMING ORG. REPORT NUMBER NA-85-1212L
9. PERFORMING ORGANIZATION NAME AND ADDRESS ROCKWELL INTERNATIONAL CORPORATION North American Aircraft Operations P.O. Box 92098, Los Angeles, CA 90009		8. CONTRACT OR GRANT NUMBER(s) F33515-80-C-5080
11. CONTROLLING OFFICE NAME AND ADDRESS Air Force Wright Aeronautical Laboratories Materials Laboratory (AFWAL/MLTN) Wright-Patterson AFB, Ohio 45423		10. PROGRAM ELEMENT, PROJECT, TASK AREA & WORK UNIT NUMBERS PE 780111F 462-0
14. MONITORING AGENCY NAME & ADDRESS (if different from Controlling Office)		12. REPORT DATE June 1985
		13. NUMBER OF PAGES 281
		15. SECURITY CLASS. (of this report) Unclassified
		16. DECLASSIFICATION/DOWNGRADING SCHEDULE
18. DISTRIBUTION STATEMENT (of this Report) Distribution limited to U.S. Government agencies only; test and evaluation, April 1985. Other requests for this document must be referred to AFWAL/MLTN, WPAFB, Ohio 45433.		
17. DISTRIBUTION STATEMENT (of the abstract entered in Block 20, if different from Report)		
19. SUPPLEMENTARY NOTES		
20. KEY WORDS (Continue on reverse side if necessary and identify by block number) Graphite/epoxy; nonautoclave process; load coupler; stub box; CAP box; Wing boxes; vertical stabilizer; moisture chamber; volatile formation. Air Frames; Beam Structures; Composite structures		
21. ABSTRACT (Continue on reverse side if necessary and identify by block number) This program established and demonstrated a generic curing technique for 177°C (350°F) organic matrix composite structure which does not require use of an autoclave and which can be used to produce composite primary and secondary aircraft structure. This was accomplished by the fabrication of elements, a subcomponent, and a full-scale component representative of low-cost bomber wing and empennage primary structure, as well as the tracking of production costs, assessment of quality for all fabricated hardware, and preparation of preliminary and final material and process specifications. keywords:		

DD FORM 1473 EDITION OF 1 NOV 83 IS OBSOLETE

UNCLASSIFIED

SECURITY CLASSIFICATION OF THIS PAGE (When Data Entered)

## FOREWORD

Rockwell International, North American Aircraft Operations (NAAO), under Air Force contract F33615-80-C-5080, has conducted a three-phase 42-month technical effort to establish and demonstrate generic curing techniques for 177°C (350°F) organic matrix advanced composite structures which do not require the use of an autoclave. The resultant processes may be used to produce primary and secondary aircraft structures.

This program was sponsored by the Air Force Wright Aeronautical Laboratories, Materials Laboratory (Manufacturing Technology Division), Air Force Systems Command, Wright-Patterson Air Force Base, Ohio 45433. The Air Force program monitor is Mr. D. Beeler (AFWAL/MLTN); program inquiries should be directed to him at (513) 255-7277. NAAO key personnel associated with this program are:

B. A. Burroughs - Program Manager  
R. L. Hunziker - Deputy Program Manager  
T. W. McGann - Phase I, Project Administrator  
G. Hanneman - Phase II, Project Administrator  
J. Rosenthal (Tulsa Facility) - Phase III, Project Administrator

Accession For	
NTIS CRA&I	<input type="checkbox"/>
DTIC TAB	<input checked="" type="checkbox"/>
Unannounced	<input type="checkbox"/>
Justification	
By	
Distribution/	
Availability Codes	
Dist	Avail and/or Special
B-3	57



Section	TABLE OF CONTENTS	Page
1.0	INTRODUCTION	1
2.0	SUMMARY	2
3.0	BACKGROUND	7
4.0	TECHNICAL DISCUSSION	12
	4.1 PHASE I - MANUFACTURING METHOD VERIFICATION	
	4.1.1 TASK 1 - METHOD PARAMETER ESTABLISHMENT	12
	4.1.1.1 Material Selection & Characterization	12
	4.1.1.1.1 Material Selection	12
	4.1.1.1.2 Net Resin Material Characterization	18
	4.1.1.1.3 Adhesive Compatibility Demonstration	18
	4.1.1.1.4 Storage Life Extension Study	30
	4.1.1.2 Nonautoclave Process Development	30
	4.1.1.2.1 Nonautoclave Process Cycle	34
	4.1.2 TASK 2 - FABRICATION OF VERIFICATION ELEMENTS	38
	4.1.2.1 Integral Structure Beam Fabrication	38
	4.1.2.2 Integral Structure Box Assembly Fabrication	48
	4.1.2.2.1 Element Design	50
	4.1.2.2.2 Element Fabrication	50
	4.1.2.2.3 Quality Assessment	85
	4.1.3 ANCILLARY INVESTIGATIONS	113
	4.1.3.1 AS4/3501-5A Material Evaluation	113
	4.1.3.2 Tooling Gap Evaluations	113
	4.1.3.3 AS4/3501-5A Gr/Ep Element Verification	117
	4.1.4 SUMMARY PHASE I - MANUFACTURING METHOD VERIFICATION	130

## TABLE OF CONTENTS (Continued)

Section	Page
4.2 PHASE II - MANUFACTURING METHOD SCALE-UP	132
4.2.1 TASK 1 - FABRICATION OF SUBCOMPONENT	132
4.2.1.1 Subcomponent Design	132
4.2.1.2 Tool Design and Fabrication	139
4.2.1.3 Subcomponent Detail Fabrication and Assembly	145
4.2.2 TASK 2 - QUALITY ASSESSMENT	162
4.2.2.1 Nondestructive Inspection	162
4.2.2.2 Subcomponent Test	170
4.2.3 SUMMARY PHASE II - MANUFACTURING METHOD SCALE-UP	190
4.3 PHASE III - FULL-SCALE FABRICATION	191
4.3.1 TASK 1 - FULL-SCALE PART FABRICATION	191
4.3.1.1 Component Design	191
4.3.1.2 Tool Design and Fabrication	195
4.3.1.3 Component Detail Fabrication and Assembly	214
4.3.1.3.1 Scale-Up Evaluation	214
4.3.1.3.2 Skin Fabrication	214
4.3.1.3.3 Substructure Fabrication	221
4.3.1.3.4 Assembly and Cocure	227
4.3.2 TASK 2 - QUALITY ASSESSMENT	241
4.3.3 SUMMARY PHASE III - FULL SCALE FABRICATION	241
4.4 COST BENEFIT ANALYSIS	247
4.4.1 WEIGHT ANALYSIS	247
4.4.1 ENERGY ANALYSIS	249
4.4.2 COST AND BENEFIT ANALYSIS	258
5.0 CONCLUSIONS AND RECOMMENDATIONS	277

# LIST OF ILLUSTRATIONS

<u>FIGURE</u>		<u>PAGE</u>
1.	Phase III Full-Scale Nonautoclave Demonstration Component . . . . .	3
2.	Program Components. . . . .	4
3.	Schedule. . . . .	5
4.	Diagram of NAAO Process - Complete Entrapped Air Removal During Degassing Step. . . . .	9
5.	Typical NAAO Nonautoclave Staging and Cure Cycles . . . . .	11
6.	Phase I Flow Diagram. . . . .	13
7.	Nonautoclave Cure Mechanical Properties - T300/5208 . . . . .	19
8.	Nonautoclave Cure Mechanical Properties - AS1/3501-5A . . . . .	19
9.	Fiberite AS1/976 and Hercules AS1/3501-5A Staged Laminate (0) <sub>15</sub> Storage Life Extension Short-Beam Sear Strength (Ksi) Test Results. . . . .	32
10.	Fiberite AS1/976 and Hercules AS1/3501-5A Staged Laminate (0) <sub>15</sub> Storage Life Extension Short-Beam Sear Strength (Ksi) Test Results. . . . .	33
11.	Comparison of Viscoelastic Staging Properties for Tape/Fabric/Resin Film . . . . .	35
12.	Viscoelastic Properties During Cure of B-Staged Laminates. . . . .	35
13.	Nonautoclave Cure Cycle - AS4/976 Net Resin . . . . .	37
14.	Typical Integral Structure Beam Element Fabricated with NAAO Nonautoclave Cure Process (Vacuum Pressure Only) . . . . .	39
15.	Sine Wave I-Beam Element - As Staged (Release Fabric Attached). . . . .	40
16.	Phase I Element Assemblies. . . . .	41
17.	T-Specimen Comparison - Autoclave Cure Versus Nonautoclave Cure Test (RT/Dry). . . . .	45
18.	Comparison of Tee Specimen Flatwise Tension Tests for Different Load Couplers. . . . .	47
19.	Different Load Couplers 40-Inch Verification Bending Beams. . . . .	49
20.	40-Inch Box Beam Detail Drawings. . . . .	51
21.	Nonautoclave Fabrication Sequence . . . . .	55

# LIST OF ILLUSTRATIONS (Continued)

<b>FIGURE</b>		<b>PAGE</b>
22.	Spraying Silicone Rubber Staging Bags . . . . .	58
23.	Flat Nonautoclave Staging Tool. . . . .	59
24.	Nonautoclave I-Beam Staging Tool. . . . .	60
25.	Typical I-Beam Nonautoclave Staging Tool (Exploded View). . . . .	62
26.	Sine Wave Web Bladder and Strongback Tooling. . . . .	63
27.	Flat Web Bladder and Strongback Tooling . . . . .	64
28.	Electrostatic Leak Checking of a Bladder Bag. . . . .	65
29.	40-Inch Sinewave Staging Tool with Bag in Place . . . . .	66
30.	Flat Web Beam Tooling . . . . .	67
31.	Assembled Staging Tool. . . . .	68
32.	40-Inch Box Cocure Tool . . . . .	69
33.	Fiberglass Assembly Preparatory to Spray-Up of Final Cure Bladders. . .	70
34.	Removal of Internal Final Cure Bladder Molds from Assembly. . . . .	71
35.	Vacuum Pressure Forming of the End Closeout Rib . . . . .	75
36.	Placing Gr/Ep in Staging Tool . . . . .	76
37.	Partially Assembled Staging Tool. . . . .	77
38.	Staged 40-Inch Beams. . . . .	78
39.	Closeup of Staged Sinewave Web I-Beam - Web-to-Flange Radius. . . . .	79
40.	40-Inch Box Beam Element 1 in Final Cure Assembly with Manifold . . . . .	80
41.	40-Inch Box Beam Element 1 Ready for Cure . . . . .	81
42.	S/N 1 & 2 40-Inch Box Beam Elements . . . . .	82
43.	Internal View of Cured Sinewave Web Element 1 . . . . .	83
44.	S/N 1 40-Inch Test Element. . . . .	84
45.	Contact Pulse Echo Ultrasonic Inspection of Staged Beam . . . . .	87

# LIST OF ILLUSTRATIONS (Continued)

<u>FIGURE</u>		<u>PAGE</u>
46.	Photomicrographs (50X) of Cured Gr/Ep Laminates . . . . .	90
47.	Ultrasonic C-Scans of Staged Gr/Ep Laminates - 1 MHz, 6 and 12 dB . . . .	91
48.	Ultrasonic C-Scans of Staged Gr/Ep Laminates - 1 MHz, 6 and 12 dB . . . .	92
49.	Nonautoclave 102-cm (40-Inch) Verification Bending Beams. . . . .	94
50.	Strain Gage Locations for Sine-Wave Beams . . . . .	96
51.	Location of Strain Rosettes for Flat Web Beams. . . . .	97
52.	Location of Permanent Indentation of One of the Sine-Wave Nodes of First Sine-Wave Beam. . . . .	97
53.	Shear Flow Analysis Schematic . . . . .	100
54.	First Sine-Wave Beam - Static Test Setup. . . . .	101
55.	Closeup of the First Sine-Wave Beam Web Failure. . . . .	102
56.	Sine-Wave Beam - Second Test Failure. . . . .	103
57.	Closeup of Lower Cap to Web - Failure of Second Sine-Wave Beam. . . . .	104
58.	Load vs Strain for Sine-Wave Web Verification Bending Beam Specimen No. 1 (Rosette No. 1) . . . . .	105
59.	Load vs Strain for Sine-Wave Web Verification Bending Beam Specimen No. 1 (Rosette No. 1) . . . . .	106
60.	Test Setup and Failure of Flat Web Beam No. 2 . . . . .	107
61.	First Sine-Wave Beam - Web Failure. . . . .	108
62.	Load vs Strain for Flat Web Verification Bending Beam Specimen No. 2 (Rosette Nos. 5 and 6). . . . .	110
63.	Load vs Strain for Flat Web Verification Bending Beam Specimen No. 1 (Rosette Nos. 5 and 6). . . . .	111
64.	Comparison of Viscoelastic Staging Properties for Fiberite 976 and Hercules 3501-5A Resins . . . . .	114
65.	Staged 40-Inch Flat Web Beam (AS4/3501-5A) - Load Coupler Side Up . . . .	115
66.	Microexamination (50X) of Staged 40-Inch Flat Web Beam (AS4/3501-5A). . .	116

# LIST OF ILLUSTRATIONS (Continued)

<u>FIGURE</u>		<u>PAGE</u>
67.	Microexamination (50X) of Staged 40-Inch Flat Web Beam (AS4/3501-5A) . . .	118
68.	Cured 12-Ply Laminate Staged in 25-cm (10-inch) Tool with Breather System - No Porosity. . . . .	119
69.	Cured 24-Ply Laminate Staged in 25-cm (10-inch) Tool with Breather System -Acceptable-to-Unacceptable Porosity . . . . .	120
70.	Cured 24-Ply Laminate Staged in 25-cm (10-inch) Tool with Additional Vacuum Port - Unacceptable Level of Porosity. . . . .	121
71.	Cured 24-Ply Laminate Staged in 25-cm (10-inch) Tool with Additional Vacuum Line and Increased Gap - Finely Dispersed Porosity . . . . .	123
72.	Photomicrograph of Cured 12-Ply 25-cm (10-inch) Patch Test Laminate - No Porosity - Trial No. 4. . . . .	124
73.	Cured 24-Ply Laminate in 25-cm (10-inch) Tool with Total Gap of 0.635 cm (0.250 inch) - No Porosity . . . . .	125
74.	Cured 32-Ply Laminate Stated in 102-cm (40-inch) Modified Tool - No Porosity. . . . .	126
75.	Cured 40-Ply Laminate Stated in 102-cm (40-inch) Modified Tool - No Porosity. . . . .	127
76.	Sine Wave Web Section - 12-Ply Tape and Fabric Cured in Stage Tool With 2 x Gap . . . . .	128
77.	Phase II Flow Diagram . . . . .	133
78.	Phase II - Manufacturing Scale-up Test Box (Nonautoclave Process Demonstration). . . . .	134
79.	Phase II Subcomponent . . . . .	135
80.	Plaster Tool Master for Stub-Box Intermediate Rib . . . . .	140
81.	Lower Rib Tooling for Stub Box. . . . .	141
82.	Intermediate Spar Tooling for Stub Box. . . . .	142
83.	Completed Stub Box Cure Tool. . . . .	143
84.	Subcomponent Cure Tool with Fiberglass Tool Proof Parts in Place. . . . .	144
85.	Subcomponent Cure Tool Diagram. . . . .	146



# LIST OF ILLUSTRATIONS (Continued)

<u>FIGURE</u>		<u>PAGE</u>
86.	Stub-Box Bag in Place on Assembly Prior to Cure . . . . .	147
87.	Stub Box Staged Details . . . . .	149
88.	Stub Box Staged Upper Rib (untrimmed) . . . . .	150
89.	Demonstration of New Ultrasonic Cutting Device for Laminates. . . . .	151
90.	Minimal Fraying of Laminate Edges Using Ultrasonic Cutting Device . . . .	152
91.	Prefit of Stub Box Details. . . . .	153
92.	Prefit of Stub Box Rib - Closeup View . . . . .	154
93.	Placing Rib and Spar Caps on Stub-Box Assembly. . . . .	155
94.	Fiberglass Wedges Placed on Ribs - Stub-Box Assembly. . . . .	156
95.	Cocure Stub-Box Assembly - Upper Manifold in Place. . . . .	157
96.	Cured Stub Box - Adequate Pressure During Cocure as Shown by Adhesive Flow. . . . .	158
97.	Drilling Closeout Cover of Subcomponent . . . . .	160
98.	Stub Box Prior to Installation of Strain Gages. . . . .	161
99.	Nondestructive Inspection Standard to Simulate Graphite/Epoxy Staged Details . . . . .	163
100.	Nondestructive Inspection Standard to Simulate Graphite-Boron/Epoxy Staged Cover. . . . .	164
101.	Ultrasonic C-Scan (1 MHz, 20 dB) of Stub-Box Front Spar - Porosity-Free .	165
102.	C-Scan (2.25 MHz, 20 dB) of Stub-Box Rib - Porosity-Free. . . . .	167
103.	C-Scan of Covers. . . . .	168
104.	Contact Pulse Echo Inspection Results - Cured Subcomponent. . . . .	171
105.	Dimensional Inspection - Rear Spar. . . . .	172
106.	Dimensional Inspection - Intermediate Spar (Lower). . . . .	173
107.	Dimensional Inspection - Intermediate Spar (Intermediate) . . . . .	174

# LIST OF ILLUSTRATIONS (Continued)

<u>FIGURE</u>		<u>PAGE</u>
108.	Dimensional Inspection - Intermediate Spar (Upper). . . . .	175
109.	Subcomponent Box Test Setup . . . . .	178
110.	Location of Stub Box Instrumentation. . . . .	179
111.	Subcomponent Installed in Test Fixture . . . . .	180
112.	Contact Pulse Echo Results at Bondline Failure. . . . .	181
113.	Comparison of Cover Predicted Maximum Axial Strains versus Measured . . .	183
114.	Comparison of Spar Predicted Shear Strains versus Measured. . . . .	184
115.	Comparison of Front Spar Flange Predicted Axial Strains versus Measured .	185
116.	Comparison of Tip Deflections of Nonautoclave Subcomponent versus Baseline Subcomponent . . . . .	186
117.	Stub Box with Cover Coupon Specimens Removed. . . . .	187
118.	Stub Box Section Removed (Showing Nonbond). . . . .	188
119.	Bondline Auger Analysis . . . . .	189
120.	Phase III Full-Scale Component. . . . .	192
121.	Manufacturing Features and Fabrication Processes. . . . .	193
122.	Phase III Flow Diagram. . . . .	194
123.	Integral Composite Structure Demonstration Article. . . . .	196
124.	Full-Scale Component Fold-Out Drawing . . . . .	198
125.	Vertical Stabilizer Skin Cover Tool . . . . .	200
126.	Skin tool (Upper Chamber Placed on Lower Chamber) . . . . .	203
127.	Upper Cover Tool Assembly . . . . .	204
128.	Composite Vertical Stabilizer (CAP Box) Skin Tool Assembly. . . . .	205
129.	Typical Plaster Tool Master for CAP Box Intermediate Rib at Station Zvs 111.594 . . . . .	206
130.	CAP Box Intermediate Rib Tool (Strongbacks and Bag not Included). . . . .	207

# LIST OF ILLUSTRATIONS (Continued)

<u>FIGURE</u>		<u>PAGE</u>
131.	CAP Box Intermediate Rib Tool with Bag in Place - No Strongbacks. . . . .	208
132.	Completed Hardback Tooling for CAP Box (Tulsa Facility) . . . . .	209
133.	Full Scale Component Cocure Manifold. . . . .	210
134.	Closeup of Fitup Between Manifold and Part. . . . .	211
135.	Vertical Displacements for Maximum (450 pound) Load . . . . .	212
136.	Fiberglass Tool Proof Details Prior to Fabrication of Cure Bag. . . . .	213
137.	Full-Scale Component Cure Bag Fabrication Sequence. . . . .	215
138.	Spraying Process for Individual Sections of CAP Box . . . . .	216
139.	Assembly of Individual Sections of CAP Box Cocure Bag . . . . .	217
140.	Ply Drop-Off Evaluation Panel . . . . .	222
141.	Typical Photomicrographs of 100-Ply Laminate Test Panel . . . . .	223
142.	Viscosity of Hercules 3501-5A Resin During Cure Cycle - RT to 250°F at 3.2°F/min. and Held . . . . .	224
143.	Viscosity of Hercules 3501-5A Resin During Cure Cycle - RT to 250°F at 1.6°F/min. and Held . . . . .	225
144.	Viscosity of Hercules 3501-5A Resin During Cure Cycle - RT to 250°F at 1.0°F/min. and Held . . . . .	226
145.	Cure Rheology of 225°F-Staged 3501-5A Resin . . . . .	229
146.	CAP Box Stage Tool Detail . . . . .	231
147.	Surface Quality of Restaged Rib . . . . .	232
148.	Full-Scale Component Front Spar . . . . .	233
149.	Full-Scale Component Details After Assembly . . . . .	235
150.	181-Glass Breather Cloth in Place Over Manifold . . . . .	236
151.	Middle Section of Cure Bag After Installation . . . . .	237
152.	Cure Bag Sealed at All Joints . . . . .	238

# LIST OF ILLUSTRATIONS (Concluded)

<u>FIGURE</u>		<u>PAGE</u>
153.	Completed Full-Scale Component. . . . .	239
154.	Full-Scale Component After Final Cure . . . . .	240
155.	Typical Sine Wave Spar Wrinkles in Cured Component. . . . .	242
156.	Visual Quality Assessment of Cured Component. . . . .	243
157.	Summary of Ultrasonic C-Scan Nonbond Indications of Cocured Component . .	244
158.	Phase I Energy Assessment of Autoclave and Oven . . . . .	253
159.	Cure Cycle Used in Phase I Energy Assessment. . . . .	255
160.	Energy Saving - Nonautoclave versus Autoclave . . . . .	259
161.	Cost Tracking Summary Sheet . . . . .	260
162.	Phase I Cost Data Comparison. . . . .	266
163.	Phase II Cost Data Comparison . . . . .	267
164.	6-Foot IR&D Bending Subcomponent. . . . .	268
165.	Phase III Cost Data Comparison. . . . .	269
166.	Nonautoclave versus Autoclave Hours/Pound . . . . .	271

# LIST OF TABLES

<u>TABLE</u>	<u>TITLE</u>	<u>PAGE</u>
I	Gr/Ep Net Resin Content Tape Prepreg Physical Property . . . . .	15
II	Gr/Ep Nonautoclave Cure Laminate Property Evaluation . . . . .	16
III	Nonautoclave Cure Material Selection Summary Evaluation Matrix . . . . .	17
IV	No-Bleed AS4/976 Gr/Ep Tape Material Characterization. . . . .	20
V	Fabric Characterization Test Results . . . . .	23
VI	Autoclave vs Nonautoclave Cured AS1/3501-5A Laminate Strength. . . . .	24
VII	Autoclave vs Nonautoclave Cured T300/5208 Laminate Strength. . . . .	25
VIII	Unidirectional CE9000-9/CELION 6000 Laminate Strength (Flexure and Inter-laminar Shear) . . . . .	26
IX	CE9000-9/CELION 6000 Laminate Tension Strength . . . . .	27
X	Unidirectional CE9000-9/CELION 6000 Laminate Compression Strength . . . . .	28
XI	Wet Strength Retention of CE9000-9/CELION 6000 . . . . .	29
XII	Nonautoclave Cure Process Adhesive System Material Screening Test Data .	31
XIII	Nonautoclave Cure Process Limits Test Results. . . . .	36
XIV	Integral Structure I-Beam Fabrication Matrix . . . . .	42
XV	Soundnes Validation Test Results . . . . .	44
XVI	Sprayable Silicone Rubber Evaluation . . . . .	73
XVII	Staged Detail Ultrasonic C-Scan Test . . . . .	86
XVIII	Porosity Evaluation of Staged Panels . . . . .	99
XIX	Summary of 40-Inch Beam Test . . . . .	99
XX	Mechanical and Physical Property Evaluation 40-Inch Beam . . . . .	112
XXI	Residual Strength Test Results . . . . .	130
XXII	Stub Box Cocure Bag Cure Schedule. . . . .	145
XXIII	Dimensional Measurements of Subcomponent . . . . .	176

# LIST OF TABLES (Concluded)

<u>TABLE</u>	<u>TITLE</u>	<u>PAGE</u>
XXIV	Summary of Load Conditions for Subcomponent. . . . .	182
XXV	B-1 Vertical Stabilizer Weight Savings Summary . . . . .	191
XXVI	Phase III Full-Scale Component Drawings List . . . . .	201
XXVII	Nonautoclave Panel Scale-Up Summary. . . . .	218
XXVIII	RT Mechanical Property Evaluation (20 ply Tool Proof Laminate) . . . .	220
XXIX	Staging Heat-Up Rages. . . . .	228
XXX	Component Nonbond Size . . . . .	245
XXXI	Weight Analysis - Phase I Elements . . . . .	248
XXXII	Weight Analysis - Phase II Subcomponent. . . . .	250
XXXIII	Weight Analysis - Full-Scale Component . . . . .	251
XXXIV	Preliminary Energy Savings . . . . .	254
XXXV	Autoclave vs Oven Energy Savings Summary . . . . .	259
XXXVI	Glossary of Fabrication Cost Operations. . . . .	261
XXXVII	Nonautoclave Cost Analysis Phase I Elements. . . . .	262
XXXVIII	Nonautoclave Cost Analysis Phase II Subcomponent . . . . .	263
XXXIX	Nonautoclave Cost Analysis Phase III Component . . . . .	264
XL	Nonautoclave Cost Analysis Average Detail Hours Savings. . . . .	272
XLI	Tool Fabrication Cost Analysis . . . . .	273
XLII	B-1 Vertical Stabilizer Cost Analysis Assumptions. . . . .	274
XLIII	Cost Analysis B-1 Vertical Stabilizer Component. . . . .	275

## 1.0 INTRODUCTION

The use and application of advanced composite to the construction of aircraft structures have advanced dramatically during the past two decades. This is evidenced by projections of up to 50 percent of structural weights of advanced composites for the next generation of fighter aircraft. These high projections are the result of structural trades showing substantial reduction in cost and weight of future aircraft through the use of new and innovative advanced composites manufacturing and design concepts.

The new composite manufacturing methods have emphasized the advantages of monolithic, integral construction over built-up, mechanically attached or secondarily bonded components that resemble the more conventional metallic structures. They have reduced weight and cost primarily by reducing part count and manufacturing operations, and by elimination of fasteners. However, even those innovative fabrication methods that use nonbleed materials, broadgoods, and integral cocuring concepts have used autoclaves as a source of pressure and energy traditionally associated with the matrix curing process.

Use of the autoclave has historically been energy, capital, and labor intensive and because of the extended periods required for cure of single components, a limiting factor in obtaining the assembly production rates required of modern systems. Elimination of the autoclave, therefore, is a logical goal.

The objective of this program was to establish and demonstrate a generic curing technique for 350°F organic matrix composite structures which does not require use of an autoclave, and which can be used to produce composite primary and secondary aircraft structure.

## 2.0 SUMMARY

This program established and demonstrated Rockwell's patented (U.S. Patent No. 4357193) generic nonautoclave manufacturing and curing techniques for curing 350°F system composite structures through the fabrication and test of significant elements and subcomponents representative of an aircraft composite empennage/wing primary structure, and the fabrication of a full-scale component of the B-1 vertical stabilizer using the techniques in a composite production environment.

The full-scale component (figure 1) selected for fabrication and producibility assessment during the last phase of this program provided for structural complexity and wide-range, generic applicability to primary and secondary aircraft structure. The complex aspects of the selected structure were its size, tapered and tailored skins, tapered chords, and volumetric effects. The specimen configuration also offered the opportunity for a complete manufacturing method validation through consideration of multiple process parameters, such as its significant volume and mass and associated cure complexities, wide laminate thickness range, joining of complete subassemblies, and the challenge of inspecting a large, real-world, multidimensional structure.

During phase I, the characteristics of Rockwell's nonautoclave process parameters were established and verified by fabrication, quality evaluation, and test of key elements of the B-1 vertical stabilizer structure to demonstrate its applicability to construction of the phase III full-scale component and, in general, the production of aircraft primary and secondary structures.

Preliminary versions of the production plan and manufacturing and process specifications directed to define the overall manufacturing approach, tooling, design details, and other aspects of the nonautoclave curing production of the phase III full-scale component were prepared. A cost-tracking plan and cost/benefit analysis was performed to project payoffs of the proposed method, including cost benefits, energy savings, process and handling savings, reduced capital expenditures, and other advantages to be derived from use of the nonautoclave cure. All fabrication costs were tracked to the manufacturing operations level of the Data Abstraction Form of the DoD/NASA Structural Composite Fabrication Guide.

Upon successful completion of phase I, phase II was initiated. During this phase a subcomponent representative of key areas of the phase III component was fabricated using tooling and procedures representative of those to be used in phase III. All fabricated hardware was subjected to sufficient NDE to verify its structural integrity, and to chemical, physical, and mechanical tests to determine its quality. Results were correlated and compared with those of similar parts cured in an autoclave. All operations were carefully cost tracked. The production plan, manufacturing and process specifications, and cost/benefit projections were updated and revised to incorporate the experience gained during the scaleup exercise of phase II.





VERTICAL STABILIZER  
● FULL SCALE COMPONENT

SPAN	133 IN.
ROOT CHORD	96 IN.
TIP CHORD	49 IN.

Figure 1. Phase III Full Scale Nonautoclave Demonstration Component

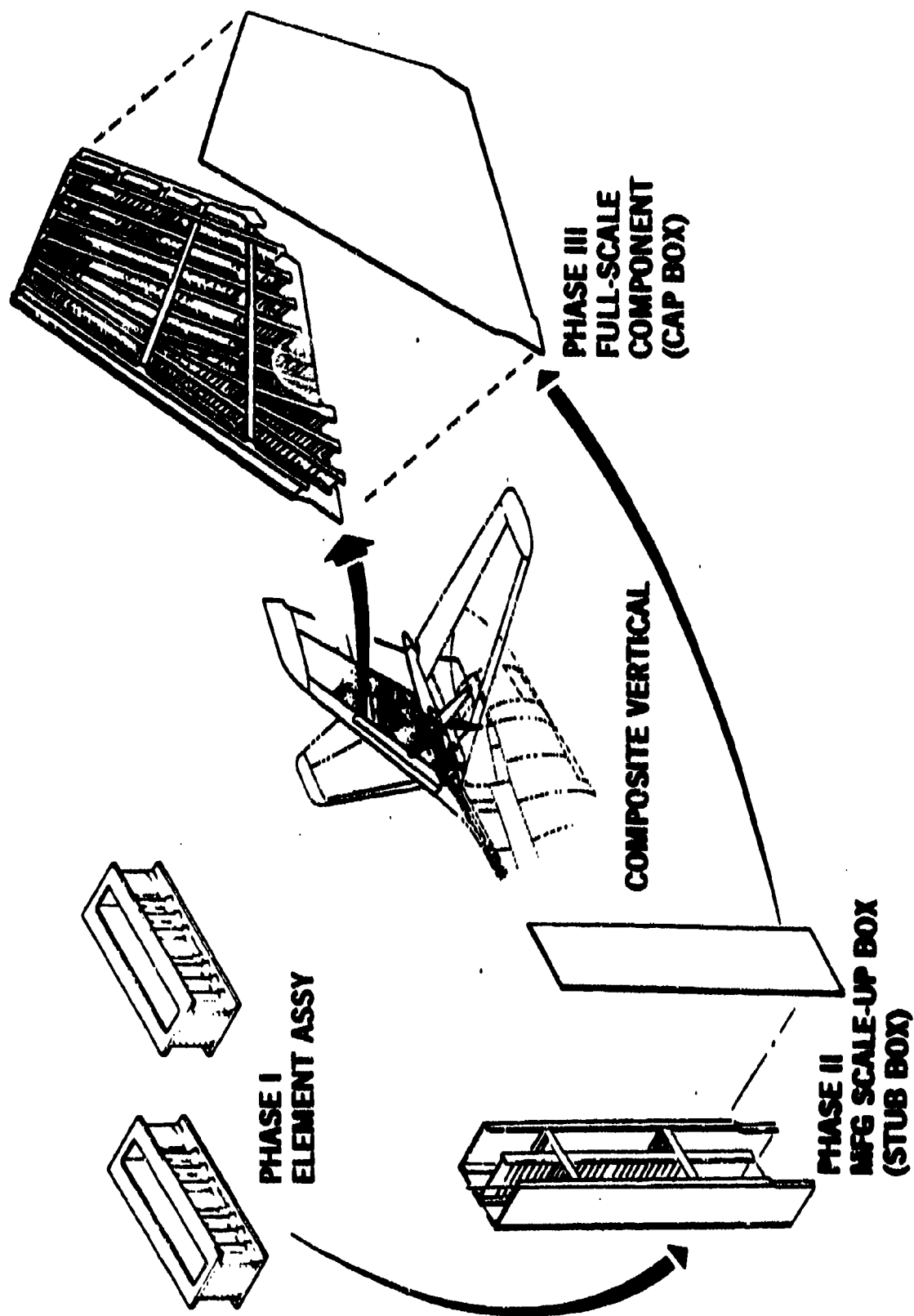


Figure 2. Program Components

During phase III a full-scale composite primary structural component of the B-1 vertical stabilizer was fabricated by the nonautoclave cure method at Rockwell's Tulsa facility in a production environment and using production facilities, equipment, and personnel. Sufficient NDE was performed on this article to verify its integrity and quality.

Production plans and the final material and process specification were prepared. Results of careful cost tracking throughout the program were used in a final cost/benefit analysis to assess the impact of the optimized non-autoclave manufacturing methods for composite structure on projected production costs.

The elements, subcomponent, and full-scale component fabricated during the three phases represent increasing levels of complexity in the manufacture of generic aircraft primary structure. Figure 2 illustrates the relationship between all components.

Figure 3 presents a summary schedule for all three phases.

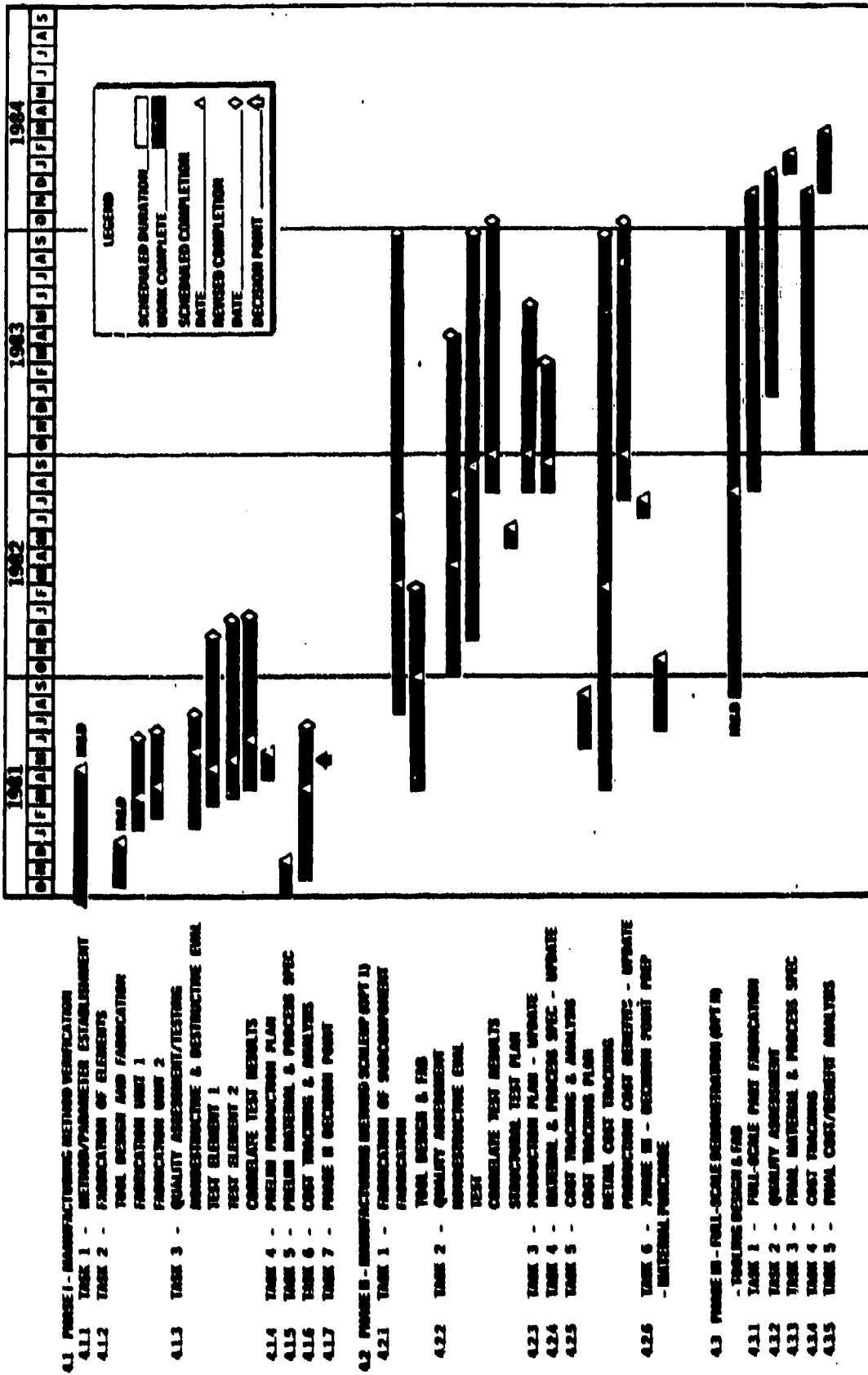


Figure 3. Program Schedule

### 3.0 BACKGROUND PROCESS DEVELOPMENT

NAAO conducted initial investigations directed at an assessment of the effects on the physical and mechanical property characteristics of graphite/epoxy (Gr/Ep) laminates cured by using conventional vacuum pressure only, coupled with standard heat-up rate and cure temperatures. These laminates exhibited the following characteristics: (1) excessive, unacceptable interlaminar and intra-ply porosity (2) reduced matrix critical mechanical properties such as interlaminar shear strength, and (3) reduced durability. Although these structural penalties might be accommodated in the design of some selected stiffness-critical secondary structure applications as some composite manufacturers have done, NAAO considered these reduced characteristics to be unacceptable for high-performance primary structures.

Initial nonautoclave process development efforts investigated the effects of relatively long cure-cycle dwell times at resin minimum viscosity temperatures of 225°F to 250°F under vacuum pressure with subsequent cure at 350° with vacuum pressure only. The results of these experiments (conducted on the Hercules' AS1/3501-5A Gr/Ep system) indicated a reduction in porosity, which was established by cross-sectional photomicrographs, and an approximate 50-percent increase in interlaminar shear strength. Subsequent evaluations involved coupling this long cure-cycle dwell time with the use of additional vacuum breather material and higher performance vacuum diffusion pumps. However, porosity levels and interlaminar shear strengths remained unchanged. At this point in the development, it was determined that an enhanced understanding of the overall curing mechanics and dynamics of Gr/Ep systems was required.

In order to attain this better understanding of the rheological characteristics of Gr/Ep materials, a series of experiments was conducted in a large bell-jar on a heated plate. Observations of several unidirectional and cross-ply laminates heated to approximately 250°F while in a vacuum environment of 28 to 30 inches of mercury (Hg) included (1) violent outgassing, as indicated by the appearance of air bubbles and vertical ply movement beginning at a temperature of approximately 150°F, (2) majority of bubble formation, appearing to be interlaminar, and (3) most efficient removal of air, occurring within the minimum viscosity temperature range. These degassed laminates were then cooled to room temperature while remaining in the vacuum environment and subsequently cured at a temperature of 350°F using vacuum pressure only. Examination of these cured laminates yielded the following results:

1. Elimination of all porosity and general appearance typical of autoclave cured laminates. This was determined by a comparison study of the cross-sectional photomicrographs. These laminates were 40 plies in thickness with a quasi-isotropic orientation of  $[0/\pm 45/90]_{5S}$ .

2. Thickness/ply corresponding to the nominal associated with an 85 psi autoclave cure laminate.
3. Interlaminar shear strength equivalent to autoclave cured laminates.

Based upon these data, it was concluded that adequate degassing of a composite material represented the highest potential for ultimately eliminating the need for autoclave curing thus forming the basis of NAAO nonautoclave technology.

Subsequent "bell" jar experiments strongly augmented NAAO's understanding of the processing characteristics of composites. Initial investigations were implemented to determine the source of air entrapment in composite laminates. Candidate regions included (1) resin matrix resulting from formulation and mixing operations (2) graphite fiber possible entrapment caused by fiber production, and (3) interlaminar resulting from layup operations. Microscopic evaluation of a laminate whose plies had been individually degassed prior to layup and subsequently cured with vacuum pressure only indicated extensive porosity. Based upon these data and the bell jar observations, it was concluded that the majority (80 percent) of the entrapped air in laminates can be attributed to the layup operation.

Processing a composite material in an autoclave at 85 psi has a dual effect on the interlaminar entrapped air. Transport of the air occurs as a result of resin flow. In addition, compaction of the air occurs as a result of the high pressure (85 psi). Thus, although microscopic, some air remains in the laminate.

Processing of a composite structure using conventional vacuum pressure only results in a highly porous, low-quality laminate. This can be attributed to insufficient pressure for air compaction and resin flow. Additionally, the minimum consolidation pressure which is applied tends to seal the individual plies, thus preventing random air migration or transport.

To create an environment similar to that in the bell jar, simplified tooling coupled with flat laminate processing, was used. Figure 4 illustrates the basic nonautoclave curing process. Tooling consists of an inner elastomeric bag and outer metallic or hard tooling representing two independent chambers. When vacuum pressure is applied to both chambers, a condition of equilibrium pressure occurs. This means that the laminate is essentially in a vacuum or bell jar environment; unlike conventional vacuum-pressure curing, no consolidation pressure is applied to the laminate thus enhancing air flow and migration. Air removal is further augmented by reducing the matrix resin viscosity with the application of heat. The laminate is then held at a minimum viscosity temperature in a vacuum environment until degassing is complete. Subsequent to this operation, the upper chamber, identified as hard tooling, is vented to the atmospheric pressure (14.7 psi) on the laminate. The laminate is heated to a temperature of 350°F and cured with vacuum pressure only. Figure 5 is a typical nonautoclave cure cycle. It must be remembered that the basic requirements of time and temperature to cure the resin remain unchanged.

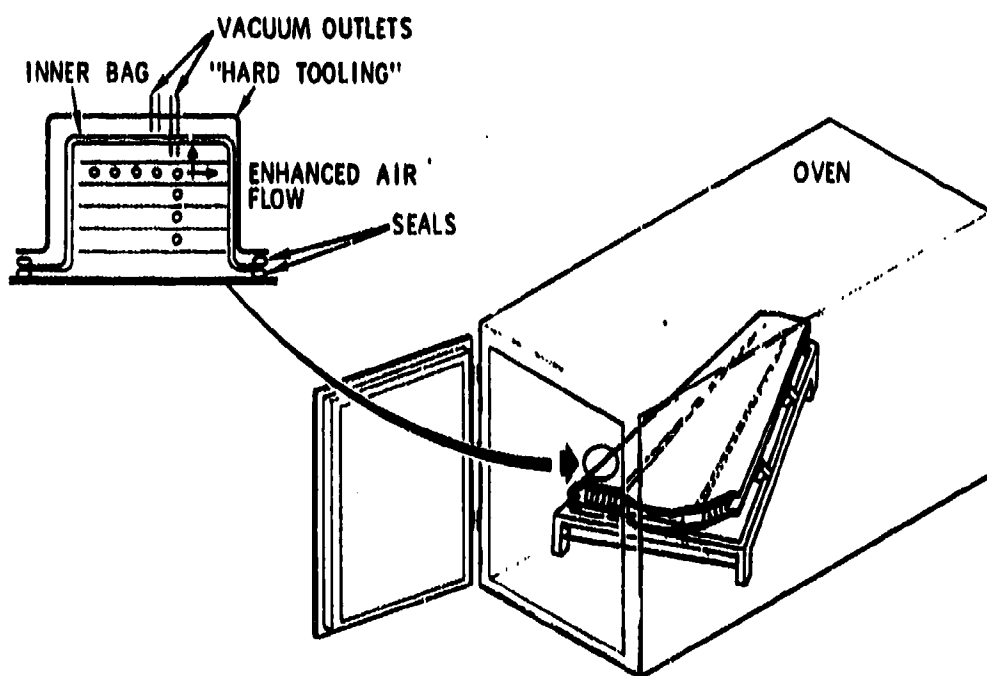
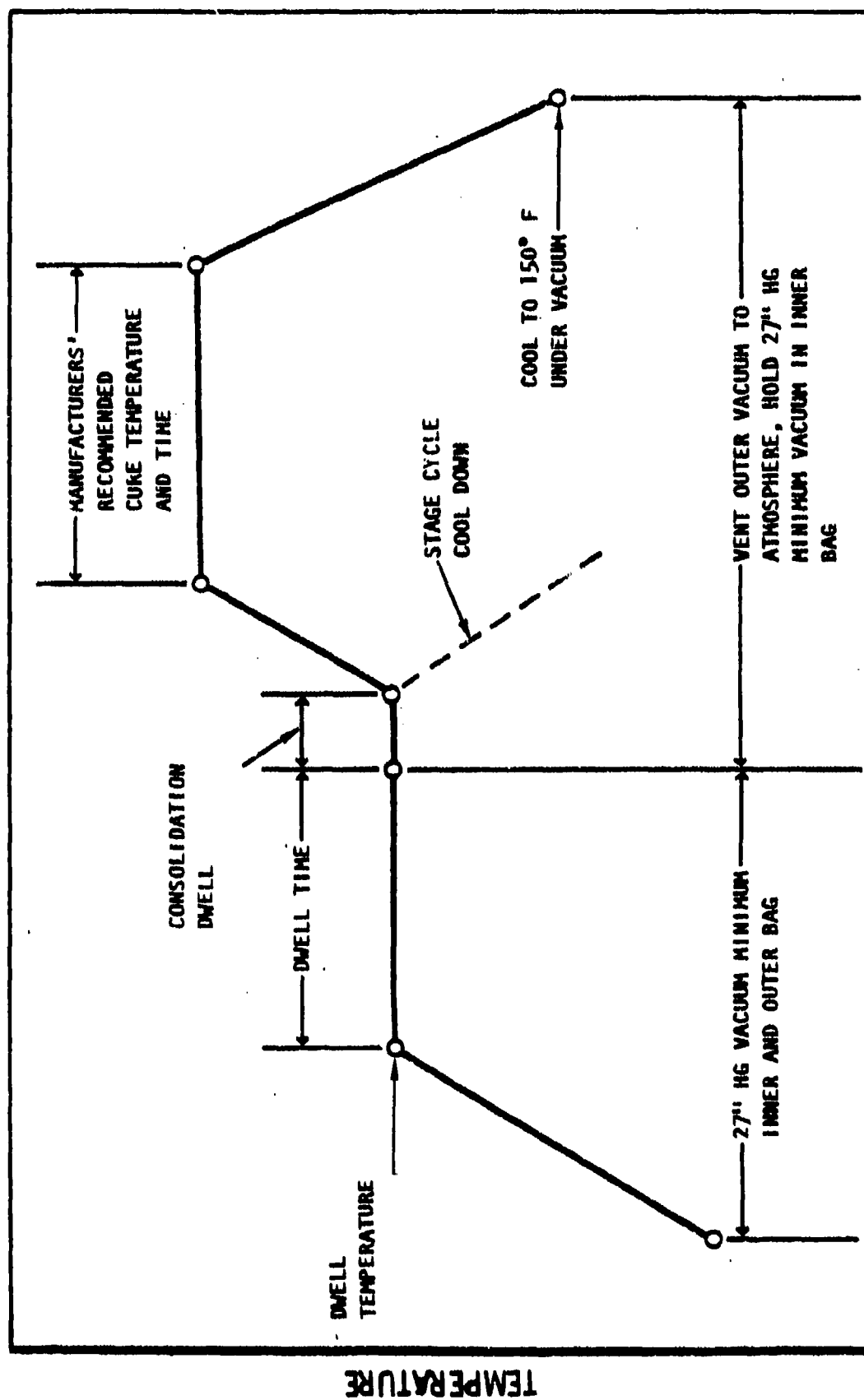


Figure 4. Diagram of NAO Process - Complete Entrapped Air Removal During Degassing Step

A review of figure 5 indicates the flexibility of the nonautoclave cure process. Following the degassing operation, laminates can be cooled under vacuum pressure and cured in a separate operation. This option is very compatible with structural details to be subsequently integrally cured. It should be noted that laminates subjected to the degassing operation have handleability at room temperature equivalent to cured laminates; however, the application of minimum heat precipitates flow and associated flexibility.





TIME

Figure 5. Typical MAAO Monoclave Staging and Cure Cycle

## 4.0 TECHNICAL EFFORT

### 4.1 PHASE I - MANUFACTURING METHOD VERIFICATION

During Phase I the feasibility of the nonautoclave cure manufacturing method was validated. Sufficient processing parameter, element verification, quality assurance, cost, and energy tracking data were generated to provide a basis for assessing the process. Through the fabrication and testing of two 102-cm (40-inch) long, integral structure boxes (which contained a flat web and a sine-wave spar with integrally cocured covers and close out ribs) the manufacturing feasibility of the process was validated. From these boxes, which were representative of critical areas of Phase II and Phase III components, verification bending beam test elements were fabricated and subjected to room temperature static test to failure. The resultant test data confirmed the capability of the nonautoclave process to produce parts that meet the structural integrity for which they were designed and to provide a valid basis for fabrication of the Phase II subcomponent and the Phase III component. Figure 6 shows the flow of activity for Phase I of the program.

#### 4.1.1 TASK 1 - METHOD/PARAMETER ESTABLISHMENT

These activities were divided into two generic categories: material selection and process demonstration. Three interdependent efforts which fully support the intent of the material selection were material selection/net resin content material characterization (tape and fabric), coupon verification testing, and structural adhesive selection and storage life extension evaluation. Three closely integrated efforts which logically fit into the category of process demonstration include process development, process limits and generic methods demonstration.

##### 4.1.1.1 Material Selection and Characterization

##### 4.1.1.1.1 Material Selection

The successful fabrication of low-cost integral composite airframe structures requires that certain raw material physical property constraints be observed. These material constraints are:

1. Minimal volatile generation during cure
2. Minimum prepreg bulk factor
3. Prepreg resin content approaching anticipated cured laminate optimum
4. Prepreg resin content control within narrow limits
5. Low, nonautoclave process staging temperature

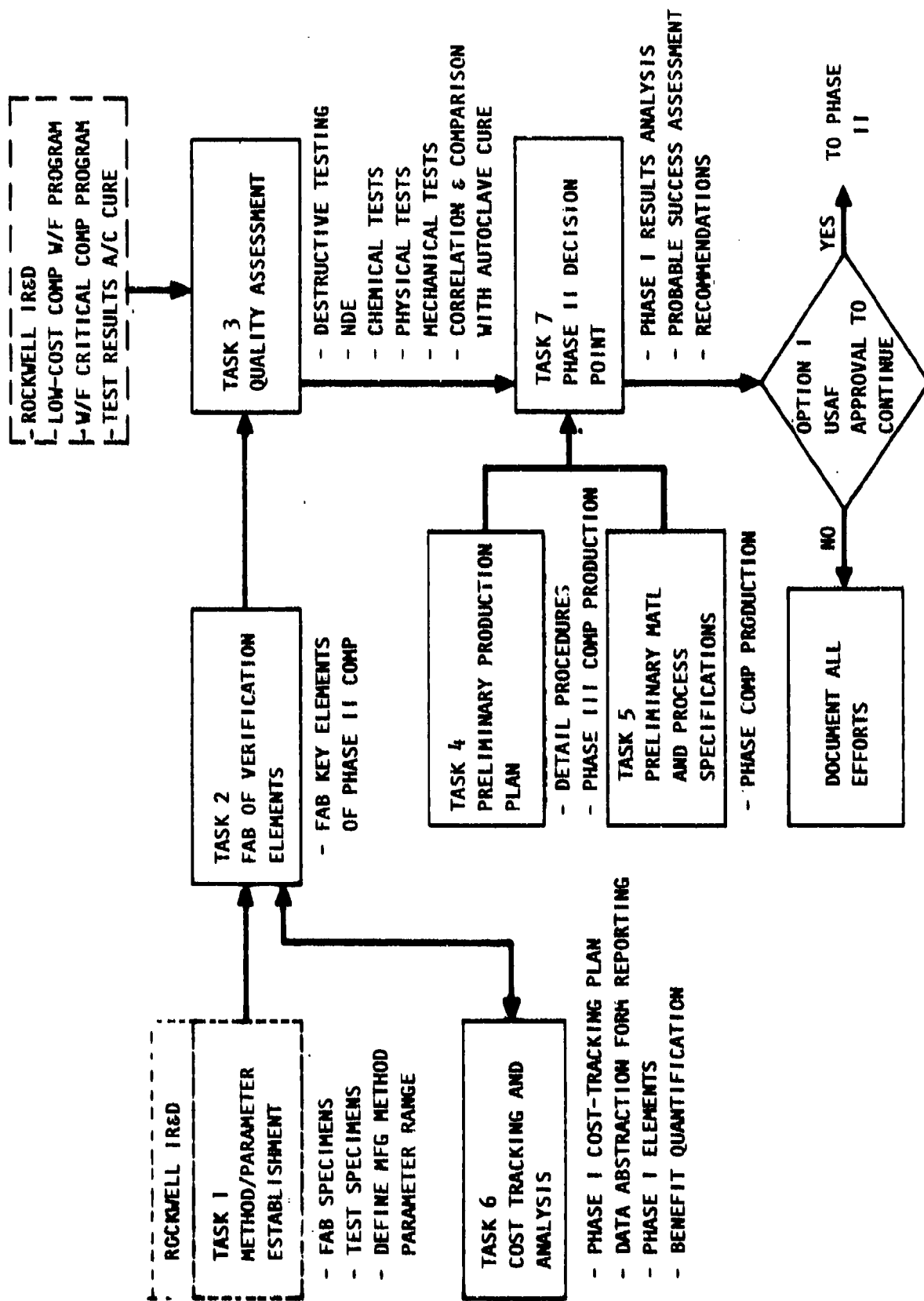


Figure 6. Phase I Flow Diagram

Effort was conducted to select a material system for the program. The selection criteria for this material investigation were:

1. Demonstration of the prepregger capability to manufacture net resin content ( $31\frac{1}{2} \pm 1\frac{1}{2}$  percent by weight) material on production equipment and in a production environment.
2. Demonstration of NAAO's proprietary nonautoclave process for compatibility/productibility with each of these material systems
3. Conformance with specification LB0130-028, revision C, 350°F cure graphite/epoxy procurement specification requirements
4. Minimum near-term and projected prepreg costs

Agreements were made with candidate material suppliers to evaluate 12-inch-wide Gr/Ep tape material systems in the range of 5- to 6-mil cured thickness/ply material. Those systems were:

1. Hercules     ASI/3501-5A  
                  ASI/3502
2. Ferro        C-6000/CE9000-9
3. Fiberite     ASI/976
4. Narmco       C-6000/5208

The selected approach was to standardize on ASI fiber because it represented NAAO's broadest data base. However, tape raw material costs for the minimum amount of material required for evaluation and the necessity of obtaining prepreg material manufactured on production equipment dictated a mixed-fiber prepreg evaluation.

The net-resin content Gr/Ep material evaluation was divided into prepreg physical property evaluation and laminate property evaluation. The physical and mechanical property evaluation test data generated during the material selection effort are presented in tables I and II. An evaluation of these test data included microscopic examination of the laminates fabricated. The results of this evaluation are quantified with weighting factors in table III. It was apparent from the data review and associated evaluation effort that each candidate material satisfied the material selection criteria. It was therefore concluded that each of the candidate material suppliers were capable of producing material to the requirements in accordance with the applicable NAAO specification. The material selection effort further reflects the generic applicability of the nonautoclave cure process technology.

Table I

## GR/EP NET-RESIN CONTENT TAPE PREPREG PHYSICAL PROPERTY EVALUATION DATA

Material	Tape		% Resin Content (1, 2)					Fiber Area Weight (Avg)(gm/in <sup>2</sup> )				
	Tack	Visual Quality	Start Edge/Ctr/Edge	Middle Edge/Ctr/Edge	End Edge/Ctr/Edge	Start	Mid	End	% Vol (Avg)	Gel Time		
Mercurles AS1/7501-5A	Light tack	Good	31.2/32.0/30.8	30.0/30.5/31.8	30.9/30.7/30.2					(5' 15")		
			Avg. 31.5 (31)**	Avg. 30.7	Avg 30.6	15.2	15.1	15.2	0.31			
Ferro C-6000 CE9000-9	Little tack	Excellent	30.2/32.6/32.1	29.6/32.8/31.5	31.9/33.0/35.0					(8'25")		
			Avg. 31.6 (31)**	Avg. 31.3	Avg. 33.3	13.2	14.6	14.7	0.4			
Fiberlite AS1/7576	Medium tack	Excellent	31.7/32.0/33.5	32.5/31.9/32.4	32.8/32.2/33.7					(10.3)		
			Avg. 32.4 (33.0)**	Avg. 32.3	Avg. 32.9	14.1	16.1	15.9 0.2				
Maruco C-6000 5200	Medium- heavy tack	Excellent	31.0/31.3/31.5	31.1/31.3/30.9	31.4/31.6/31.1					(20'20")		
			Avg. 31.3 (30.8)**	Avg. 31.1	Avg. 31.4	15.3	17.1	17.1	0.3			
Mercurles AS1/7502	Light tack	Good	31.0/31.1/29.9	32.5/33.5/33.6	33.3/33.0/31.0					4'30"		
			Avg. 30.7 (29.3)**	Avg. 33.2 (29.7)**	Avg. 32.7	15.2	15.2	15.2	0.24			

1. Requested prepreg resin content is 31.5 (+1.5)%
2. (X) vendor certification value.

Table II  
GR/EP NONAUTOCLAVE CURE LAMINATE PROPERTY EVALUATION

Material	15-Ply Unidirection Laminate						40-Ply [0/+45/90]s Laminate					
	Shear Str (ksi) RT 270 F 350 F	Thickness Per Ply (mil)	Specific Gravity	Resin Content (%)	Fiber Volume		Thickness Per Ply (mil)	Specific Gravity	Resin Content (%)	Fiber Volume	Inocured/Cured Thickness Per Ply	
Berkales KSI/3501-SA	16.4 12.0 9.2	4.92	1.61	29.3	0.628		5.19	1.61	28.2	0.648	1.10/1.13	
	15.4 11.3 9.6											
	17.6 12.1 9.6											
	16.3 11.0 9.5											
Ferro C-6000 CE9000-9	16.1 10.6 8.5	5.17	1.60	30.1	0.633		5.23	1.57	32.6	0.597	1.05/1.03	
	16.1 10.8 8.6											
	16.7 10.9 8.3											
	16.3 10.0 8.5											
Fiberite KSI/976	14.9 10.9 9.1	5.19	1.62	28.6	0.639		5.57	1.61	29.6	0.626	1.11/-	
	16.9 10.0 8.7											
	17.1 9.9 9.5											
	16.3 10.3 9.1											
Berkales C-6000 5200	15.4 10.7 9.4	5.56	1.63	25.1	0.600		5.75	1.60	28.3	0.649	1.05/1.01	
	15.3 10.7 9.2											
	15.9 11.1 9.3											
	15.5 10.0 9.3											
Berkales KSI/2502	16.1 11.4 9.4	5.01	1.62	27.2	0.649		5.14	1.60	29.4	0.624	1.16/1.13	
	17.7 11.2 9.7											
	17.5 11.8 9.5											
	17.1 11.5 9.5											

Table III  
NONAUTOCLAVE CURE MATERIAL SELECTION SUMMARY EVALUATION MATRIX

Material System	Selection Criteria (Weighting Factor)						
	Resin Content Control (10)	Area Fiber Wt Control (5)	Resin Film Wt Control (10)	Nonautoclave Process Compatibility (10)	Bulk Factor (8)	Tack (5)	Staging Temp (7)
Ferro C-6000/CE-9000-9	7	3	8	10	8	3	7
Fiberite AS1/976	7	2	9	10	7	5	7
Marmco C-6000/5208	10	3	9	10	8	5	5
Hercules AS1/3501-5A	8	5	10	10	7	4	7
Hercules AS1/3502	5	5	9	10	7	4	7
							46
							47
							50
							51
							47

Because of the attractive manufacturing benefits from the use of graphite woven-fabric material, the application of fabric potentially hybridized with Gr/Ep tape was evaluated. Although the Hercules AS1 10K filament graphite fiber represents NAAO's largest data base, its lack of weaveability precluded its selection for the fabric material to be used in this substructure.

Candidate fibers which contain fewer filaments per tow (3K and 6K), which ensures good weaveability characteristics, included Celanese Celion, Union Carbide T300, and Hercules AS4. Selection of the AS4 material was based upon (1) projected potential for significant cost savings (2) comparability with the baseline AS1 fiber, and (3) near-term availability of both type A and B allowables for tape and fabric.

Based on the selection of the AS4 fiber, quotations for production quantities, coupled with an acknowledgement to certify to the net-resin-content material requirements for prepreg tape, were solicited from each prepregger who participated in the material screening effort. Based on responses to this solicitation, the material selected was Fiberite which quoted a lower price than Hercules and didn't take exception to the tight ( $\pm 1\frac{1}{2}$  percent) net resin content tolerance of LB0130-128.

#### 4.1.1.1.2 Net-Resin Material Characterization

As a result of the selection of Fiberite AS4/976 prepreg tape and fabric for the program, characterization of these materials was conducted. The tape and fabric net-resin-content material test data are presented in tables IV and V, respectively. In addition to developing data on AS4/976 the generic nature of the nonautoclave process was demonstrated by conducting similar testing on AS1/3501-5A, T300/5208 and CE 6000/9000-9. The results of these tests are shown in tables VI, VII, VIII, IX, X, and XI. A graphic comparison of key properties of T300/5208 and AS1/3501-5A is shown in figures 7 and 8.

#### 4.1.1.1.3 Adhesive Compatibility Demonstration and Characterization

Nonautoclave cure processing had been used primarily for the fabrication of flat laminated structures. The cocure joining of laminate layups to precured staged or metal details by the nonautoclave cure process requires a film adhesive. In addition, cocured integral structure fabrication may also require adhesive bonding material to improve critical joint toughness. The compatibility of the adhesive with the composite matrix resin and the nonautoclave cure process was established and validated under an NAAO-funded program.

The adhesive selection task, conducted under an internally funded program, consisted of a literature survey and a series of screening tests. Four adhesive systems were procured and subjected to screening tests. These adhesives were FM-400, FM-300, AF143, and Metlbond 1515. Screening tests included cocured-to-cocured and precured-to-cocured lap-shear-joint tests at several test temperatures with and without film adhesive. The nonautoclave cure process was used to establish the desired basic process compatibility.



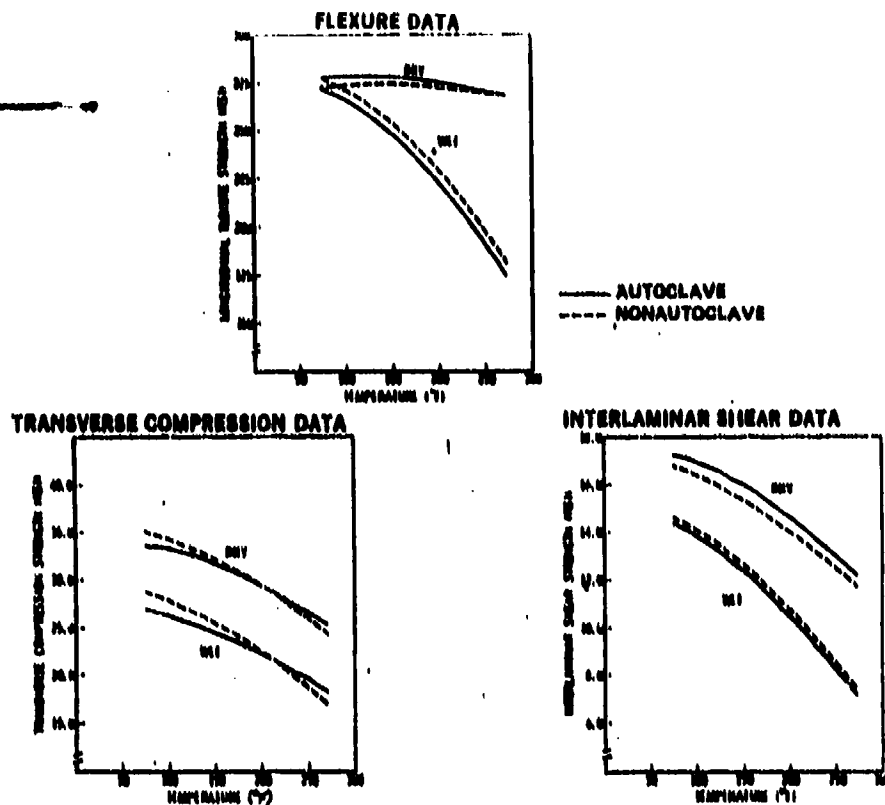


Figure 7. Nonautoclave Cure Mechanical Properties - T300/5208

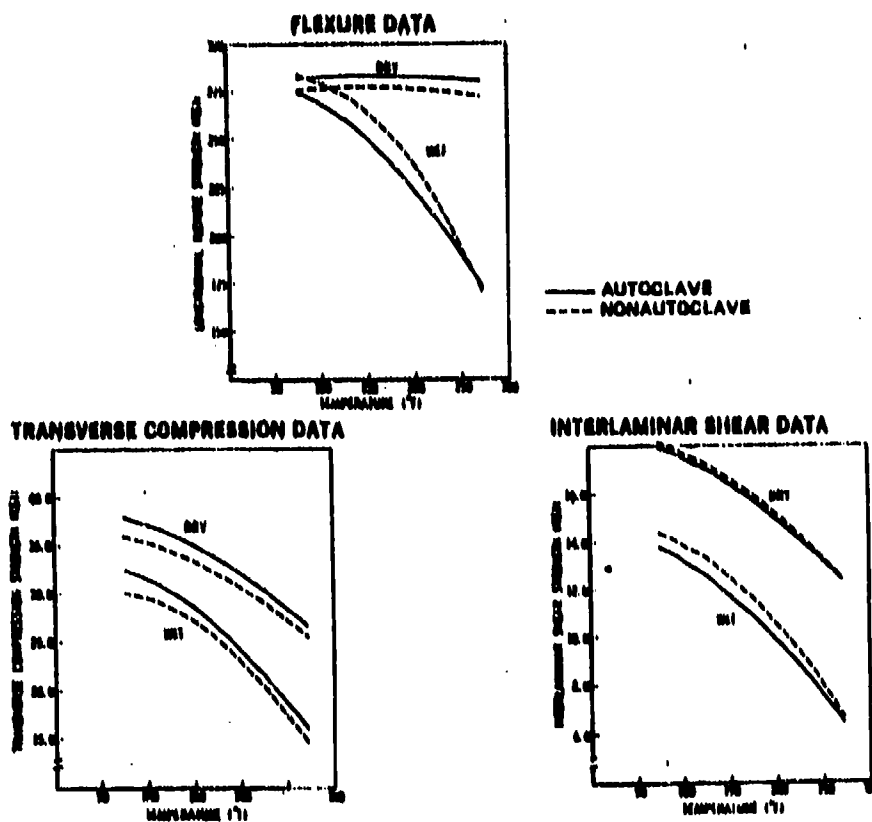


Figure 8. Nonautoclave Cure Mechanical Properties - AS1/3501-5A

Table IV

**NO-BLEED AS4(6K)/976 GRAPHITE/EPOXY TAPE MATERIAL CHARACTERIZATION 15-PLY  
UNIDIRECTIONAL LAMINATE MECHANICAL PROPERTY TEST RESULTS**

Mechanical Property	Test Temperature and Condition		
	RT Dry/Wet	270° F Dry/Wet	350° F Dry/Wet
0° flexural strength, ksi (fiber v/f - 0.650)	314.8/293.6 201.9/310.4 329.2/303.5 334.1/327.8 <u>313.9/298.8</u>	257.3/175.3 254.6/154.6 247.8/170.0 245.8/168.8 <u>261.1/153.2</u>	202.2/112.1 189.0/102.4 196.1/107.0 174.1/110.2 <u>195.2/110.8</u>
Average value	318.8/305.8	253.3/164.4	191.3/108.5
Wet/dry strength retention	95.9%	64.9%	56.7%
Interlaminar shear strength, ksi (fiber v/f - 0.650)	14.5/11.7 15.7/10.8 15.7/11.0 16.0/12.1 <u>16.1/11.9</u>	8.7/4.9 9.0/4.7 8.5/5.1 8.9/5.0 <u>8.9/4.6</u>	5.7/3.5 5.9/3.2 6.4/3.4 6.4/3.5 <u>5.8/3.5</u>
Average value	15.6/11.5	8.8/4.9	6.0/3.4
Wet/dry strength retention	75.7%	55.7%	56.7%

NOTE: 1. Wet conditioning: 30 ± 1 day in an 95% relative humidity (RH) environment at 120°F prior to test.

Table IV (cont.)

NO-BLEED AS4(6K)/976 GRAPHITE/EPOXY TAPE MATERIAL  
CHARACTERIZATION TENSILE TEST RESULTS

Mechanical Property	Test Temperature and Condition						
	Ultimate Strength (ksi)			Tensile Modulus. (msi)			
	RT Dry/Wet	270° F Dry/Wet	350° F Dry/Wet	RT Dry/Wet	270° F Dry/Wet	350° F Dry/Wet	350° F Dry/Wet
90° compression beams (Fiber v/f-0.613)	246.2/237.8 273.7/268.4 <u>223.4/248.5</u>	170.0/144.4 178.5/148.9 <u>161.3/141.4</u>	165.7(1) 139.4/ <u>179.9/</u>	18.9/20.9 -/- <u>-/-</u>	19.2/19.0 -/- <u>-/-</u>	19.5/(1) -/- <u>-/-</u>	19.5/(1) -/- <u>-/-</u>
Average value	247.8/251.6	169.9/144.9	161.7(1)	18.9/20.9	19.2/19.0	19.5/(1)	19.5/(1)
Wet/dry retention	100%	85.3%	--	100%	99%	--	--
Ball shear (Fiber v/f-0.602)	11.6/(1) 11.5/- <u>11.6/-</u>	9.2/(1) 7.9/- <u>8.1/-</u>	6.1/(1) 6.4/- <u>7.0/-</u>	(2)/(1) -- --	0.4/(1) 0.3/- <u>-/-</u>	0.4/(1) 0.4/- <u>-/-</u>	0.4/(1) 0.4/- <u>-/-</u>
Average value	11.6/(1)	8.0/(1)	6.5/(1)	(2)(1)	0.4(2)	0.4(1)	0.4(1)
NOTES: 1. Specimens not tested at this condition 2. Strain-gage failure 3. Wet conditioning: 30 ± 1 day in a 95% RH environment at 120°F prior to test							

Table IV (Cont.)

NO-BLEED AS4(GK)/976 GRAPHITE/EPOXY TAPE MATERIAL  
CHARACTERIZATION TENSILE TEST RESULTS

Mechanical Property	Test Temperature and Condition						
	Ultimate Strength (ksi)			Tensile Modulus, (mst)			
	RT Dry/Met	270° F Dry/Met	350° F Dry/Met	RT Dry/Met	270° F Dry/Met	350° F Dry/Met	350° F Dry/Met
90° tensile (Fiber v/F-0.604)	7.3/5.2 8.9/5.3 <u>8.1/5.6</u>	5.4/2.1 5.5/2.4 <u>5.0/2.1</u>	4.1/1.2 4.1/1.2 <u>3.9/1.2</u>	1.3/1.3 1.3/1.3 <u>1.2/1.3</u>	1.1/0.9 1.2/1.0 <u>1.1/0.4</u>	1.1/0.4 1.1/0.4 <u>1.1/0.4</u>	1.1/0.4 1.1/0.4 <u>1.1/0.4</u>
Average value	8.1/5.4	5.3/2.3	4.0/1.2	1.3/1.3	1.2/1.0	1.1/0.4	1.1/0.4
Met/dry retention	66.7%	43.4%	20.0%	100%	83.3%	36.4%	36.4%
0° tensile (Fiber v/F-0.509)	259.5/263.8 261.7/273.9 <u>261.8/269.5</u>	222.3/213.8 232.6/225.1 <u>226.2/222.2</u>	209.9/(1) 226.0/ <u>231.5/</u>	20.4/20.3 20.1/20.4 <u>19.8/20.0</u>	(2)/21.2 /21.4 <u>/20.0</u>	20.2(1) 21.3/ <u>21.5/</u>	20.2(1) 21.3/ <u>21.5/</u>
Average value	261.0/269.1	227.0/226.2	222.4/(1)	20.1/20.2	(2)/21.0	21.9/(1)	21.9/(1)
Met/dry retention	100%	99.6%		100%			
Cross-ply Tensile (Fiber v/F-0.631)	83.4/(1) 82.2/ <u>68.8/</u>	85.3/(1) 76.0/ <u>79.1/</u>	77.9/(1) 79.9/ <u>79.9/</u>	7.2/(1) 8.6/ <u>7.5/</u>	7.3(1) 7.0/ <u>7.2/</u>	6.9(1) 7.9/ <u>7.0/</u>	6.9(1) 7.9/ <u>7.0/</u>
Average value	78.1/(1)	80.3/(1)	79.2/(1)	7.8(1)	7.2/(1)	7.5/(1)	7.5/(1)
NOTES: 1. Specimens not tested at this station 2. Strain-gage failure 3. Met conditioning: 30 ± 1 day in a 95% RH environment at 120° F prior to test.							

Table V

FABRIC CHARACTERIZATION TEST RESULTS  
NONAUTOCLAVE CURE, FIBERITE HMF 133/76, LOT  
B1-105, ROLL 2A

Mechanical Test	Results	
	Strength (ksi)	Modulus (msi)
	RT/270F	RT/270° F
Warp Flexure	108.7/112.6 112.7/113.5 118.9/115.9 104.0/113.5 <u>115.9/108.8</u>	
(Spec Requirement) (1)	112.0/112.9 (100/73)	
Interlaminar Shear	10.8/8.0 10.8/8.2 9.4/8.1 11.0/8.3 <u>10.4/7.8</u>	
(Spec Requirement) (1)	10.5/8.1 (7.0/5.5)	
Warp Tension	72.9/93.8 81.8/92.6 <u>70.7/76.9</u> 75.1/87.8	9.6/10.0 9.7/10.0 <u>10.0/9.8</u> 9.8/9.9
(Spec Requirement) (1)	(75.0/70.0)	(9.3/8.5)
Fill Tension	70.7/85.9 71.4/83.7 <u>65.4/88.7</u> 69.5/86.1	8.8/ -- 8.5/10.0 <u>8.3/9.9</u> 8.5/10.0
(Spec Requirement) (1)	(73.0/65)	(9.3/8.5)
Warp Compression	83.5/66.9 71.8/72.5 <u>78.0/67.6</u> 77.8/69.0	8.5/8.5 8.6/8.5 <u>9.0/8.8</u> 8.7/8.6
(Spec Requirement) (1)	(60.0/45)	(8.5/8.0)
Fill Compression	81.1/67.5 94.0/80.6 <u>90.3/76.4</u> 88.5/74.8	8.4/8.6 8.4/8.3 <u>8.4/8.3</u> 8.4/8.4
(Spec Requirement) (1)	(60.0/45)	(8.5/8.0)
Roll Shear	14.9/12.9 15.8/13.3 <u>14.8/13.3</u> 15.2/13.2	0.50/0.37

NOTE: 1. Minimum requirements for strength and modulus at room temperature/350° F per LBQ128-120.

Table VI

AUTOCLAVE VERSUS NONAUTOCLAVE-CURED  
AS1/3501-5A DRY-WET LAMINATE STRENGTH

MECHANICAL PROPERTY/ SPECIMEN CONFIGURATION	TEST TEMP OF	AUTOCLAVE CURE STRENGTH (KSI)			NONAUTOCLAVE CURE STRENGTH (KSI)		
		DRY	WET	% RET	DRY	WET	%
0° F FLEXURE/[0] <sub>15</sub> V/f = 64.9/62.6	RT	282.2 298.1 <u>289.9</u>	275.9 276.1 <u>272.3</u>		278.9 267.2 <u>291.2</u>	290.8 303.9 <u>286.3</u>	
AVG.		289.9	274.8	94.8	278.3	293.7	105.5
0° F FLEXURE/[0] <sub>15</sub>	270	285.8 284.1 <u>288.5</u>	168.1 172.2 <u>173.6</u>		268.9 261.7 <u>273.3</u>	156.9 174.3 <u>167.6</u>	
AVG.		286.1	171.3	59.9	167.9	166.3	62.2
SHORT BEAM SHEAR/[0] <sub>15</sub> V/f = 64.9/62.6	RT	17.7 18.7 18.7 18.3 <u>17.9</u>	13.9 14.3 12.7 13.8 <u>14.2</u>		18.3 18.3 19.0 18.3 <u>18.6</u>	14.5 14.6 14.2 14.3 <u>14.5</u>	
AVG.		18.3	13.8	75.4	18.5	14.4	77.8
SHORT BEAM SHEAR	270	12.4 12.1 12.3 12.6 <u>12.5</u>	6.5 6.6 6.4 6.5 <u>6.5</u>		12.2 12.1 12.5 12.5 <u>12.5</u>	6.8 6.8 6.9 6.6 <u>6.6</u>	
AVG.		12.4	6.5	52.4	12.4	6.7	54.0
90° COMPRESSION/[90] <sub>22</sub> V/f = 63.3/61.2	RT	37.9 38.4 <u>36.1</u>	33.5 33.6 <u>30.3</u>		36.7 38.2 <u>32.7</u>	32.2 26.9 <u>31.0</u>	
AVG.		37.9	32.5	85.6	35.9	30.00	83.6
90° COMPRESSION/[90] <sub>22</sub>	270	26.7 27.5 <u>25.7</u>	15.3 15.6 <u>16.4</u>		25.3 25.6 <u>25.9</u>	14.6 14.9 <u>13.4</u>	
AVG.		26.6	15.8	59.4	25.4	14.3	56.3
NOTE: 1. Wet conditioning: 30 ± 1 day in 95% RH environment at 120 F prior to test.							

Table VII

AUTOCLAVE VERSUS NONAUTOCLAVE-CURED  
T300/5208 DRY-WET LAMINATE STRENGTH

MECHANICAL PROPERTY/ SPECIMEN CONFIGURATION	TEST TEMP OF	AUTOCLAVE CURE STRENGTH (KSI)			NONAUTOCLAVE-CURE STRENGTH (KSI)			
		WET	DRY	WET	% RET	DRY	WET	% RET
0° FLEXURE/[0] <sub>14</sub>	RT		273.7 274.8 <u>291.7</u>	278.6 278.4 <u>279.2</u>		268.2 269.8 <u>274.4</u>	275.5 288.9 <u>271.93</u>	
AVG.			280.1	278.7	99.5	270.8	279.4	103.2
0° FLEXURE/[0] <sub>14</sub> V/o = 63.8/65.0	270		259.0 266.9 <u>259.1</u>	179.0 179.2 <u>165.4</u>		252.0 269.4 <u>263.1</u>	186.4 189.4 <u>193.7</u>	
AVG.			261.7	174.5	66.7	261.5	189.8	72.6
SHORT BEAM SHEAR/[0] <sub>14</sub> V/o = 63.8/65.0	RT		17.5 17.9 17.5 16.1 <u>17.3</u>	14.6 13.8 ----- 14.3 <u>14.7</u>		16.7 17.3 16.5 17.1 <u>16.6</u>	14.9 14.6 14.9 14.4 <u>14.0</u>	
AVG.			17.3	14.4	83.2	16.8	14.6	87.0
SHORT BEAM SHEAR/[0] <sub>15</sub>	270		11.7 12.1 12.2 12.2 <u>12.2</u>	7.0 7.3 7.2 7.3 <u>7.4</u>		10.9 12.2 11.8 11.5 <u>11.9</u>	7.4 7.4 7.4 7.4 <u>7.4</u>	
AVG.			12.1	7.2	59.4	11.7	7.4	63.2
90° COMPRESSION/[90] <sub>20</sub> V/o = 60.9/62.5	RT		34.9 33.9 <u>31.9</u>	28.7 25.2 <u>26.8</u>		37.0 33.4 <u>35.0</u>	27.0 29.1 <u>29.9</u>	
AVG.			33.6	26.9	80.1	35.1	29.7	81.8
90° COMPRESSION/[90] <sub>20</sub>	270		25.7 24.5 <u>25.5</u>	17.2 17.8 <u>19.2</u>		23.5 24.6 <u>26.3</u>	16.5 16.7 <u>17.6</u>	
AVG.			25.2	18.1	71.8	24.3	16.9	69.5
NOTE: Wet conditioning: 30 ± 1 day in 95% RH environment at 120°F prior to test.								

TABLE VIII

**UNIDIRECTIONAL [0]<sub>15</sub> Gr/Ep (FERRO CE9000-9/CELION 6000, ROLL 6051)  
LAMINATE FLEXURE AND INTERLAMINAR SHEAR PROPERTIES (1,4)**

Property	Ultimate Strength (ksi)		Dry/Wet 3500F	Flexure Modulus (ksi)		
	RT	2700F		RT	2700F(2)	3500F(2)
90° Flexure (3)	266.1/241.3	266.2/196.9	249.1/104.5	17.9	16.3	20.6
	250.1/281.9	256.2/189.6	259.3/99.5	17.3	16.8	21.3
	242.1/290.5	275.4/194.2	230.1/94.8	17.4	17.5	18.4
	267.8/289.2	275.6/207.2	225.3/85.3	17.1	17.1	17.4
	----/272.7	----/199.3	----/88.3			
Average	256.8/275.1	268.1/197.5	240.7/94.5	17.4	16.9	19.4
	240.0/-----	200.0/-----	155.0/-----	17.5	17.0	16.0
Short-beam shear(3)	15.9/12.2	9.8/6.0	7.6/3.7			
	16.0/12.6	10.0/5.9	7.7/3.8			
	16.3/12.3	9.8/0.0	7.9/3.9			
	15.5/12.2	9.9/6.3	8.0/3.9			
	16.4/12.0	9.9/6.3	8.1/4.0			
Average	16.0/12.3	9.9/6.1	7.9/3.9			
	14.0/-----	9.5/-----	7.0/-----			
NOTES: 1. Cured laminate fiber volume -64 percent 2. Elevated-temperature flexure modulus determined from cross-head travel 3. Moisture content of wet-test laminate = 1.10 percent 4. Laminate cured 2 hours at 3600F and 85 psig using TX1040 separator and no other bleeder material						



TABLE IX

## Gr/Ep (FERRO CE9000-9/CELIOM 6000, ROLL 6051) LAMINATE TENSILE PROPERTIES

Property Laminate Configuration Temp.	Ultimate Strength (ksi) Dry/Wet		Tensile Modulus (ksi) Dry/Wet	
	RT	270°F	RT	350°F
0° Tension [0] <sub>g</sub> (3)				
Fiber v/f-0.616	226.7/219.2	219.0	18.9(1)/18.7	20.3(1)
Average	190.7/221.0	220.4	19.1/22.3	18.5
LB0130-128 Requirement	209.0/194.0	210.2	17.8/19.9	18.4
	209.0/221.4	217.5	18.6/20.3	19.3
	200.0/-----	180.0	19.4 (19.0 min)/-----	18.5 (18.0 min)
90° Tension [90] <sub>g</sub> (4)				
Fiber v/f 0.626	5.2/5.1	4.7/1.5	1.4(1)/1.3	1.1(1)/0.8
Average	8.1/4.5	4.9/2.2	1.3/1.3	1.1/0.8
LB0130-128 Requirement	5.9/4.5	4.8/2.0	1.3/1.4	1.1/0.8
	6.4/4.7	4.8/1.9	1.3/1.3	1.1/0.8
	7.4/-----	-----	1.3/-----	0.94/0.3
0° Tension/[0/+45/90] <sub>g</sub>				
Fiber v/f-0.622	60.4	69.3	6.6(1)	6.5(1)
Average	62.4	67.7	6.7	7.5
	63.8	72.0	6.5	6.7(1)
	67.5			
	63.7	69.7	6.5	7.1
NOTES: 1. Denotes values determined by strain-gage readout				
2. Specimen laminate configuration 90/24				
3. 0° tension wet-test laminate moisture content = 1.24 percent				
4. 90° tension wet-test laminate moisture content = 1.15 percent				

Table X

UNI-DIRECTIONAL GR/EP (FERRO CE9000-9/CELIION 6000, ROLL 6051)  
LAMINATE COMPRESSION PROPERTIES

Property/ Laminate Configuration Temp.	ULTIMATE STRENGTH (ksi) DRY/WET		COMPRESSION MODULUS (ksi) DRY/WET	
	RT	270°F	RT	270°F
Beam compression/[0] <sub>90</sub> (1) Fiber v/f-0.608	255.8/246.4 229.3/266.2 241.7/225.3	217.9/143.6 239.2/145.5 190.5/149.3	19.7/19.0 19.1/19.3 18.3/19.9	18.7 18.4 19.8
Average L80130-128 requirement	242.3/245.9 220.0/200.0	215.5/146.1 180.0/100.0	19.0/19.4 18.9/18.9	19.1 17.0
ARTC-11 compression/[90] <sub>24</sub> (2) Fiber v/f-0.628	28.0/25.7 29.7/28.9 30.6/27.9	23.6/17.6 22.9/17.1 23.7/17.8		
Average	29.7/27.4	23.4/17.5		
NOTES: 1. Beam compression wet-test laminate moisture content = 1.20 percent 2. ARTC-11 compression wet-test laminate moisture content = 1.08 percent				

Table XI

## WET-STRENGTH RETENTION OF FERRO CE9000-9/CELIION 6000 LAMINATES

Mechanical Property	Laminate Configuration	Fiber Volume/ Moisture Content (%)	Ultimate Wet Strength/% Retention					
			RT		270°F		350°F	
			ksi	%	ksi	%	ksi	%
0° flexure	[0]15	64.7/1.10	275.1	107.0	197.5	73.0	94.5	39.3
Short-beam shear	[0]15	64.7/1.10	12.5	76.9	6.1	61.7	3.9	49.3
Short-beam shear	[0]16	62.6/1.08	12.3	76.9	6.6	66.7	4.4	62.8
0° tension	[0]8	61.6/1.24	211.4	101.3	—	—	—	—
90° tension	[90]16	62.6/1.15	4.7	72.5	1.9	39.6	0.9	20.0
0° compression (beam)	[0]6	60.8/-1.20	245.9	101.6	146.1	67.8	—	—
90° compression	[90]24	62.8/1.08	27.4	92.3	17.5	74.5	10.5	56.6

During the adhesive selection screening effort, nonautoclave-cure processing variables that could rule out the acceptability of an adhesive material were considered. In addition, adhesive peel strength was assessed for nonautoclave-cured metal-to-metal peel specimens. The pertinent adhesive screening test data are presented in table XII. Based upon the adhesive screening test results, as well as previously generated B-1 program adhesive evaluation data and Vought Corporation data generated under Air Force contract F33615-76-C-3138 "Advanced Technology Wing," American Cyanamid FM-300 was selected for this program.

#### 4.1.1.1.4 Storage Life Extension Study

A storage life extension study of staged graphite/epoxy laminates of the two epoxy resin systems (Fiberite AS1/976 and Hercules AS1/3501-5A) evaluated the effect of nonautoclave staging on the ambient temperature storage life of graphite/epoxy laminates. It was expected that B-staging of the graphite/epoxy material would extend its ambient temperature storage life, thereby eliminating costly freezer storage and excessive handling in the fabrication sequence of integral structures. Through bringing the resin up to a level of cure the T<sub>g</sub> is raised above ambient conditions; below gel, therefore, the advancement of the resin is slowed at ambient conditions.

The storage life extension data include the results from a company-sponsored program which utilized the same graphite/epoxy laminates (AS1/976 and AS1/3501-5A). The results for laminates that were staged, exposed to 360 days of ambient temperature environment (the laminates were sealed in a moisture proof bag), cured and tested are shown in figures 9 and 10. These data indicate a lack of any significant degradation of the Hercules AS1/3501-5A flexure and interlaminar shear strength properties for the duration of the program exposure periods as well as for the 360-day exposure period. A 360-day exposure for Fiberite AS1/976 flexure and interlaminar shear strength properties was not obtainable because the Fiberite AS1/976 laminates severely delaminated during specimen machining.

Based on the data accumulated during the study, a 90-day ambient temperature storage life was established for all details to be fabricated from Fiberite 976 epoxy material. The use of Hercules 3501-5A epoxy material would allow a 360-day ambient temperature storage life.

#### 4.1.1.2 Nonautoclave Process Development

The objective of this effort was to establish optimal or nominal staging operation parametric data for the selected materials. The staging process is a degassing operation which is performed at a selected temperature for the specified duration required for complete removal of entrapped air. It represents the key feature of nonautoclave curing process which permits the subsequent use of vacuum pressure only to obtain autoclave-processed quality components. The information generated during this task provided baseline cure cycle parameters such as required heatup rate, minimum viscosity dwell temperature, and nominal dwell time.

TABLE XII

NONAUTOCURE CURE PROCESS ADHESIVE SYSTEM  
MATERIAL SCREENING TEST DATA

Material	Avg Lap Shear Strength (psi)			Peel Strength (ppt)		
	Cocure Compatibility (Al to Al)		Cocure Compatibility (Gr/Ep to Gr/Ep)	Gr/Ep to Aluminum Peel		
	RT	220°F		-65°F	RT	220°F
FM-400	3,420	2,940	1,980	1,900	18	12
AF-143	3,040	2,520	2,270	1,970	24	12
FM-300	3,530	2,400	4,270	3,500	20	31
MB-1515	2,670	2,200	2,900	2,760	13	19

\*All specimens vacuum pressure cured at 350°F for 1 hour.

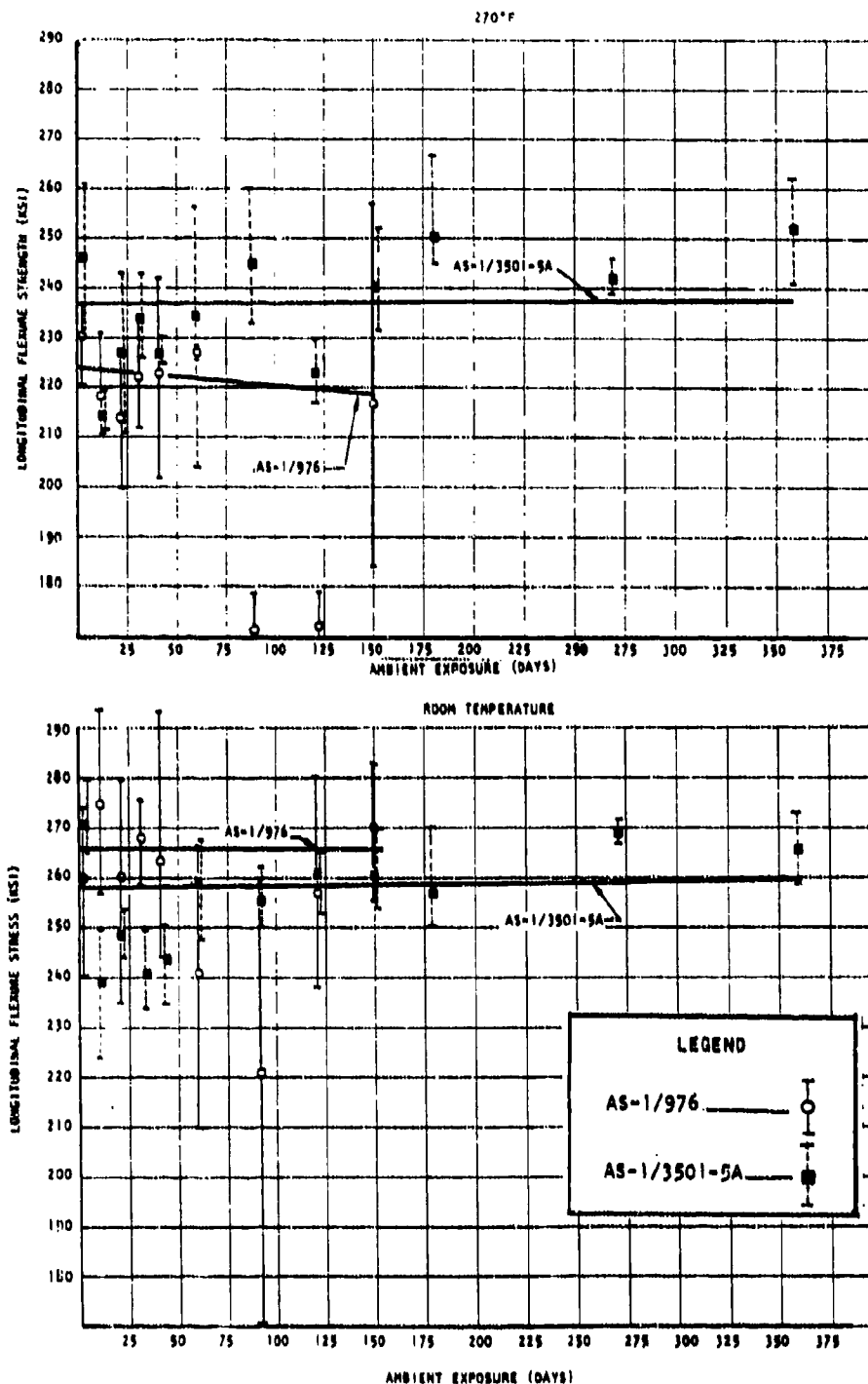


Figure 9. Fiberite AS1/976 and Hercules AS1/3501-5A Staged Laminate (0)<sub>15</sub> Storage Life Extension Longitudinal Flexure Strength (Ksi) Test Results

270°F

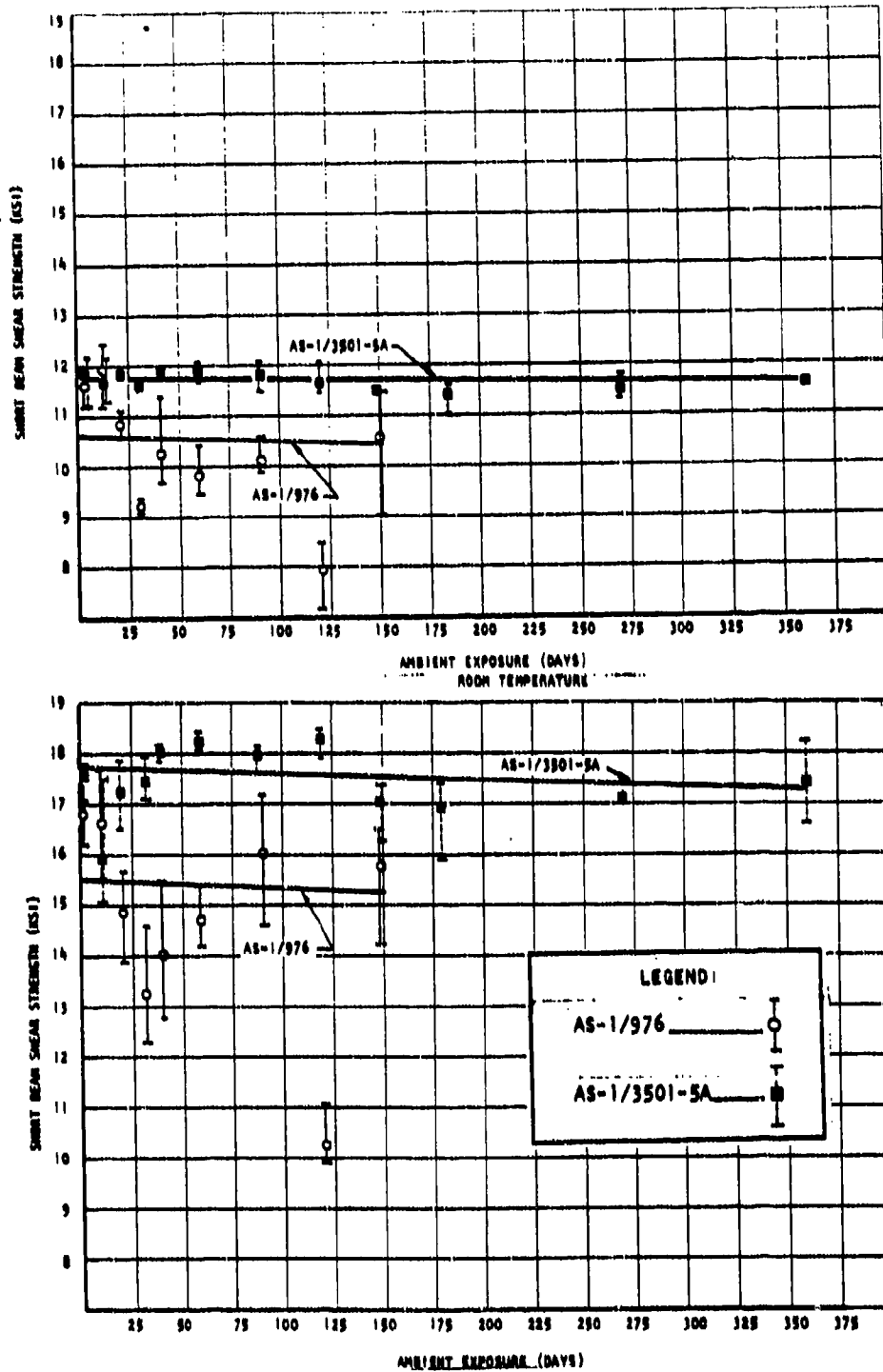


Figure 10. Fiberite AS1/976 and Hercules AS1/3501-5A Staged Laminate (O)<sub>15</sub> Storage Life Extension Short-Beam Shear Strength (Ksi) Test Results

#### 4.1.1.2.1 Nonautoclave Process Cycle Development

Realistic manufacturing process parameter ranges or limits for various materials (tape and fabric) and material advancement were evaluated employing a nominal staging process. Limits in heatup rate, dwell temperature, dwell time, subsequent required consolidation pressure, and application time were independently assessed while maintaining the other variables at the considered nominal. Subsequent to subjecting 6- by 6-inch  $[0]_{5T}$  oriented AS4/976 Gr/Ep panels to the selected staging conditions, all panels were identically cured using vacuum pressure only. Evaluations were based upon cross-sectional microscopic examination for porosity and five interlaminar shear specimen test replicates at RT and 270°F.

Resin rheology studies investigated the time-versus-temperature viscoelastic characteristics of the 976 tape, fabric, and resin film. Conclusions reached as a result of the studies were: The time-versus-temperature viscoelastic characteristics of the tape are somewhat higher than both the fabric and the resin film (see figure 11). It was also shown that variations in the staging dwell length permanently alters the viscosity properties of the resin system for subsequent processing (see figure 12).

Based on these initial viscoelastic studies a staging window was established and verified through process evaluation. The results of the nonautoclave cure process limits laminates, table XIII, indicate that a 20-minute dwell at 220°F produced a laminate with unacceptable mechanical and physical properties while a 180-minute dwell at 250°F produced a laminate acceptable based on shear strength but not acceptable based on staged laminate characteristics and cured laminate porosity.

A difficulty encountered during the testing of the nonautoclave staging limits was the excessive flow characteristics of the Fiberite 976 epoxy resin. In the 220° to 270° range, the resin had an extremely low viscosity for a very long time. The preferred staging dwell is in the range of 30 to 45 minutes as demonstrated for AS1/3501-5A and -6 and T300/934 and T300/5208 material systems compared with the 60 to 120 minutes associated with the 976 resin system. A shorter dwell time is especially critical when processing net-resin content material in a tooling system without edge dams such as the nonautoclave tooling. It was imperative to advance the resin to a viscosity where it would not flow excessively upon pressure application thus insuring proper fiber volume in the cured detail.

Based on the results of a number of tests conducted to determine the optimum cure processing parameters, the nonautoclave staging dwell limits when processing graphite material impregnated with Fiberite 976 epoxy were established as  $250^{\circ} \pm 20^{\circ}\text{F}$  for  $45 \pm 15$  minutes utilizing a minimum vacuum of 27 inches of mercury (Hg). A typical cure cycle is shown in figure 13. These staging dwell limits consistently produced laminates which meet or exceed the laminate quality of standard autoclave processed parts in terms of handling, thickness, porosity, and strength.



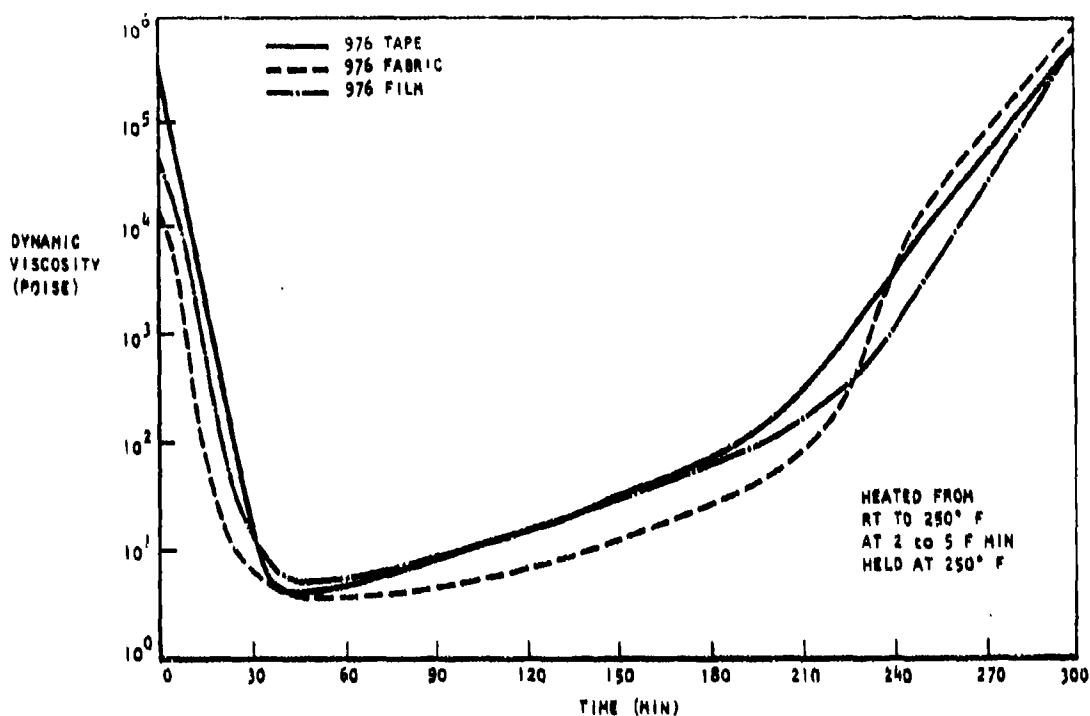


Figure 11. Comparison of Viscoelastic Staging Properties for Tape/Fabric/Resin Film

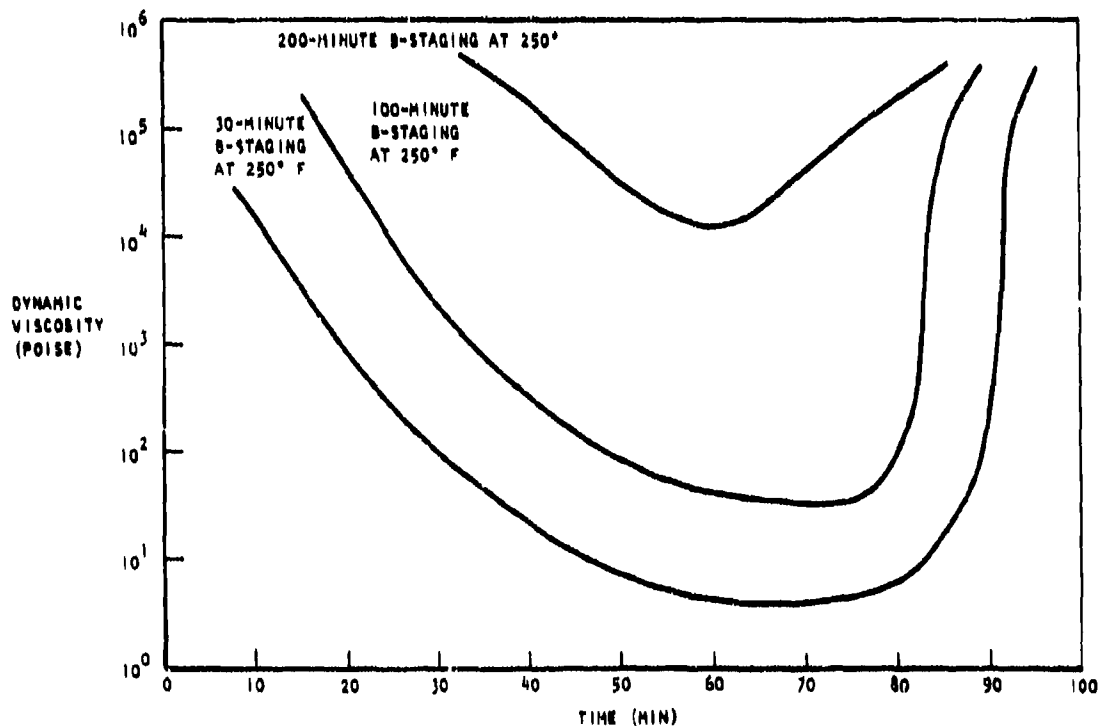


Figure 12. Viscoelastic Properties During Cure of B-Staged Laminates

TABLE XIII

NONAUTOCLAVE CURE PROCESS LIMITS TEST RESULT  
Fiberite Fy-E 1379 F, Lot No. C1-303, Roll 3

Trial Description	STAGED LAMINATES			CURED LAMINATES	
	Handling Charact	Avg Thickness	Porosity Charact	Avg Thickness	Avg Shear Strength
Temp/Dwell/Vacuum					RT/270°F
NOM/NOM/NOM	Acceptable	0.0811	None	0.0830	15.5/8.7
220/NOM/NOM	Acceptable	0.0792	None	0.0798	15.7/7.8
230/NOM/NOM	Acceptable	0.0785	None	0.0798	16.3/8.5
240/NOM/NOM	Acceptable	0.0756	None	0.0768	15.7/8.2
260/NOM/NOM	Acceptable	0.0795	None	0.0799	15.2/8.5
270/NOM/NOM	Acceptable	0.0791	None	0.0801	15.6/8.4
280/NOM/NOM	Unacceptable	0.0783	None	0.0830	16.4/9.0
NOM/NOM/15"	Unacceptable	0.0847	Unacceptable	0.0848	7.7/5.3
NOM/NOM/20"	Acceptable	0.0805	Unacceptable	0.0812	8.4/6.1
NOM/NOM/25"	Acceptable	0.0782	Marginal	0.0788	10.6/7.7
NOM/NOM/26"	Acceptable	0.0781	Acceptable	0.0792	11.3/7.4
NOM/NOM/27"	Acceptable	0.0071	None	0.0772	15.6/8.5
NOM/10+15/NOM	Marginal	0.0849	Marginal	0.0767	15.6/8.4
NOM/15+15/NOM	Marginal	0.0805	Marginal	0.0789	15.5/8.2
NOM/20+15/NOM	Acceptable	0.0813	None	0.0814	15.9/8.2
NOM/30+0/NOM					
NOM/120+15/NOM					
NOM/150+15/NOM					
220/20+15/NOM					
270/20+15/NOM					

NOM: - 20°F/min heat rate  
 - 250°F  
 - 30 ± 15 min  
 - 30 inch vacuum

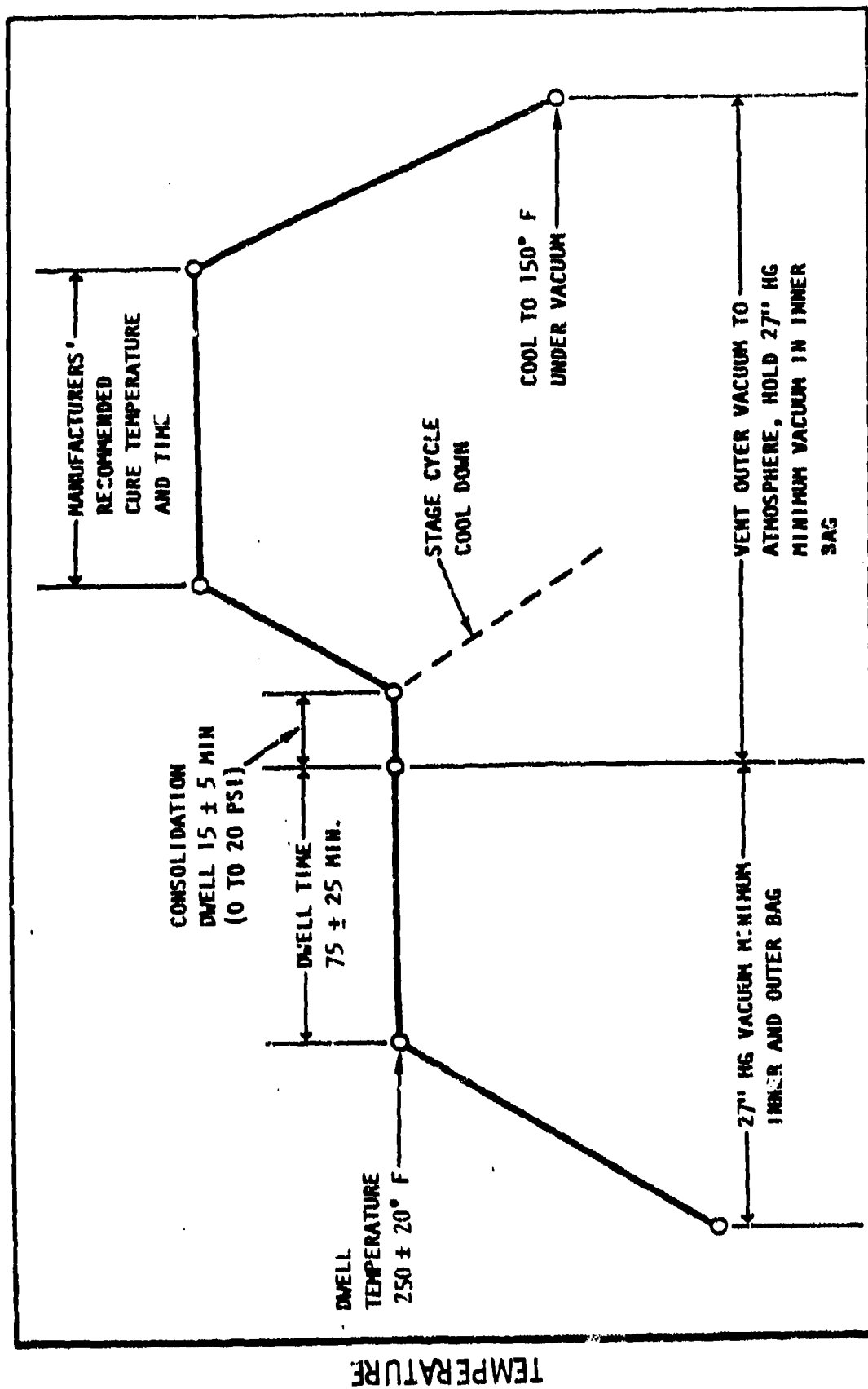


Figure 13. Monoclave Cure Cycle - ASA/976 Net Resin

## 6.1.2 TASK 2 - FABRICATION OF VERIFICATION ELEMENTS

During Task 1 it was established that the nonautoclave process is capable of producing Gr/Ep laminates of acceptable physical and mechanical properties. A basic cure cycle and cure cycle limits were established for the AS4/976 net resin Gr/Ep material. During this task the objective was to verify that the nonautoclave process was capable of producing structural hardware representative of the elements of a critical aircraft structure.

As a starting point elements of the main demonstration component, the B-1 vertical stabilizer, were selected. Several reasons for this existed: prior available data produced during the B-1 composite vertical stabilizer program and the generic nature of these elements to represent typical aircraft structure.

The composite elements selected for nonautoclave cure verification (figures 14 and 15) consisted of two types: small 10- by 10-inch flat-web and sine-wave-web I-beams. The smaller beam elements were sufficiently complex to fully interrogate baseline and candidate manufacturing methods and to identify any manufacturing methods modifications necessary to supplement fabrication of the larger element assemblies; thus, these beams represented logical elements for nonautoclave technology transition from flat laminates to larger element assemblies. In addition, an extensive autoclave processed data base existed for the "tee" specimens which were removed from the smaller beams thus amplifying cure process comparisons. All tee specimens and sine-wave pull specimens were fabricated and tested using in-house funding.

As shown in figure 16, integral box assemblies were selected because they are representative of structural and manufacturing critical regions of primary composite airfoil structure and because a substantial autoclave processed data base is available for process comparisons in terms of structural integrity, cost, quality, and weight. This extensive data base was established during the B-1 Vertical Structural Qualification and the Low-Cost Wing-Fuselage Manufacturing Technology Demonstration programs (AFFDL-TR-78-5 and AFML-TR-79-9110, respectively).

### 4.1.2.1 Integral Structure Beam Fabrication (Tee I-Beam Specimens)

The integral structure beam fabrication matrix is delineated in table XIV. This fabrication matrix plan was conducted to maximize the manufacturing method data available for program implementation and to demonstrate the generic aspects of the nonautoclave process in terms of material form, element construction, supporting materials, staging approaches, forming, and cure techniques.

Over 30 material and process and construction variables were evaluated. Prepreg tape and fabric material were included in the verification element plan to provide correlation with the autoclave-processed all-tape-material data base. Both flat-web and sine-wave construction, representative of both types of substructure, were evaluated. The use of structural adhesive in the load coupler/cover joint region appeared to have significant potential for increasing flatwise tensile strength and

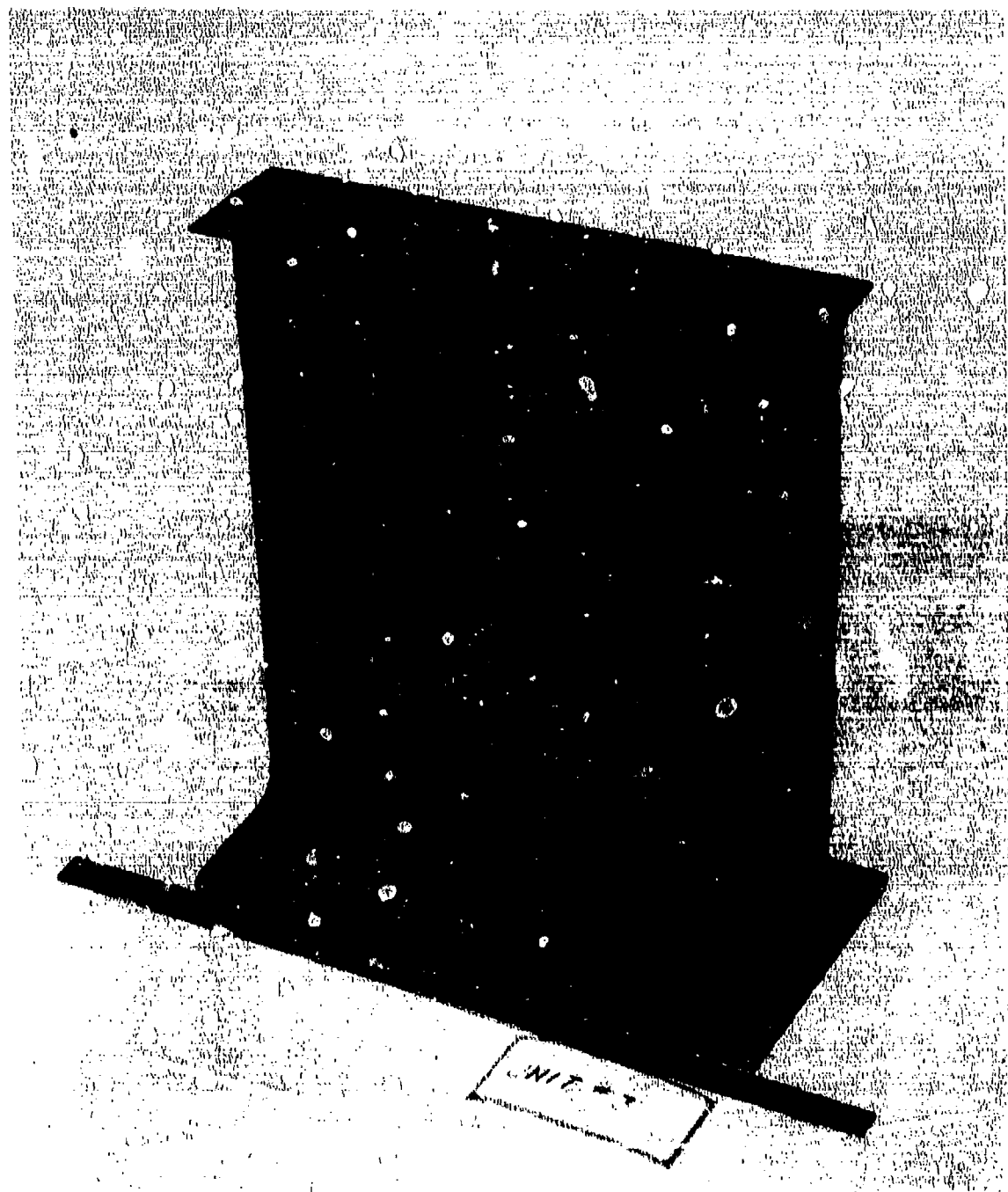


**Figure 14. Typical Integral Structure Beam Element Fabricated with NAAO Nonautoclave Cure Process (Vacuum Pressure Only).**

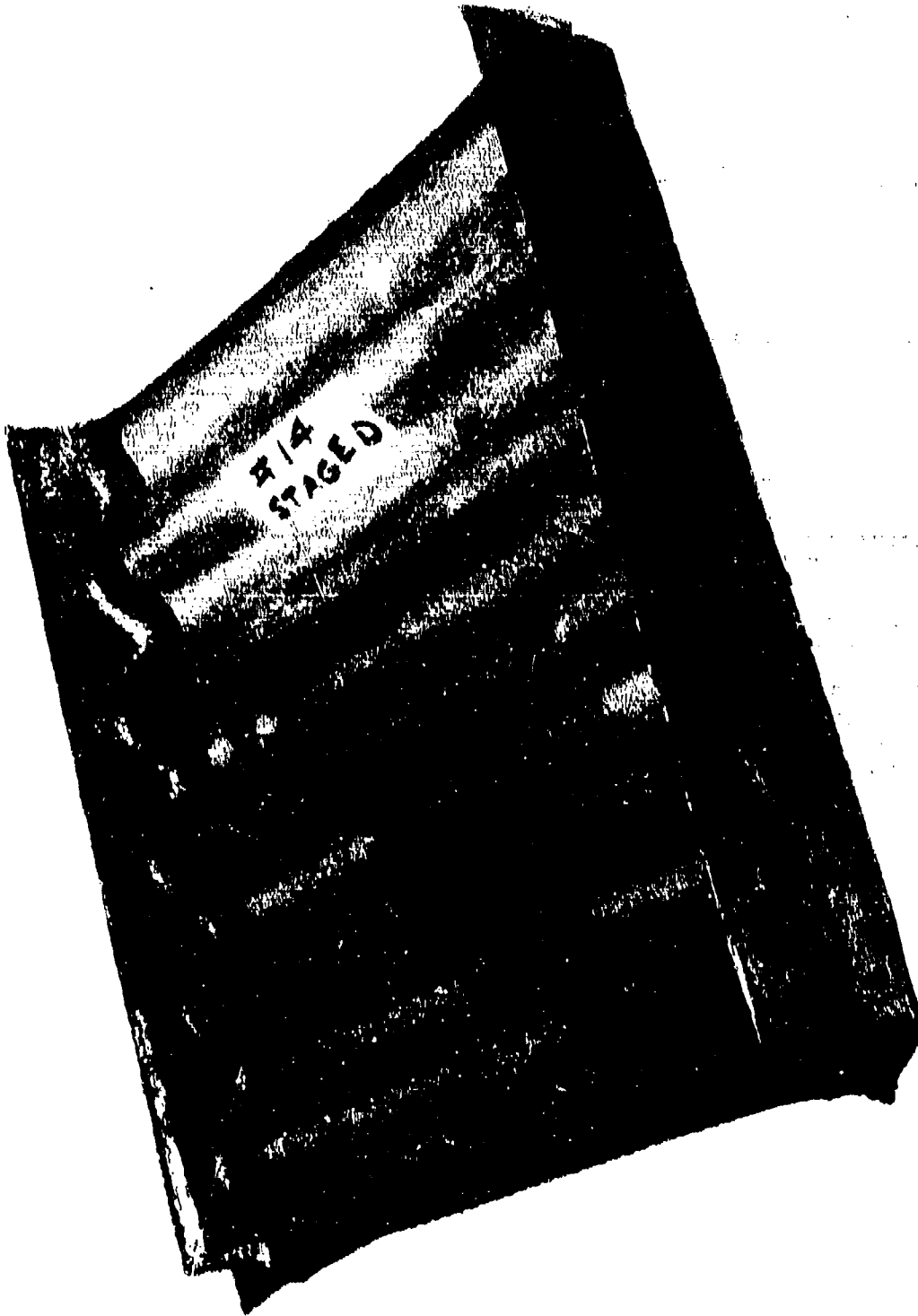


Figure 15. Sine Wave I-Beam Element - As Staged (Release Fabric Attached)

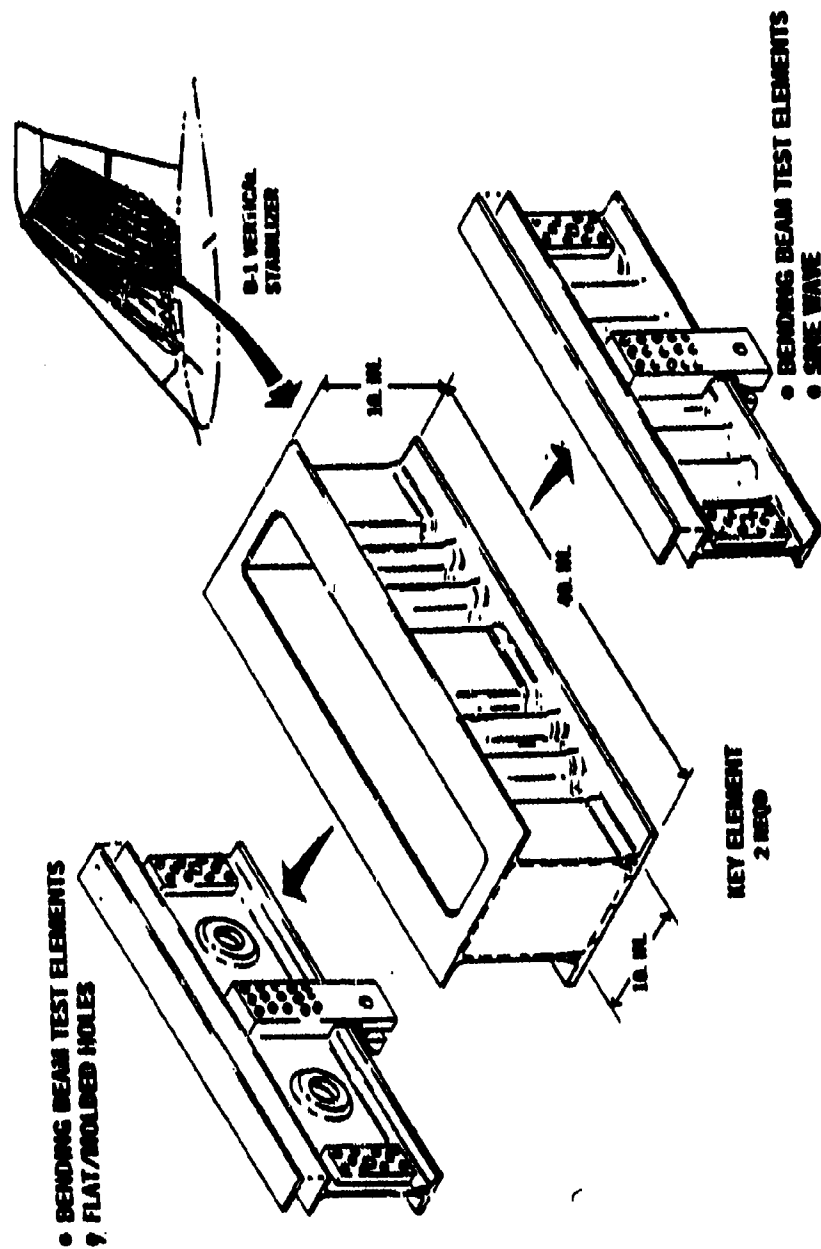


Figure 16. Phase I Element Assemblies

TABLE XIV  
INTEGRAL STRUCTURE BEAM FABRICATION MATRIX

Mfg Method Description	Material Form			Construction		Additional Materials		Staging Approach		Forming		Cure Approach				
	Gr/Ep Tape	Gr/Ep Fabric	Flat-Web Spar	Sine Wave Spar	Struct Adhesive Load	Coupler/Cover Joint	Struct Adhesive Cover Joint	Asy, Integrally Heated Wood Molds	Asy, Oven Heated Fiberglass Molds	Flat Form, Oven	Vacuum Pressure Heated Tooling	Hand-Pressure, Heat Gun	Conventional Bladder, Thin Rubber	Conventional Improved Seals	Conventional Self-Vented	Polyulfide Vacuum Bag
1	X				X		X	X					X			X
2	X												X			X
3	X												X			X
4	X												X			X
5	X												X			X
6	X												X			X
7	X												X			X
8	X												X			X
9	X	X	X	X	X	X	X	X	X	X	X		X	X	X	X
10	X	X	X	X	X	X	X	X	X	X	X		X	X	X	X
11	X	X	X	X	X	X	X	X	X	X	X		X	X	X	X
12	X	X	X	X	X	X	X	X	X	X	X		X	X	X	X
13	X	X	X	X	X	X	X	X	X	X	X		X	X	X	X



substantially reducing historical fitup problems. The staging operation (associated with the nonautoclave cure process) was successfully performed on flat laminates which were subsequently formed and cured with vacuum pressure only. The staging operation was also accomplished in an assembled state using integrally heated prototype wood or fiberglass tooling augmented by an oven. Hand and vacuum forming techniques were demonstrated on laminates staged in a flat condition as well as by hand pressure/heat gun forming. Simulation, using thin-rubber bagging material, of bladder molds (extensively used for final cure throughout the previous B-1 vertical stabilizer and the low-cost wing/fuselage programs) was established as the baseline curing approach. Cost savings and risk-reducing sprayable bagging materials were demonstrated as compatible with the NAAO nonautoclave cure process.

Beam evaluation included sectioning and polishing of selected regions (i.e., cover, web, flanges) and microscopic examination for porosity. Photomicrographs were taken of representative areas of all beams. Test data generated from the first three integral structure beams (table XV) fully validated the equivalence of the nonautoclave cure process and conventional 85 psi cure autoclave processing. Based upon these evaluations, 10 beams were converted to tee elements, similar to those presented in figure 17, and submitted for test. The load coupler provides a coupling between integral wing skins and substructure capable of transferring fuel pressure loads. In a conventional integral wing/substructure joint, (figure 17), fuel pressures normal to the wing skin will peel the substructure flange from the skin.

The load coupler transfers the fuel pressure loads by providing a structural component that can react these applied loads in flatwise tension and transfer them to the substructure web in shear.

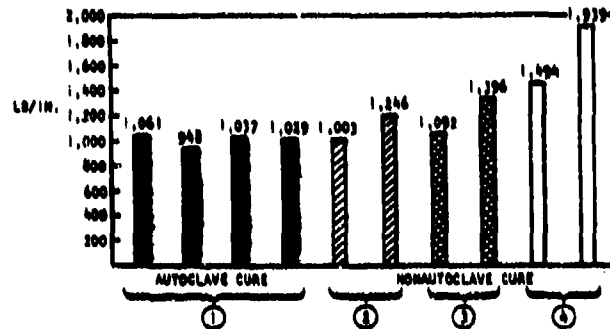
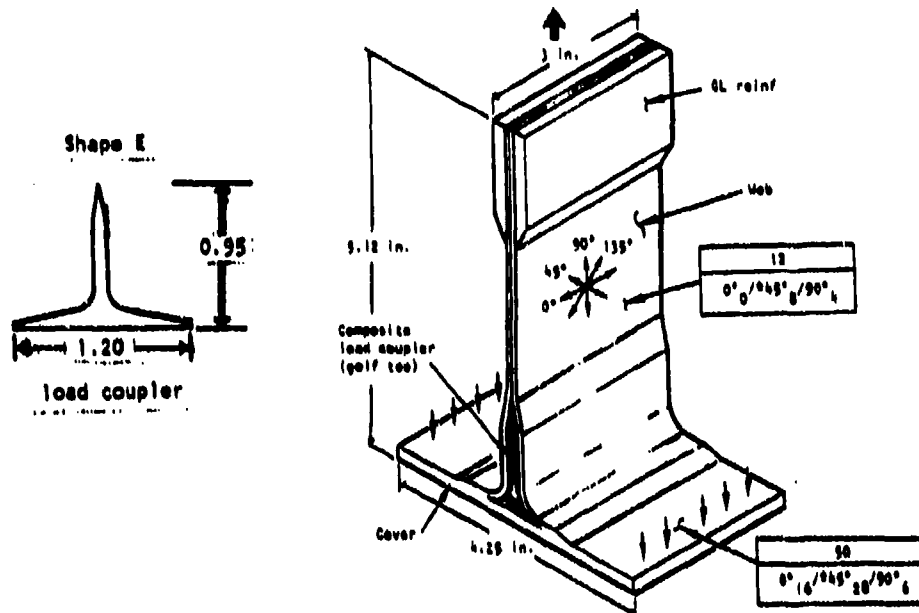
Examination of the flatwise tensile strength of tee elements fabricated by both the nonautoclave method and autoclave method indicated that they are structurally equivalent. The average autoclave value was 1018 lb/in. and the nonautoclave value was 1361 lb/in. It is evident that the inclusion of adhesive at the faying surface of the load coupler improved the strength approximately 30 percent. Consequently, this method of fabrication was used throughout the remainder of the program.

Two load coupler materials were also evaluated: 0- and 90-degree orientations made from both 3M Scotchply 1007 tape and Gr/Ep AS4/3501-5A tape. This investigation into the use of fiberglass as coupler material was based on material costs. Each specimen was preconditioned prior to test at 150°F, 90-percent relative humidity, to attain a 1.09-percent moisture content by weight in the web area. Small traveler coupons, 2.0- by 2.0-inch, of the web layup were placed in the moisture chamber along with the specimens to ascertain when the web had attained the 1.09-percent moisture level.

Failure modes for these coupons were typical for this kind of specimen. Interlaminar tension failure of the outer  $\pm 45$  ply of the cover laminate initiated the failure sequence. As the load increased, the total interface area between the load coupler and the cover failed.

TABLE XV  
SOUNDNESS VALIDATION TEST RESULTS

Element Designation	Bending Beam 1		
Element Laminate Properties	Cover	Flat Web	Sine Wave Web
Ply Thickness, mils (mm)	5.52 (1.40)	5.00 (1.27)	4.75 (1.21)
Fiber Content, v/o	60.1	67.3	66.9
Resin Content, v/o	33.5	27.3	27.1
Void Content, Calculated, v/o	0.2	-0.6	-0.5
Specific Gravity	1.59	1.63	1.63
Compression Stress, ksi (MPa)  RT  220°F (104°C)		69.6 (479.9)  49.9 (344.1)	
Element Weight Performance	Web Type	Calculated Weight (lb)	Actual Weight (lb)
Bending Beam 1 Sine wave	Flat 7.51	10.66 -0.62	10.80
For Calculated Weight: Ply Thickness = 0.0053 in. Density = 0.057 lb/in. <sup>3</sup>			



- NOTES:
1. FORMED ON RUBBER/FIBERGLASS TOOL - STARTED AND CURED IN AUTOClave
  2. FORMED AND STAGED ON THIN-LINE RUBBER HOLD/WOOD TOOL WITH ELECTRICAL HEATERS - CURED IN OVEN
  3. MATERIAL STAGED IN PLAT - FORMED OVER RUBBER/WOOD TOOL AND CURED IN OVEN
  4. FORMED AND STAGED ON THIN-LINE RUBBER HOLD/WOOD TOOL WITH ELECTRICAL HEATERS - CURED IN OVEN; SPECIMEN HAS ADHESIVE ON ALL SIDES OF LOAD COUPLER

Figure 17. T-Specimen Comparison - Autoclave Cure Versus Nonautoclave Cure Test (RT/Dry)

Average ultimate flatwise tension strength for the fiberglass/epoxy load couplers was 1017 lb/in. for the room temperature wet (RTW) specimens and 1046.7 lb/in. for the elevated temperature wet (ETW) tests. The Gr/Ep load couplers provided a 25-percent increase in ETW ultimate strength to 1,229 lb/in. Figure 18 graphically illustrates these test data. Included in the figure is the 800-lb/in. load requirement which is typically used as a minimum design criterion for structure subjected to full pressure loads.

Both the fiberglass and Gr/Ep load couplers provided adequate static strength to meet the 800-lb/in. design criterion (figure 18). While both load coupler materials provide adequate strength, the fiberglass material exhibited bulk problems during processing which caused some wrinkling of the test component. The problem is attributed to thermal expansion between the fiberglass and the Gr/Ep and/or the fact that the fiberglass was fabric. The conclusion reached was that the fiberglass caused processing problems, and the Gr/Ep had improved strength; therefore, fiberglass load couplers, while structurally sound, are not preferred over those of Gr/Ep.

A review of the data just described coupled with failure mode analysis yields the following conclusions:

1. The nonautoclave cure process using vacuum pressure only for cure produces typical integral structural sections equivalent to a slightly better than identical sections manufactured in an autoclave using 85 psi positive pressure.
2. The nonautoclave staging process is sufficiently flexible and generic to be used on composite components either as an assembled detail or in flat form capable of being postformed with a minimum application of heat.
3. The use of structural adhesive in the structurally and manufacturing critical regions, identified as the region adjacent to the load couplers and the lower flange to cover interface, substantially improves the tensile characteristics of integral structures.

It should be noted that all autoclave and nonautoclave cured specimens except the test elements containing the structural adhesive failed similarly in terms of region and mode. The failure mode of these elements was characterized by net tensile failure in load coupler and flat web, which is indicative that full exploitation of the integral design is being approached.

4. Compatibility of the FM-300 structural adhesive and the staging operation was demonstrated.
5. Use of fiberglass (Scotchply 1007) load couplers provide adequate strength to meet the anticipated design loads.

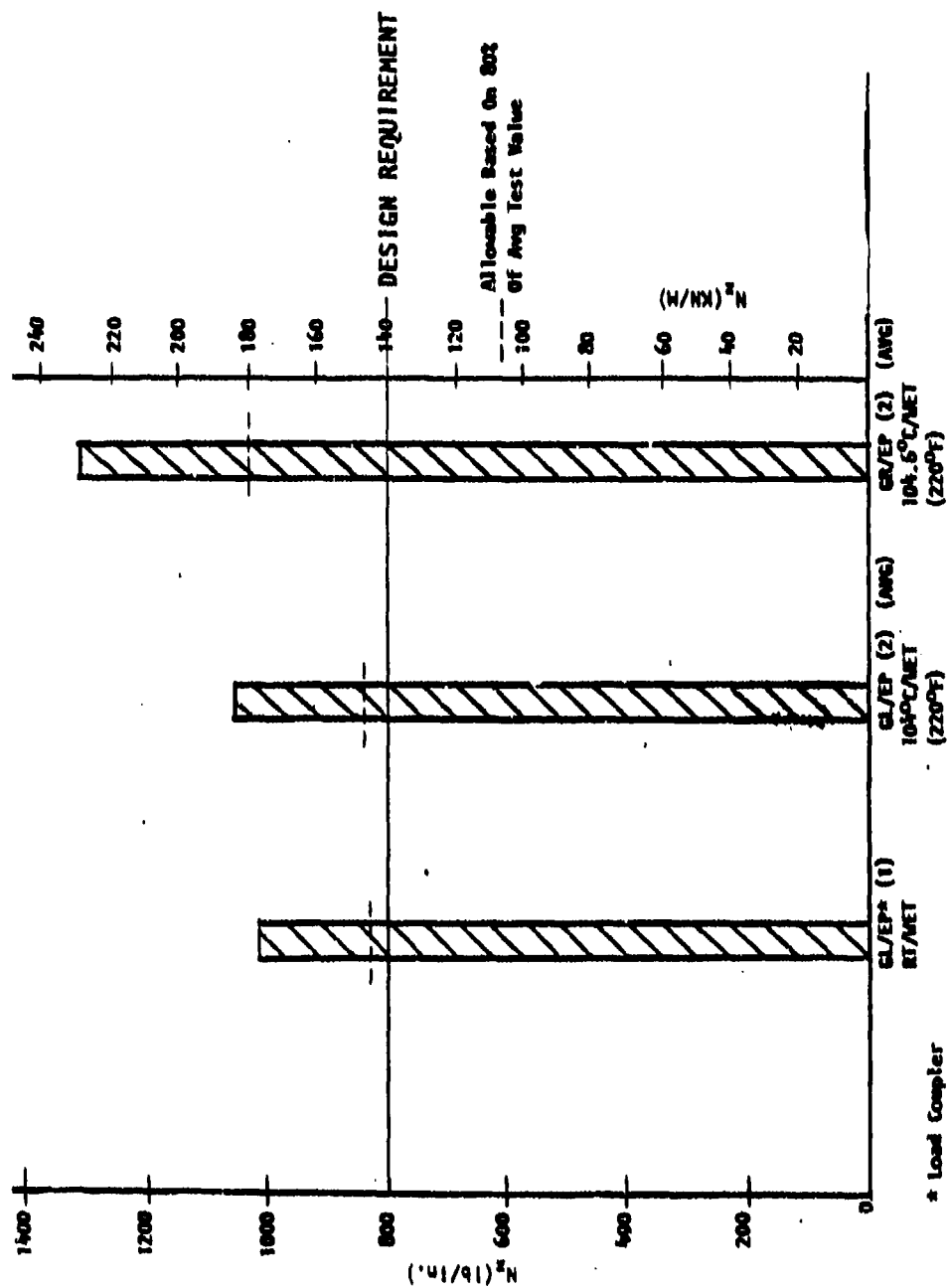


Figure 18. Comparison of Tee Specimen Flatwise Tension Tests for Different Load Couplers

#### 4.1.2.2 Integral Structure Box Assembly Fabrication

The elements manufactured during this task were integral structure box assemblies simulating a flat-web and a sine wave spar joined together by a lower cover and close out ribs (figure 19). These elements represented critical portions of airfoil structure and were selected to exercise the implementation and scaleup of the nonautoclave cure process. Materials, tooling, and the nonautoclave cure processes were representative of the general baseline full-scale manufacturing concept.

The selected element validated the nonautoclave manufacturing method and verified the reproducibility capability of the proposed nonautoclave curing process. These elements, with varying gauges and structural shapes, combined with the integral structure design concept provided a variety of generic applications and manufacturing challenges and demonstrated the unique nonautoclave manufacturing approach. These challenges include the following:

1. A 64-ply laminate, representative of empennage/wing covers.
2. A medium-gauge 32-ply laminate flat-web with fuel holes representative of ribs, fuselage frames, and intercostals.
3. A light-gauge, 12-ply laminate formed to complex sine-wave shapes.
4. Graphite/epoxy material forms, including fabric (ribs and spars, webs and caps) and tape (covers).

The selection of this element also allowed a direct comparison in cost and structural integrity with identical parts fabricated during the Low-Cost Composite Wing/Fuselage program (F33615-77-C-5278). The results were also compared with data from the Low-Cost Composite Vertical Stabilizer program where a large number of sine-wave and flat-web spars were fabricated utilizing state-of-the-art autoclave curing procedures.

A total of three box beams were fabricated with two (under the contracted effort) utilizing the selected AS4/976 Gr/Ep material system and (one under in-house effort) using AS4/3501-5A Gr/Ep.

After fabrication of the box beam and evaluation of the producibility aspects (such as inspection of the bond lines and C-scan of the laminates), the box was machined to yield two bending beams which were structurally tested to evaluate the structural integrity of both the integral structure concept and the nonautoclave processing. Detail cost tracking of the fabrication hours was also conducted to establish the cost impact of the nonautoclave process.

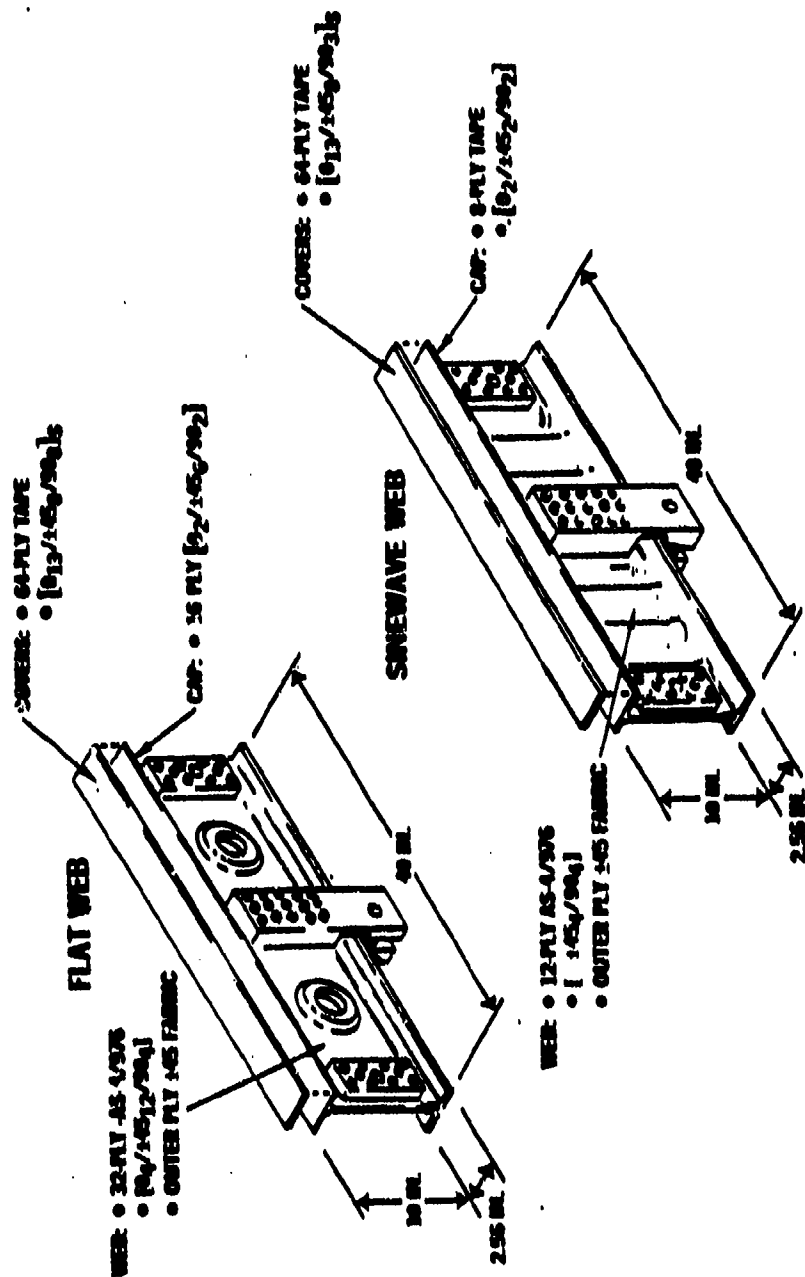


Figure 19. 40-Inch Verification Bending Beams

#### 4.1.2.2.1 Element Design

The design of the box beam and subsequent bending beam elements were identical to those fabricated under the wing fuselage critical component program. The two spars and ribs were cocured to the cover with a ply of FM 300 adhesive at the faying surfaces. The cover was a 64-ply quasi-isotropic laminate fabricated from 5 mil tape. AS4/976 net resin material was used for all details except the load couplers which were CE9000 fiberglass. Figure 19 is a schematic diagram of the sine-wave and flatweb bending beams. The 10-inch high sine-wave spar was a 12-ply web ( $\pm 45_4/90_4$ ) with the inner plies tape and one ply of fabric as the outer ply. The web increased in thickness at the transition to the 2.5-inch wide caps. The cap was an 8-ply ( $0_2/\pm 45_2/90_2$ ) all-tape laminate. After sectioning of the box beam a portion of the cover was utilized at the mechanically fastened cover. 0.25-inch diameter titanium H1-loks fasteners attached the cover to the cap. The flat web beam, with a web thickness of 32 plies ( $0_4/\pm 45_{12}/90_4$ ), had an inner section of tape with one outer ply of fabric. Two 4-inch diameter fuel holes were included in the web with a 6-ply donut buildup around the hole. The caps were 16-ply tape ( $0_2/\pm 45_6/90_2$ ) and, again, the 64-ply cover was mechanically attached to the cap using H1-loks. Steel-loading hardware was added to the beams for testing purposes.

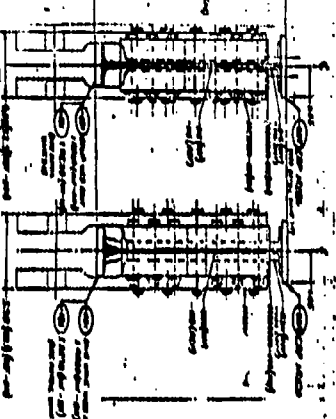
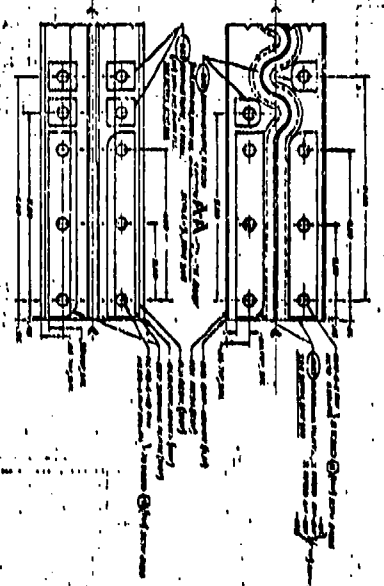
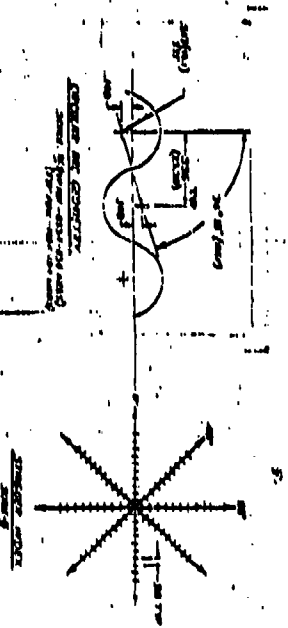
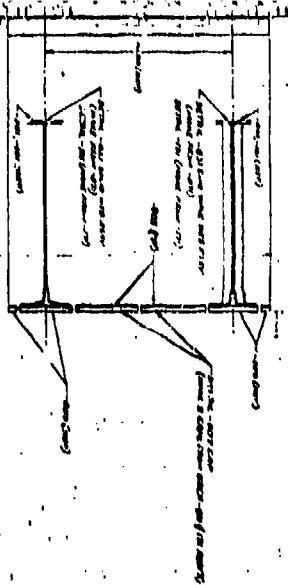
The predicted design ultimate shear flow in the webs was 1100 lb/in. for sine wave and 3250 lb/in. for the flat web. These values include knock-down factors for environmental conditioning to 1-percent moisture in the web and testing at 220°F. During test, the integrally bonded side of the beam was in tension. Figure 20 is the detailed drawing of the elements.

#### 4.1.2.2.2 Element Fabrication

Fabrication of the three 40-inch long box beams (two under contract and one funded in-house) followed directly from the 10-inch I-beam work, described previously. Three main areas developed the capability to fabricate the 40-inch beams: (1) a production plan was prepared (2) tools were designed and fabricated, and (3) the actual parts were fabricated. Inspection of the parts is discussed in the Quality Assessment section.

A preliminary production plan was prepared to guide the fabrication of the element. The plan or flow chart, shown in figure 21 is described in the following sequence. (1) After detail design drawings are complete templates for fabricating the staging tools are produced which allow for the correct dimensional tolerances for tool thermal expansion, web configuration, and offset between tool halves. (2) Using the templates plaster tools are produced which are used as female master tools. Fiberglass hardbacks are then laid up over the plaster, creating a tooling surface which has dimensional configurations identical to the Gr/Ep part to be produced. (3) Next, a rubber bag is sprayed over the fiberglass tool (figure 17). (4) After curing the rubber the Gr/Ep is



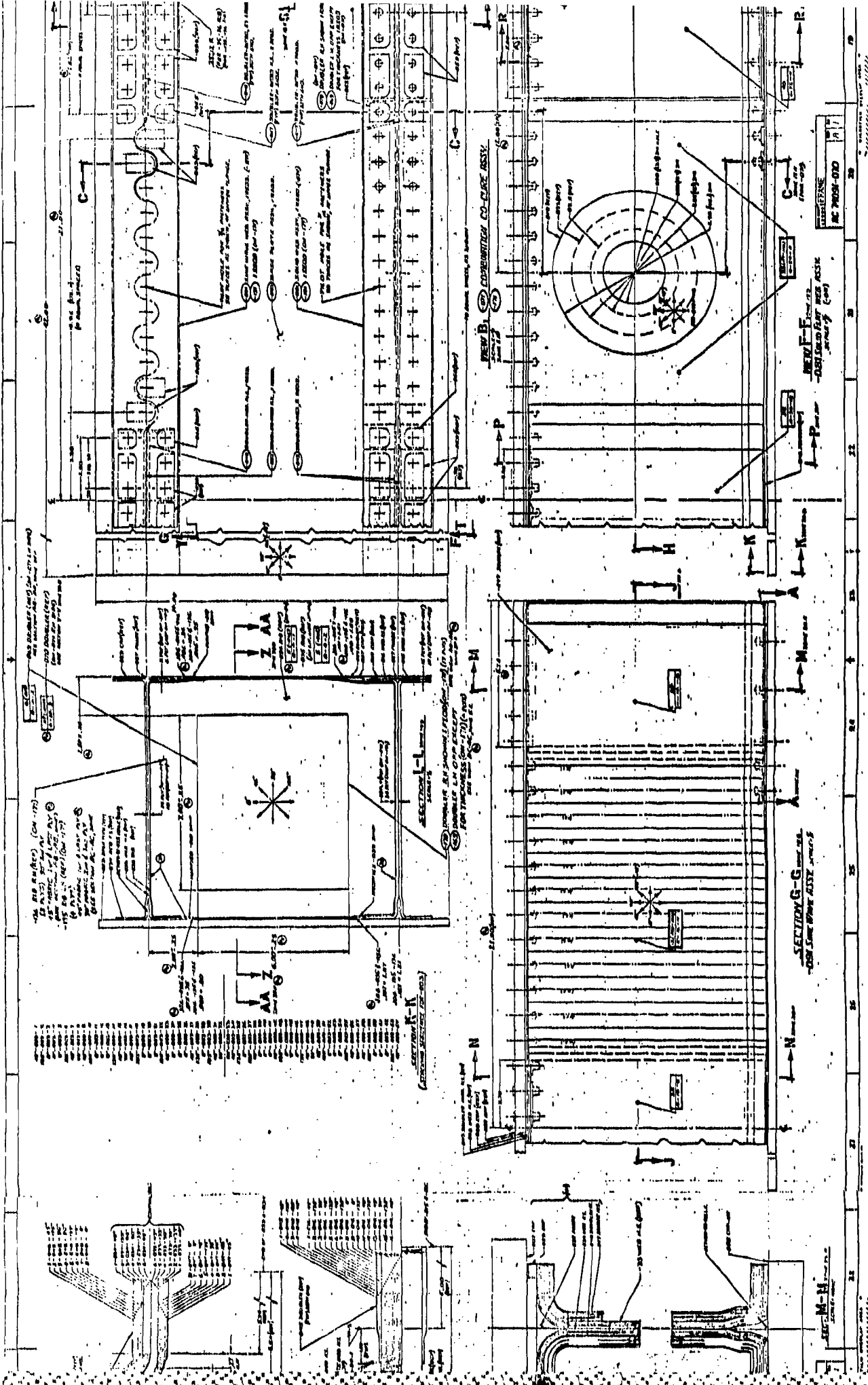


1. The component is made of 1/2 inch thick plate steel. The dimensions are given in inches. The component is shown in four views: top, front, side, and bottom. The top view shows a rectangular shape with dimensions 1/2 inch by 1/4 inch. The front view shows a rectangular shape with dimensions 1/2 inch by 1/4 inch. The side view shows a rectangular shape with dimensions 1/2 inch by 1/4 inch. The bottom view shows a rectangular shape with dimensions 1/2 inch by 1/4 inch.

Item	Material	Quantity	Unit	Notes
1	1/2 inch thick plate steel	1	piece	Top view (Fig. 1)
2	1/4 inch thick plate steel	1	piece	Front view (Fig. 2)
3	1/8 inch thick plate steel	1	piece	Side view (Fig. 3)
4	1/2 inch thick plate steel	1	piece	Bottom view (Fig. 4)

Figure 20. 40-Inch Box Beam Detail Drawings





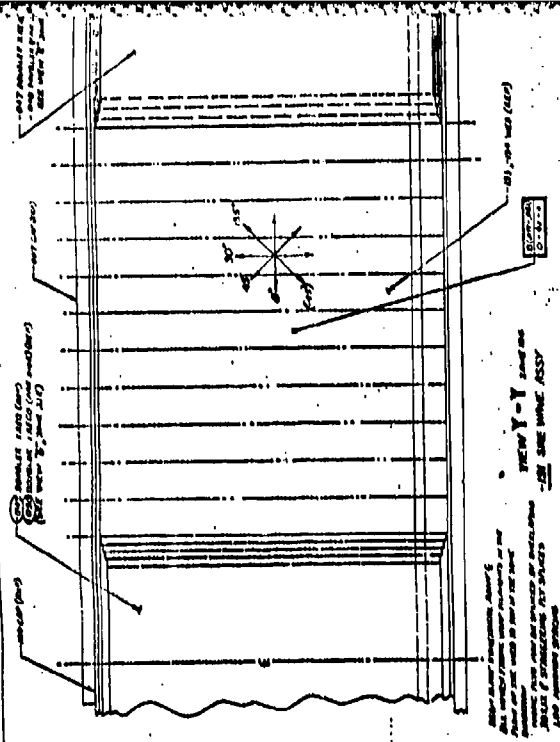
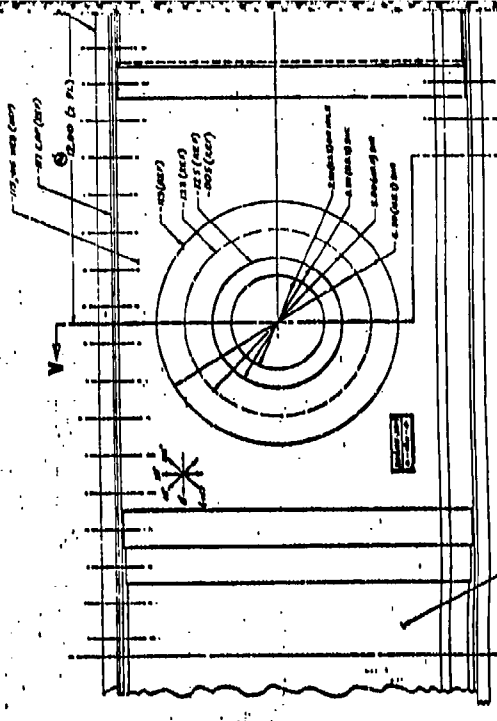
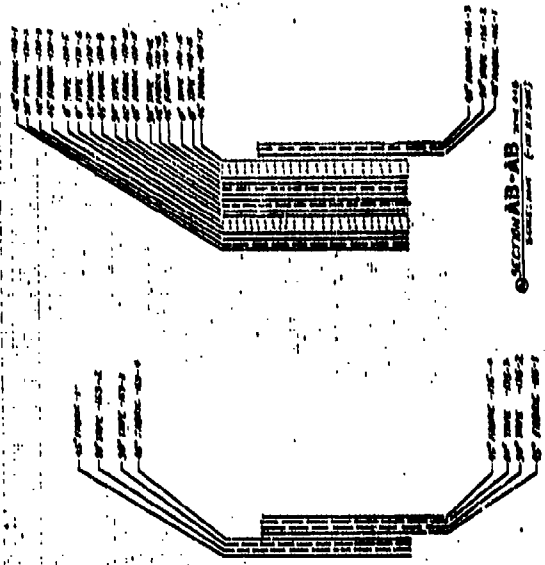
4 of 3



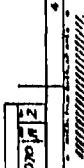
VIEW T-T  
-82 SOLID PLATE (1.475) WEG ASSY  
SCALE 1/4" = 1"

SECTION AB-AB  
SCALE 1/4" = 1"

SECTION AC-AC  
SCALE 1/4" = 1"



1



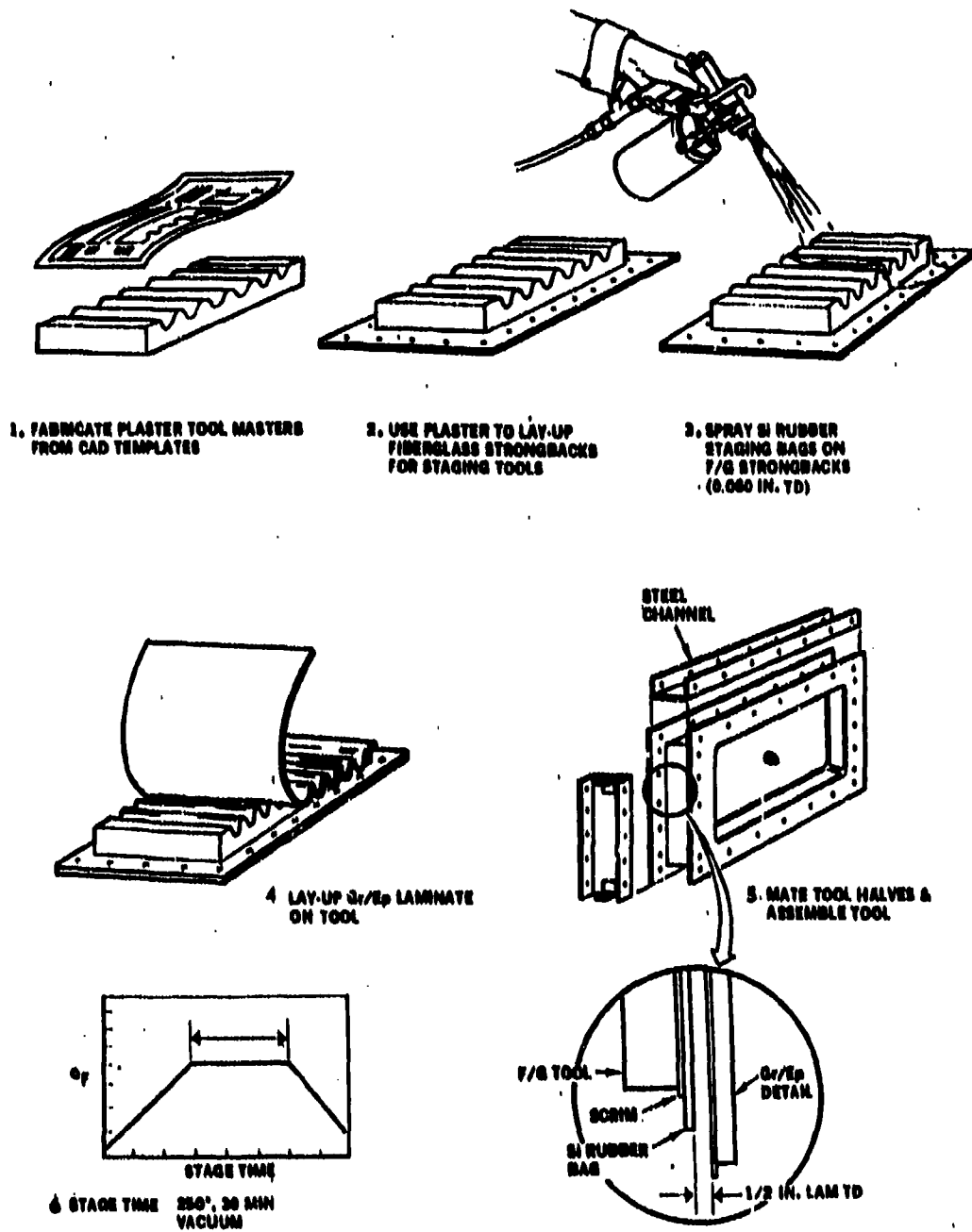


Figure 21. Nonautoclave Fabrication Sequence

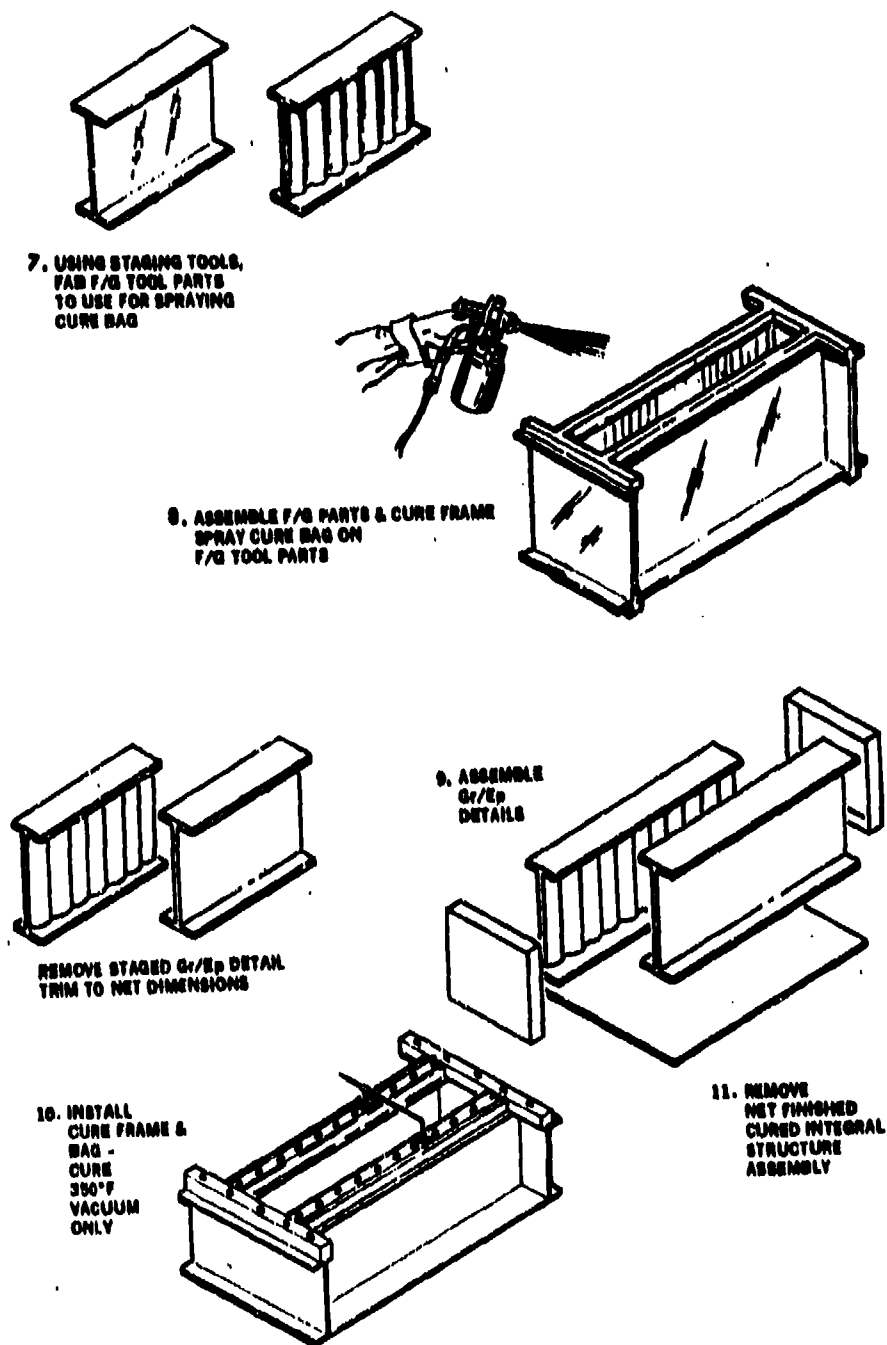


Figure 21. Nonautoclave Fabrication Sequence (Concl.)



laid up on each half of the tool (5) The halves are joined and the tool assembled. (6) The detail is staged using the prescribed cycle. After staging and inspection the details are trimmed to final dimensions and are ready to be assembled into the cocure tool. (7) Fiberglass mockups of the individual details are produced with the same staging tools to produce a rubber bag which is used to cocure the structures, (8) These mockups are assembled into the final cocured configuration and a silicone rubber is sprayed over the details. (9) Once the cocured silicone bag is cured the Gr/Ep details are assembled, (10) The cocure bag is placed around them. The cocure fixture comprises a manifold which provides the vacuum path, maintains vacuum during cure and to maintain the correct chordal height of the spars during cure. After curing the Gr/Ep (using the prescribed cycle) the completed integral cocure structure is removed for final trim to remove any excess resin flash for final inspection. This basic approach was used throughout the program. Improvements in silicone rubber bagging material and cocure tool design were incorporated during Phases II and III. More complete descriptions of the tooling and manufacturing procedures are presented in the following paragraphs.

**Tool Design.** An understanding of the nonautoclave process begins with an understanding of what occurs during the curing process. As previously discussed the initial nonautoclave development work (which proved that Gr/Ep laminates could be fabricated with the aid of only vacuum pressure) was conducted in a bell jar. This bell jar provides a vacuum atmosphere which allows the Gr/Ep laminate to cure unrestrained by bag pressure. When fabricating structural details this environment must be recreated. For flat laminates the tooling is relatively simple (as shown in figure 23). Basically, the tooling consists of a layup tool and a chamber over the laminate. The vacuum is drawn between the bag and Gr/Ep laminate and the bag and the chamber. Breather material is placed between the laminate and the bag to prevent sealoff. Since net resin material was used, no bleeder was required. Tedlar, Teflon or some similar release agent is placed on the layup tool to prevent the Gr/Ep from adhering to the tool. Another layup can be placed between the Gr/Ep and the breather. Both 181 fiberglass cloth and Air Tech 1010 airwave breather have been successfully used.

The same concept can be used to fabricate C-channels. It is important, however, that the edges of the laminate are not sealed off thus preventing the volatiles from escaping from the laminate during cure. As demonstrated in the early bell jar experiments and also by General Dynamics during the Processing Science programs, 90 to 100 percent of the volatile migration occurs along the fiber direction in a planar fashion, not normal to the lamina.

To fabricate I-beams the basic principles that were developed for flat laminates must be followed: (1) sufficient room for the laminate to expand during cure and (2) keeping the edges of the laminate free of any obstructions which would sealoff the ends. Figure 24 is a cross section of a typical I-beam tool used throughout this program. As can be seen, the basic concept remains; however, some additional design considerations are required. A more controlled gap or space between the

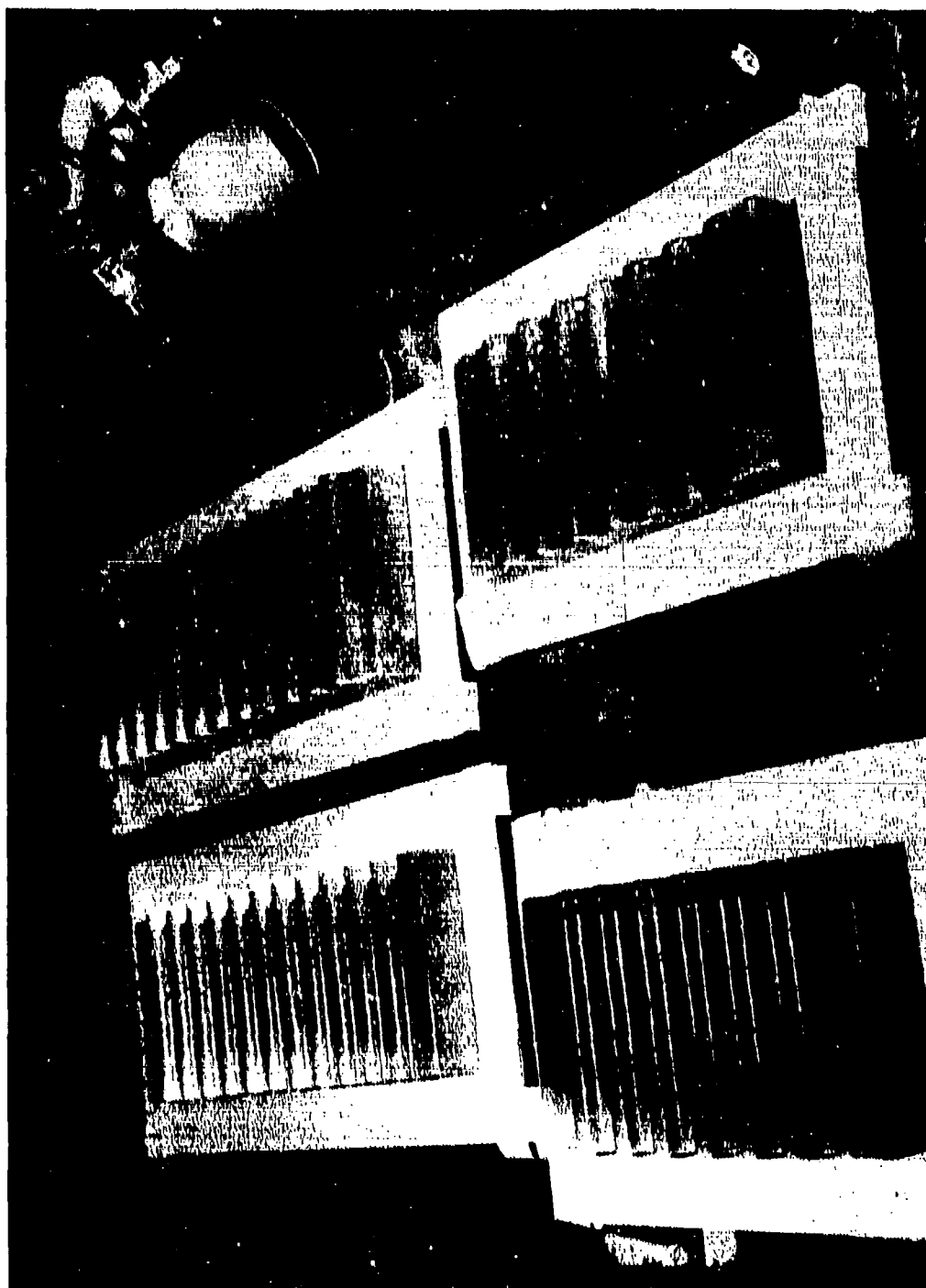


**Figure 22. Spraying Silicone Rubber Staging Bags**

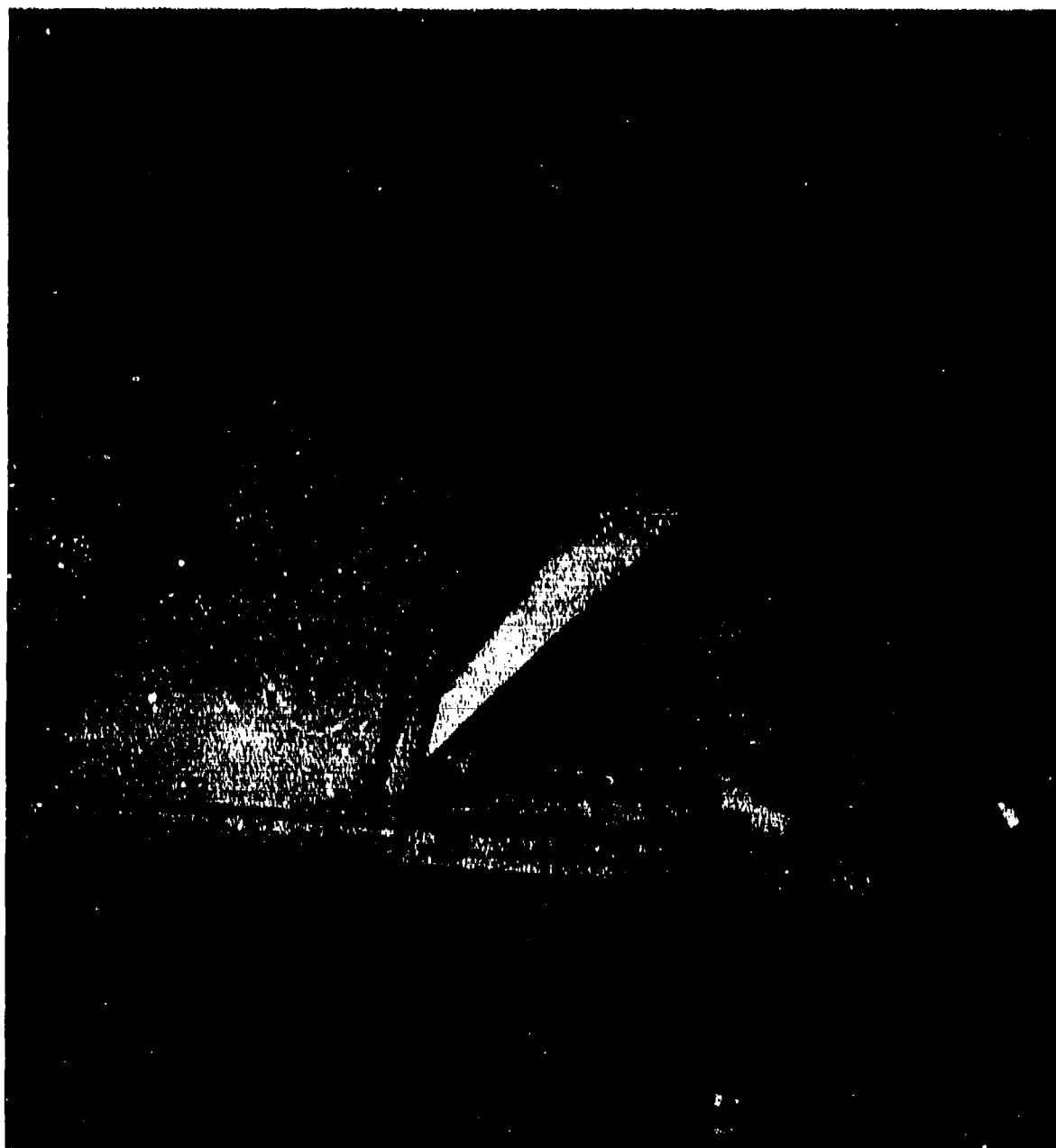


Figure 23. Flat Nonautoclave Staging Tools

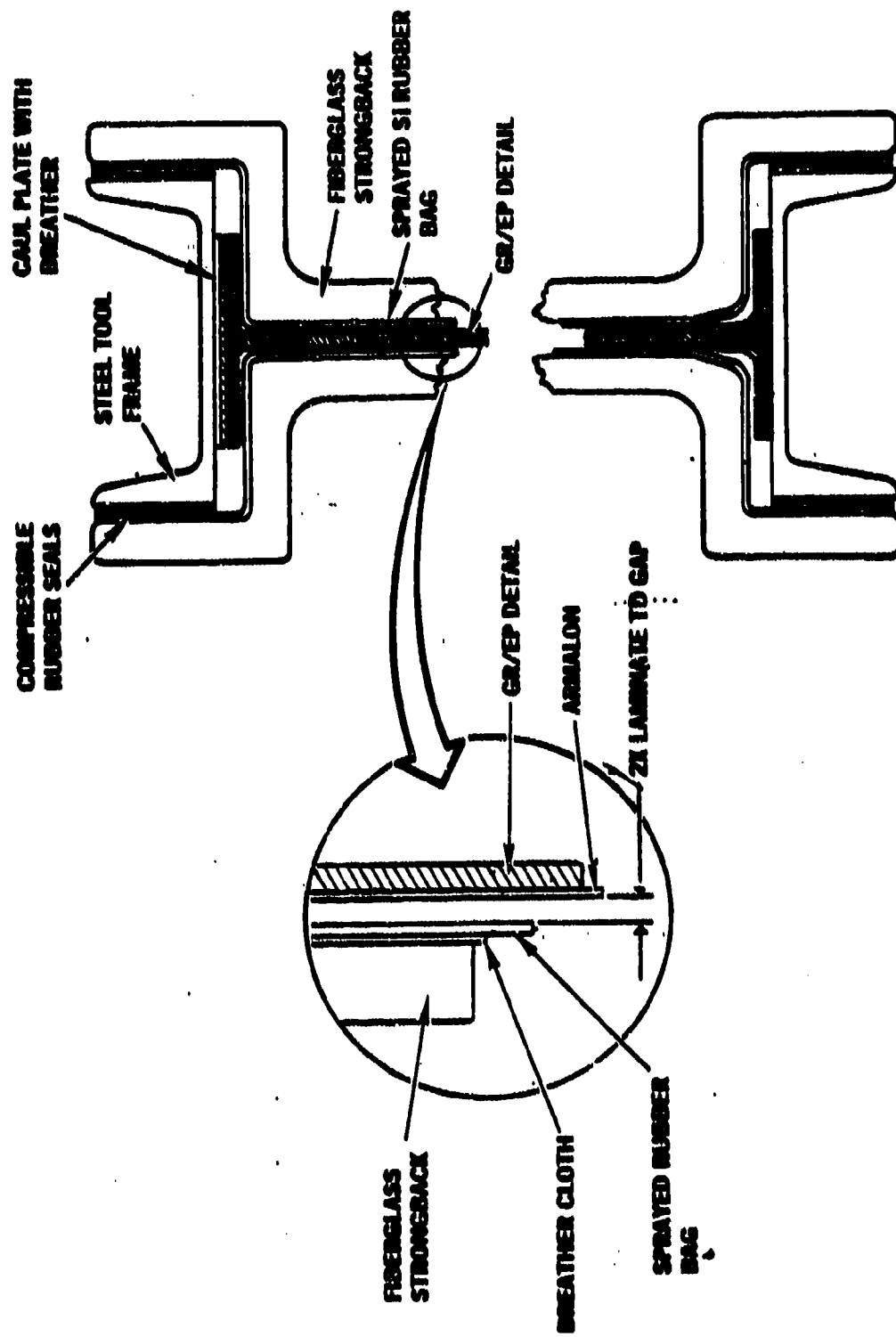


Figure 24. Nonautoclave I-Beam Staging Tool

Gr/Ep and the outer chamber or hard tool is required. While the minimum tolerances are understood, (i.e., the tool cannot be in intimate contact with the part) the maximum gap was initially set at 0.2 inch. Through a series of tooling development studies discussed in paragraph 4.1.3.2 a general rule-of-thumb gap requirement of one-half the Gr/Ep laminate thickness between the inner surface of the bag and the Gr/Ep must be maintained. The steel channel and rubber seals control this gap. The steel channels are visible in figures 29 and 30. Again, it is evident in figure 24 that there is sufficient area around the edges of the laminate to prevent sealing of the edges of the laminate.

One ply of 181 fiberglass cloth was bonded to the inner surface of the tool to prevent vacuum sealoff, and a ply of armalon was placed on the Gr/Ep detail to prevent it from adhering to the bag. Figures 26 through 30 show one-half sine-wave and flat web I-beam tools with the cured silicone rubber bags in place. The 181 breather cloth is visible on the surface of the tool in figure 26. The rubber bags are checked for holes using a static discharge tool as shown in figure 28.

Figure 25 is an exploded view of a typical tool. Note the location of the vacuum ports: one on each side of the web and one on the top and bottom of the tool. Figure 31 is an assembled tool.

The sprayed silicone rubber bags used in the staging and cocure tools are discussed under the rubber evaluation section.

Design of the cocure tool is relatively simple. The basic requirements include a form fitting rubber bag which matches the final shape of the cocure structure and a frame to support the bag and provide control of the height of the structure. Figure 32 illustrates a typical cocure tool. For the 40-inch boxes produced in this Phase and the subcomponent and component fabricated in Phases II and III the basic concept is the same. Vacuum holes (0.0125-inch) are drilled in the 2-inch-square steel tube at two-inch centers to provide a uniform vacuum path.

The cure bags were sprayed and cured on precured fiberglass/epoxy details assembled in the final cure tooling (figure 33). The fiberglass/epoxy details were fabricated for use as tooling to support spraying of the cure bladder molds and to check the dimensional accuracy of the staging tools. Hexcel F115/1581 material, a 250°F curing fiberglass/epoxy system, was utilized in fabrication of the sine-wave web beam, flat web beam, and the end close out ribs. The selected fiberglass/epoxy enabled the details to be cured at 250°F in the staging tools, using vacuum pressure only to ensure physical parameter integrity. The final cure bladders are shown in figure 34. Subsequent to fabrication, the cure bag was inspected to ensure that it was leak free. Additionally, a thickness survey was performed to ensure adequate bladder thickness and cure bladder uniformity.

During preparation of cure bagging for the first specimen, sealing difficulties were encountered which necessitated modifications to

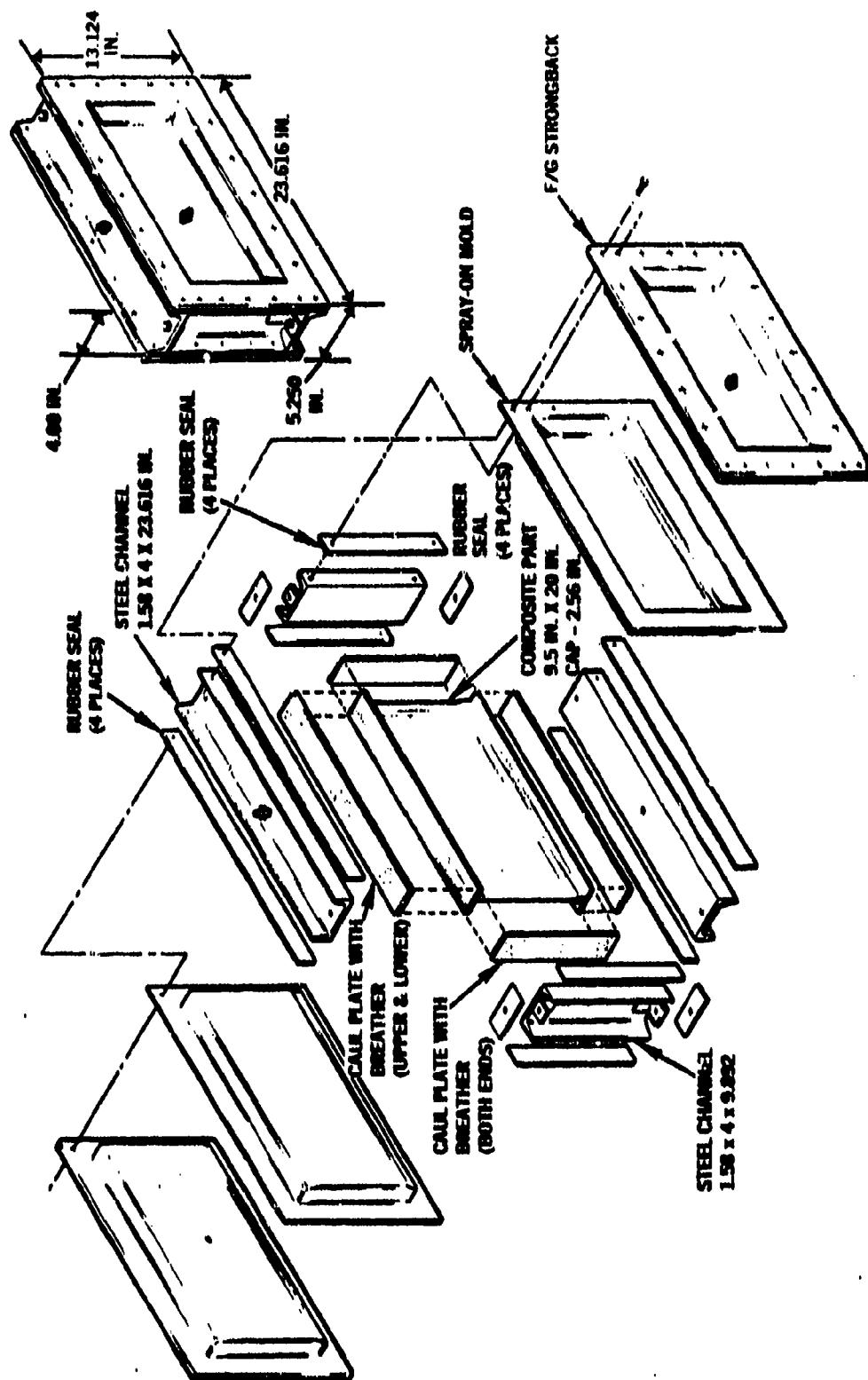


Figure 25. Typical I-Beam Monoclave Staging Tool (Exploded View)

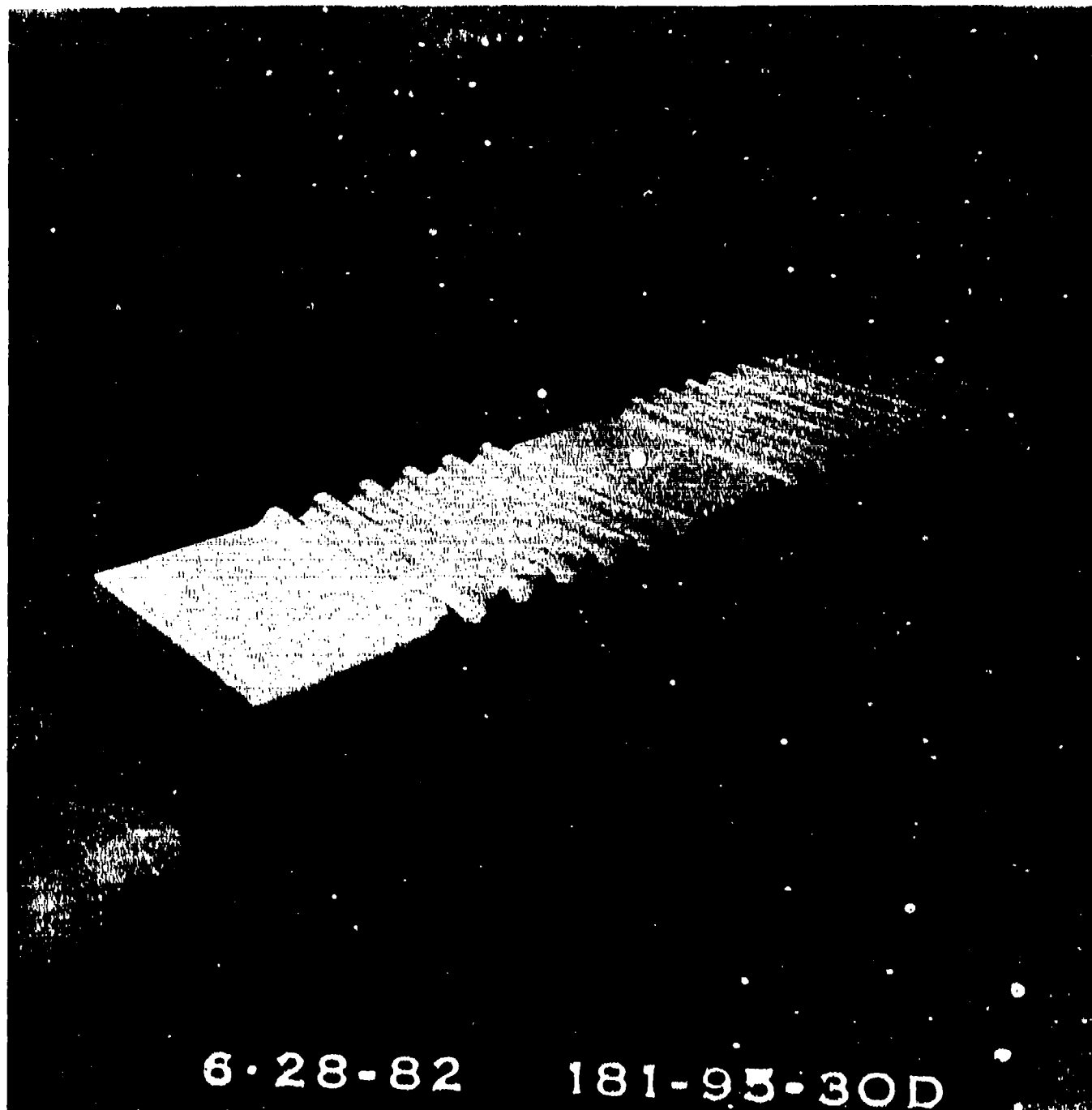


Figure 26. Sine Wave Web Bladder and Strongback Tooling



**Figure 27. Flat Web Bladder and Strongback Tooling**



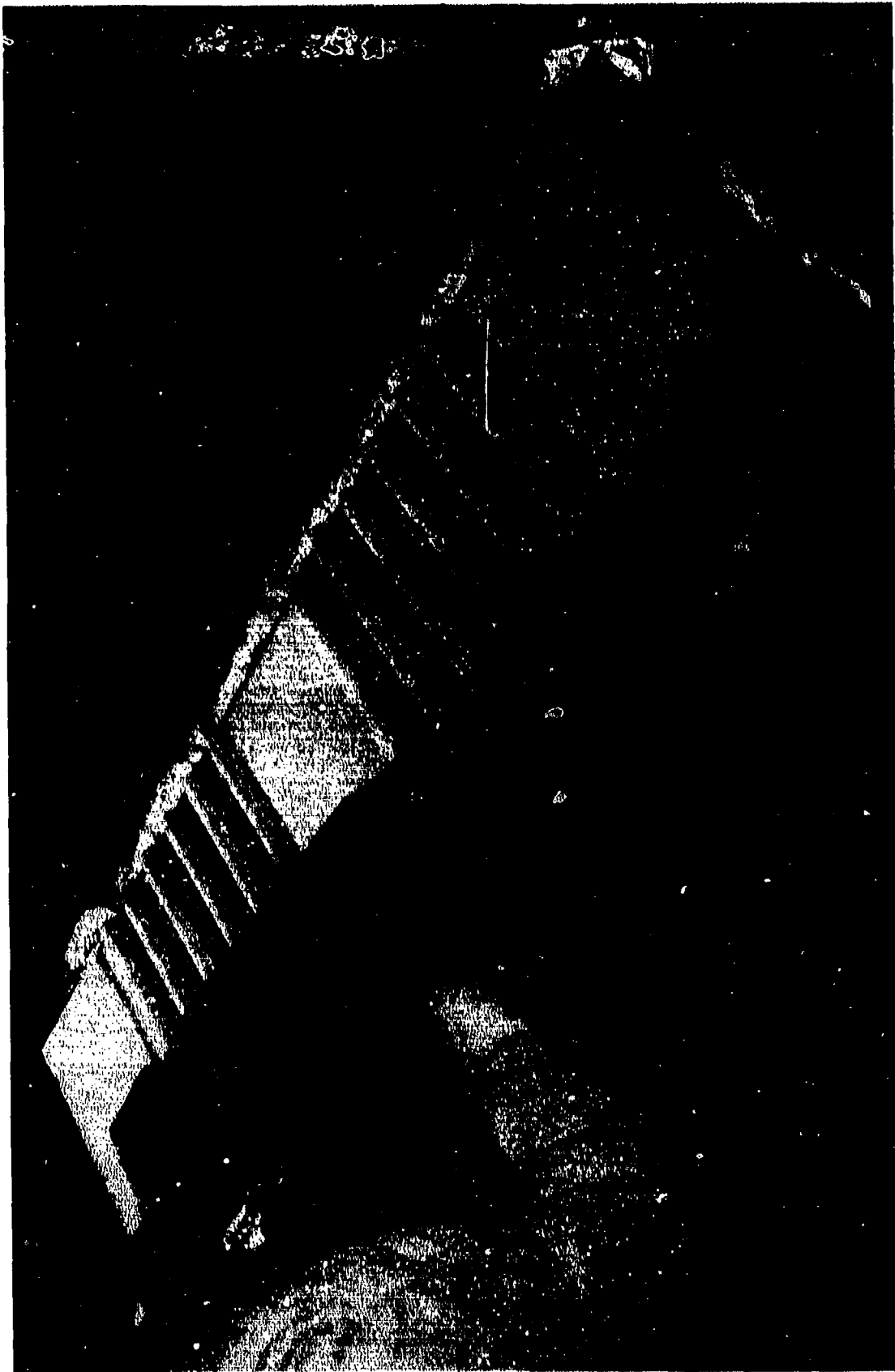


Figure 28. Electrostatic Leak Checking of a Bladder Bag

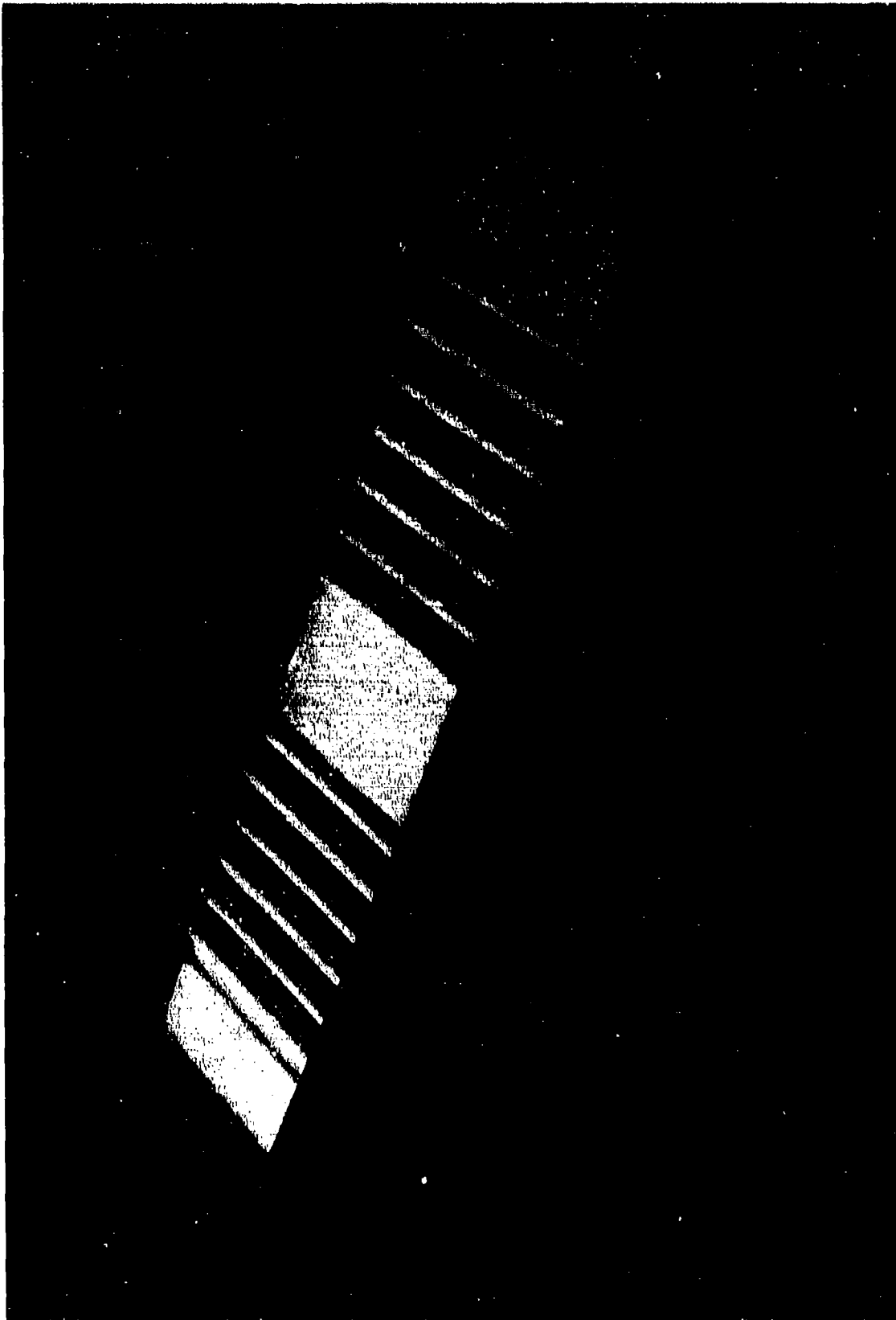
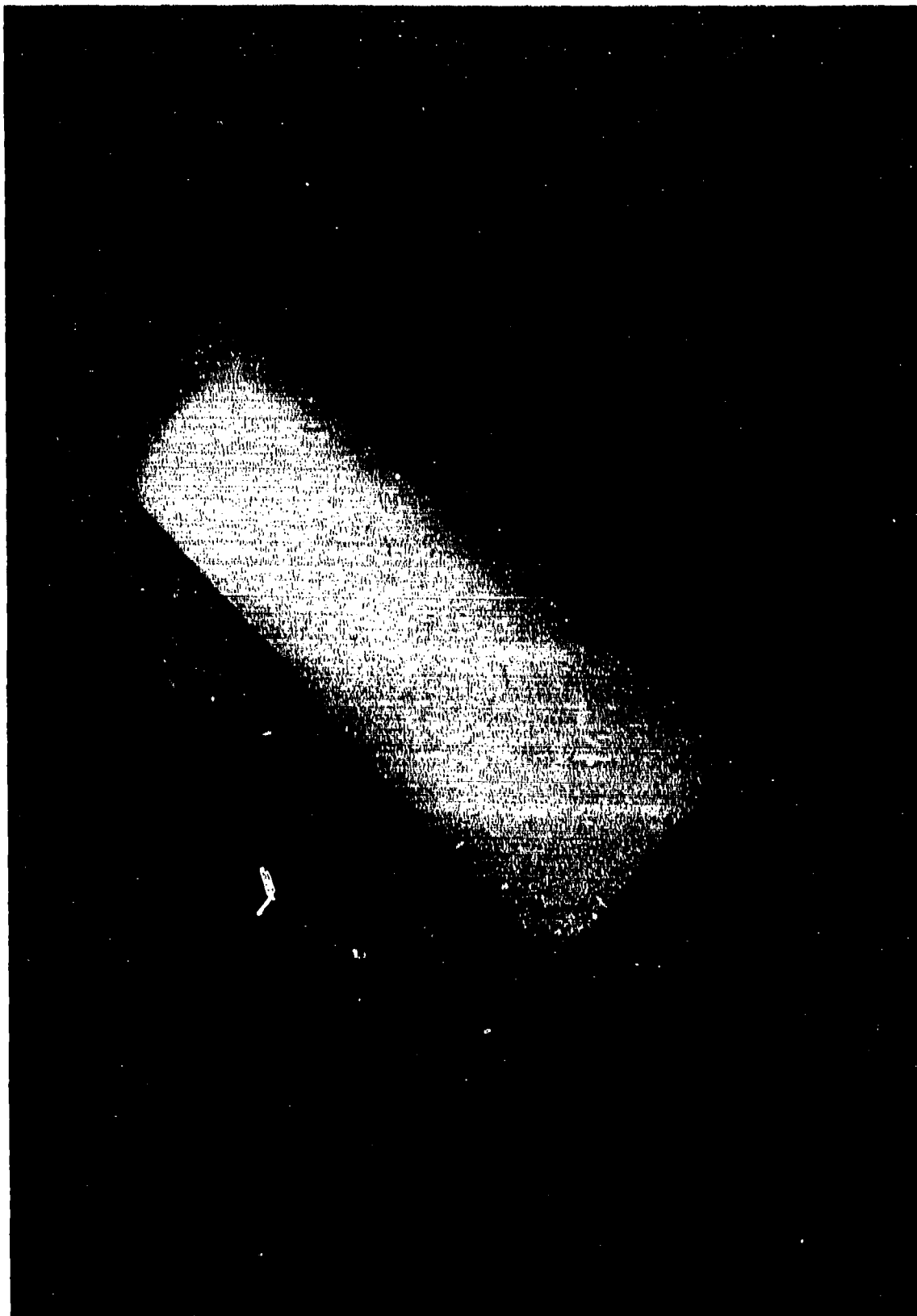


Figure 29. 40-Inch Sinewave Staging Tool with Bag in Place



**Figure 30. Flat Web Beam Tooling**



Figure 31. Assembled Staging Tool

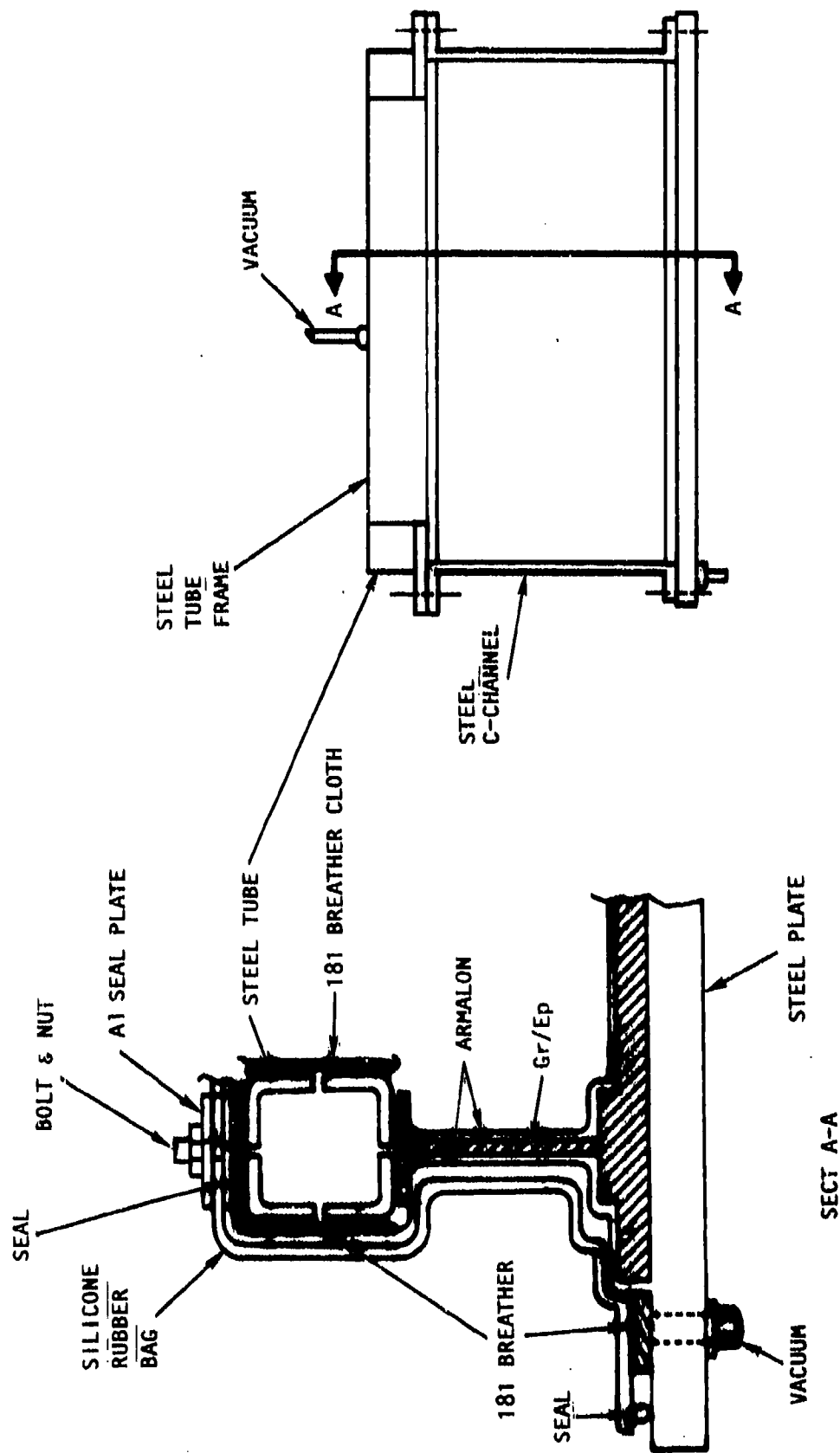


Figure 32. 40-Inch Box Cocure Tool

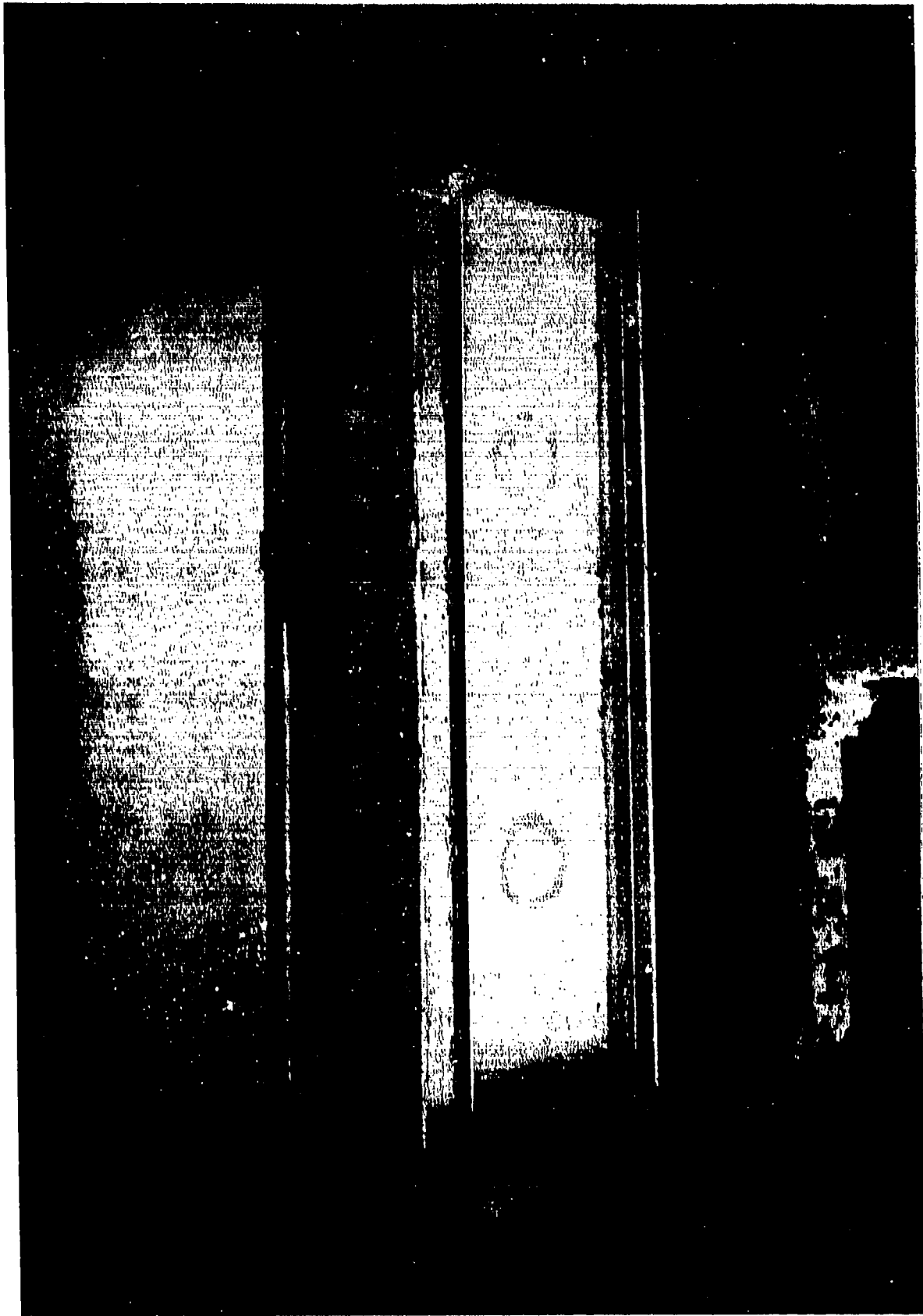


Figure 33. Fiberglass Assembly Preparatory to Spray-Up of Final Cure Bladders

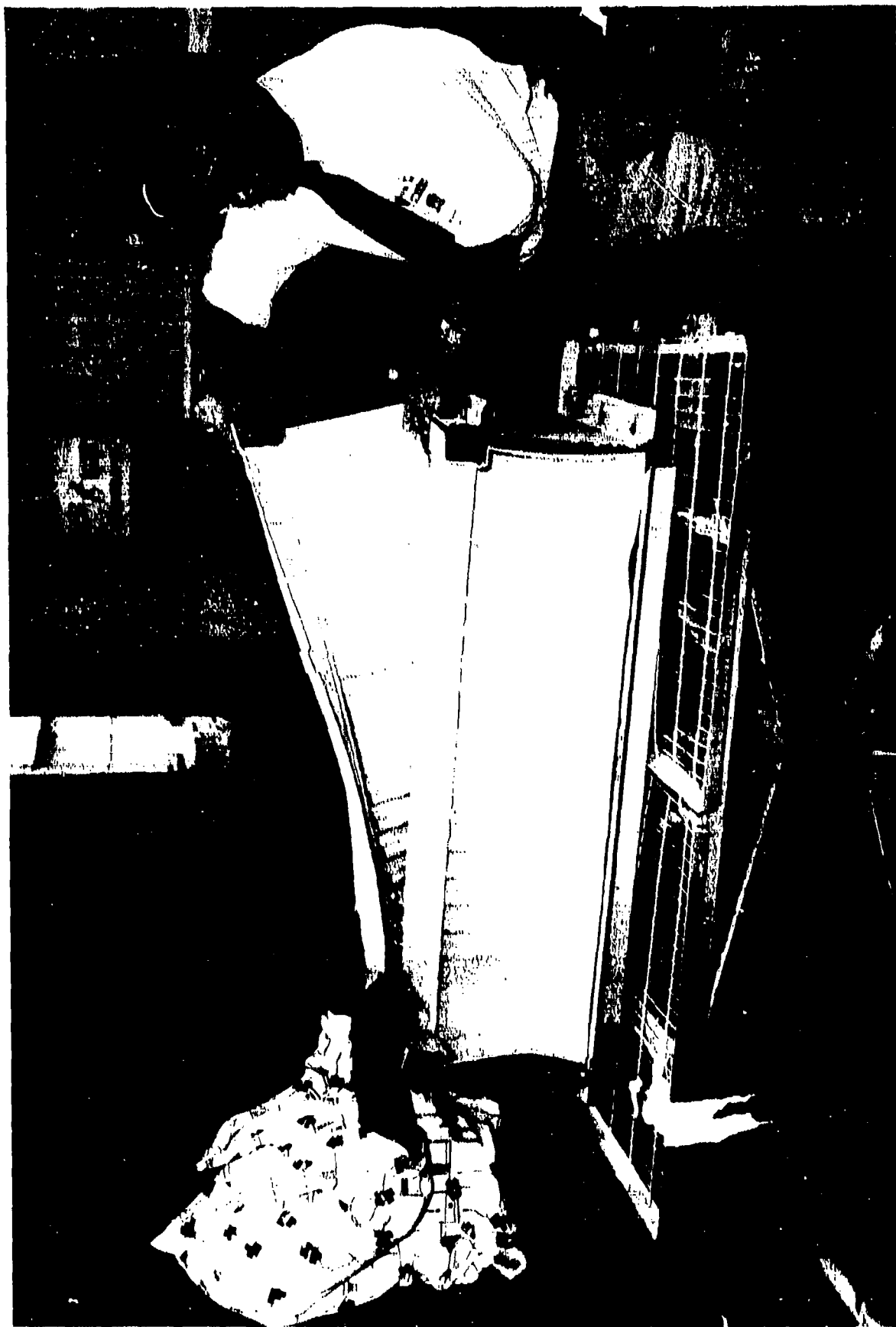


Figure 34. Removal of Internal Final Cure Bladder Molds from Assembly

the final cure tool assembly. The sealing difficulties were attributed to the low adhesion characteristics of the rubber cure bladders. An adequate bag seal was obtained by the use of positive pressure applied to the seal joint with aluminum strips mechanically fastened to the tool, thereby satisfying minimal vacuum and vacuum decay requirements.

**Rubber Evaluation.** A key portion in the development of both the nonautoclave staging and cocure tools is the bag. Previous attempts at fabricating cocured structure have relied on cast rubber bags or on cutting and fabricating bags using calendered rubber or solid rubber tooling. To improve the bag and reduce its cost, silicone rubber was sprayed on the tool to shape a form fitting bag. Initial work on the cocure bag utilized D-aircraft compound 56-rubber. It was found that it could be sprayed, when thinned, using either a standard spray gun or an airless sprayer. Both methods were used in this program with equal success. It should be noted that some expertise is required by the user to assure that a uniform bag is produced [the rubber is sprayed on the tool in several coats, with each coat allowed to air dry 4 to 8 hours, until a final thickness of 0.05 to 0.075-inch is reached for the staging bags and 0.75 to 0.125 inch for the cure bag]. Once the bag spray-up operation is complete, the bag is cured according to the prescribed schedule:

Air dry at room temperature	18 hours
Oven dry at 65.5°C (150°F)	4 hours
Oven dry at 93.3°C (200°F)	2 hours
Oven cure at 121.1°C (250°F)	2 hours
Oven cure at 165.6°C (330°F)	2 hours
Shut oven off and let cool.	

Subsequently, a film of release agent (DAPCO No. 3400, produced by D-aircraft) is sprayed on the inside of the bag. Figure 22 shows the staging tools being sprayed with the silicone rubber.

In order to establish and verify the optimum rubber bladder mold material, the mechanical and physical properties of present and candidate sprayable rubber compound systems used to fabricate the staging and cure tool rubber bladder molds were evaluated. Two sprayable rubber compound systems were also evaluated and the results were compared with Dapocast System 56-1 (refer to table XVI). As the evaluation indicated, both new sprayable rubber compound systems, Dapocast 56-2 and Dapocast 62, had improved tensile strength and elongation properties compared with the compound 56-1. The compound-56-2 system did not have improved hardness and tear strength properties over the 56-1 system, while the compound-62 system did have improved hardness and tear strength properties. The supplier data for the rubber systems are included in table XVI. Upon comparison, it was noted that the only property value in agreement with the supplier data was hardness. The results for tensile strength elongation and the tear strength of the three systems fell short of supplier values.



TABLE XVI  
 SPRAYABLE SILICONE RUBBER EVALUATION

	SUPPLIER'S DATA		AVERAGE TEST RESULTS/		
	COMPOUND NO.		COMPOUND NO.		
Property	56	62	56-1	56-2	62
Hardness (shore A)	45	45+5	58/6	57/14	62/12
Tensile strength (PSI)	900	900	438/3	566/4	848/4
Elongation (%)	300	400	142/3	238/4	388/4
Tear strength (PL <sub>1</sub> )	90	150	86/5	80/3	97/3

To further evaluate the compound-62 rubber, a set of flat web 102-cm (40-inch) silicone rubber staging tool bladder molds were fabricated. The compound-62 silicone bladder mold handling properties were examined and compared with those of the compound-56 silicone rubber molds. The compound-62 molds were similar in appearance and thickness when compared with the compounds 56-1 molds, although the compound-62 exhibited improved handleability and flexibility.

Element Fabrication. The individual details of the cocure structure were laid up in flat; and the close-out ribs and spars were formed over the tooling. Debulking the flat packs is not required in the nonautoclave process. Figure 35 shows the end close-out ribs being vacuum formed. Figure 36 illustrates the method that was used to form the Gr/Ep pack into the sine-wave tool. The I-beams were laid up on each half of the tool forming C-channels. The two halves were mated as shown in figure 37. Note that the Gr/Ep laminates are laid up on the tool with the silicone rubber bag in place. Once the two halves of the I-beam tool are mated, the load couplers are located into what will become the integrally bonded side of the part. The load couplers were fabricated using a clicker die. After insertion of the load couplers the cap strips are placed on the part and the steel channels are added around the tool to complete the tool assembly.

Following the manufacturing process, the details were removed for inspection and trimming to final dimensions for incorporation into the cocure structure. Figure 38 shows the flat web and sine-wave staged details. The fiberglass load couplers are visible in the two center beams. Figure 39 is a close-up of one of the sine-wave beams showing the web to flange radius area and the uniform compaction of the radii.

The Gr/Ep details were trimmed using either a utility knife or a hand-held hacksaw blade. While these methods seemed basic and time-consuming, they were necessary to avoid damage to the staged laminates. The staged laminates appear to be as solid as a cured laminate; however, they are more susceptible to edge delamination and, because the resin is not completely cured, use of a high-speed cutter causes the resin to liquify and foul the blade.

After trimming the details were assembled into the cocure frame (figure 40) with a ply of FM300 at the faying surfaces. The cocure bag was placed over the assembly (figure 41) and the assembly placed in the oven under prescribed cure cycle (RT to 350°F at 5-7°F/min.; hold for 60 minutes). 28-Hg vacuum was maintained throughout the cure. The cocure assemblies are shown in figures 42 and 43. Note that the assembly in the foreground has the two end ribs removed in preparation for fabricating the test beams.

A 2-inch wide section of the 64-ply cocure box cover was removed during sectioning and utilized as the bending beam cover. Hi-Lok fasteners (0.25-inch Ti) were used to attach the cover to the beams. The steel loading hardware (shown in figure 44) was attached to complete the assembly operation.

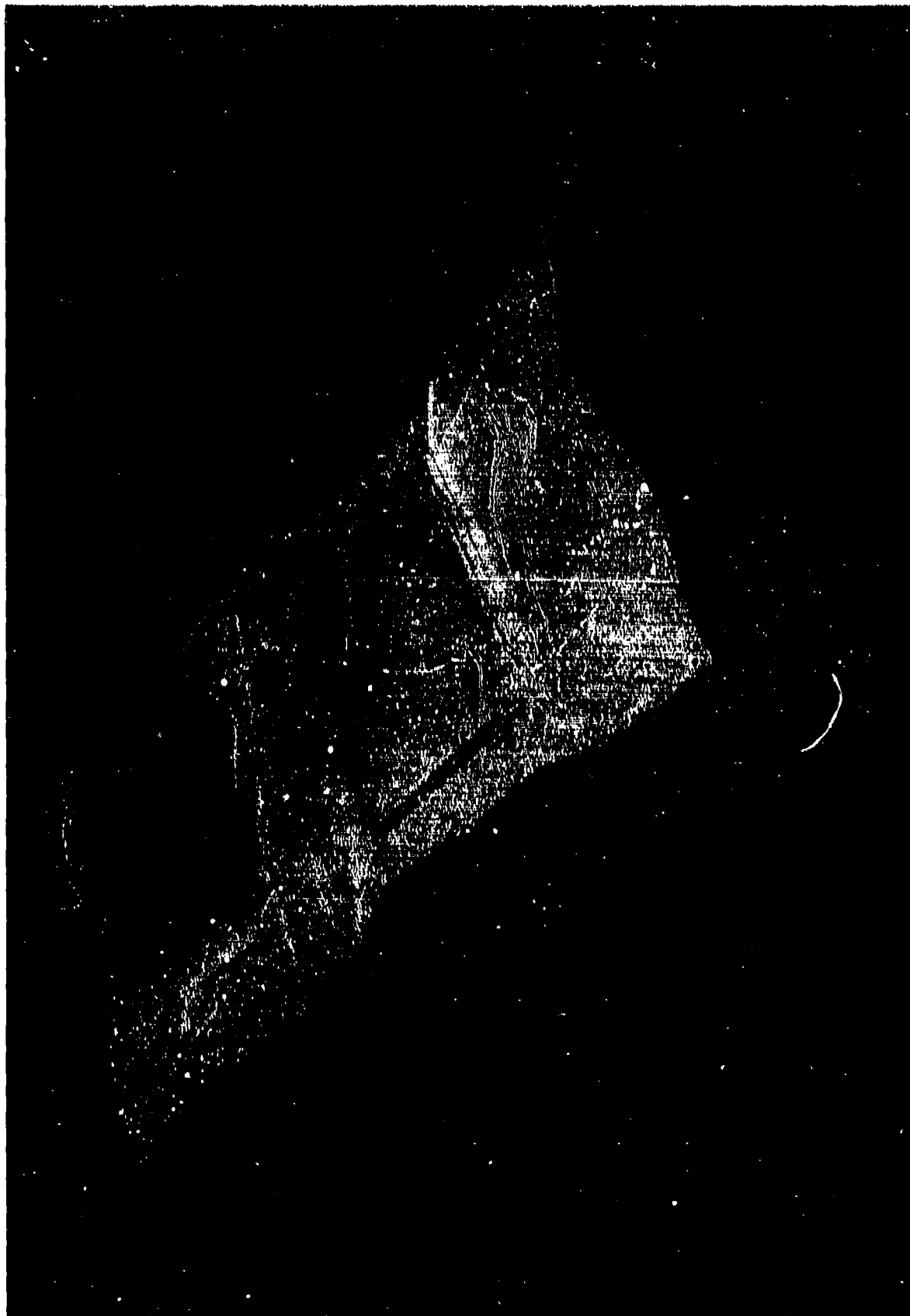


**Figure 35. Vacuum Pressure Forming of the End Closeout Rib**

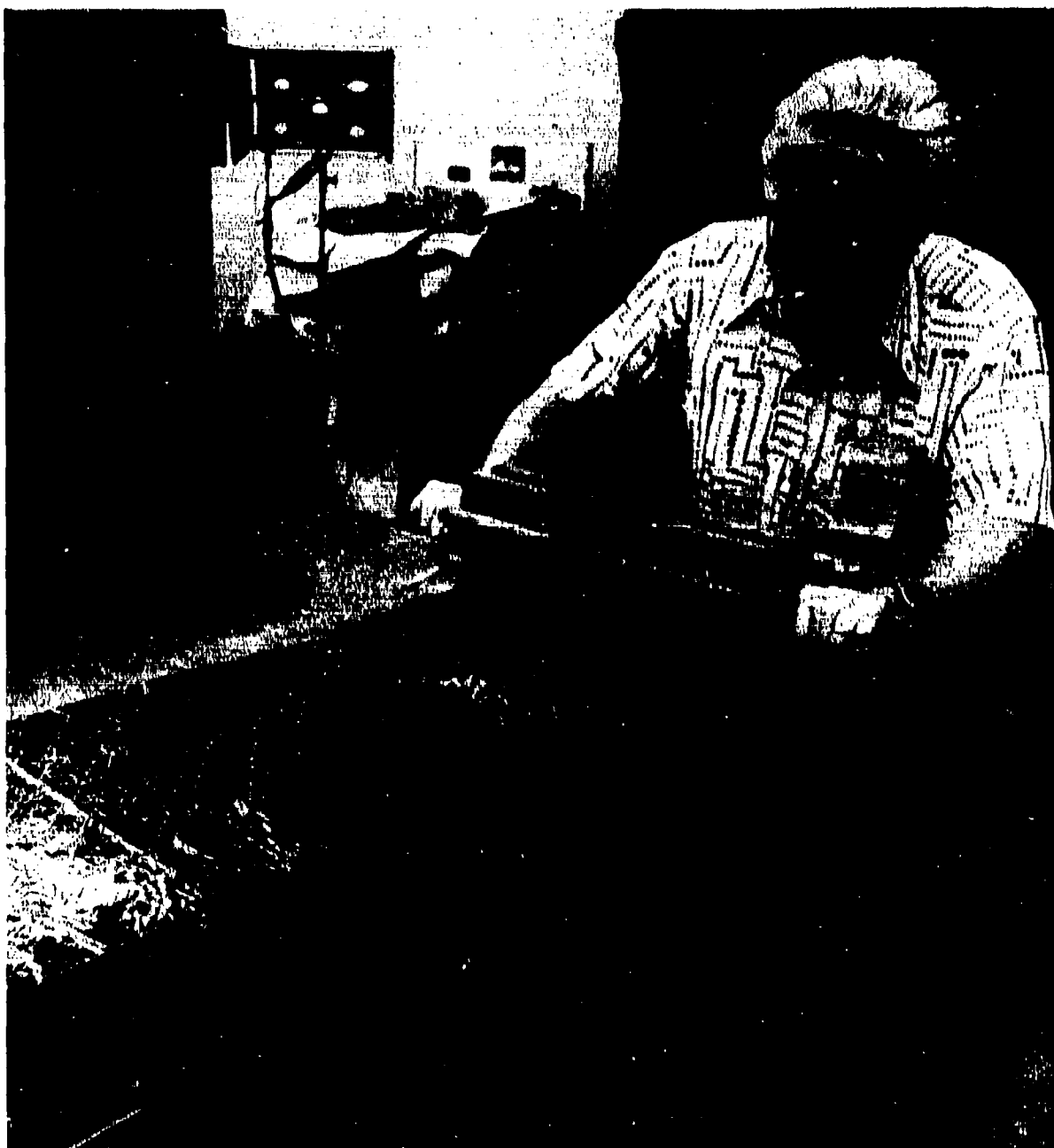


Figure 36. Placing Gr/Ep, Staging Tool



**Figure 37. Partially Assembled Staging Tool**



Figure 38. Staged 40 Inch Beams



Figure 39. Close-up of Staged Sine-wave Web I-Beam - Web-to-Flange Radius



Figure 40. 40-Inch Box Beam Element 1 in Final Cure Assembly with Manifold





Figure 41. 40-Inch Box Beam Element 1 Ready for Cure

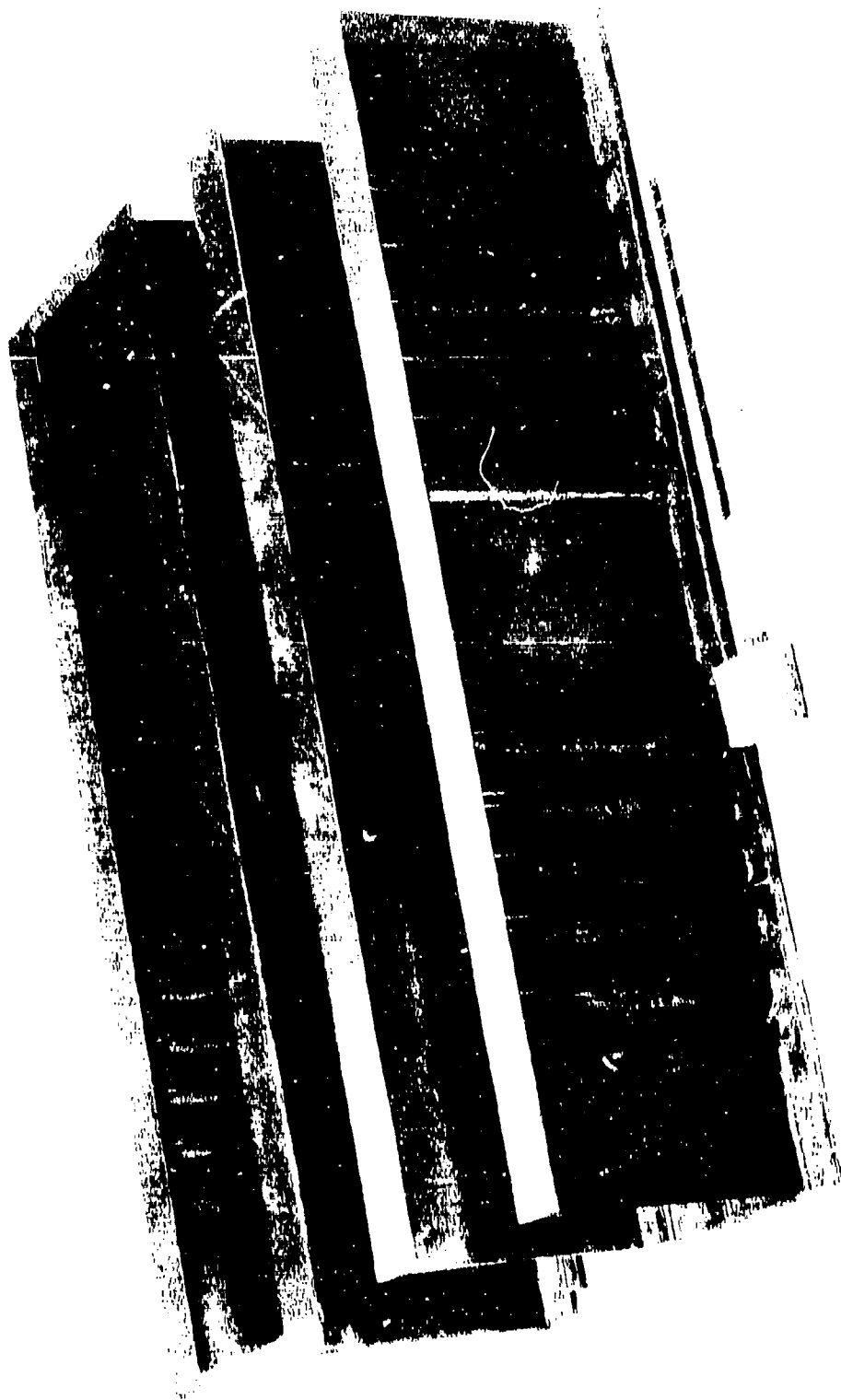


Figure 42. S/N 1 & 2 40-Inch Box Beam Elements



Figure 43. Internal View of Cured Sinewave Web Element 1.

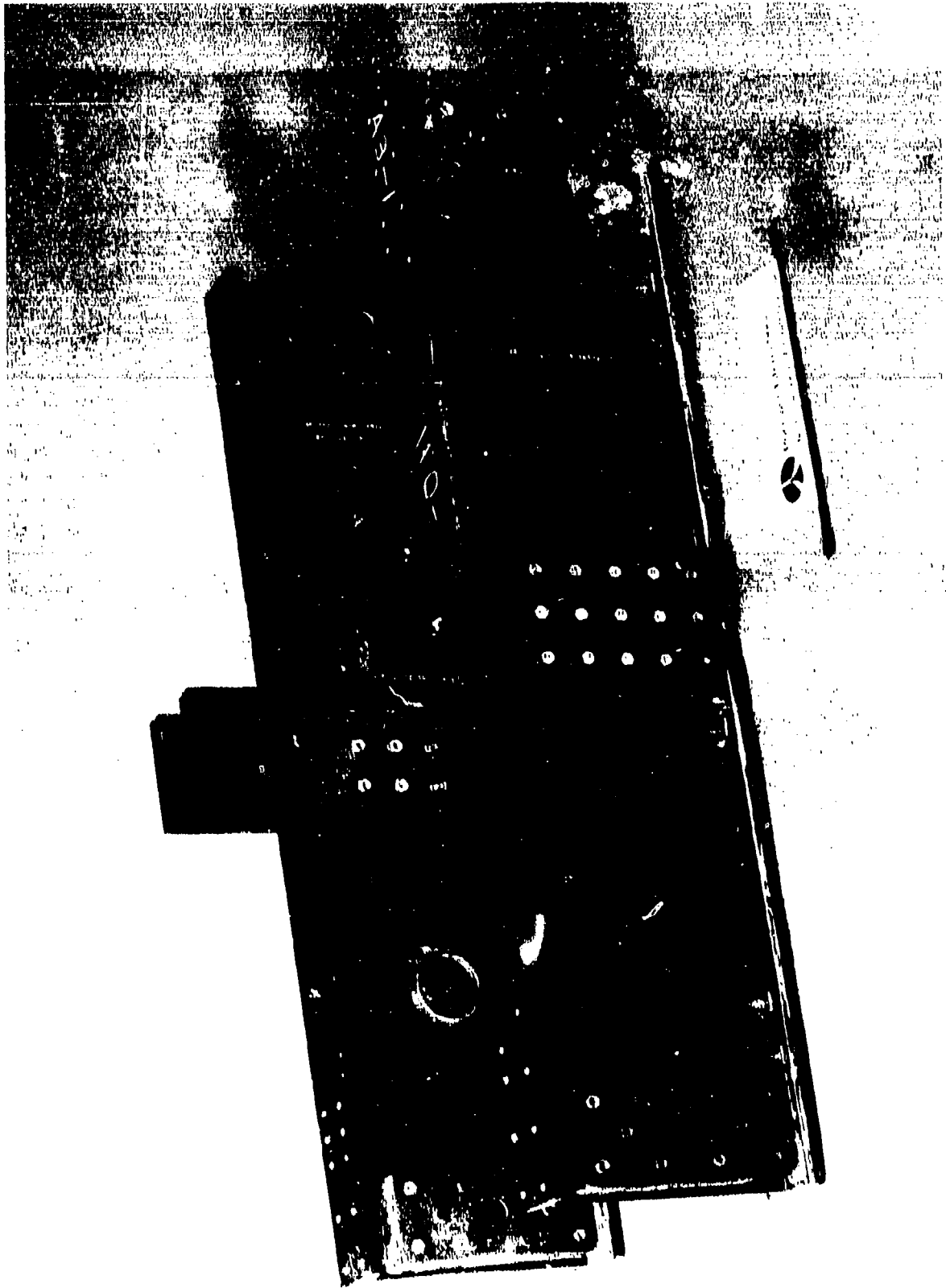


Figure 44. S/N 1 40-Inch Test Element

#### 4.1.2.2.3 Quality Assessment

A three-point plan to evaluate the integrity of the nonautoclave process for fabricating structures was conducted. The plan included nondestructive evaluation of the staged and cured details, static testing of the bending beams and destructive evaluation of the beams (which included mechanical property testing of coupons removed from the beams and photomicrographic examination of sections of both the staged and cured structures).

Ultrasonic Inspection. Nondestructive testing techniques have traditionally been used for defect detection in cured composite integral structures. One of the risks associated with integral structure is the commitment of large complex assemblies to final cure without adequate assurance that each of the detail assemblies meets acceptance standards. It is necessary to establish nondestructive testing (NDT) procedures for staged laminates to detect any anomalies. The staged details were inspected for defects, thereby eliminating the cost and time of nondestructive inspection of the final assembly and reworking the cured component should the details be defective.

The mechanical properties of staged laminates subjected to the traditional ultrasonic C-scan test (water immersion) were compared to the results of staged laminates not exposed to ultrasonic test defect detection. The test was performed on both tape and fabric prepreg. The results (refer to Table XVII) indicate that ultrasonic C-scanning has minimal or no effect on the properties of cured laminates; however, it was not possible to run the ultrasonic C-scans with the separator material on the staged detail because the separator material had disbanded from the staged detail in areas. It was established that removal and replacement of the separator material risks bridging of the detail during the curing operation; removal and replacement of the separator material was therefore not allowed.

To verify the detail testing techniques, a test specimen was fabricated with intentional defects in four locations. Attempts were made to locate the defects using the water immersion, ultrasonic C-scan method without removing the separator materials (porous Armalon and TX-1040). Frequency attenuation was varied throughout the entire decibal range of the instrumentation without improving the C-scan flaw detection sensitivity. The disbonding of both the porous Armalon and TX-1040 separator materials (that typically occur during processing) prevented proper defect detection using ultrasonic C-scan equipment. Additional testing was completed on the flawed specimen using a hand-held contact pulse echo transducer (figure 45) with water as a coupling agent. The pulse echo transducer technique was capable of consistently detecting flaws as small as 0.5 inch  $\pm$  0.125-inch diameter at any ply level.

The ability of C-scan to integrate staged laminates containing porosity was also aimed at establishing reliable standards for use in the inspection of Gr/Ep structures which have been staged using the nonautoclave process. Because these staged laminates have physical

TABLE XVII  
STAGED DETAIL ULTRASONIC C-SCAN TEST

<u>MECHANICAL PROPERTIES</u>		<u>RESULTS</u>	
Fiberite 976, Lot CI-303, Roll 3 Tape Prepreg		Control Laminate	C-Scanned Laminate
		RT/270°F/350°F	RT/270°F/350°F
<u>LONGITUDINAL FLEXURE</u>		336.7/240.3/180.5 333.0/236.8/173.0 332.7/225.7/145.9 330.8/224.3/166.5	334.0/260.6/178.7 331.2/250.8/172.1 345.3/248.2/177.9 336.8/253.2/176.2
<u>INTERLAMINAR SHEAR</u>		15.3/8.0/5.8 16.0/8.0/5.7 15.6/8.1/5.8 15.6/8.1/5.8	14.2/7.9/5.6 15.4/7.9/5.8 15.0/7.4/6.0 14.9/7.7/5.8
<u>TRANSVERSE COMPRESSION</u>		32.5/22.5/16.7 33.8/22.6/17.0 32.8/22.9/17.0 33.0/22.7/16.9	28.9/22.0/15.6 29.0/20.3/16.0 29.1/20.9/15.5 29.0/21.1/15.7
Fiberite HMF 133/79, Lot B1-105, Roll 2A Fabric Prepreg			
<u>WARP FLEXURE</u>		128.0/104.8/95.5 121.8/113.5/92.1 125.0/110.3/97.2 124.9/109.5/94.9	119.3/110.0/84.1 120.6/120.1/85.5 112.0/113.1/88.6 117.3/114.4/86.1
<u>INTERLAMINAR SHEAR</u>		9.9/8.3/7.3 10.2/8.0/7.1 9.8/7.0/7.0	8.2/7.8/6.8 9.3/7.6/6.4 9.7/8.0/6.5
<u>WARP COMPRESSION</u>		85.8/71.0/64.7 83.4/71.0/63.8 84.0/73.6/58.8 84.4/71.9/62.4	81.5/70.8/63.7 80.3/76.2/64.3 78.7/72.6/64.1 80.2/73.2/64.0



**Figure 45. Contact Pulse Echo Ultrasonic Inspection of Staged Beam**

properties which differ from the fully cured laminates, current inspection standards developed for other Gr/Ep structures are not valid. Ability to inspect structural details before they are cocured into a complete integral structure will lead to higher reliability.

Sixteen-ply Gr/Ep unidirectional laminates were prepared by the nonautoclave staging process utilizing different levels of vacuum differentials outside and inside the bag as a means of producing several levels of porosity in test specimens. A portion of each of the specimens was then fully cured to allow sectioning and polishing for visual determination of the degree of porosity. The specimens, both staged and cured, were inspected by ultrasonic through-transmission at 2.25 MHz with a three-quarter-inch diameter lens at six-inch focal length. Information from these tests reinforced the feasibility of quantitative measurement of porosity in staged laminates. Fabrication procedures, NDT, and visual examination results are shown in table XVIII.

Figure 46 presents photomicrographs of the cured specimens. Sections were taken of the cured laminate, polished, and photographed at 50X magnification. Items a and c in figure 46 show approximately the same level of porosity. However, the size of the individual pores in item c of figure 46 is typically much larger throughout the specimen. This would account for the increased ultrasonic attenuation shown in the C-scans of the staged specimens (figure 47) while figure 48 shows the cured specimen C-scans. The scans at 12 dB attenuation are at a power setting that shows the approximate size of the lead tape utilized as defect reference points. The ability of the staged laminates to transmit the applied ultrasonic signal more readily than the cured laminate would appear to be anomalous. Any indication of porosity in a staged laminate would be amplified in the cured laminate. It was also observed the laminates which appeared to be porosity-free in staged condition were indeed porosity-free after cure.

It can be concluded from this work that the ability to evaluate staged laminates with ultrasonic C-scan does provide a reasonable method of ensuring cured part quality. The amount of porosity present in a laminate, staged or cured, cannot be gauged by the C-scan.

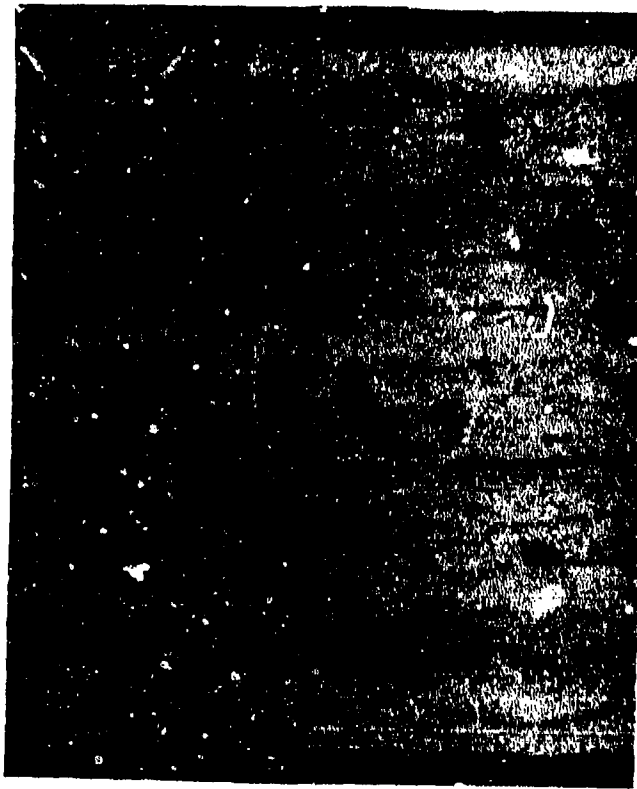
As a further method of ensuring the accurate evaluation of staged laminates, typical C-scan standards were developed. The standard was a 12- by 12-inch Gr/Ep laminate having varying ply thicknesses representative of those thicknesses that would be found in the actual structure. Lead tape and pull-out type anomalies were used as references.

All staged laminates in this program were subjected to ultrasonic C-scan and contact pulse echo. Pulse echo through-transmission of the staged box-beam element 1 details detected a few localized areas of porosity within the end doubler areas on the sine-wave and flat-web beams. It was felt that porosity in these regions could be eliminated during the final cure operation. Because the porosity was located in the doubler areas where the steel loading hardware attached for the structural test of 40-inch beams, it was felt that the porosity



TABLE XVIII  
POROSITY EVALUATION OF STAGED PANELS

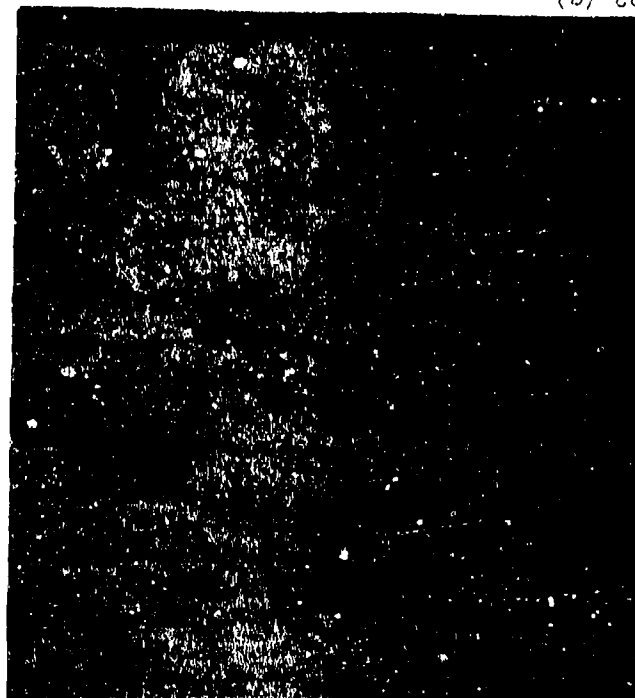
Panel No.	Staging Fabrication Procedure	Visual Examination	NDT Conclusions	DB Attenuation	
				Staged	Cured
1	Vacuum bag only	Moderate porosity	Moderate	12	21
2	Place in bag and in vacuum chamber. Bag and chamber at 28 in. Hg vac (standard nonautoclave procedure).	Minor porosity Acceptable	No porosity	0	0
3	Place in bag and in vacuum chamber. Bag and chamber at 12 in. Hg vac.	Heavy porosity Unacceptable	Heavy porosity	18	39



(a) COUPON No. 1



(b) COUPON No. 2



(c) COUPON No. 3

Figure 46. Photomicrographs (50X) of Cured Gr/Ep Laminates

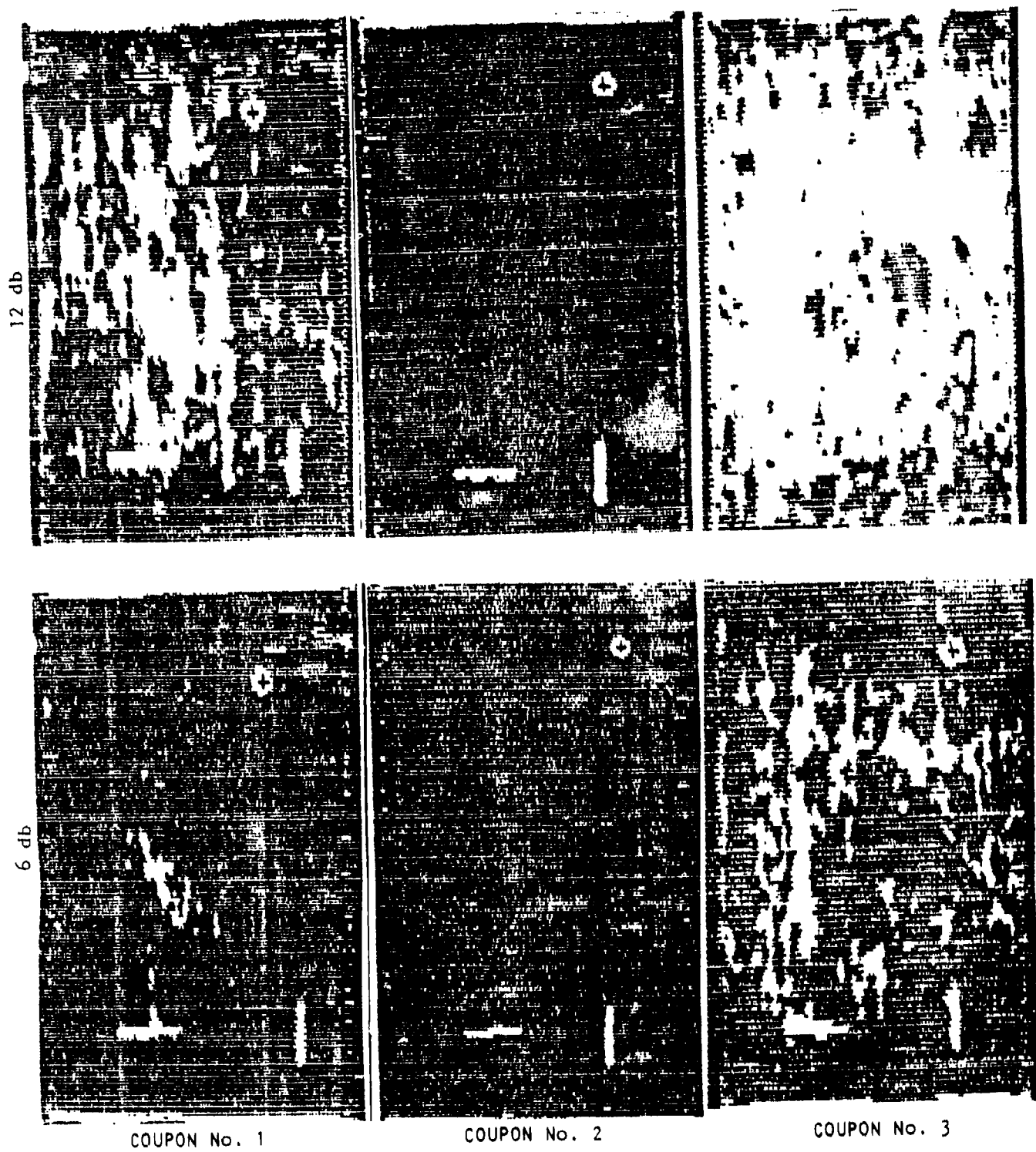


Figure 47. Ultrasonic C-Scans of Staged Gr/Ep Laminates - 1 MHz, 6 and 12 dB

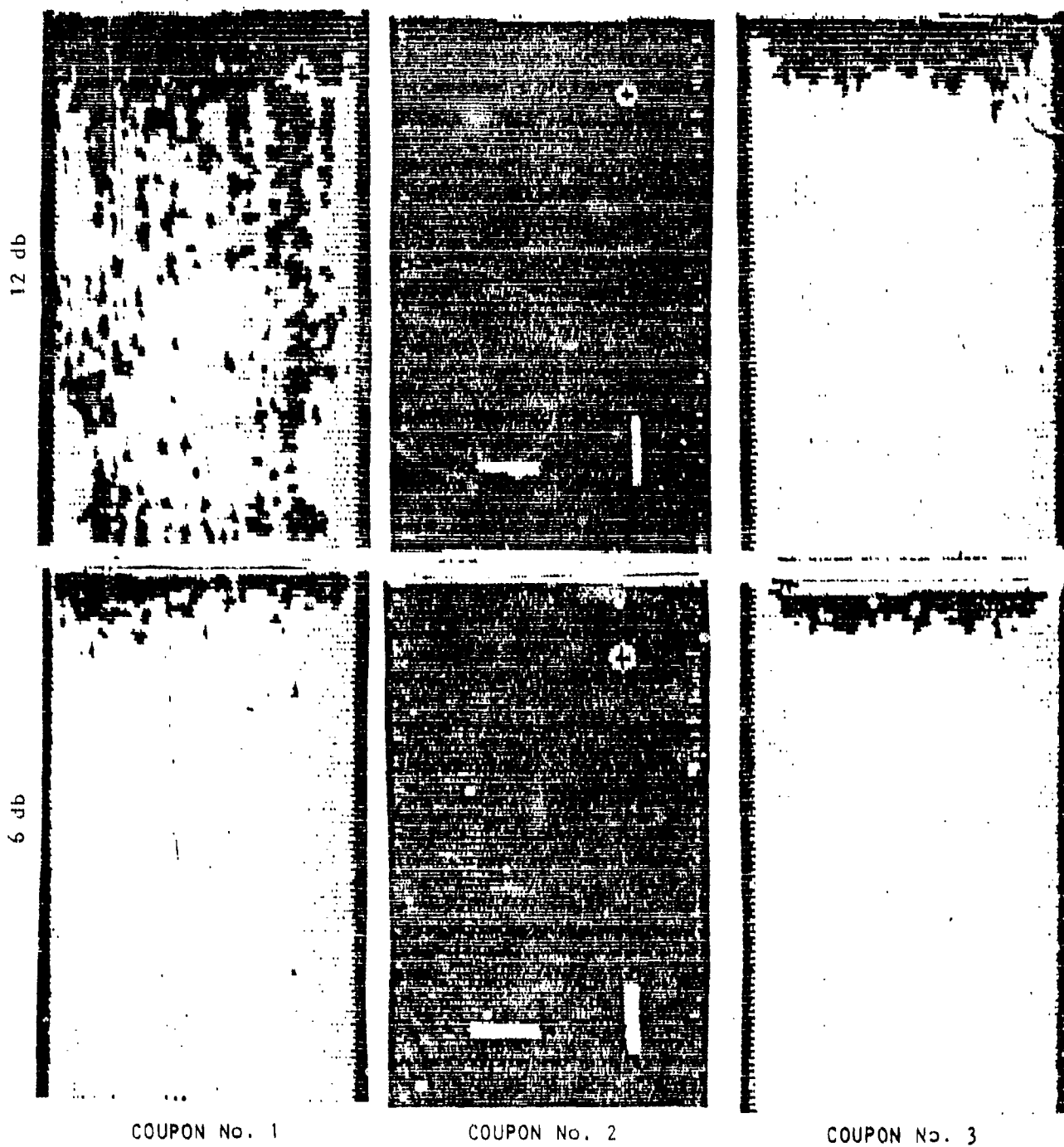


Figure 48. Ultrasonic C-Scans of Cured Gr/Ep Laminates - 1 MHz, 6 and 12 dB

would not affect the validity of the test. The porosity was not severe and thus did not affect the fastener bearing or shear properties of the laminate. There was no porosity detected in the covers.

Visually, the cured box beam was of excellent quality. There were some localized indications of reduced pressure in the radii of the sine-wave member. Subsequently, the box beam was nondestructively inspected for defects and porosity using both ultrasonic C-scan and X-ray. These tests revealed porosity in the same areas as revealed by the pulse echo through-transmission test of the staged details. The box beam assembly trim material was then sectioned, polished, and examined for porosity. Fine, dispersed porosity was detected in the web doublers and cap-to-cover bondline. A study was conducted to determine the cause of the porosity in these regions and the results are contained in section 4.1.3.2 Tooling Gap Evaluations.

The second 40-inch box beam was visually acceptable; however, there were some localized areas of reduced pressure as well as a very minor wrinkle in the radii of the sine-wave member. These local defect conditions were similar but slightly larger than areas associated with the first 40-inch box beam assembly. There were also indications of localized delaminated areas in the outer ply of the cover which were attributed to inadequate vacuum during cure because of sealoff of the staged box laminate cover to the nonporous Armalon coated tool surface. The second box-beam component was sectioned and compared with the first component. Sectioned areas of the second assembly were polished and, upon examination, porosity was detected. Porosity was present in the end doubler areas on both the sine-wave and flat-web beams and in the cap-to-cover adhesive bondline. Ultrasonic C-scan inspection of the elements confirmed the presence of porosity in the same areas as the sectioning revealed.

Prior to preparation of the second sine-wave and flat-web 40-inch verification bending beam test elements, the delaminated areas in the outer ply of the cover were repaired.

Element Tests and Test Result Correlation. The criterion for judging the success of the manufacturing method was a capability of the element to perform structurally as required by the B-1 composite vertical stabilizer design. Test results were compared with the test results of similar parts fabricated using conventional autoclave pressure manufacturing methods. The objective of these tests was to demonstrate that NAAO's proprietary nonautoclave curing process was capable of producing integral structures with spars having shear strength equivalent to the autoclave parts. Sine-wave and flat-web beam test results from the composite vertical and horizontal programs further substantiated the test results.

Four beam elements were obtained from the two integral beam/cover structural assemblies (figure 44). These beams were tested as a simple center loaded beam, as shown in figure 49. The sine-wave and flat-web beams are typical of configurations used on the Low-Cost Composite Wing/Fuselage program. In addition, the sine-wave beams were

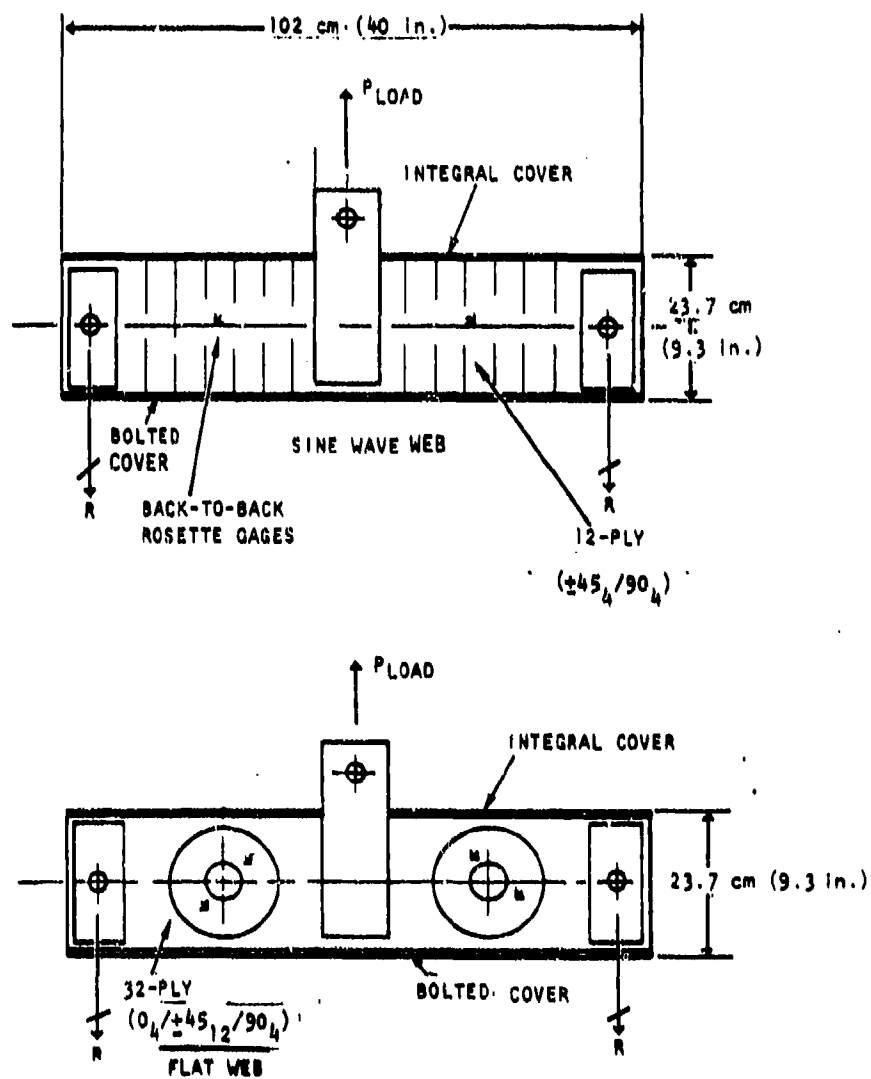


Figure 49. Nonautoclave 102-cm (40-Inch) Verification Bending Beams

similar to and were compared with sine-wave beams tested on the composite vertical and horizontal tail programs for the B-1. Each sine-wave beam test element was instrumented with four rosette strain gages (as shown in figure 50) and the flat web beams were instrumented with eight rosette strain gages (as shown in figure 51). Four thermocouples were installed on each beam to measure temperature during testing.

Each of the four beams (2 sine-wave, 2 flat-web) fabricated from the two 40-inch boxes were subjected to static elevated temperature wet test.

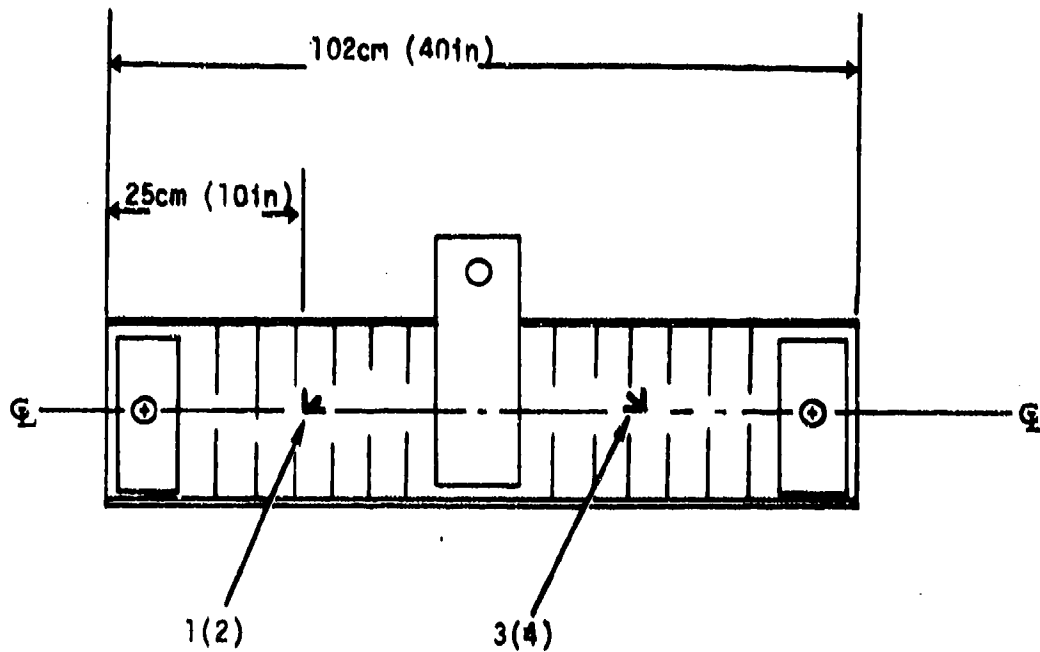
Prior to test, the beams were preconditioned at 70°C (175°F), 95-percent relative humidity. The 12-ply sine-wave-web beams were conditioned to a minimum of 1.09-percent moisture content by weight and the 32-ply flat-web beams to 0.9-percent. These moisture levels represent predicted worst case moisture levels for the cover and substructure elements of a composite vertical stabilizer of the B-1 aircraft over a 20-year in-service environment. These moisture levels matched those used on the low cost composite wing/fuselage (contract F33615-77-C-5278) I-beams, which were identical in configuration and layup to those tested here. This allowed for correlation and comparison of the structural test data of similar beams (utilizing conventional autoclave material and fabrication techniques) with those employing nonautoclave cure technology and material.

Moisture content, using moisture traveler coupons, was monitored on a scheduled basis throughout conditioning. The traveler coupons measured approximately 2.0- by 2.0-inches. The edges were painted with moisture resistant polyurethane to prevent rapid diffusion into the laminate through the exposed edges.

After preconditioning, the elements were installed in the environmental test fixture and brought to a test temperature of 140°C (220°F), 95 percent relative humidity.

The beams were loaded through an Edison load proportioning unit. Load link and strain gage output were read on an SR-4 strain gage and balance unit, and thermocouple measurement were read on a Leeds Northrop temperature indicator.

The beams were loaded in three point bending, placing the integral cover in tension, as shown in figure 49. Loading was applied in 20-percent increments from 0 to 40 percent of predicted failure, then in 10-percent increments to failure. Strain levels were recorded at each load level. Predicted ultimate failure load for the sine-wave beams was 22,000 pounds. This produced a nominal shear strain at failure in the 12-ply sine-wave web of approximately  $4800 \times 10^{-6}$  inch/inch. The flat-web beam ultimate failure load was predicted to be 65,000 pounds. The 32-ply web had a shear stress of 21,000 psi and  $5200 \times 10^{-6}$  inch/inch strain at failure.



( ) Backside Gage

Figure 50. Strain Gage Locations for Sine-Wave Beams



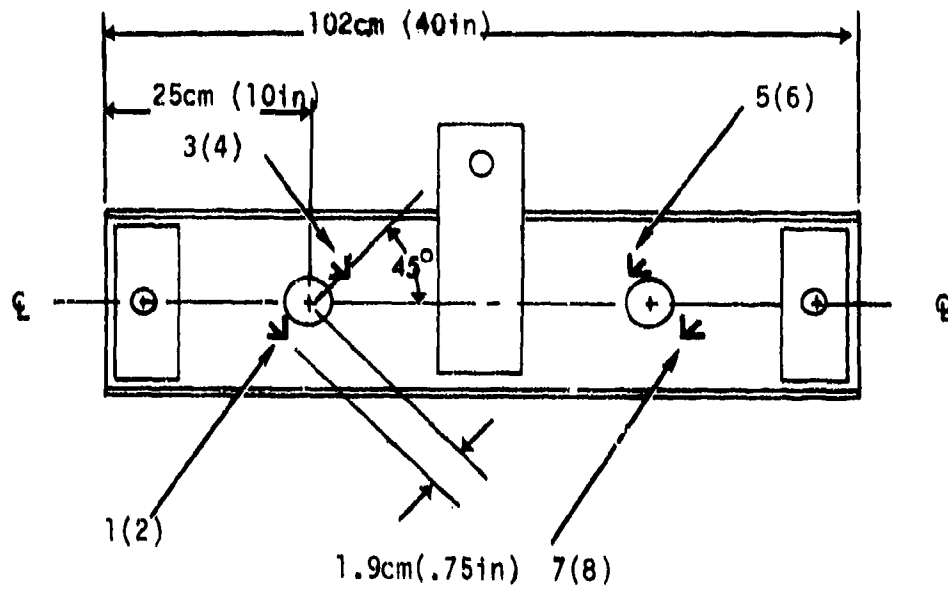


Figure 51. Location of Strain Rosettes for Flat Web

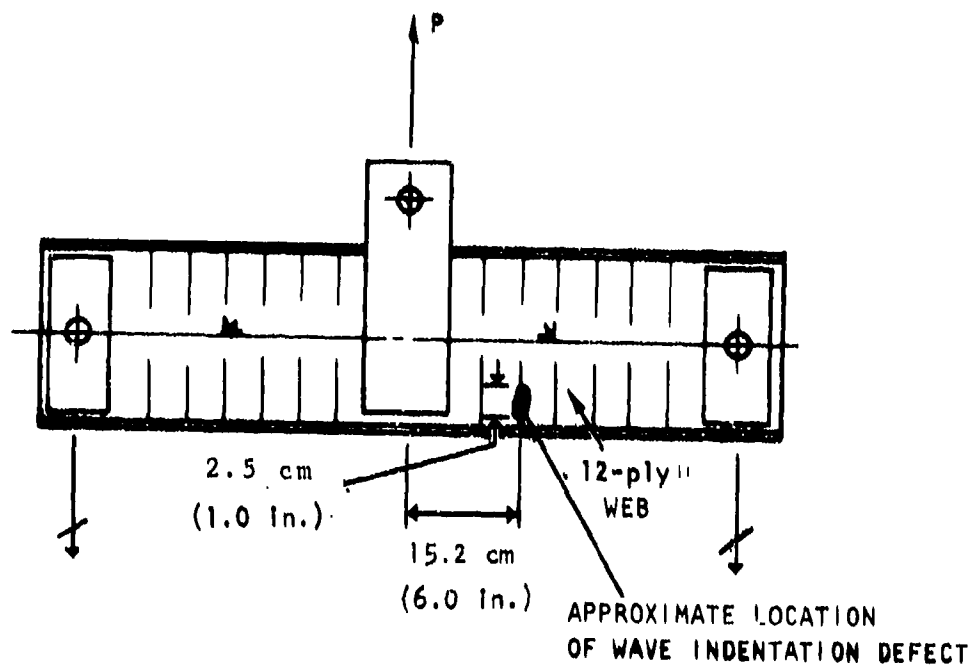


Figure 52. Location of Permanent Indentation of One of the Sine-Wave Nodes of First Sine-Wave Beam

Table XIX summarizes the test results which included failure load, web shear flow and shear strain, test temperature, and moisture content.

Inspection of the first sine-wave beam indicated a local indentation or buckle in one of the sine-waves about 15 cm (6 inches) from beam centerline (figure 52). The depth of this manufacturing defect was 0.10 cm (0.04-inch). It was determined that this defect could initiate a failure of the beam. Analysis of the defect was conducted. The results established the predicted failure shear flow as 118.4 kN/M (676 lb/in.) which is 7 percent over actual failure load.

The shear on a unit element (figure 52) surrounding this indentation is made up of tension and compression components acting at 45 degrees:

$$\text{Allow stress} = \frac{d}{t} + \frac{6M}{t^2}$$

Where

d = dent depth  
M = moment  
P = Shear load  
q = Shear flow  
t = webthickness

$$M = P \times d = q$$

With:

$$\text{Allow} = 489 \text{ MPa (71,000 psi)}$$

$$t = 0.173 \text{ cm (0.068 inch)}$$

then:

$$q \text{ predicted at failure} = 118.4 \text{ kN/m (676 lb/in.)}$$

Figures 54 and 55 show the static test setup and web failure of the first sine-wave beam. Inspection of the beam indicated that the failure originated at this local indentation defect. The failure shear flow was 126.4 kN/M (1722 lb/in.) which gave a failure to predicted ratio of 1.07 percent (accounting for the localized instability caused by the defect).

Evaluation of the test data of the second sine-wave beam indicated that the beam failed at 130 percent of the predicted failure with the mode of failure, (as seen in figures 56 and 57) in the upper cap and between the lower cap and the web. Plots of the 45-degree strain gage legs versus load for rosette No. 1 (figures 58 and 59) indicated a linear web response and no degradation to failure. The initial failure was the flatwise tension shear interaction of the integral upper cap and the load coupler, then, as it failed, the web was simply pulled away from the lower bolted cap (as previously shown).

TABLE XIX  
SUMMARY OF 102-CM (40-IN.) BEAM TESTS

Part	P Failure Load KN (LB)	Q <sub>web</sub> KN/M (LB/IN)	Test Temp. °C (°F)	Web Moisture % by Weight Before After Test Test	Average Web Shear Strain Percent	Failure Q <sub>Predicted</sub> (2)
Sine-Wave Beam No. 1	60.0 (13,500)	126.4 (722)	107 (225)	0.98 0.42	0.27	1.07
Sine-Wave Beam No. 2	128.1 (29,000)	270.0 (1542)	102 (215)	0.99 0.55	0.55	1.31
Flat Web No. 1	320.2 (72,000)	674.9 (3854)	98 (208)	1.24 1.16	0.28 9(7)	1.10
Flat Web No. 2	2643.2 (59,400)	556.7 (3179)	107 (225)	0.87 0.68	0.28 (1)	0.91
<p>NOTE: 1. Strain gage located on hole doubler 1.9-cm (0.75-in.) from hole boundary</p> <p>2. Q<sub>Predicted</sub> is from failure analysis with initial defect</p>						

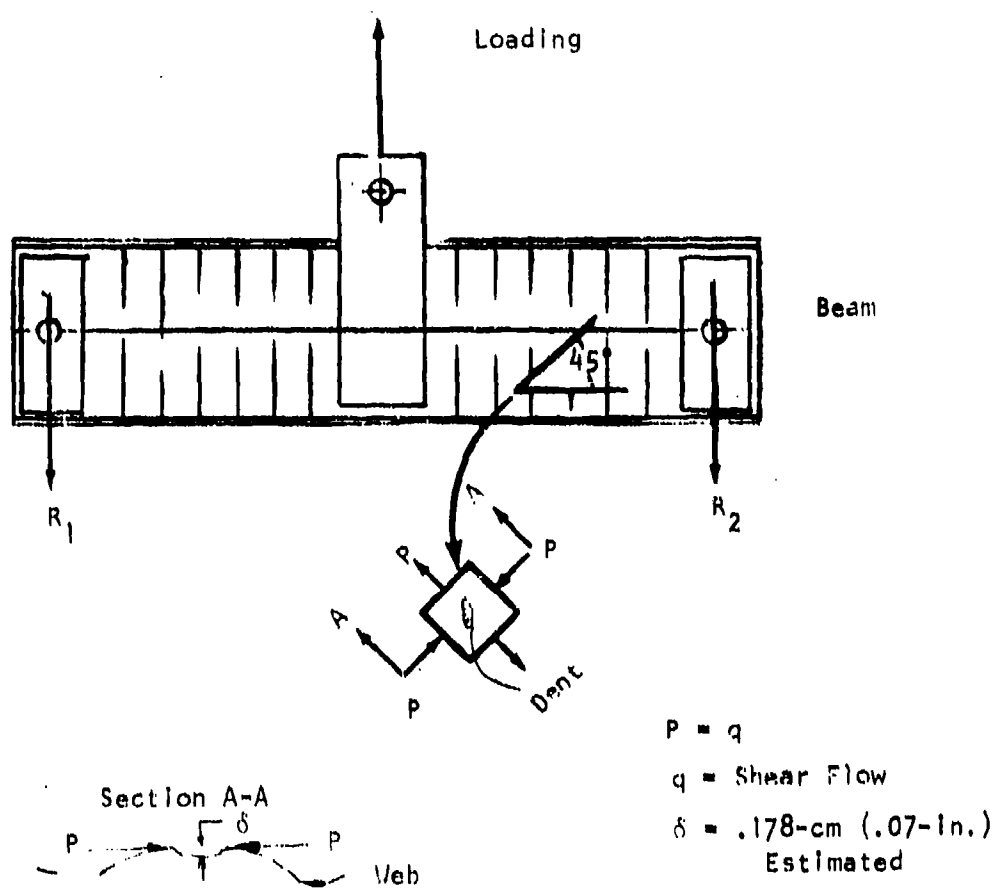


Figure 53. Shear Flow Analysis Schematic

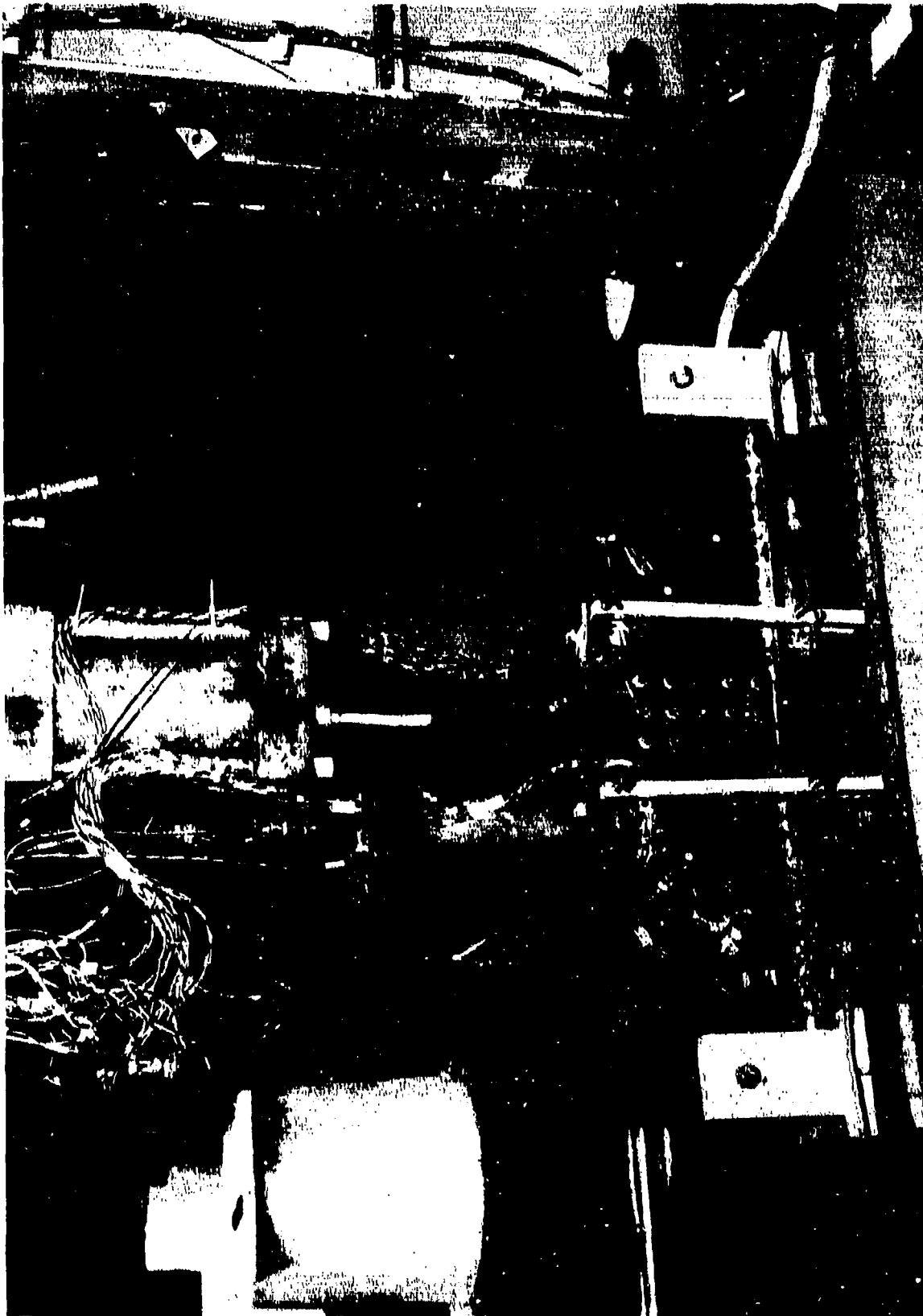


Figure 54. First Sine-Wave Beam - Static Test Setup

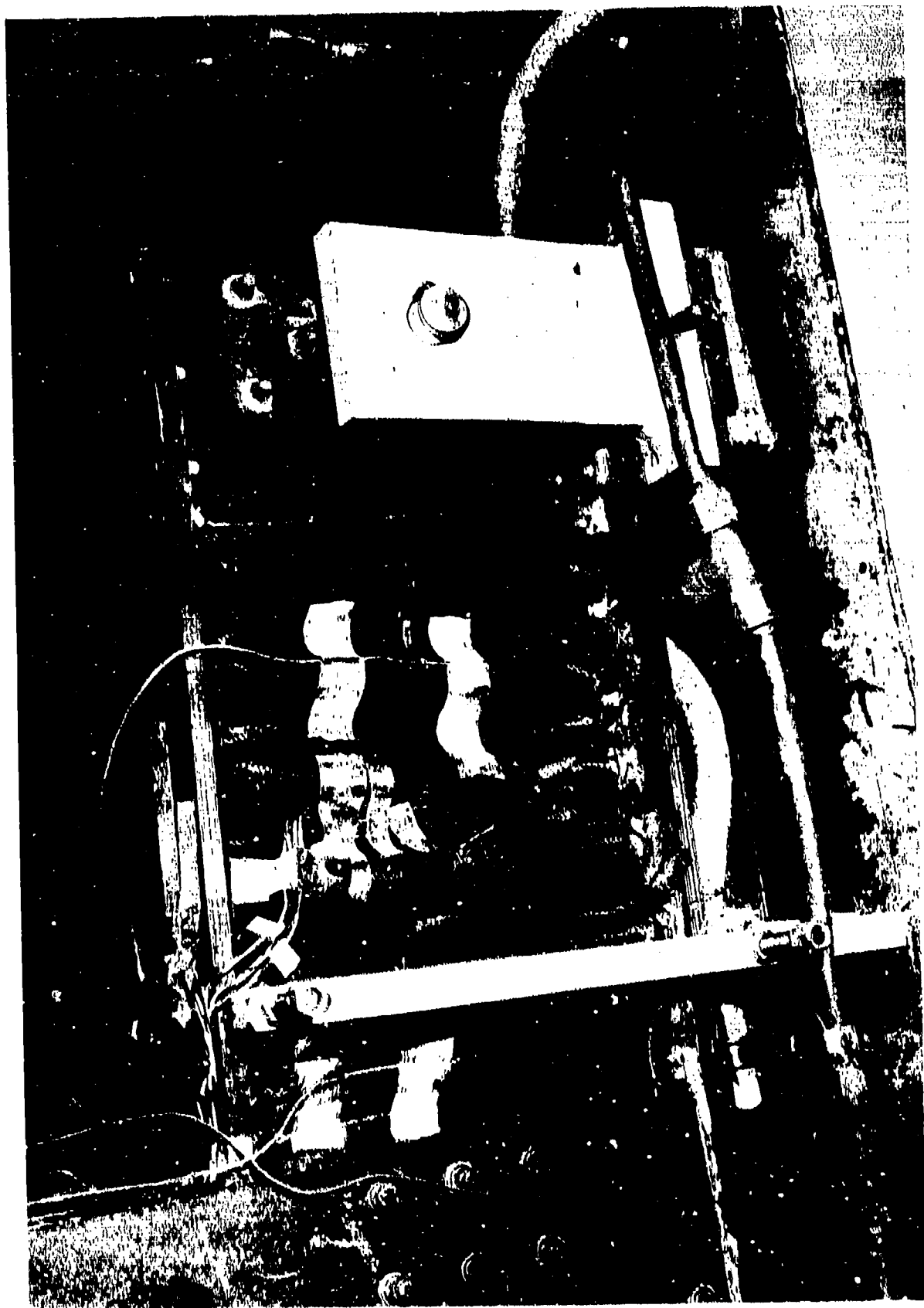


Figure 55. Closeup of the First Sine-Wave Beam Web Failure

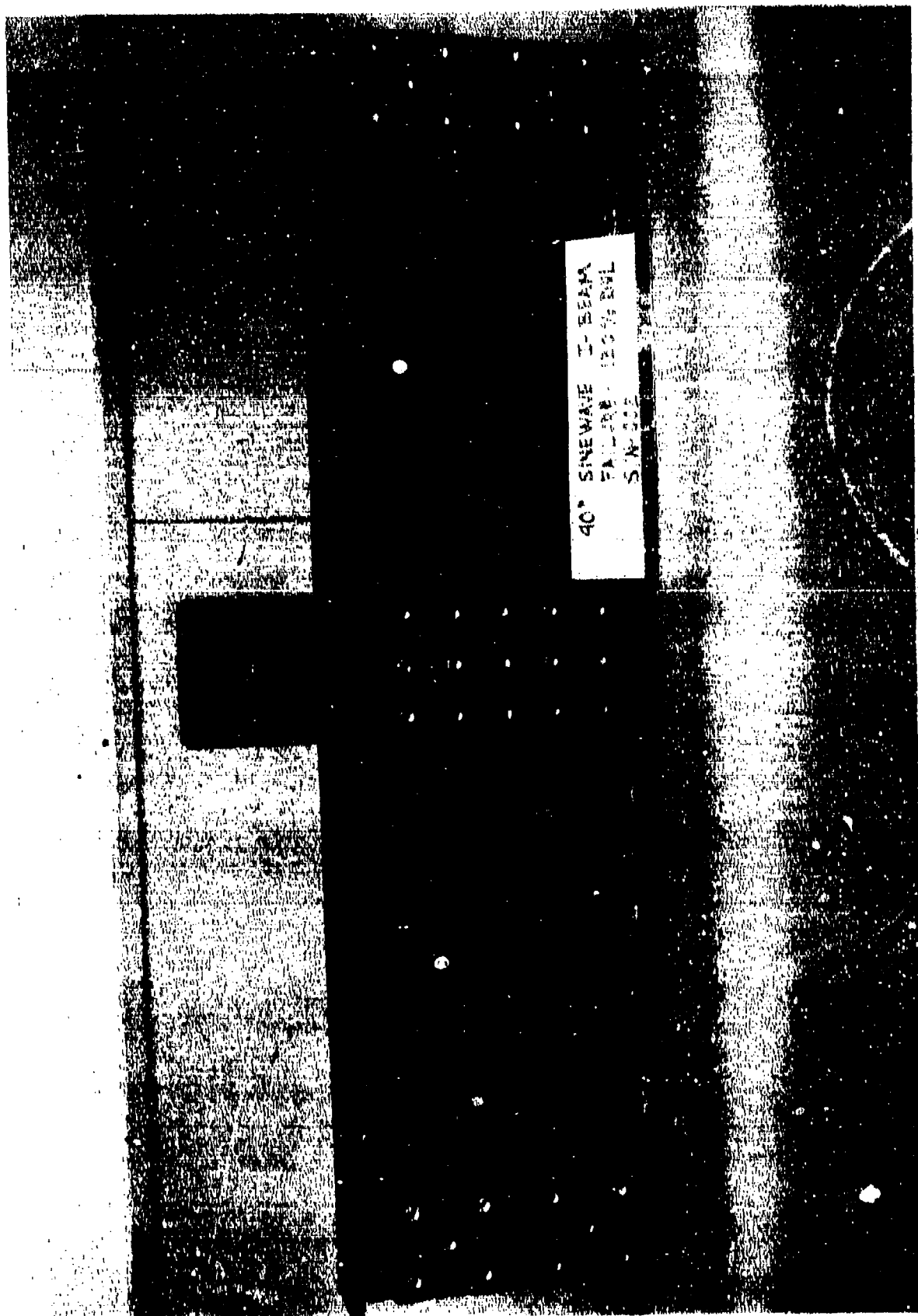


Figure 56. Sine-Wave Beam - Second Test Failure

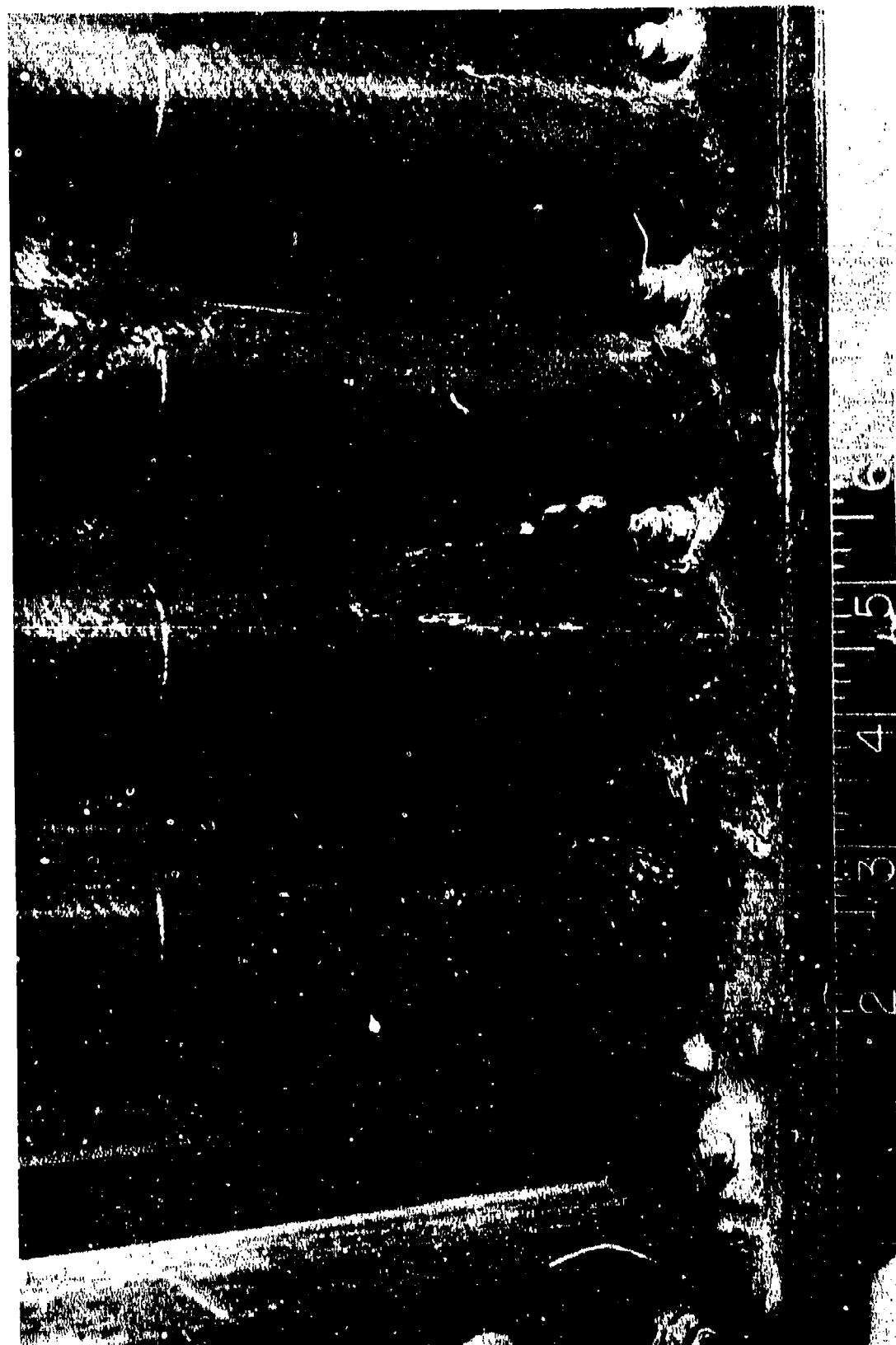


Figure 57. Closeup of Lower Cap to Web; Failure of Second Sine-Wave Beam



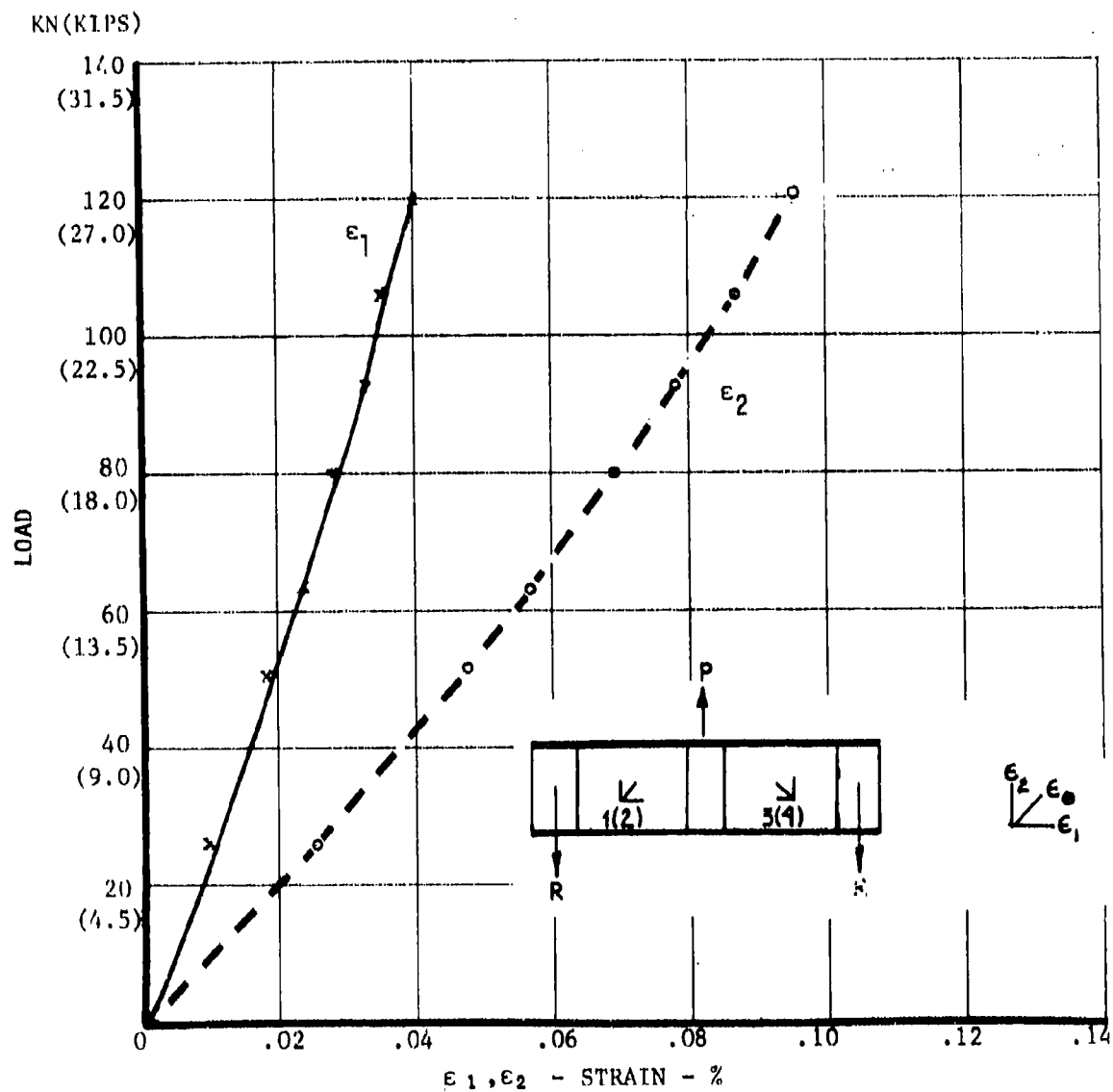


Figure 58. Load vs Strain ( $\epsilon_1$ ,  $\epsilon_2$ ) for Sine-Wave Web Verification Bending Beam Specimen No. 1 (Rosette No. 1)

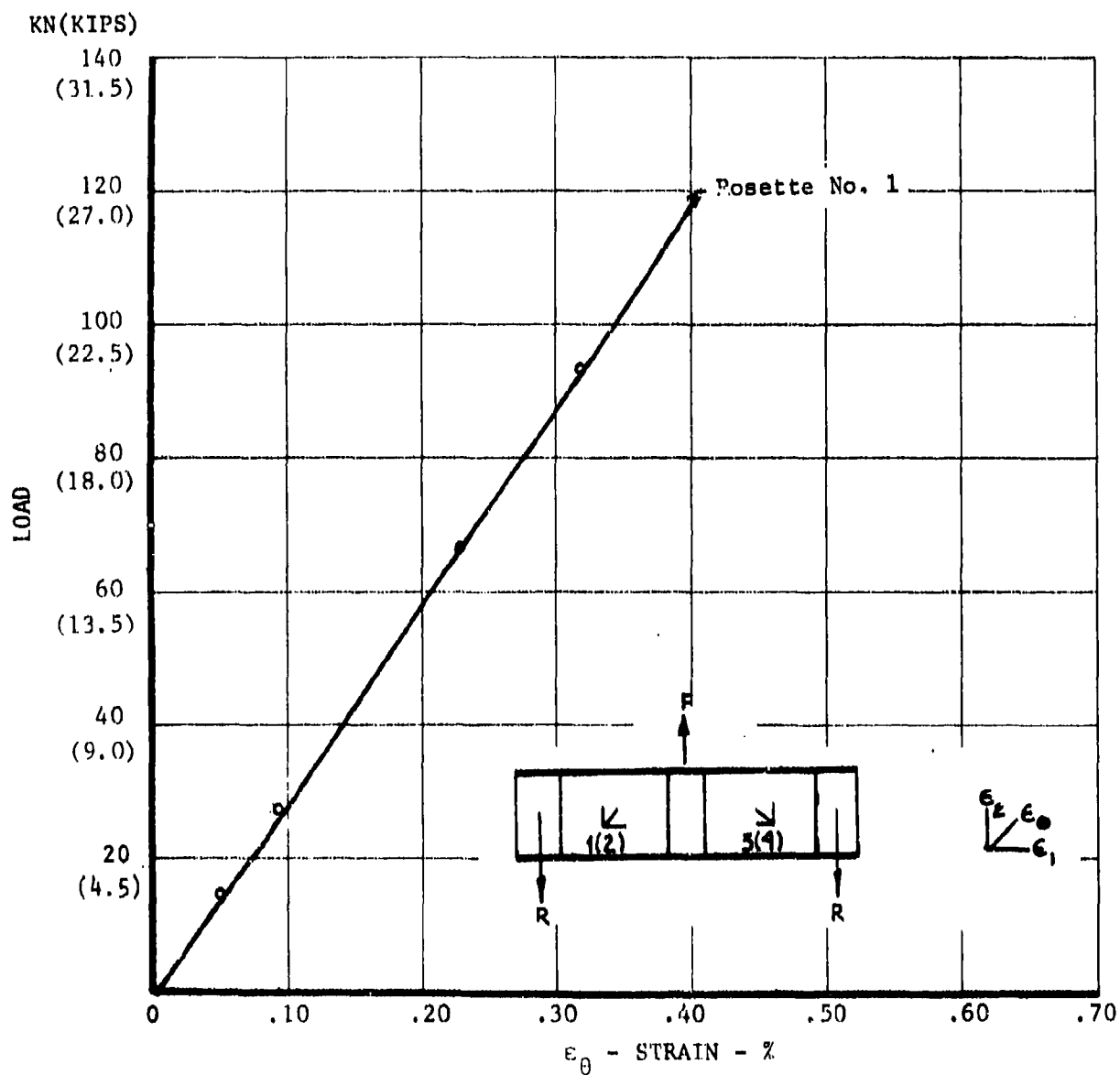


Figure 59. Load vs Strain ( $\epsilon_{\theta}$ ) for Sine-Wave Web Verification Bending Beam Specimen No. 1 (Rosette No. 1)

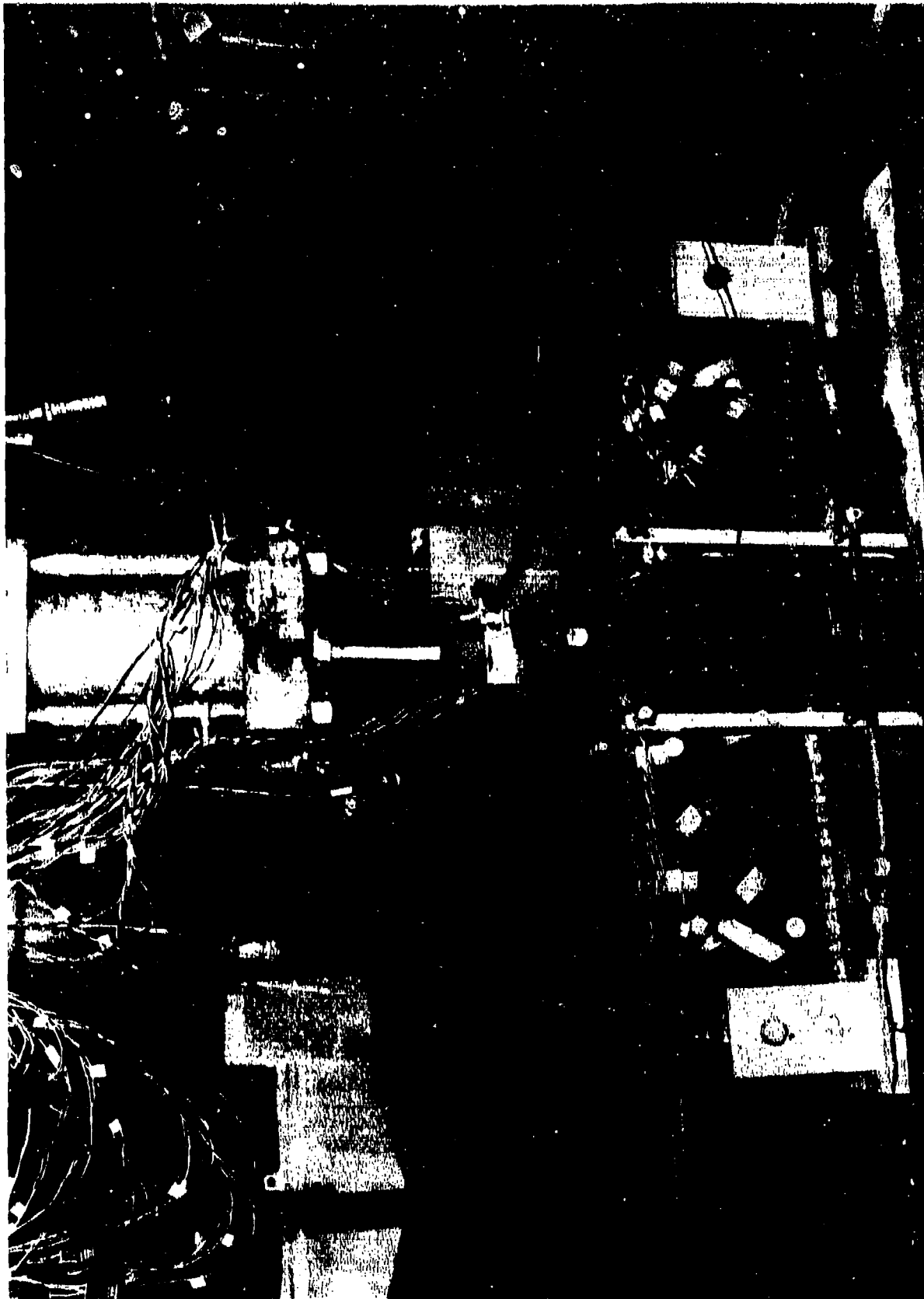


Figure 60. Test Setup and Failure of Flat Web Beam No. 2

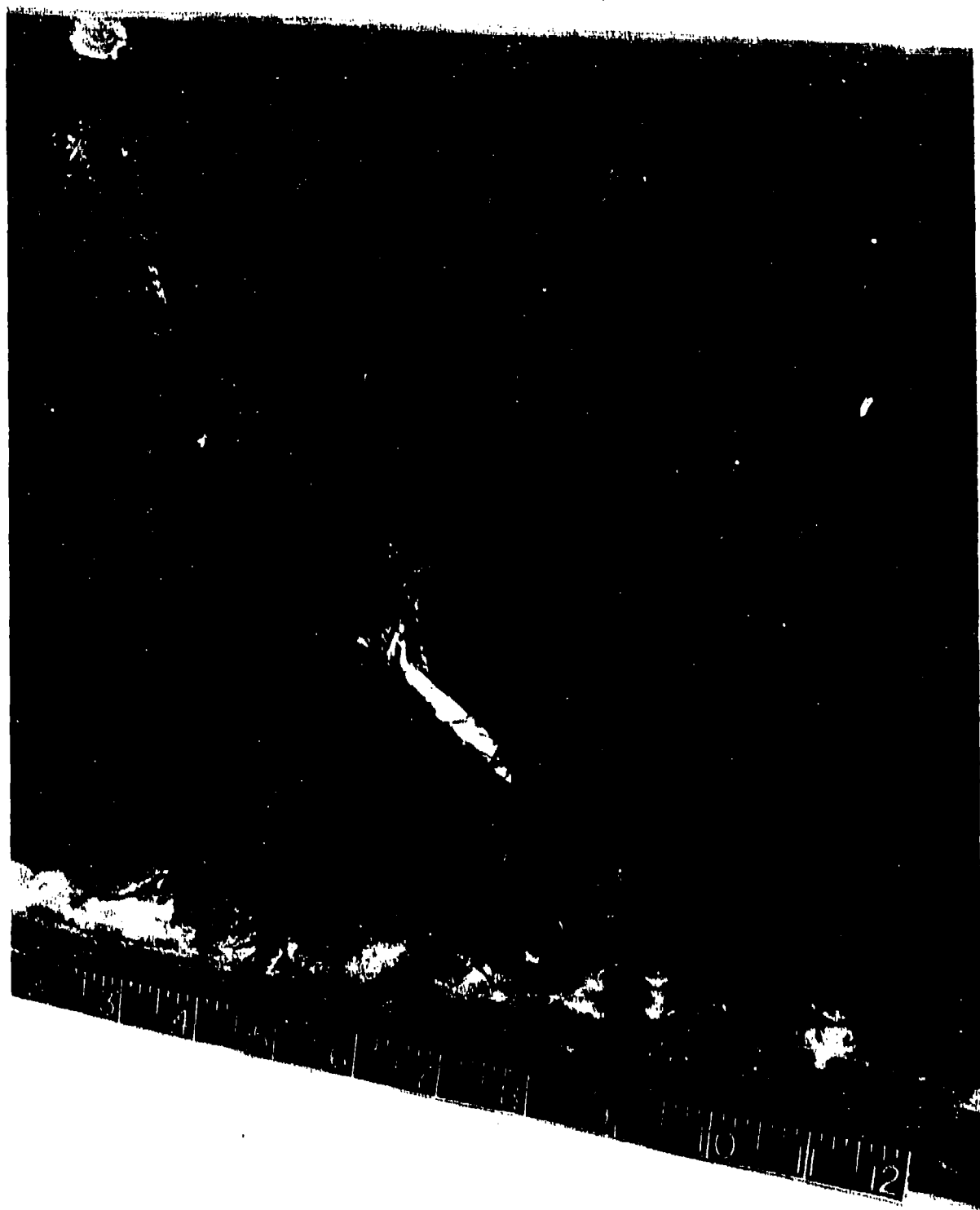


Figure 61. First Sine-Wave Beam - Web Failure

This was confirmed by taking the shear load  $V = 64 \text{ N}$  (14,400 lb) and distributing it over the 0.406 (16.0 inches) estimated length. This gives

$$P/\text{UNIT length} = \frac{14,400}{16} = (157.6 \text{ kN/m}) \text{ } 900 \text{ lb/in.}$$

Based on experimental test data of similar beam elements, it was determined that there is an allowable of approximately 157.6 kN/m (900 lb/in.)

The first and second flat web beam failures (see figures 60 and 61) were in the web at 45 degrees with respect to the centerline, as would be expected with a shear beam specimen. The first flat-web beam failed at a web shear flow of  $q = 675 \text{ KN/M}$  (3854 lb/in.) which is 110 percent of predicted failure, whereas the second beam failed at  $q = 556.7 \text{ kN/m}$  (3179 lb/in.) which is 91 percent of predicted failure.

The failures resulted from the compression component of the shear flow; hence, the strain of the middle leg of each beam rosette (oriented parallel to the 45 degree direction) was plotted in order to determine the reason the second beam failed at a lower-than-predicted shear load.

Typical load-versus-strain graphs for both the first and second flat web beams are shown in figures 62 and 63. Because of the nonlinear behavior of the second beam gage (number 6), it appears that delamination occurred around the hole, thus lowering the compression allowable. This observation was reinforced by examination of the failed laminate area which revealed a very resin-poor section which would contribute to the delamination.

Test data evaluation of the four 102-cm (40-inch) beams indicated that all the specimens failed near predicted loading. In addition, the data evaluation confirmed the capability of the nonautoclave process to produce parts which meet the structural integrity for which they were designed. Porosity levels encountered in the beams did not significantly affect the static strength of the part as expected.

Selected physical and mechanical property tests on coupons extracted from failed beams were conducted. These property tests were required for the ongoing evaluation of manufacturing methods. The tests included physical testing for per-ply thickness, specific gravity, and fiber and void content. Mechanical tests included compression tests at 104°C (220°F) on coupons extracted from the flat web area of the beam. The results are presented in table XX.

The average thickness/ply of 0.0057 (spec. req.  $0.0052 \pm 0.003$ ) for 102-cm (40-inch) flat web beams is related to the excessive bulk previously encountered with the 976 fabric. While there are no specification requirements for specific gravity or resin content, the average fiber content volume of 61.3 percent is within the specification requirement of  $62.0 \pm 3.0$  percent. Micrographic examination of both the flat-web and the sine-wave web indicated that there was porosity in the web areas of the beams. The porosity, however, did not appear to adversely affect the static mechanical properties of the laminates as evidenced by the 102-cm (40-inch) verification bending beam testing and the coupon tests discussed in the following paragraph.

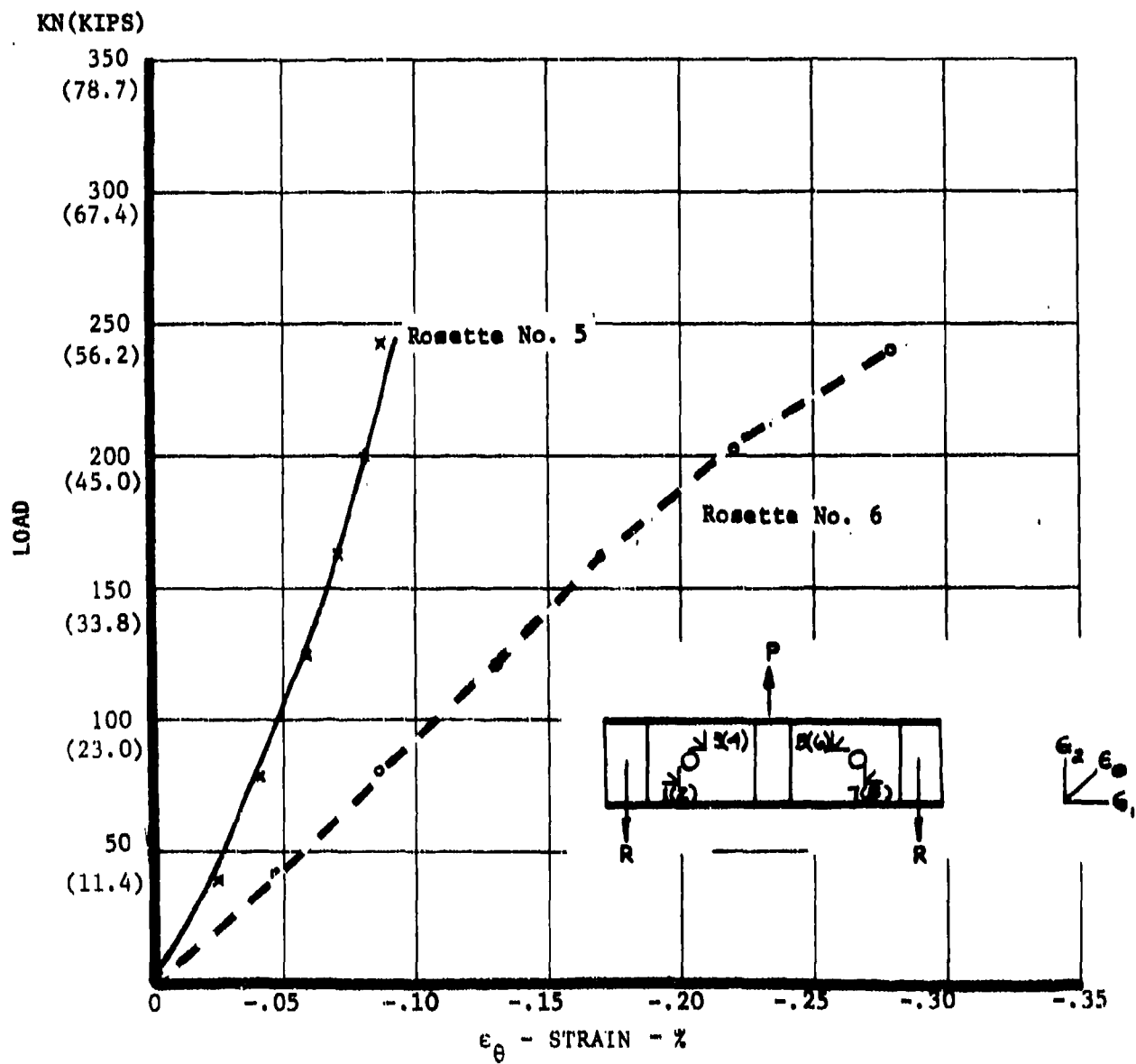


Figure 62. Load vs Strain ( $\epsilon_\theta$ ) for Flat Web Verification Bending Beam Specimen No. 2 (Rosette Nos. 5 and 6)

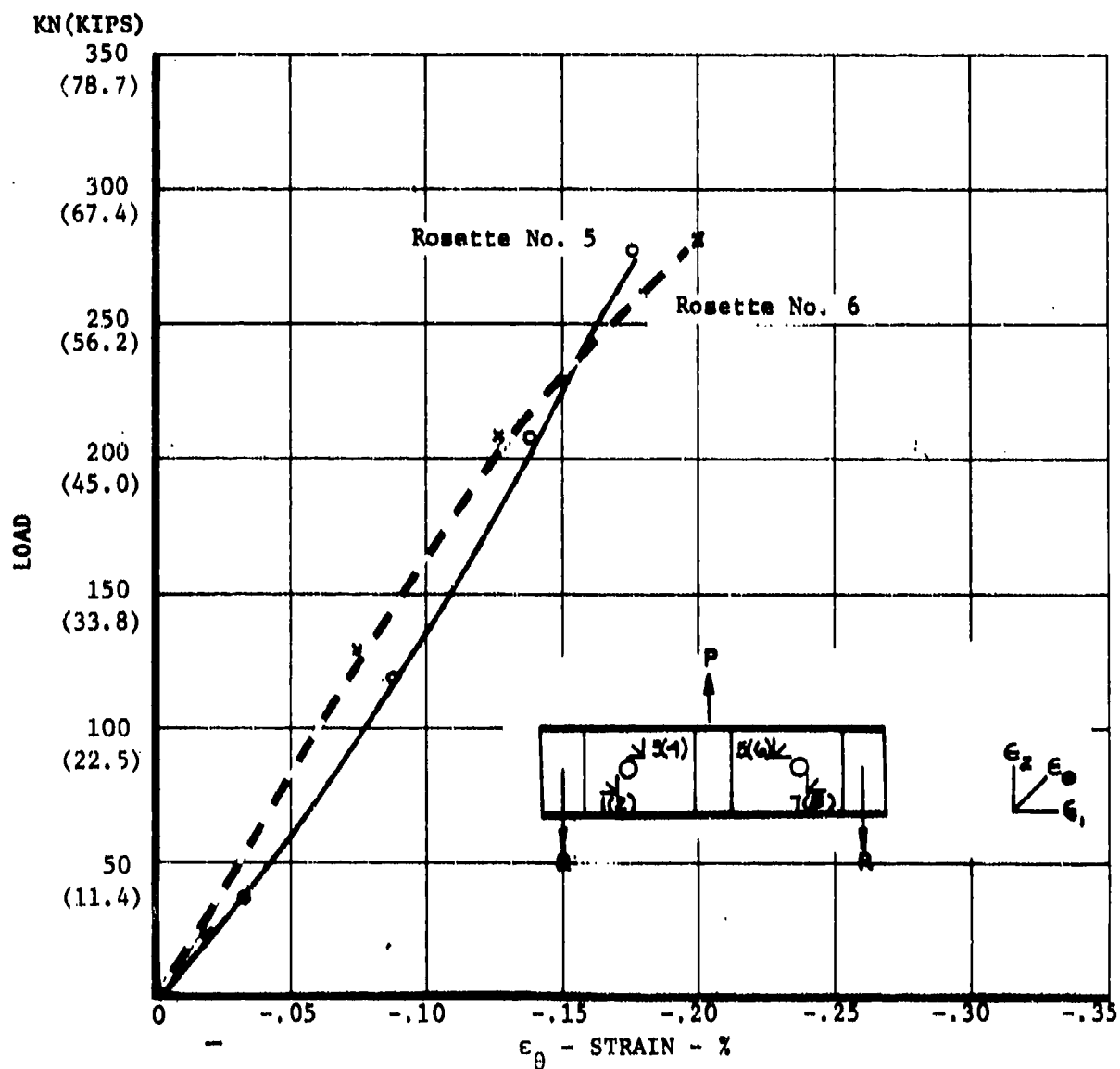


Figure 63. Load vs Strain ( $\epsilon_\theta$ ) for Flat Web Verification Bending Beam Specimen No. 1 (Rosette Nos. 5 and 6)

TABLE XX

MECHANICAL AND PHYSICAL PROPERTY EVALUATION  
40-1n. FLATWEB VERIFICATION BENDING BEAM COMPRESSION DATA

BENDING BEAM COUPON NO.	TEST TEMP (°F)	FAILURE (KSI)	AC-50 PREDICTED (KSI)	TEST PRED
1-1	RT	61.6	60.0	<u>0.97</u>
1-2		56.6		
1-3		61.7		
2-1		56.9		
2-2		57.3		
2-3	220°F	<u>56.0</u>	45.0	<u>1.08</u>
AVG		(58.4)		
1-4		49.0		
1-5		48.7		
1-6		49.3		
2-4	270°F	50.6		<u>1.02</u>
2-5		47.7		
2-6		<u>46.8</u>		
AVG		(48.7)		
1-7		45.2		
1-8	270°F	44.4		<u>1.02</u>
1-9		46.7		
2-7		44.4		
2-8		45.3		
2-9		<u>44.0</u>		
AVG		(45.0)		

NOTES: AS4/976 [0<sub>4</sub>/±45<sub>12</sub>/90<sub>4</sub>]

SP.GR = 1.57

RESIN CONTENT = 31.3%

FIBER VOL = 61.3% (SPEC REQUIREMENT 62.0 + 3.0%)



Room temperature (RT), 104°C (220°F), and 132°C (270°F) edgewise (90 degrees) compression coupon tests were conducted. The results of these compression tests showed very good correlation with predictions based on analytical models (AC-50 computer program). The average RT and 132°C (270°F) compression strengths of the laminates were within three percent of the predicted failure, and the 104°C (220°F) tests were within eight percent of predicted failure.

#### 4.1.3 ANCILLARY INVESTIGATIONS

##### 4.1.3.1 AS4/3501-5A Gr/Ep Material Evaluation

As a result of the presence of porosity in the 40-inch box beams fabricated from AS4/976 material, an investigation was conducted to determine if it was material related. A sample of net resin content AS4/3501-5A was received from Hercules and an all-tape, 10-inch Gr/Ep I-beam element was fabricated using the material. Prior to staging the element, the rheometric analysis of the resin was evaluated to identify the differences between the viscosity-versus-time profiles for the Fiberite 976 and the Hercules 3501-5A resin systems. The initial viscosity and viscosity profile during heatup of the 3501-5A were identical to that of the 976 fabric, as seen in figure 64. The differences lie in what happens at a resin temperature of approximately 82°C (180°F). The 976 viscosity continues to drop while the viscosity of the 3501-5A immediately begins to increase. The viscosity of the 976 resin does not begin to increase until a temperature of 104°C (220°F) is attained and, subsequently, the 3501-5A viscosity increases, as expected. This leads to a difference in the time for complete gel at 121°C (250°F): 145 minutes for the Hercules 3501-5A versus 235 minutes for the Fiberite 976.

Physical parameters for the Hercules AS4/3501-5A were established in order to verify the resin solids content, volatile content, and fiber a real weight. Fabrication of an AS4/3501-5A 25-cm (10-inch) flat web beam was subsequently initiated. The web configuration was [ $\pm 45/90$ ]<sub>2</sub> with a nominal thickness of 0.1587 cm (0.0624 inch). The web layers were placed in the staging tool and the fiberglass/epoxy load couplers, Gr/Ep fillers and caps were added as the tool halves were placed together. The beam was staged at 126°C  $\pm$  5.5°C (250°F  $\pm$  10°F) for 30 minutes prior to venting the outer bag and 15 minutes after venting. The staged beam was excellent in overall surface appearance and microscopic examination of a polished section revealed no porosity. The beam was subsequently cured for one hour at 177°C  $\pm$  5.5°C (350  $\pm$  10°F) utilizing vacuum pressure only. The cured beam had an excellent surface appearance, as shown in figure 65. A section of the beam was removed and polished. Microexamination revealed excellent compaction within the web area. Porosity was detected figure 66 only within the Gr/Ep filler area and was attributed to a lack of adequate resin to fill the interstices formed when twisting the Gr/Ep filler strips. This problem was remedied by the use of a higher resin content AS4/3501-5A Gr/Ep in the filler areas.

The configuration of the I-beam tooling did not contain provisions to prevent excess resin from flowing out of tool. This condition was aggravated by the fact that the 976 resin system maintained minimum viscosity for a long period of time. This allowed the resin to be drawn into the vacuum

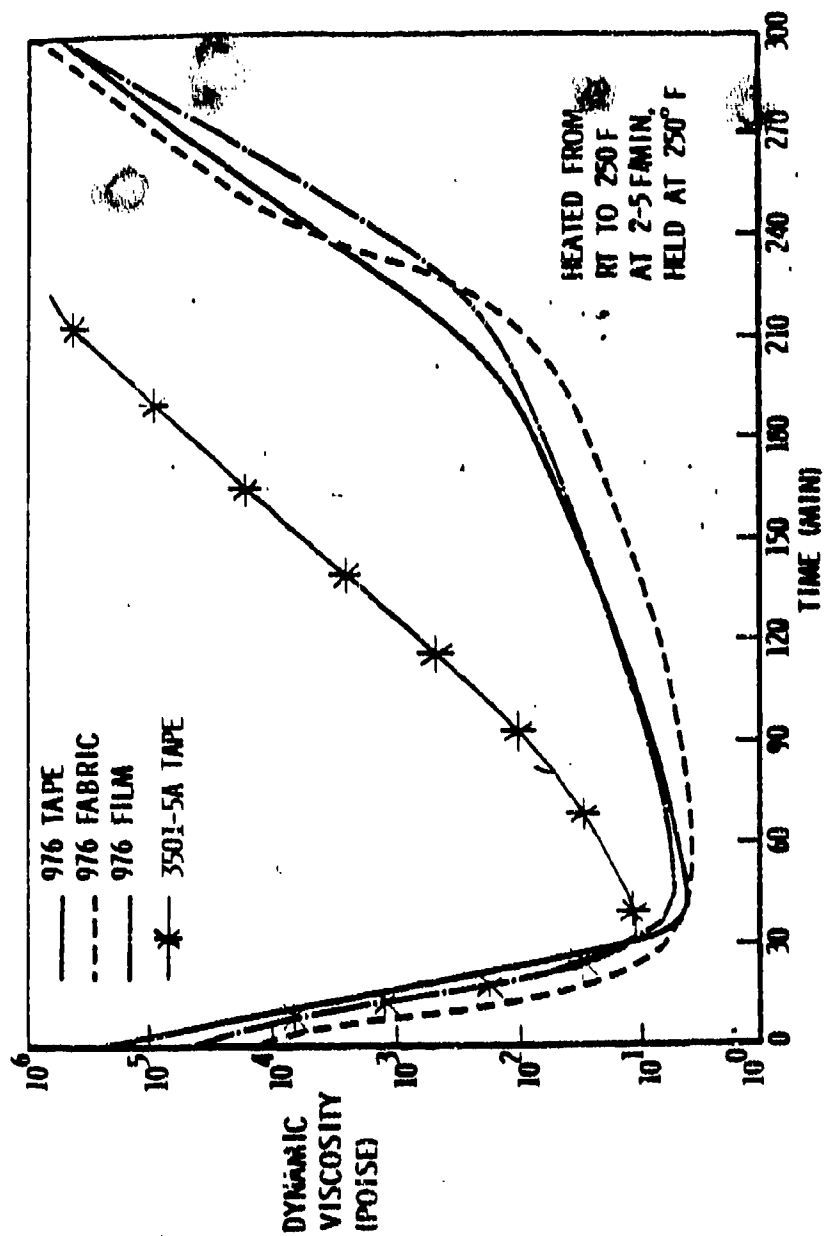


Figure 64. Comparison of Viscoelastic Staging Properties for Fiberite 976 and Hercules 3501-5A Resins

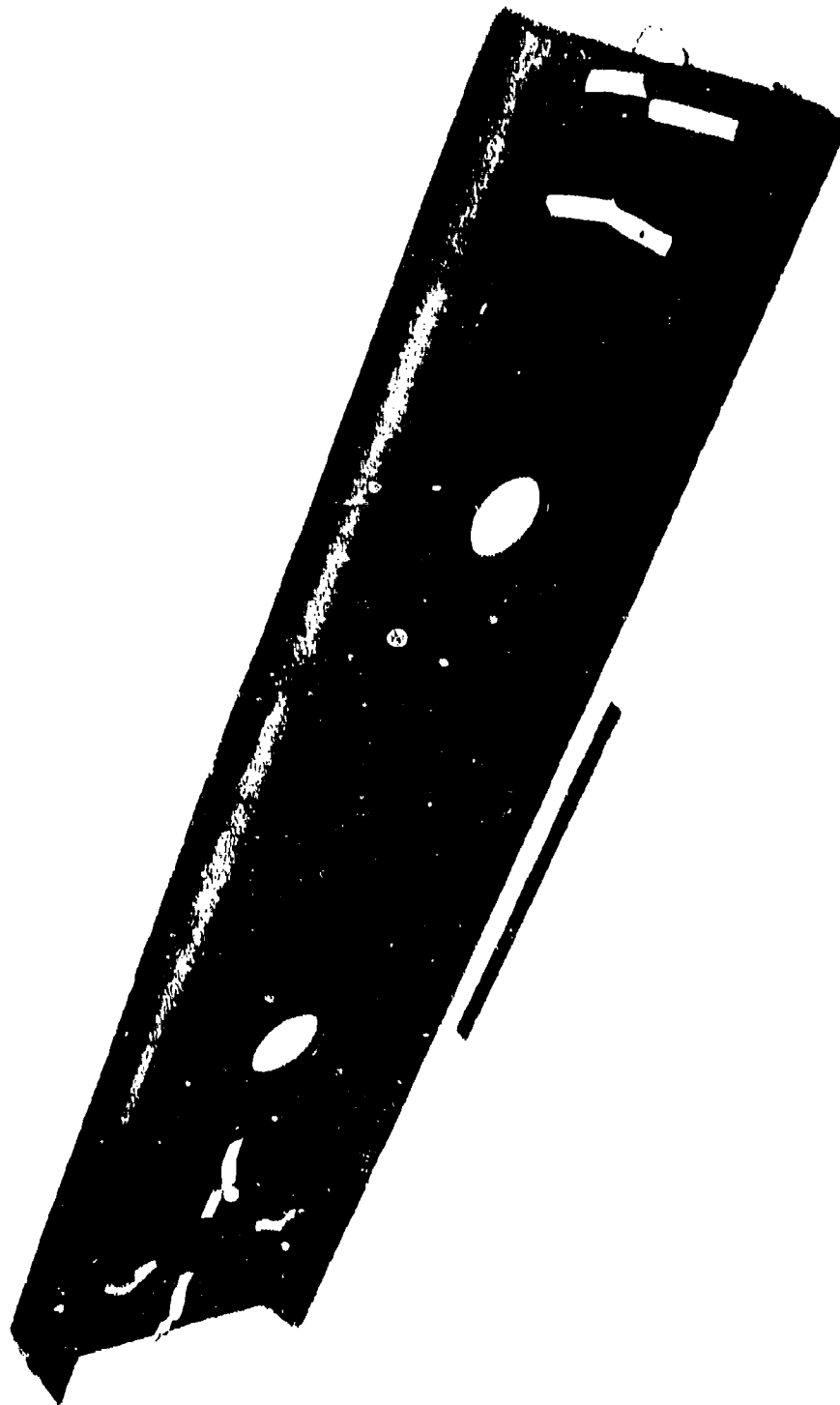


Figure 65. Staged 40-Inch Flat Web Beam (AS4/3501-5A)

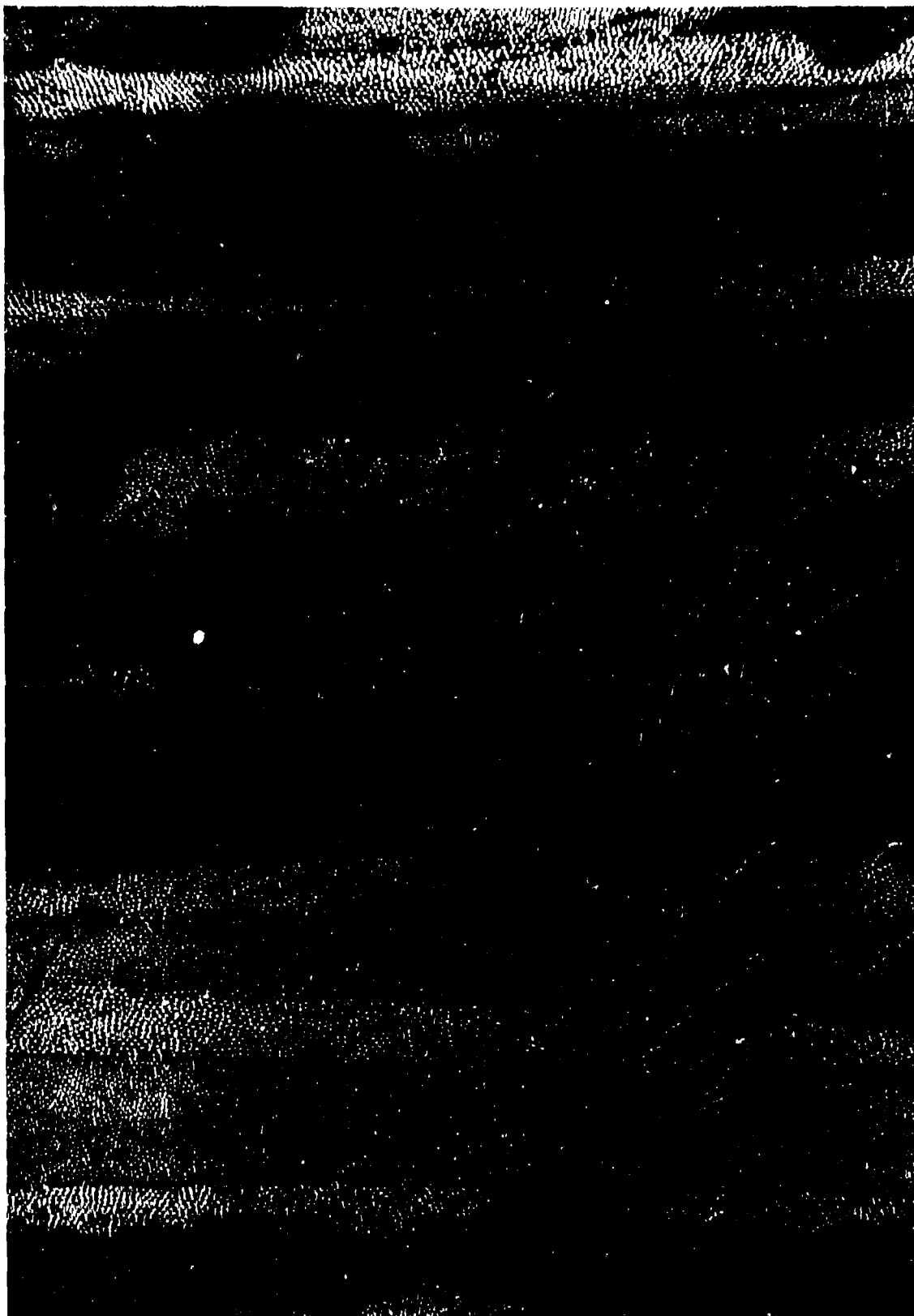


Figure 66. Microexamination (50X) of Staged 40-Inch Flat Web Beam  
(ASA/3501-5A)

lines creating resin starved areas. Because of this phenomena, it was decided that the Hercules AS4/3501-5A would be used in Phases II and III of the program. To further demonstrate the applicability of the Hercules system to the fabrication of larger structures, a 102-cm (40-inch) flat web beam was fabricated. The element was fabricated from net resin content AS4/3501-5A Gr/Ep tape prepreg.

The 102-cm (40-inch) fiberglass box tool proof element, fabricated as tooling to support spraying of the cure bladder molds, was altered to accommodate the addition of the staged flat web element. The entire element was subjected to  $177^{\circ}\text{C} \pm 5.5^{\circ}\text{C}$  ( $350 \pm 10^{\circ}\text{F}$ ) for one hour under vacuum pressure to cure the flat web beam.

The overall appearance of the beam was very good. The loosened plies in the radius areas were remedied and the radius areas were smooth with an excellent overall surface appearance. A section of the beam was removed and polished. Microexamination of the section revealed porosity (see figure 67), although the porosity in the cured element appeared to be not as extreme as that in the staged element. Based upon the extreme difficulty involved with polishing staged or partially cured specimens because of fiber displacement/ distortion, resin removal/smearing, etc., it was concluded that the porosity levels of the staged and cured laminates were equivalent.

#### 4.1.3.2 Tooling Gap Evaluations

Three conditions may contribute to inadequate air/volatile removal: (1) insufficient minimum viscosity dwell-time selection (2) unacceptable breather system design, and (3) tooling/laminate interference which causes positive pressure application on the laminate.

Investigations of each of these three parameters were conducted to isolate the critical factor. Based on NAAO's extensive nonautoclave processing background and processing experience data, the acceptability of the dwell time for an AS4/3501-5A laminate was verified.

For purposes of evaluating the breather system adequacy and comparing the 102-cm (40-inch) and 25-cm (10-inch) staging tools, 12-ply and 24-ply laminates were simultaneously staged in the 25-cm (10-inch) tool utilizing a breather system and a staging cycle identical to those used in the 102-cm (40-inch) box beam elements. Prior to staging the laminates were vacuum debulked at room temperature. After staging and sectioning, microexamination of the cured 12-ply and 24-ply laminates revealed no porosity in the 12-ply laminate (see figure 68), while a porosity gradient of acceptable-to-unacceptable was present across the 24-ply laminate, as shown in figure 69. The 25-cm (10-inch) staging tool had only one vacuum port located directly adjacent to the 12-ply laminate, possibly enabling more efficient removal of air and volatiles during the staging operation.

An additional vacuum port was added directly opposite the existing port in the 25-cm (10-inch) staging tool, and the 12-ply and 24-ply experiment was duplicated. The staged laminates were cured and sectioned which revealed no porosity in the 12-ply laminate, but the 24-ply laminate had an unacceptable level of porosity, as shown in figure 70.

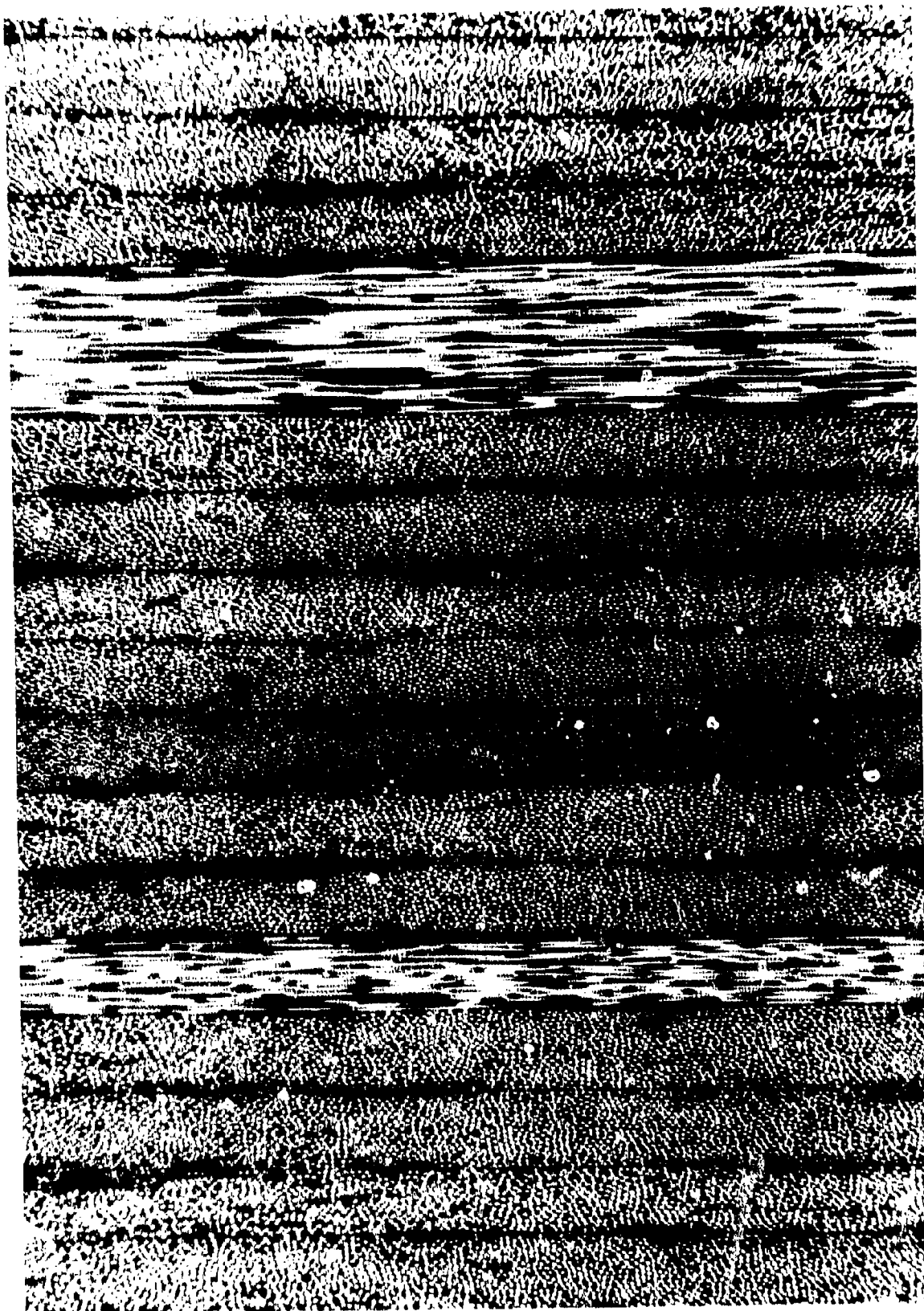


Figure 67. Microexamination (50X) of Staged 40-Inch Flat Web Beam  
(AS4/3501-5A)

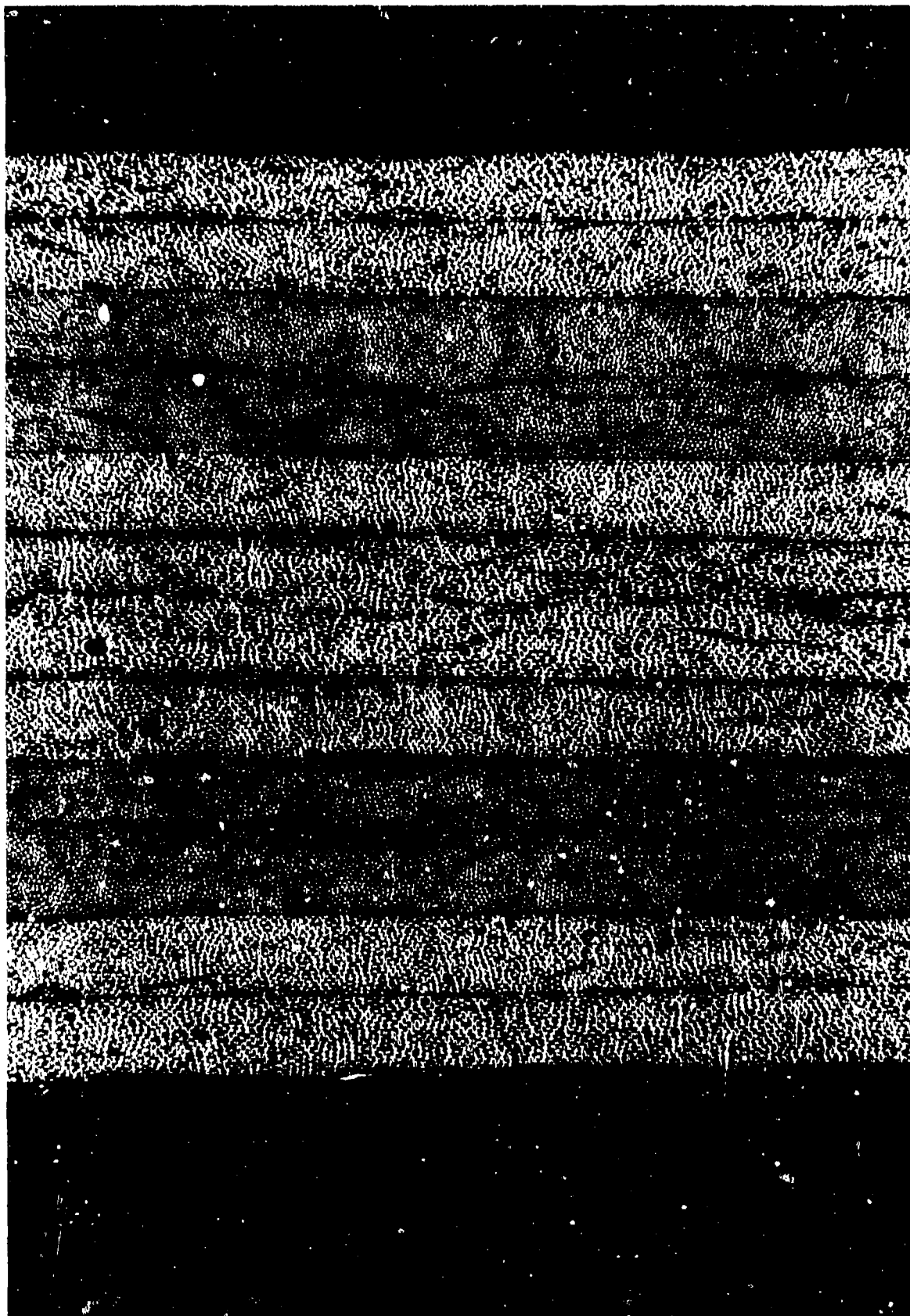


Figure 68. Cured 12-Ply Laminate Staged in 25-cm (10 inch) Tool with Breather System; No Porosity

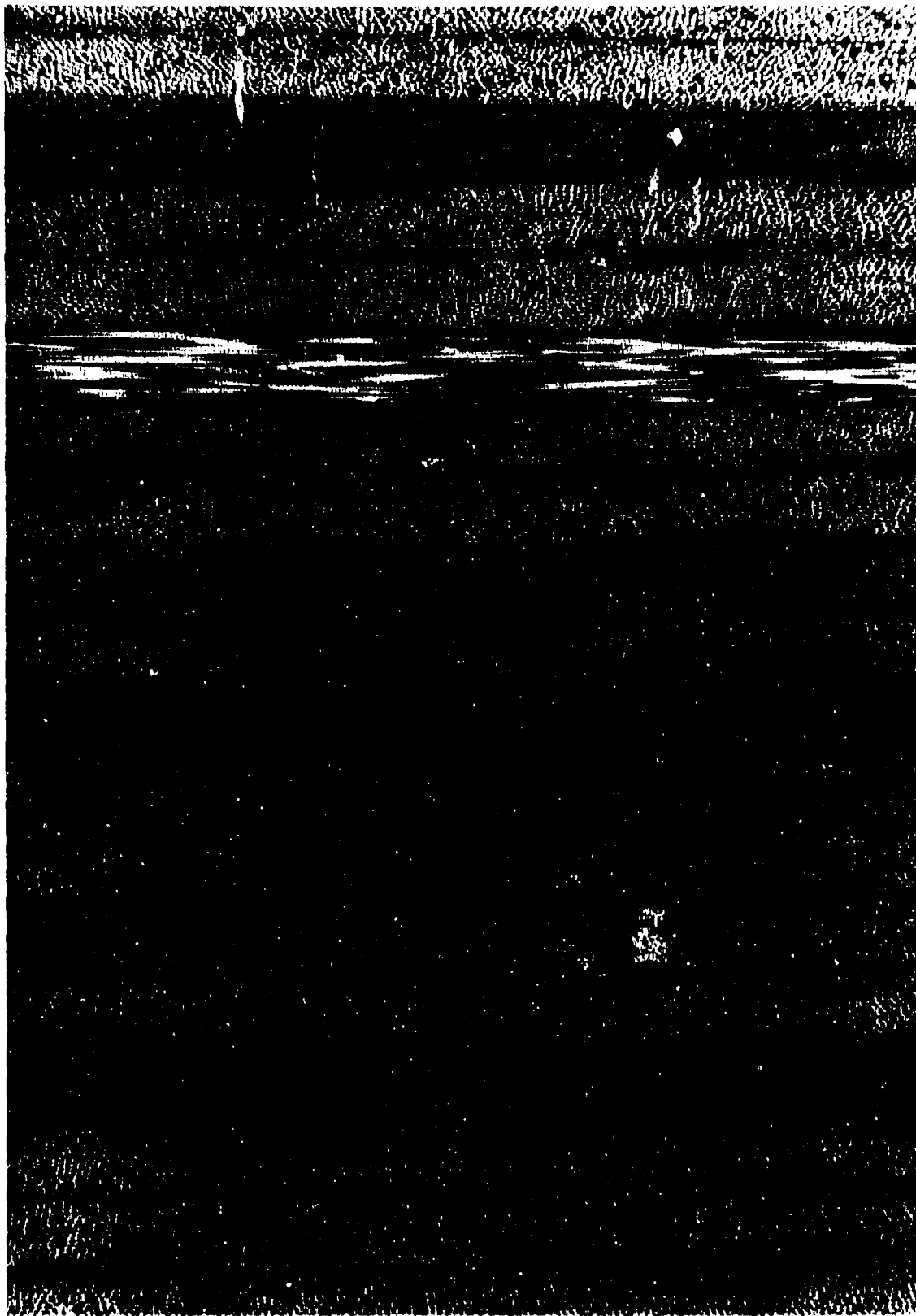


Figure 69. Cured 24-Ply Laminate Staged in 25-cm (10 inch) Tool with Breather System; Acceptable-to-Unacceptable Porosity



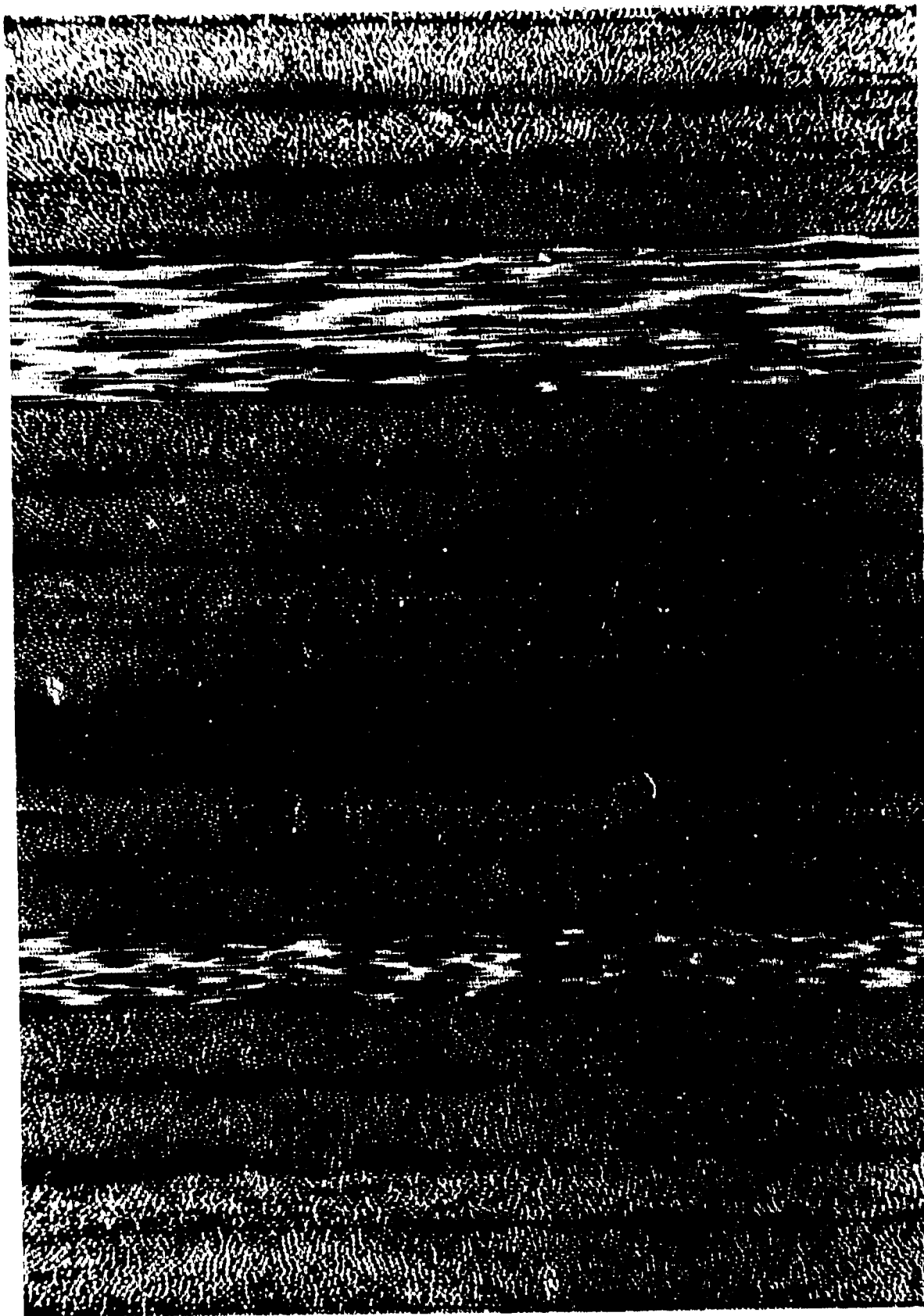


Figure 70. Cured 24-Ply Laminate Staged in 25-cm (10 inch) Tool with Additional Vacuum Port; Unacceptable Level of Porosity

Based on the results of this experiment utilizing the 25-cm (10-inch) modified tool, it was determined that the porosity in the 24-ply laminate was the result of pressure placed on the laminate by the thermal expansion of the rubber bladder mold during staging cycle. Pressure can prevent free expansion of the laminate, which in turn can adversely affect the migration of air and volatiles from the laminate. To eliminate laminate/bladder mold interference, the gap between the strongbacks was increased by adding a 0.152-cm (0.060-inch) compressible rubber shim to the flange area of each rubber bladder mold. The net increase in the gap between the strongbacks was 0.127 cm (0.050 inch) which resulted in a total gap of 0.051 cm (0.200 inch).

Using the 25-cm (10-inch) tool with an additional vacuum line as well as an increased gap between strongbacks, the experiment was duplicated. Micro-examination of the cured laminates revealed no porosity in the 12-ply laminate, and only a small amount of finely dispersed porosity (as shown in figure 71) in the 24-ply laminate (see figures 72 and 73).

The results confirm that positive tool pressure exerted on the laminate during staging caused the observed porosity. Additionally, the results indicate that a tooling gap-to-laminate thickness ratio of two-to-one is required to produce porosity-free laminate. Based on this assumption, the 102-cm (40-inch) tool was modified by: (1) adding three 0.152-cm (0.060-inch) compressible rubber shims to the flange area of each rubber bladder mold and (2) adding vacuum ports to the vertical channels.

The modified tool was utilized to simultaneously stage 32-ply and 40-ply laminates. After cure these laminates were microexamined and the results indicated no porosity in the laminates (see figures 74 and 75).

Studies were initiated to evaluate the possibility of creating a pressure differential within the 25-cm (10-inch) flat-web staging tool that would reduce thermal expansion of the rubber bladder molds. Two trials (using the 25-cm (10-inch) tools) were accomplished with 97.9 kPa (29 inches Hg) vacuum in the outer bag, while reducing the vacuum in the inner bag. The first trial evaluated a 23.6 kPa (7 inches Hg) differential, while the second evaluated a 13.5 kPa (4 inches Hg) differential. The 12- and 24-ply laminates, staged with differential pressure, contained an unacceptable level of porosity. The use of differential pressure as a viable alternative was eliminated because of the inability of the reduced inner vacuum to accommodate adequate air/volatile removal.

Studies evaluated the effect of an increased tool gap on staging Gr/Ep sine-wave details. A 12-ply Gr/Ep tape 25-cm (10-inch) web section with no flanges was staged in the 25-cm (10-inch) sine-wave web tool with an increased gap. The web section was subsequently cured and micro-examination revealed no porosity (see figure 76).

A Gr/Ep tape/fabric hybrid (8 plies of tape and 2 plies of fabric) sine-wave section was fabricated. Microexamination after curing found it to be porosity free. A complete tape/fabric hybrid 25-cm (10-inch) sine-wave beam was then fabricated. The web section was wrinkle free and the overall

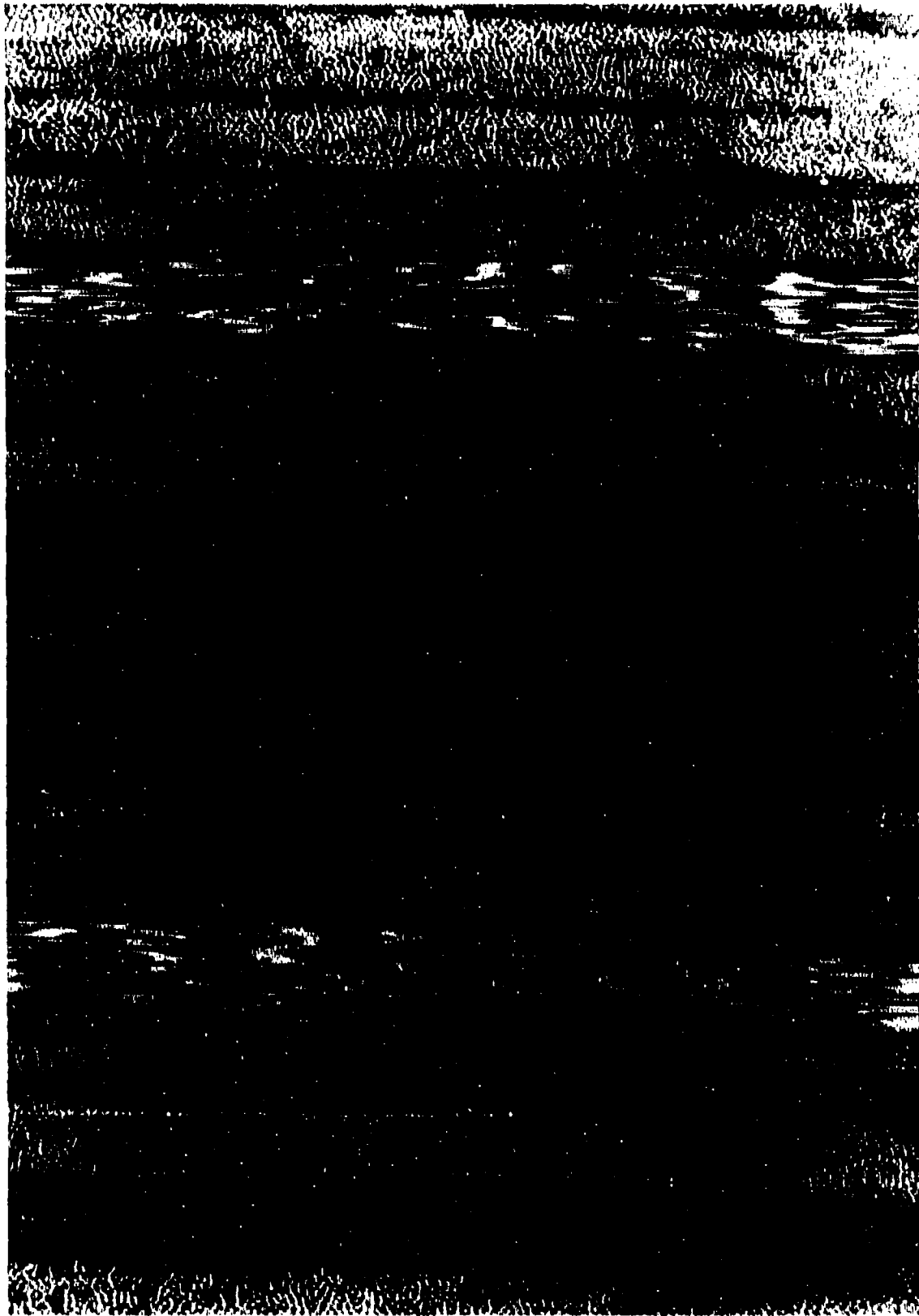
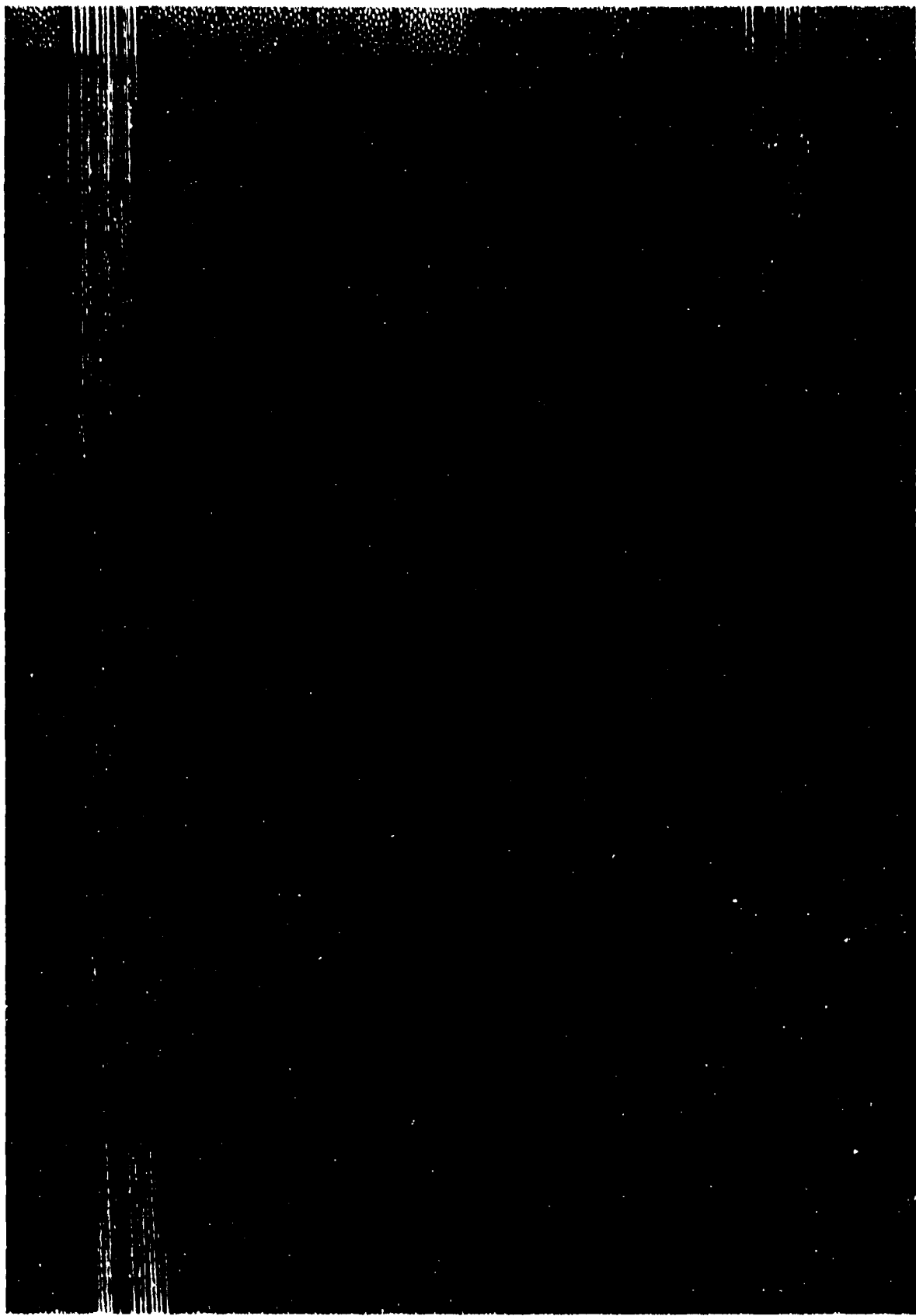


Figure 71. Cured 24-Ply Laminate Staged in 25-cm (10 inch) Tool with Additional Vacuum Line and Increased Gap; Finely Dispersed Porosity



Figure 72. Photomicrograph of Cured 12-Ply 25-cm (10-inch) Patch Test Laminate; No Porosity; Trial No. 4



**Figure 73. Cured 24-Ply Laminate Stage in 25-cm (10-inch) Tool with Total Gap of 0.635-cm (0.250 inch); No Porosity**

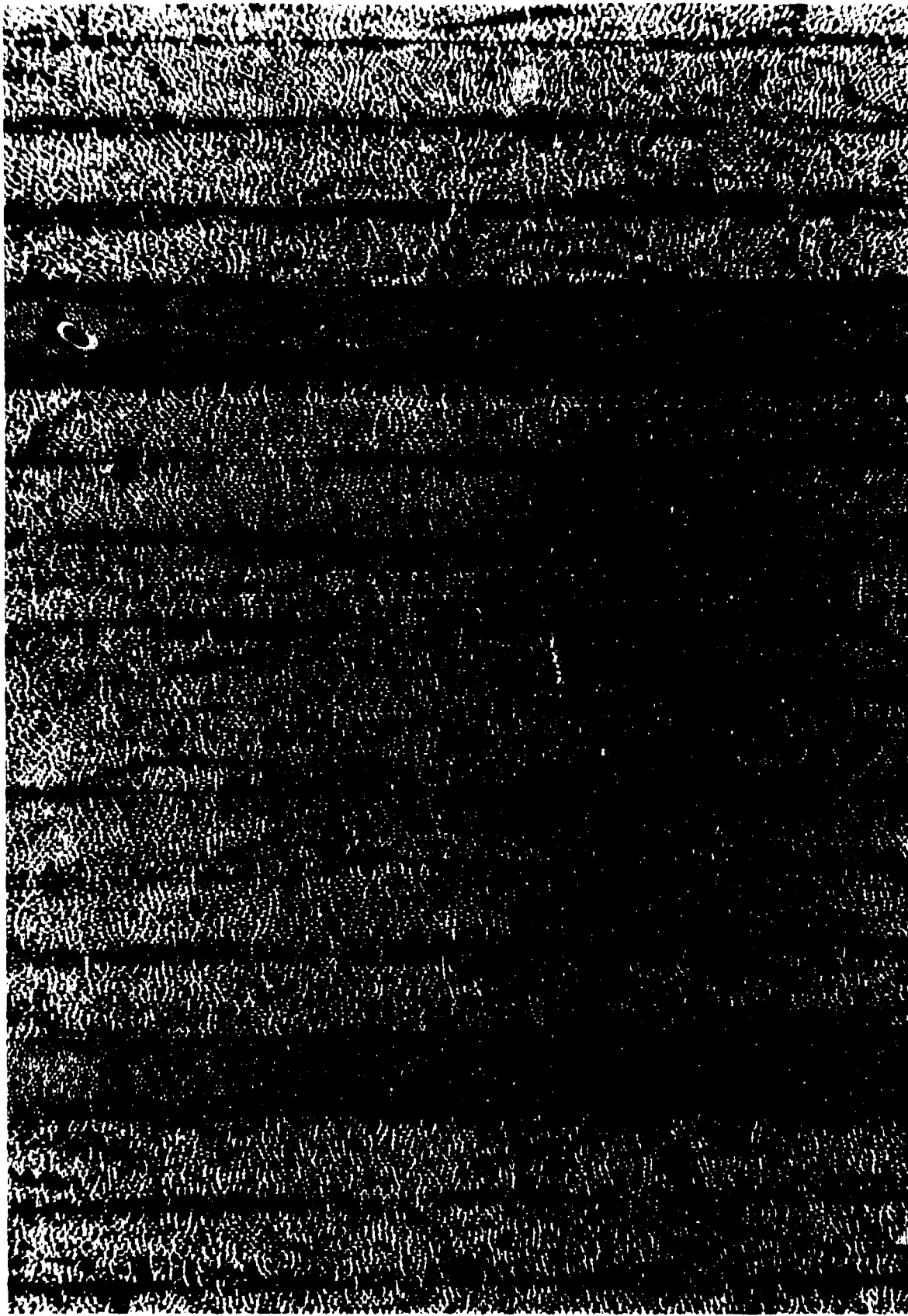
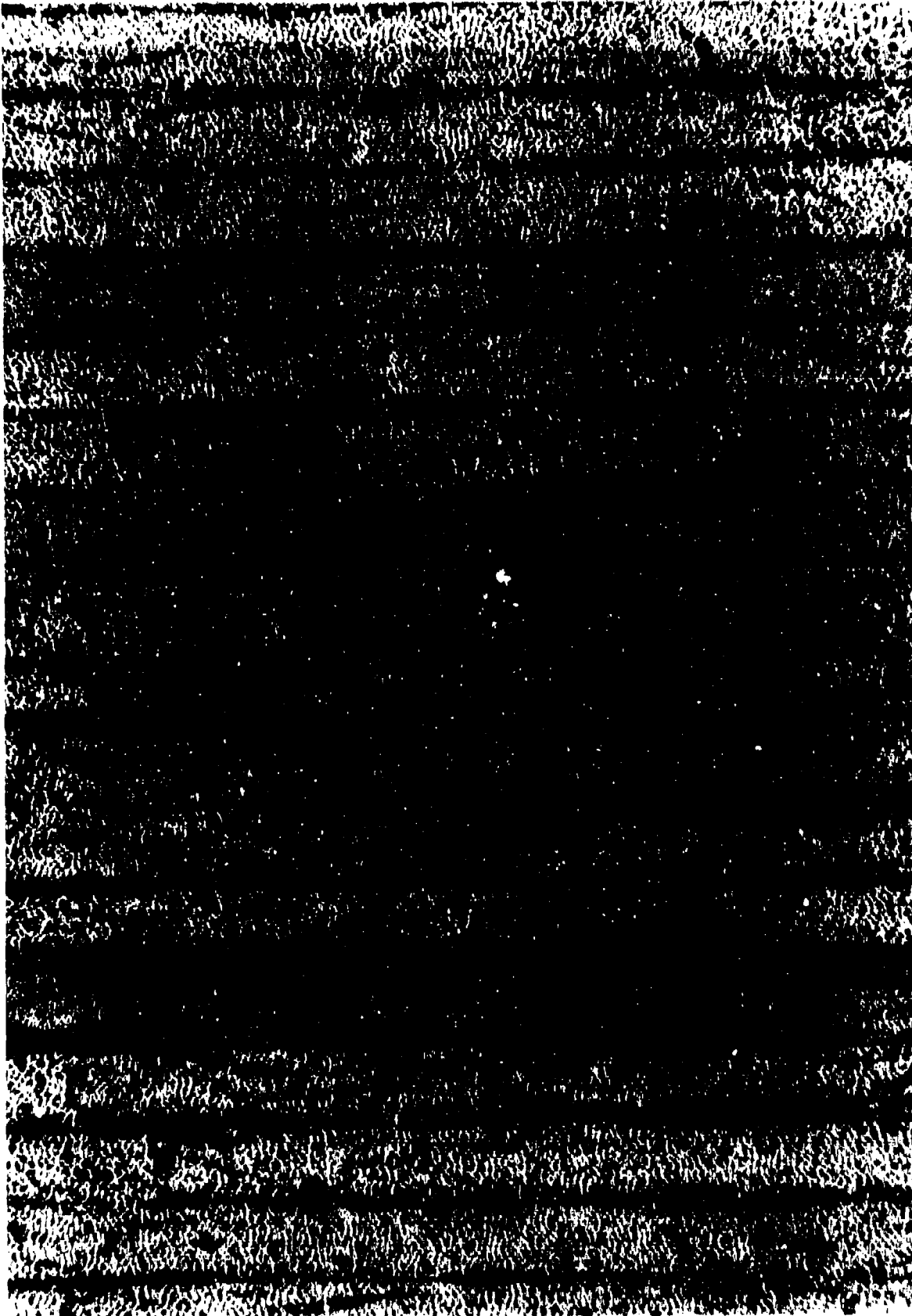


Figure 74. Cured 32-Ply Laminate Staged in 102-cm (40 inch) Modified Tool;  
No Porosity



**Figure 75. Cured 40-Ply Laminate Staged in 102-cm (40 inch) Modified Tool;  
No Porosity**

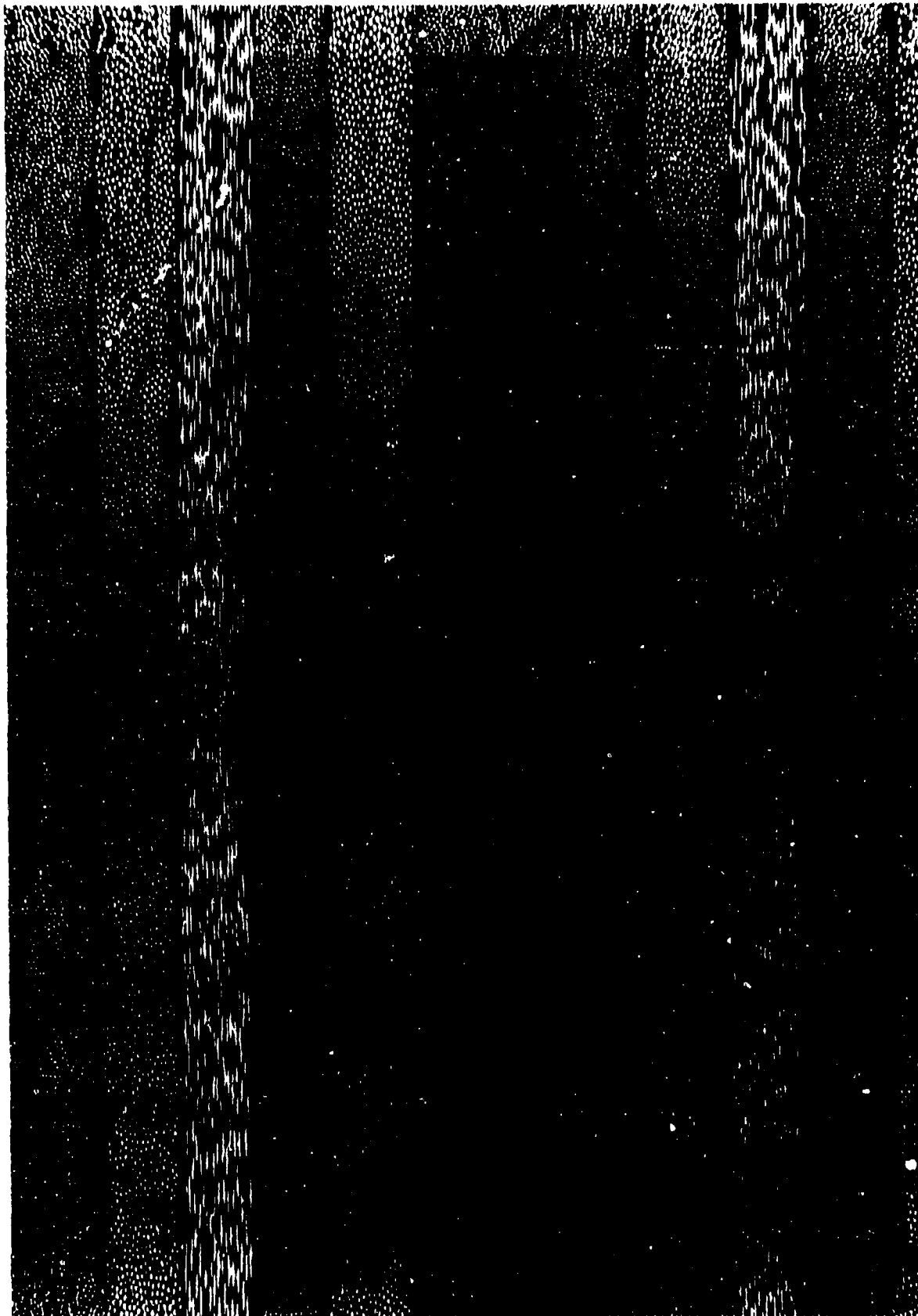


Figure 76. Sine Wave Web Section; 12-Ply Tape and Fabric; Cured in Stage Tool with 2 x Gap



surface appearance of the beam was good, although there was some resin buildup in localized radius areas on the load coupler because of inadequate pressure in the outermost plies only. This kind of porosity has been previously noted and is associated with the reduced resin content of the fabric.

The result of these investigations proved that an improper gap was the cause of the observed porosity in the larger 40-inch box beam elements fabricated from AS4/976 and tested. The tooling parameters established here were utilized in the remainder of the program.

#### 4.1.3.3 AS4/3501-5A Gr/Ep Element Verification

To further evaluate the net resin (31 percent) graphite/epoxy AS4/3501-5A tape and fabric and the two-to-one gap-to-laminate ratio thickness, a 102-cm (40-inch) box beam element was fabricated. The box was identical in configuration and dimensions to the two boxes fabricated under Phase I of this program and utilized AS4/3501-5A graphite/epoxy in the beams and load couplers. In addition, staging tools were modified to accommodate the two-to-one tooling gap-to-laminate ratio that was determined during earlier experimentation.

The sine-wave web and flat web beams, ribs, and cover were staged using the same procedures as before. Staging operations for the sine-wave web and flat-web beams were satisfactory, and no major leaks were encountered during the process. Moreover, the sine-wave web had excellent radius definition and surface appearance. In the vertical plane, the sine waves appeared to have a few surface wrinkles created in the outer ply. There was no slippage of either load coupler on the filler material. Preliminary thickness and height measurements are comparable with the sine-wave beams previously fabricated.

The staged flat web beam also had excellent radius definition and surface appearance. Preliminary thickness and height measurements are comparable with previously fabricated flat web beams. Ultrasonic and contact pulse echo inspection of the details revealed that no porosity was present.

A further confirmation of the integrity of the nonautoclave process was validation of the fatigue strength of such components. Additionally, there was concern about the fatigue strength of integral structure, which up to this time had not been validated. To alleviate these two concerns, the flat web beam was removed from the box and fabricated into a test beam. After fabrication of the beam, it was moisturized to 0.87 percent by weight and subjected to a constant-amplitude fatigue test at 150°F and a static residual strength test-to-failure at 220°F.

The constant-amplitude fatigue test had an R-factor of 0.1 with a minimum applied load of 19,500 pounds. This represented 30 percent of the average static failure load of the previous beams. The beam successfully completed 272,000 cycles of loading, which is equivalent to two B-1A vertical stabilizer ribs, without failure or observable damage. Strain surveys, conducted at 1/2-life intervals, showed linear responses in all strain gages. Table XXI is a comparison of the test results of IR&D beam with the previously fabricated beams.

Table XXI

## RESIDUAL STRENGTH TEST RESULTS OF A NONAUTOCLAVE INTEGRAL STRUCTURE COMPONENT

Flat Web No.	Predicted	Test	Test Predicted
1 (contract)	11.70 kN (52,452 lb)	16.18 kN (72,000 lb)	1.37
2 (contract)	11.79 kN (52,452 lb)	13.35 kN (59,400 lb)	1.13
3 IR&D	11.79 kN (52,452 lb)	13.15 kN (58,500 lb)	1.12

After completion of the fatigue test, the static residual strength test at 220°F was conducted to beam failure at 112 percent of predicted strength. The failure initiated along a 45-degree line with respect to the web reference axis through the left reinforced cutout and then split away the upper and lower beam caps.

The maximum cap strain and the rosette shear strain (at the edge of the cutout) were 0.24 percent for the cap strain and 0.29 percent for the rosette shear strain.

Based on this test the conclusion is that both the integral method of fabricating structures (in which one cover is cocured to the substructure) and the nonautoclave method of fabricating structures meet the structural integrity requirements to which these structures were designed.

#### 4.1.4 SUMMARY PHASE I - MANUFACTURING METHOD VERIFICATION

Phase I, Manufacturing Method Verification, validated the nonautoclave manufacturing process through the fabrication and testing of structural elements representative of critical areas of Phase II and Phase III components.

Two 102-cm (40-inch) long, integral structure boxes containing a flat web and a sine-wave spar with integrally cocured covers and close-out ribs were fabricated using AS4/976 Gr/Ep. From these boxes, 102-cm (40-inch) verification bending beam test elements (two flat-web and two sine-wave web) were fabricated. Prior to testing, the elements were preconditioned to moisture levels to simulate predicted worst case moisture levels for the cover and substructure elements of the B-1 composite vertical stabilizer equivalent to those used during the Low-Cost Composite Wing/Fuselage Critical Component program which fabricated and tested similar beams using conventional autoclave techniques.

After preconditioning, the elements were subjected to static test to failure. Test data evaluation of the four 102-cm (40-inch) beams indicated that all of the specimens failed at predicted loading. In addition, the data confirmed the capability of the nonautoclave process to produce structurally acceptable parts.

Selected physical and mechanical property tests on coupons extracted from the failed beams were conducted as a requirement of an ongoing evaluation of manufacturing methods. These tests included physical testing for per-ply thickness, specific gravity, and fiber and void content. Mechanical tests included compression tests at 104° (220°F) on coupons extracted from the flat-web area of the failed beam. The results of the compression tests showed very good correlation with predictions based on analytical models.

Fabrication and fatigue test of a 40-inch box beam elements utilizing AS4/3501-5A Gr/Ep confirmed fatigue strength of the design and the ability to use AS4/3501-5A Gr/Ep in the remainder of the program.

In summary, the test and evaluation processes accomplished under Phase I provided a valid basis for fabrication of the stub box under Phase II and Phase III of the program.

## 4.2 PHASE II - MANUFACTURING METHOD SCALE-UP

Phase II of the program consisted of validating manufacturing methods and cost benefits through the fabrication of a scale-up section of the B-1B vertical stabilizer structure. The subcomponent was fabricated using the process parameters established in Phase I with production-type tooling. The subcomponent was nondestructively evaluated prior to structural testing. Cost tracking and economic analysis of the process to validate initial cost benefits projections continued throughout Phase II.

After fabrication and nondestructive inspection and evaluation, the component was structurally tested under representative loading conditions. A structural test plan comprised inspection requirements, static test loads, environmental conditions, instrumentation, and the test procedures necessary to determine the structural integrity of the stub box.

The test data from the nonautoclave-cured subcomponent was compared with data from tests of an autoclave-cured article (fabricated during a previous program) to evaluate the relative structural integrity of the nonautoclave-processed part. Figure 77 illustrates the task flow of Phase II.

Results of these tests and component evaluations were incorporated in the manufacturing plan and tooling approach for the fabrication of the Phase III full-scale demonstration article.

### 4.2.1 TASK 1 - FABRICATION OF SUBCOMPONENT

To demonstrate the high payoffs associated with the nonautoclave process, a scale-up portion of the vertical stabilizer structure was fabricated (figure 78). This section represented a portion of a full-scale vertical stabilizer and incorporated important design complexities:

1. Integral spar/cover design
2. Net molded substructure to match close out cover
3. Sine-wave and flat web integral components
4. Molded, reinforced hole penetrations in rib webs

The design complexities of the Phase II subcomponent permitted interrogation of the phase II major objectives to verify the high-cost payoffs of the nonautoclave approach and the fabricability of this large, highly-loaded, primary composite structure. The scale-up subcomponent selected for the proposed program was similar to the subcomponent fabricated and tested in support of the Low-Cost Composite Vertical Stabilizer Program under contract F33651-74-C-5164. The subcomponent was 287-cm (113-inches) long, 38-cm (15-inches wide, and 25-cm (10.0-inches) deep.

#### 4.2.1.1 Subcomponent Design

To simplify the design, a constant chordal height box was used to represent the vertical stabilizer construction. Detail drawings of this component are shown in figure 79.

The depth of this part was representative of the vertical

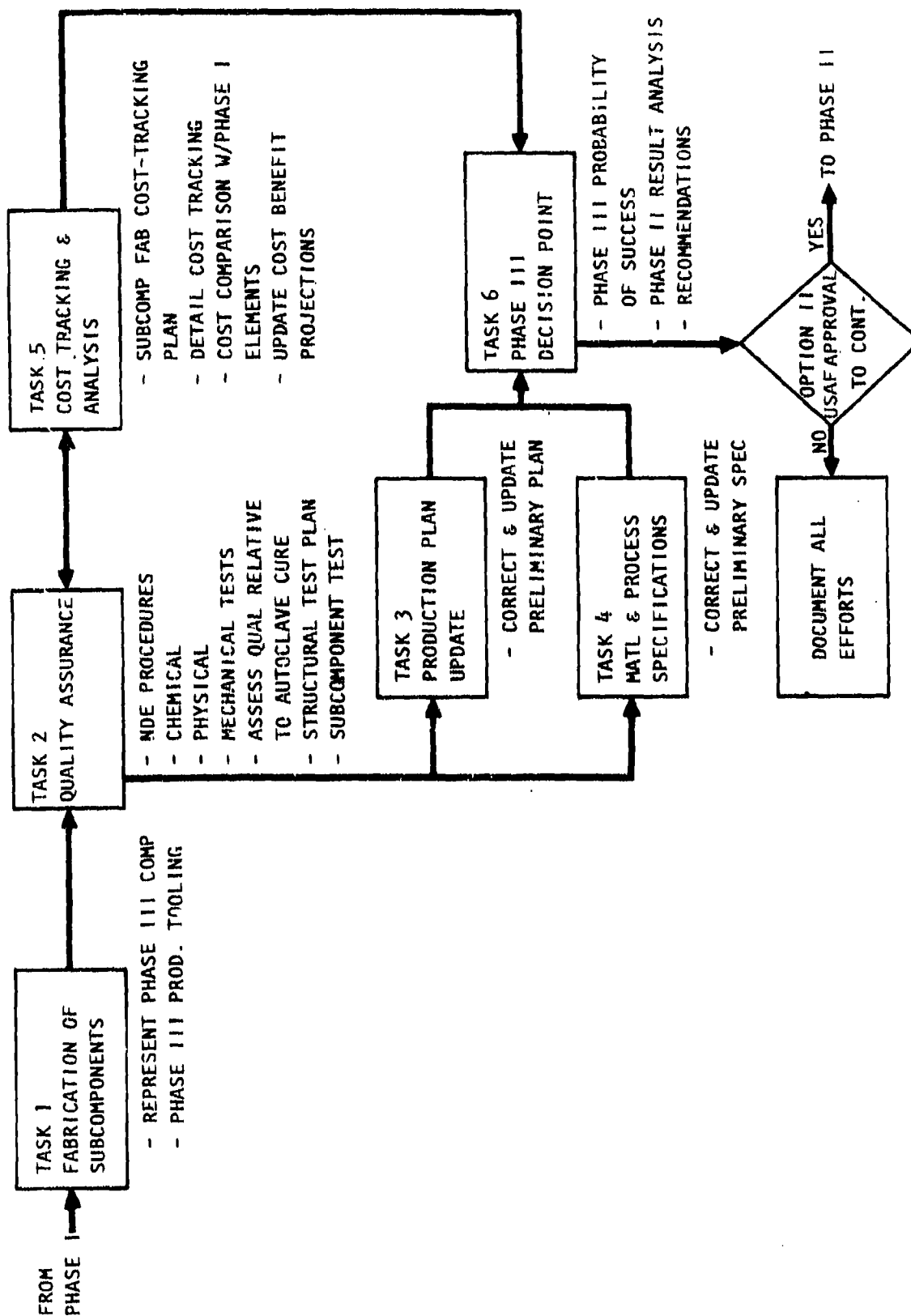


Figure 77. Phase II Flow Diagram

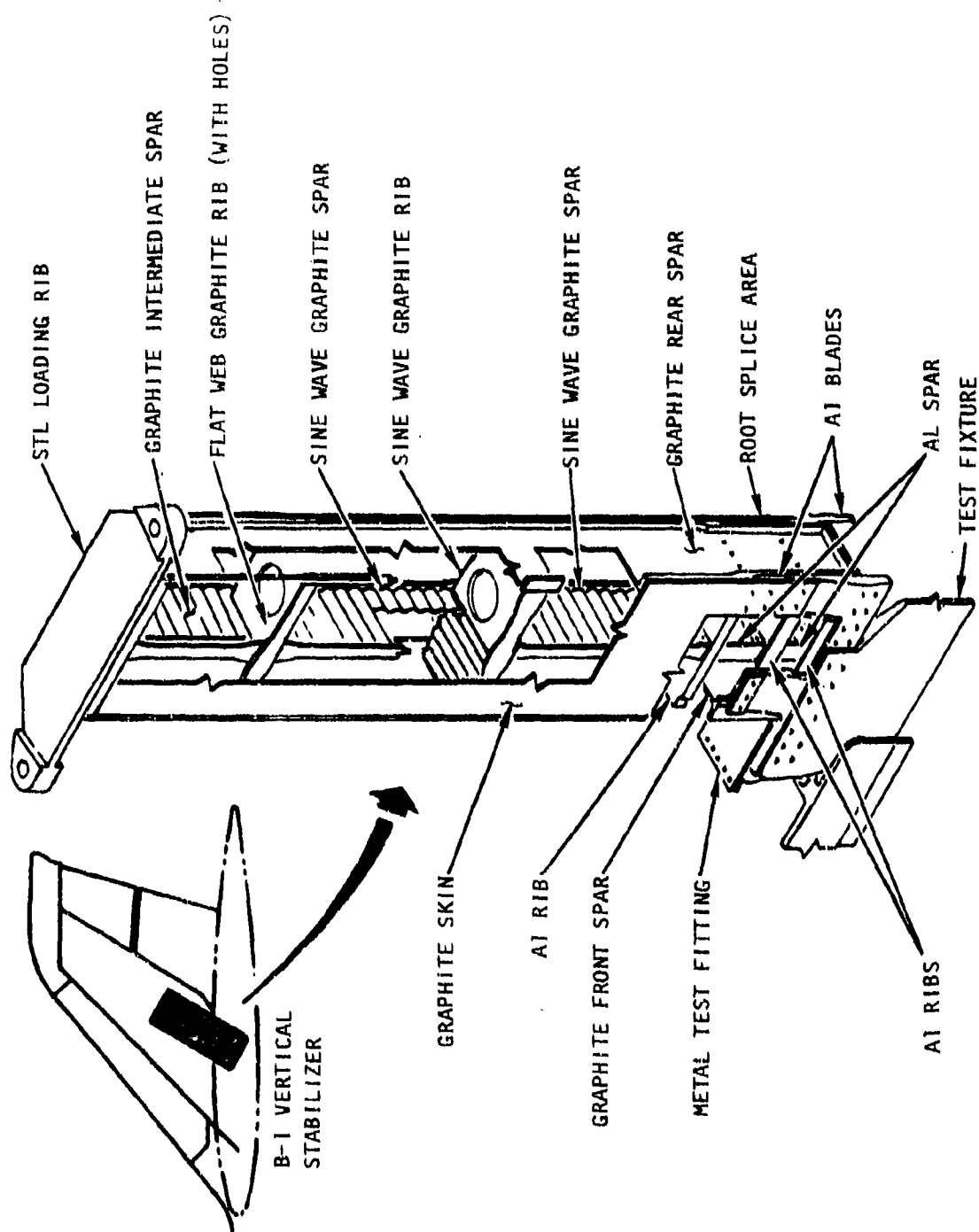
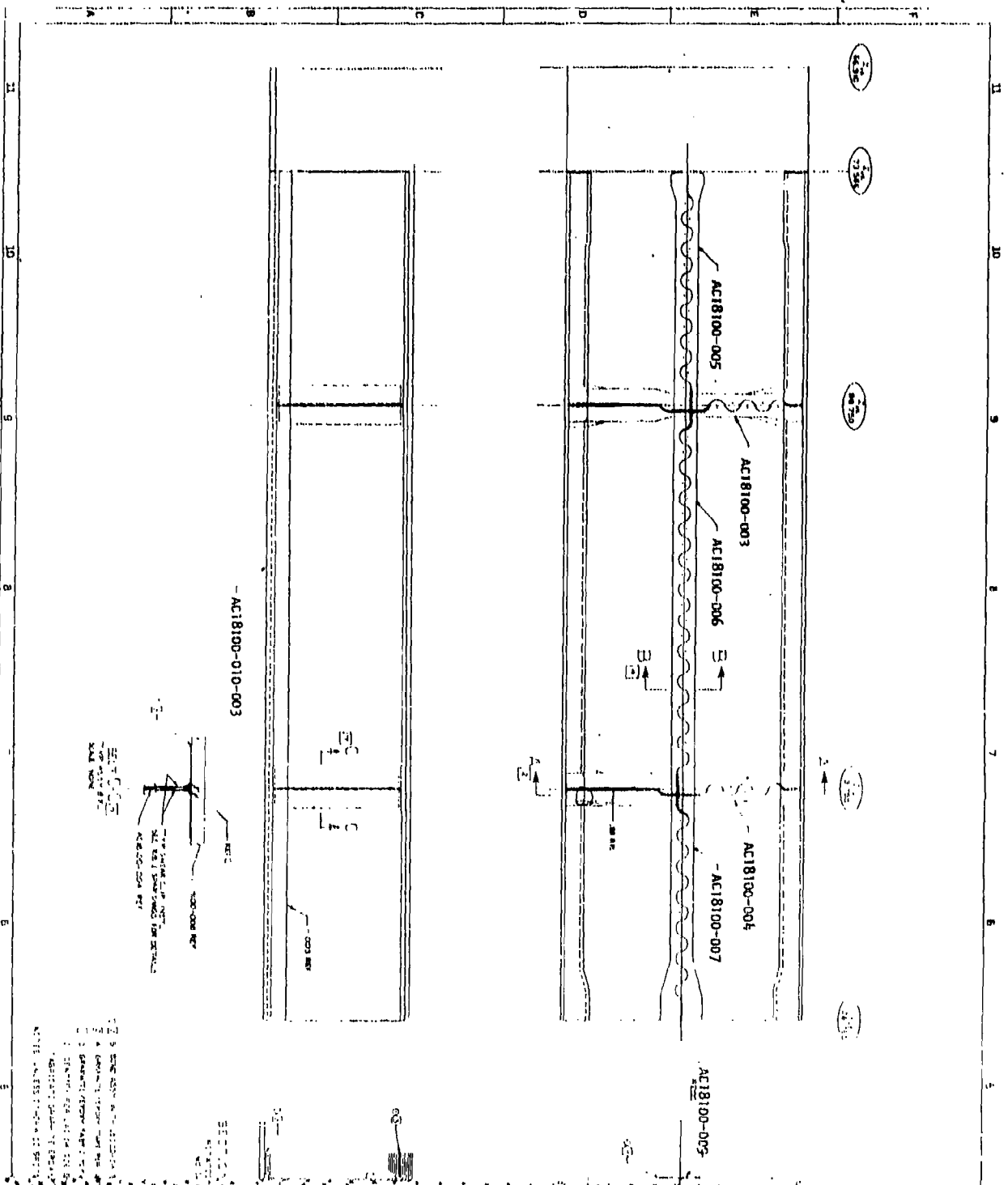
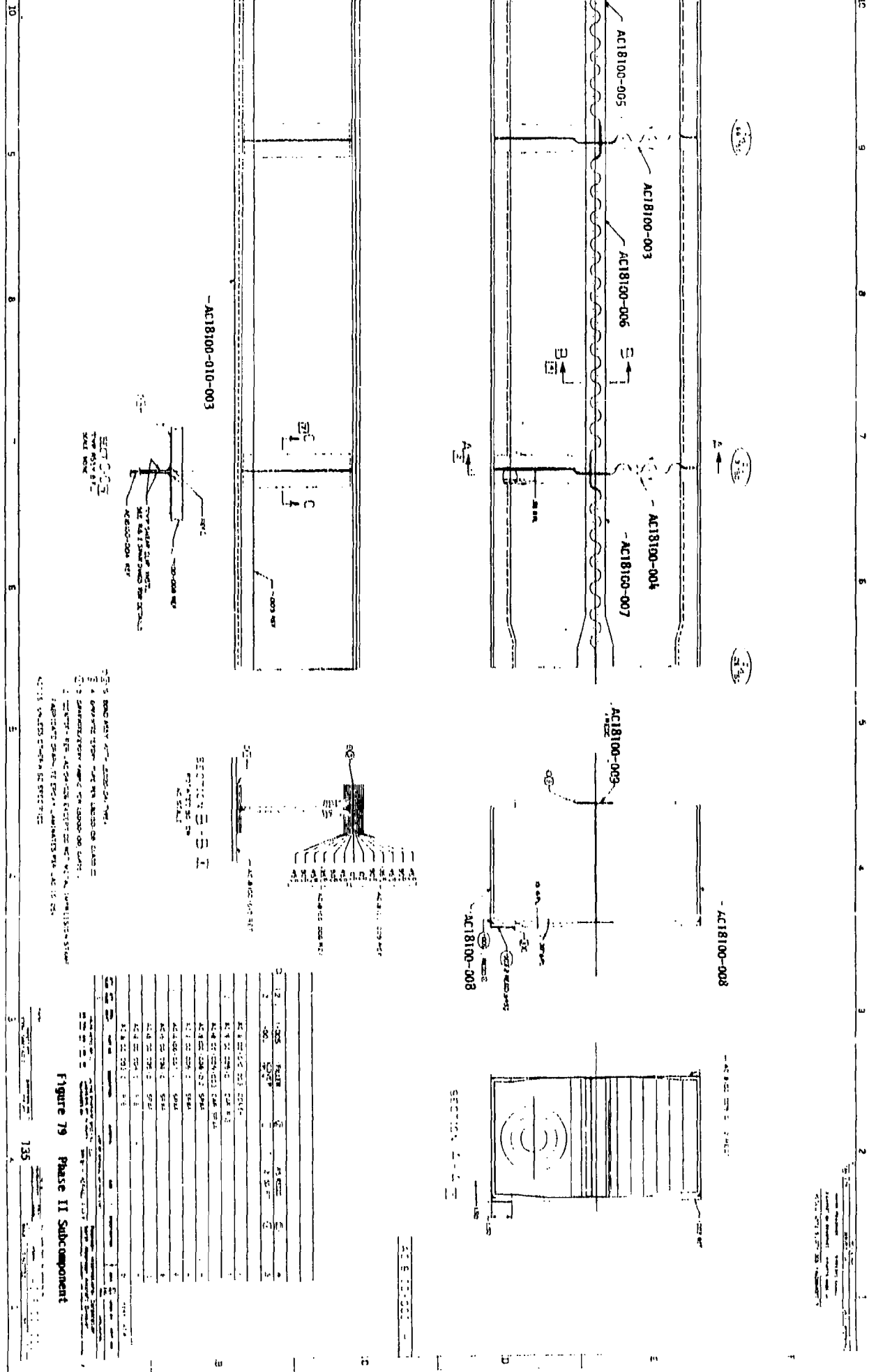


Figure 78. Phase II - Manufacturing Scale-up Test Box (Monotoclave Process Demonstration)



1. Name of the Project  
 2. Name of the Engineer  
 3. Name of the Designer  
 4. Name of the Checker  
 5. Name of the Approver  
 6. Date of Issue  
 7. Date of Revision  
 8. Date of Approval  
 9. Date of Completion  
 10. Date of Submission





stabilizer structure. The intermediate composite sine-wave spar lies on the centerline of the box. The front and rear spars were continuous composite C-beam design. Chordwise composite ribs were continuous from front to rear spars and were built integrally with the spars and one cover.

Features of the design for the Phase II subcomponent exercised key manufacturing and tooling approaches. The structure was of sufficient size and complexity to permit realistic assessment of potential manufacturing problem such as:

1. Prepreg outtime
2. Handling
3. Achievable heatup rates
4. Maintenance of intended shape
5. Dimensional tolerances
6. Integral composite box to aluminum root structure interface
7. Cost analysis
8. Tooling design and fabrication

The two covers measured 156.92-cm by 40.49-cm (61.78- by 15.92-inches) and tapered from 72 plies at the root to 48 plies at the tip. The lower 34.3 cm (13.5 inches) of the cover contained boron/epoxy in the zero-degrees plies which constituted approximately 45 percent of the laminate at the thickest portion. The covers were fabricated from graphite/epoxy (AS4/3501-5A) tape with boron/epoxy (AVCO 4 mil) in the root attachment end only. The upper cover was mechanically attached to the stub-box assembly while the lower cover was integrally bonded to the substructure. The forward and rear spars were C-channels and were also fabricated from AS4/3501-5A graphite/epoxy tape. The web area of the 25.4 cm (10-inch) high 139-cm (55-inch) long spar was 44 plies; the cap areas were 55 plies. The non-integral cap contained joggles to accommodate the rib caps. The intermediate spars and the two ribs were fabricated from graphite/epoxy tape prepreg with one outer ply of graphite/epoxy fabric prepreg.

The front and rear composite spars of the stub-box were analyzed to evaluate the graphite/epoxy integral cover design. This design differed from the baseline subcomponent (i.e., Composite Vertical Stabilizer (CVS) program) which had an aluminum rear spar. The nonautoclave stub-box design utilized an integral graphite/epoxy composite front and rear spar to demonstrate the integral structures concept. The rear spar was highly loaded and was strong enough to resist the failure loads of the blade-to-cover joint. The design ultimate shear flow (DUL) of the rear spar was 2294 lbs/in., and the CVS subcomponent failed at 160 percent of design ultimate load (DUL) resulting in a 3670 lbs/in failure load. Shear ultimate of the web was 8080 lbs/in and the buckling allowable was 5320 pounds per inch. This resulted in an allowable load that was 45-percent larger than the failure load of the original subcomponent. This high margin of safety in the spar ensured that failure would be initiated in the blade-to-cover joint, as in the baseline subcomponent thus ensuring comparative test results.

The two ribs were identical except for height because of the variation in cover thickness from the root to tip. Clips and upper and lower

flanges are cocured with the web. Half of the web was sine-wave; the other half was flat-web with a reinforced hole to simulate systems routing. The web area was 6-ply graphite/epoxy tape with the outer ply  $\pm 45$  degrees graphite/epoxy fabric. The web area increased to 16-ply around the access holes.

The three-piece intermediate spar was similar in construction to the ribs having a 6-ply web with the outer ply  $\pm 45$  degree graphite/epoxy fabric and local buildups to 16-ply at the substructure intersection areas. As with the ribs, shear clips and upper and lower flanges were integrally cured with the web. The upper cap was one piece spanning the three-piece spar.

All of the Gr/Ep details were fabricated from net resin ( $31 \pm 2$  percent) AS4/3501-5A graphite/epoxy tape prepeg. Where a ply of fabric was used, it was  $36 \pm 3$  percent AS4/3501-5A Gr/Ep.

Load couplers were used between the substructure and integral cover in the first bay between the base rib and the first outboard rib. The couplers assured that the integral joint was capable of transmitting any secondary out-of-plane bending loads induced in the area of the base rib from the cover to the substructure. The configuration was the same as that used in fabrication of the Phase I elements.

In the root splice area of the stub-box, the integral flat 44 ply graphite/epoxy front and rear spars were terminated and, through a mechanical joint, were attached to aluminum spars. The aluminum spars provided the required strength and stiffness for proper load introduction from the test fixture into the graphite/epoxy structure of the box. The joint between the graphite/epoxy and aluminum sections of the spar was analyzed for load transfer between the flanges. Relative stiffness between the spar and cover remained constant in the area of the splice. Therefore, it was only necessary to examine the load transfer between the two spar sections because there was no interaction with the cover. This resulted in a maximum bearing load in the graphite of 2610 pounds. The accompanying margin of safety of the flange splice joint was +0.58. The aluminum part of the joint had a high bearing allowable and was not as critical to the integrity of the joint.

In a comparison of the design of this subcomponent with that fabrication in the earlier program several dissimilarities were present. The major dissimilarity was that the substructure of the nonautoclave version was integral with one of the covers. The other cover (i.e., the close-out cover) was attached with mechanical fasteners as with the conventional composite subcomponent. On the original subcomponent, both covers were mechanically fastened to the substructure. The integral design concept incorporated other changes to the construction of the box such as two-piece composite front and rear spars, load couplers on the integral side, and integral joints between substructure elements. However, while these changes affect the construction of the box, there was no change from the original design in form, fit, or function. These requirements insured accurate data correlation between the two boxes.

#### 4.2.1.2 Tool Design and Fabrication

Tooling designs prepared for the detail staging tools and cocure tool incorporated the lessons learned during the Phase I development. The tooling bag-to-part gap ratio of 2:1 was incorporated in the staging tools and the use of cocure bags continued with a major improvement.

The basic tool sequence of using CAD generated templates to fabricate plaster master tools on which the fiberglass strongbacks were produced was continued in this phase.

Figure 80 shows the plaster tool masters for fabrication of one of the intermediate ribs. A total of four tool masters were fabricated. There was one tool for each of the three intermediate sine-wave spars and one tool for both of the ribs. The ribs are identical except for length. The staging tool for the rib details contained provisions for adjusting the fixture to hold the two sizes. A removable insert was used to alter the length from 39.2 cm (15.44 inches) to 36.9 cm (14.56 inches). Tooling for the front and rear spars was aluminum channel.

Utilizing the four completed fiberglass staging tool hardbacks, the silicone rubber bags were sprayed for the intermediate spars and rib tool. Conventional nylon bag material was used for the front and rear spars and covers. The rubber used for these bags was "D" Aircraft Products Compound No. 62, the recommendation from the material study which determined that this rubber compound provided the best strength and tear resistance (table XVI). The compound-62 rubber proved to be more durable than the compound 56 used in Phase I.

The lower rib staging tooling is shown in figure 81. Also shown in the photograph (left to right) are the fiberglass/epoxy tool proof parts and the two halves of the fiberglass strongback with the sprayed silicone rubber bags in place and the steel channel frame that surrounds the tools. Figure 82 is a photograph of the intermediate spar tooling and shows the two fiberglass hardbacks with the sprayed silicone rubber bags in place and the assembled steel frame.

The cocure assembly manifold (see figure 83) was mounted on a revolving mandrel to ease fabrication of the cocure bag. The base was 1.90-cm (0.75-inch) steel plate reinforced with two I-beams. The upper manifold assembly was 0.31-cm (0.125-inches) thick square tubing with a set of 0.31-cm (0.125-inch) diameter holes drilled on 5-cm (2-inches) centers along the length of the manifold. Vacuum ports were located in the base and manifold. The height of the cocured assembly is was controlled by the manifold.

The fiberglass tool proof articles fabricated from the detail staging tools were trimmed and assembled to form the tooling necessary to spray the cure bag as shown in figure 84. The front, intermediate, and rear spars and the two ribs were placed in the cure fixture without the cover to facilitate spraying the hard-to-reach areas of the spar/rib intersection. EA934 epoxy resin filled gaps and fillets to achieve a smooth transition surface between the part assembly and the tool.



Figure 80. Plaster Tool Master for Stub-Box Intermediate Rib

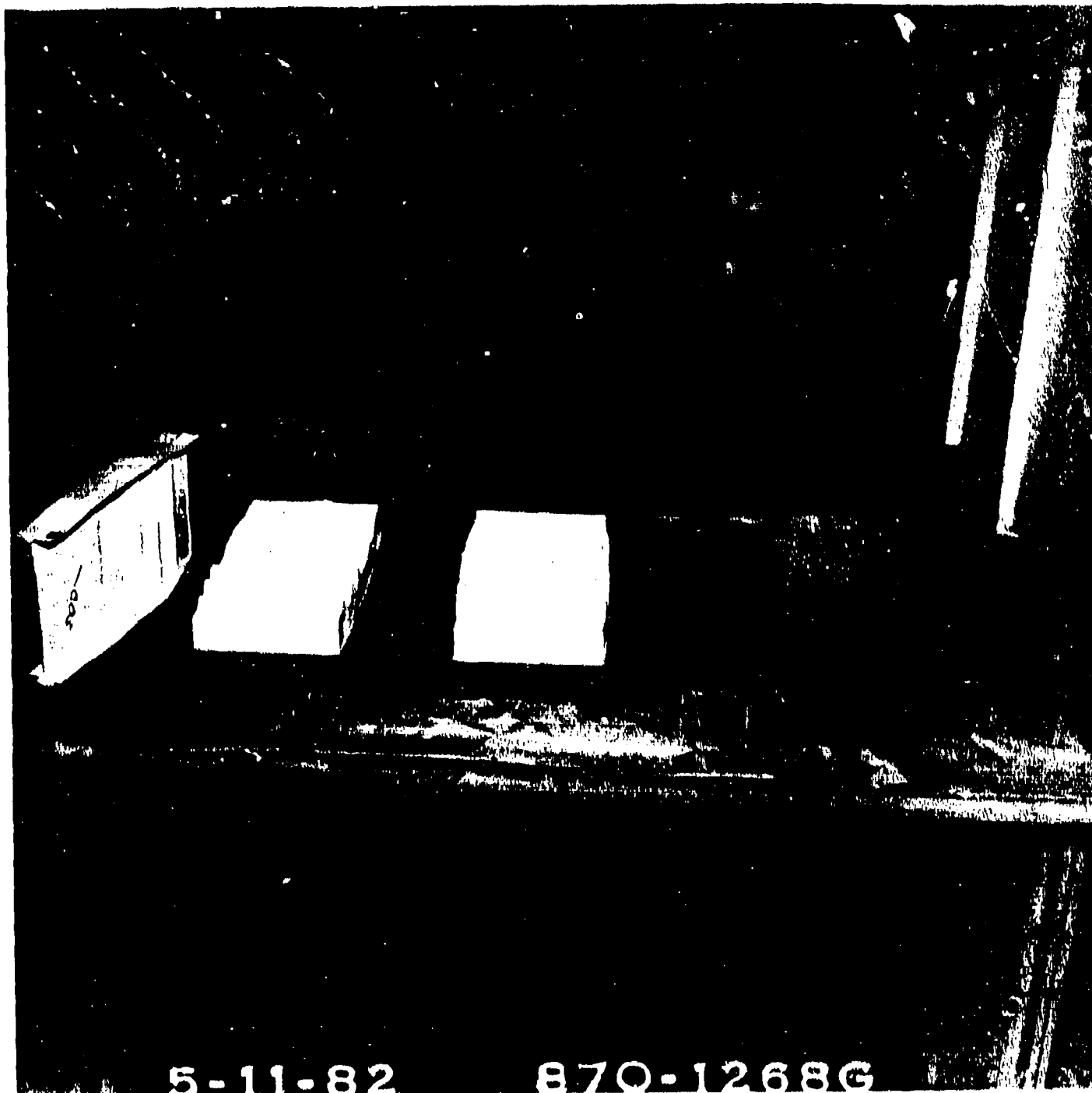


Figure 81. Lower Rib Tooling for Stub Box

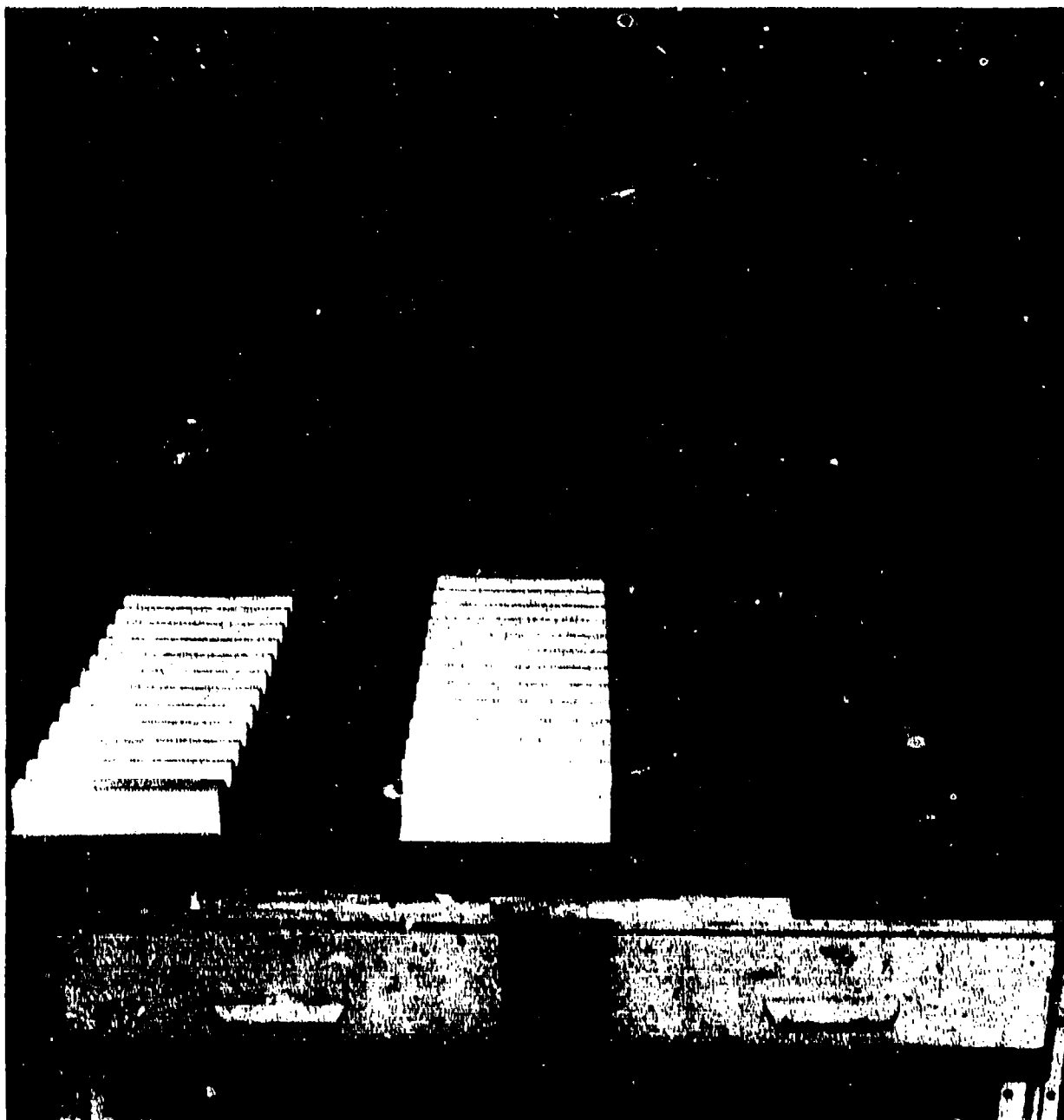


Figure 82. Intermediate Spar Tooling for Stub Box



Figure 83. Completed Stub Box Cure Too!



Figure 84. Subcomponent Cure Tool with Fiberglass Tool Proof Parts in Place



Unlike the three-piece cocure bag used to fabricate the Phase I 40-inch box beams, the Phase II subcomponent cocure bag was designed to be fabricated as one piece. The one-piece, multi-cell bag eliminated the need for sealing the seam along the top of the manifold thus reducing the sealing time required for installation of the bag and reducing the possible setups for leaks to develop. The bag was sealed only to the base plate using silicone adhesive. As shown in figure 85, expansion joints were used in the design to aid in the removal and installation of the bag.

The web areas of the cocure bag were sprayed to a thickness of approximately 0.38 cm (0.150-inches). After the web areas were sprayed, the lower cover and base of the tool were installed, and the spraying continued to form the lower cover area.

With the bag spray-up operation complete, the bag was cured according to the prescribed schedule shown in table XXII.

TABLE XXII. STUB-BOX CURE SCHEDULE

Air dry at room temperature	18 hours
Oven dry at 65.5°C (150°F)	4 hours
Oven dry at 93.3°C (200°F)	2 hours
Oven cure at 121.1°C (250°F)	2 hours
Oven cure at 165°C (330°F)	2 hours
Shut oven off and let cool	

The sprayed silicone rubber cure bag was cured and leak checked. Figure 86 shows the cure bag in place on the fiberglass tool proof part. The expansion joints are visible on the top of the manifold (in figure 85). These joints enabled the use of a one-piece bag for the six cells of the stub box; otherwise, as many as seven separate bags (one for each cell and one for the exterior) would be required and would entail intensive mechanical sealing techniques and greatly increase the risk of vacuum leaks which would ultimately affect the quality of the cured article.

On completion of the cure, the rubber bag was inspected using a static arc rod. Several small holes were evident and were repaired. Further inspection revealed several thin areas near the transition zones where the web and cap flanges joined. To eliminate problems during thermal processing, sprayable rubber compound without naphtha thinner was applied to build up the thin areas to the required thickness. Following this application, the bag was again subjected to cure and a thorough inspection showed the built-up areas to be acceptable. A coat of release agent (Dapocast 3200) was sprayed on the inner side of the bag.

#### 4.2.1.3 Subcomponent Detail Fabrication and Assembly

The same fabrication techniques used during Phase I were employed during this phase to layup the Gr/Ep material and form it onto the staging tools. After assembly of the tools, all details were staged using the prescribed cycle: RT to 250°F at 5-60°F/minutes hold for 30 minutes  $\pm$  15 minutes with vacuum drawn on both sides of the bag; release the vacuum between the bag and the tool to atmospheric pressure and maintain for 15 minutes, then cool down. A 14 psig positive pressure was found to be an aid in forming the sine wave details. Figure 87 shows the staged details prior to trimming. Figure 88 is a close-up view of one of the ribs. Notice the good surface finish and radii compaction of the web-to-cap transition. The reinforcement for the access hole is also visible in the photograph.

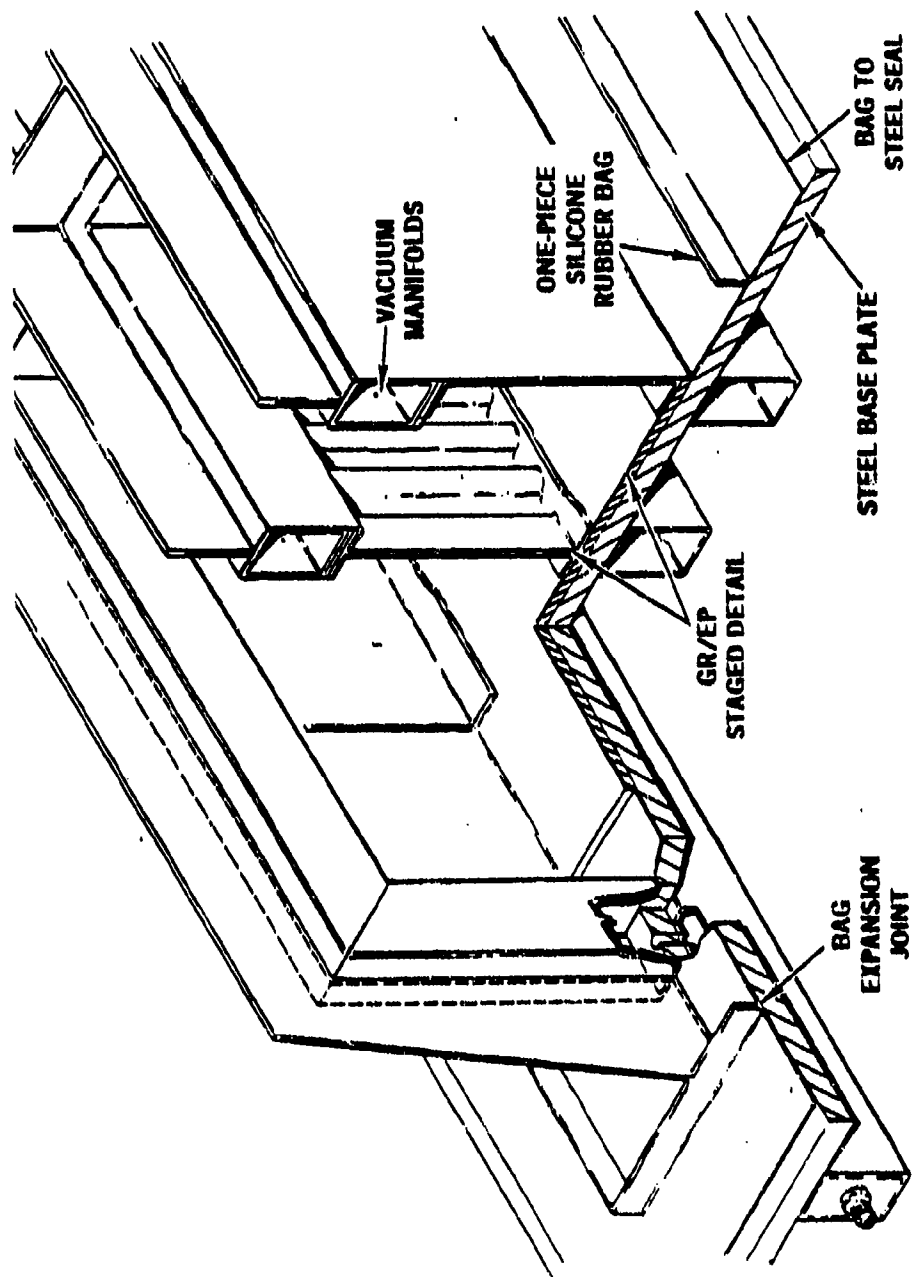


Figure 85. Subcomponent Cure Tool Diagram

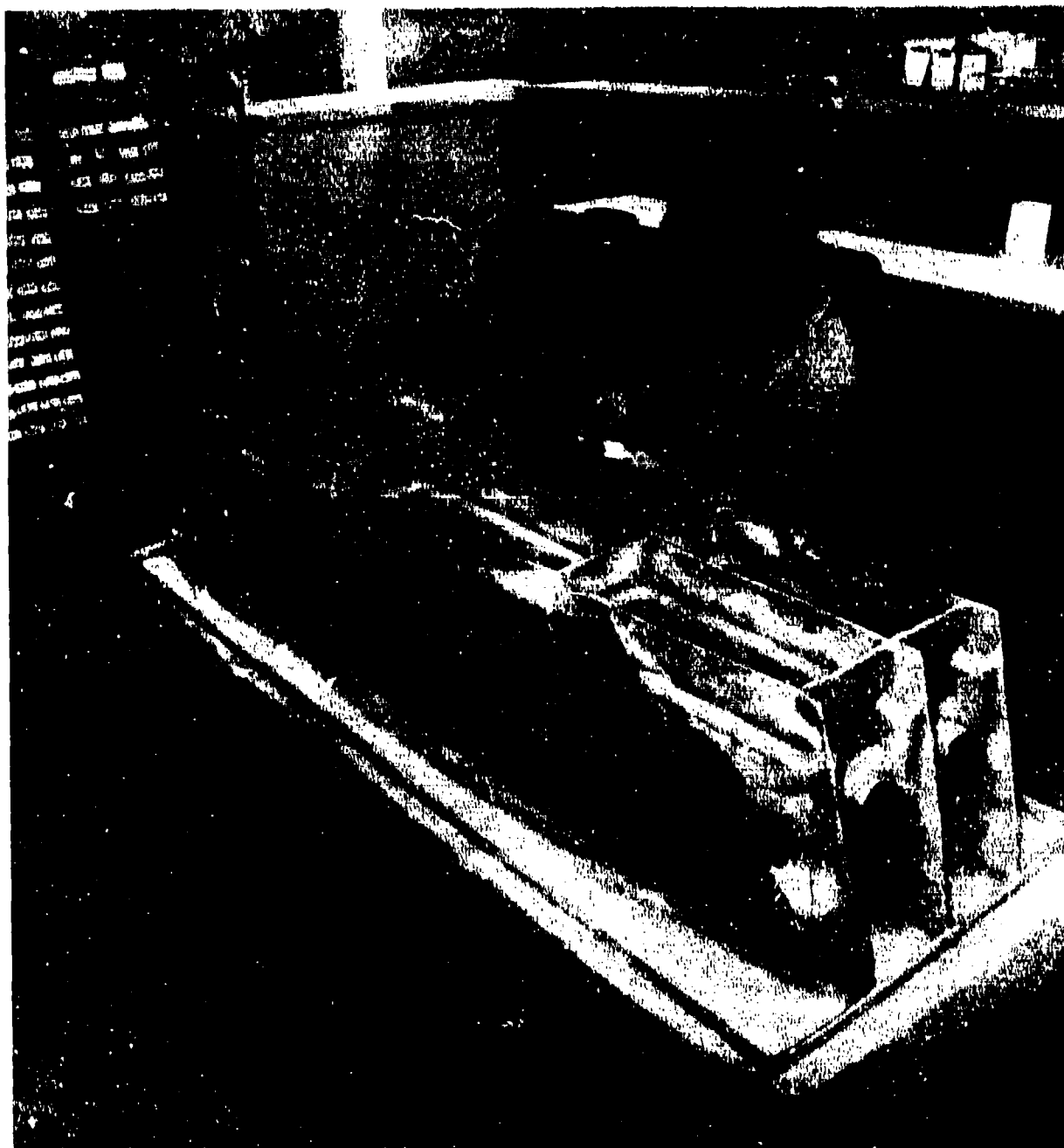
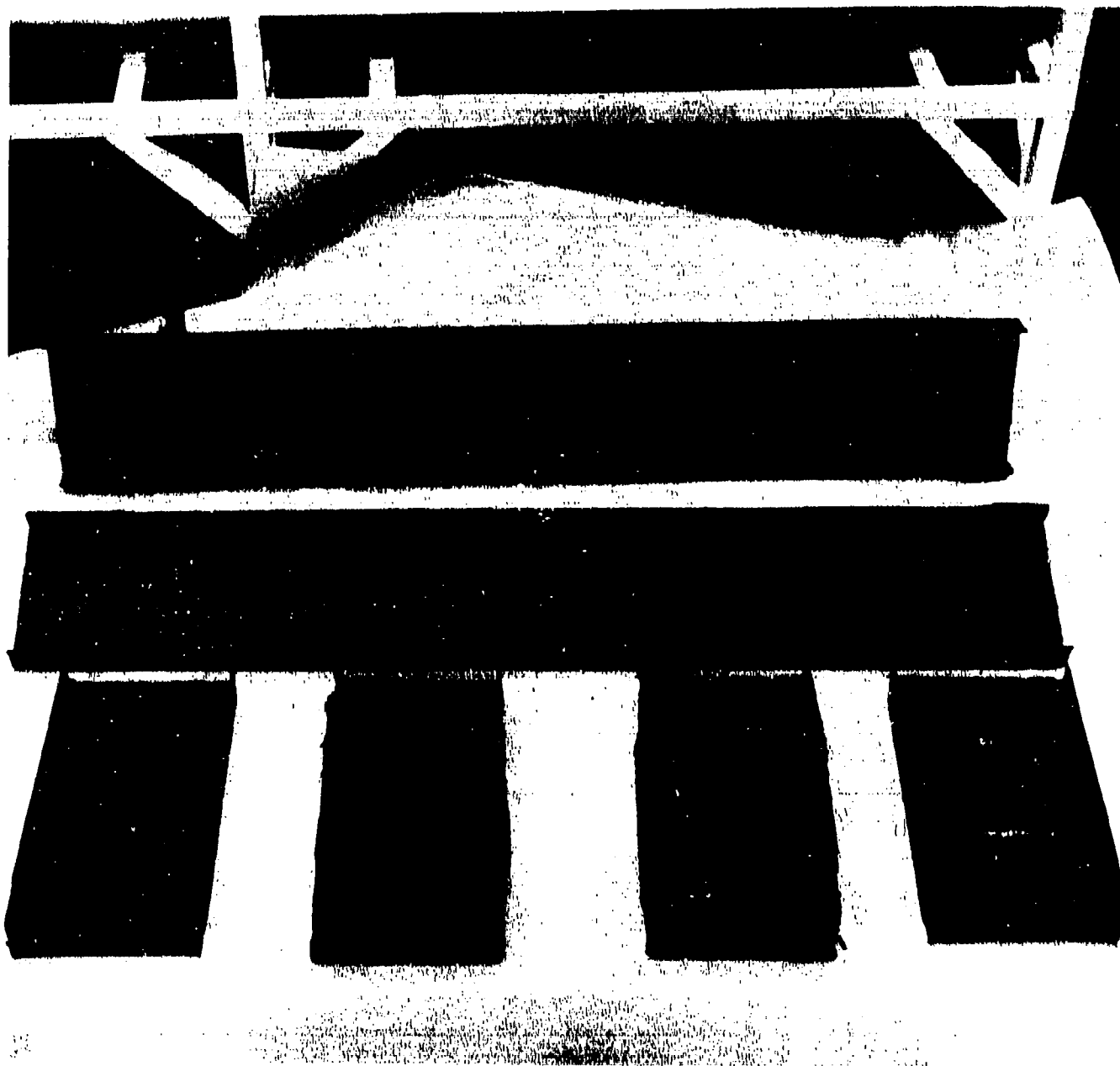


Figure 86. Stub-Box Bag in Place on Assembly Prior to Cure



**Figure 87. Stub Box Staged Details**

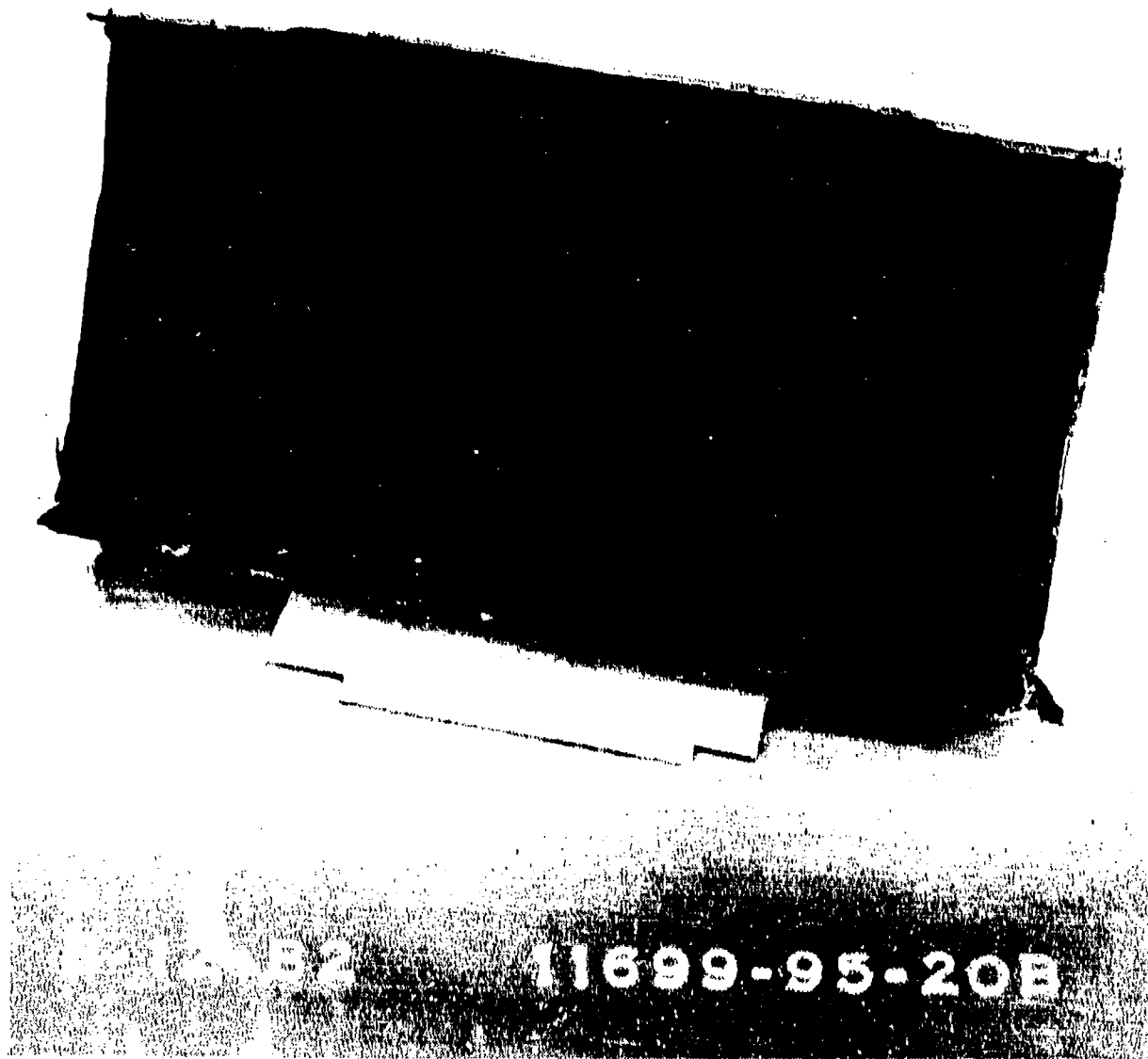


Figure 88. Stub Box Staged Upper R1b

Prior to assembly, the details were trimmed and prefitted to the lower cover with the aid of a new device used for the first time by North American Aircraft Operations and developed in conjunction with Energy and Minerals Research, Inc., Exton, Pennsylvania. Using low-frequency ultrasonics with a tuned holding fixture, the staged details were cut with minimal fraying of the edges. Figure 89 shows the trimming of the 44-ply rear spar. The use of the device eliminated the tedious task of hand-cutting the graphite/epoxy laminate with utility knives which caused fraying and delamination of the plies. This device augmented the water-jet cutter which was used at NAAO-Tulsa facility during CAP box fabrication. The quality of the trimmed surface is apparent in figure 90. Laminates up to 80 plies were cut using the device. Feed rate varied according to thickness but, on the average, use of this device cut the trimming time by half.

After prefit, (figures 91 and 92) Armalon was placed on the details and FM-300 adhesive was applied to the faying surface of the spars, ribs, and skin covers. The accuracy of the fitup of the various details is visible in figure 92. The rib and spar caps are in place in figure 93. The spar caps were continuous from root to tip. Fiberglass wedges were fitted at the intersections of the ribs and front and rear spars (see figure 94) and twisted graphite/epoxy tows were placed at the front and rear spar intersection with the cover. The spar caps were then added and thermocouple wires were attached to the spars and lower cover to monitor the cure temperatures. The steel manifold was installed, and a fiberglass breather was placed over the manifold and baseplate. (See figure 95.)

Following installation of the cure bag and vacuum lines, the assembly was placed in the oven for final cure. The cure cycle was  $60 \pm 10$  minutes at  $177 \pm 60^\circ\text{C}$  ( $350 \pm 100^\circ\text{F}$ ) which is typical for all 3501-5A resin systems.

A vacuum of 27-inches Hg was held in the tool during the heatup to  $177^\circ\text{C}$  ( $350^\circ\text{F}$ ). After reaching  $177^\circ\text{C}$  ( $350^\circ\text{F}$ ), a leak developed in the bag. Five of the six vacuum lines maintained the 27-inches Hg, and the sixth static vacuum line fell to 18-inches Hg which was maintained for the remaining cure portion of the cure cycle.

Following cure the stub box assembly was removed from the oven and the cure bag lifted off. Inspection of the bag after cure revealed a tear at the corner of the skin. The tear, which was approximately 2.54-cm (1.0-inch) long, caused a loss of pressure during the cure cycle but did not appear to have caused any problem to the article.

The porous and nonporous Armalon was removed from the part. The cured stub box had excellent surface appearance and the sine-wave radii maintained outstanding definition with no wrinkling of sine wave convolutions. Sufficient pressure was applied to all the bond joints as evident from the flow of adhesive (figure 96) at the joints.

Two-inch diameter access holes were drilled in the two ribs and twisted Gr/Ep tows were placed at the intersection of the front and rear spars and the cocured cover. Two plies of fabric were bonded with FM-300 over the exterior of the spar/cover joint to enhance the peel strength of the cocured joint.



Figure 89. Demonstration of New Ultrasonic Cutting Device for Laminates



Figure 90. Minimal Fraying of Laminate Edges Using Ultrasonic Cutting Device



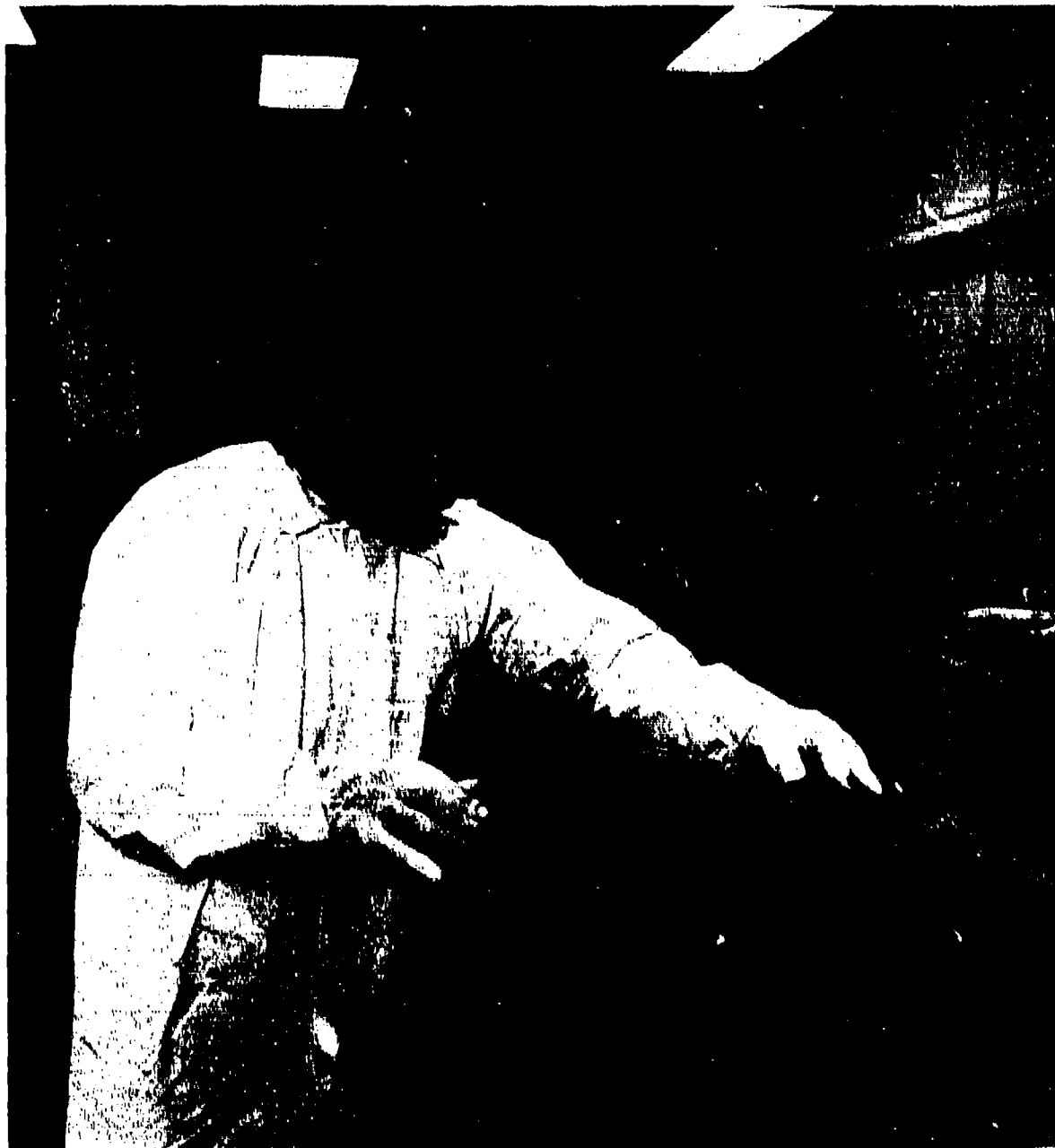


Figure 91. Prefit of Stub Box Details

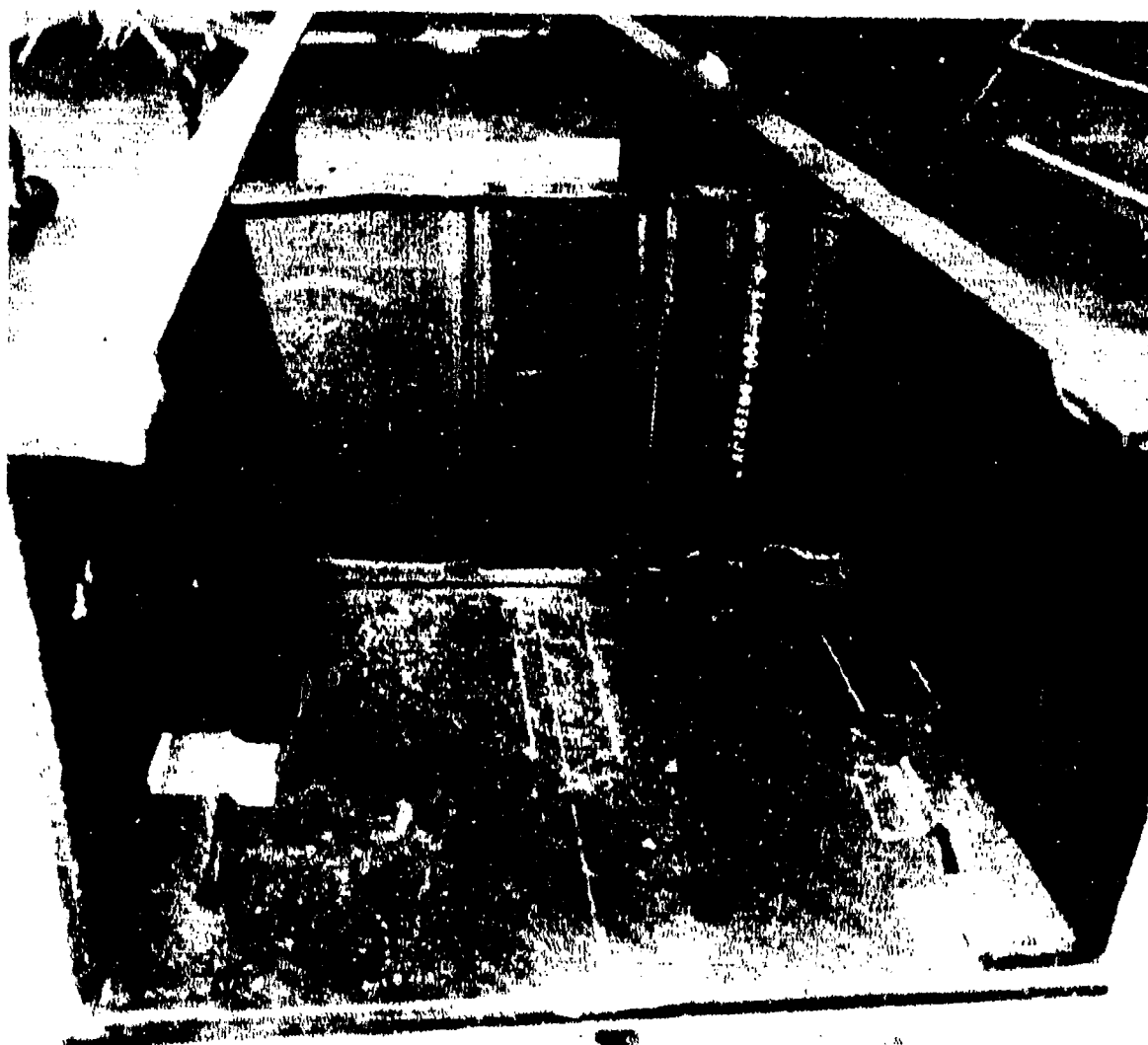


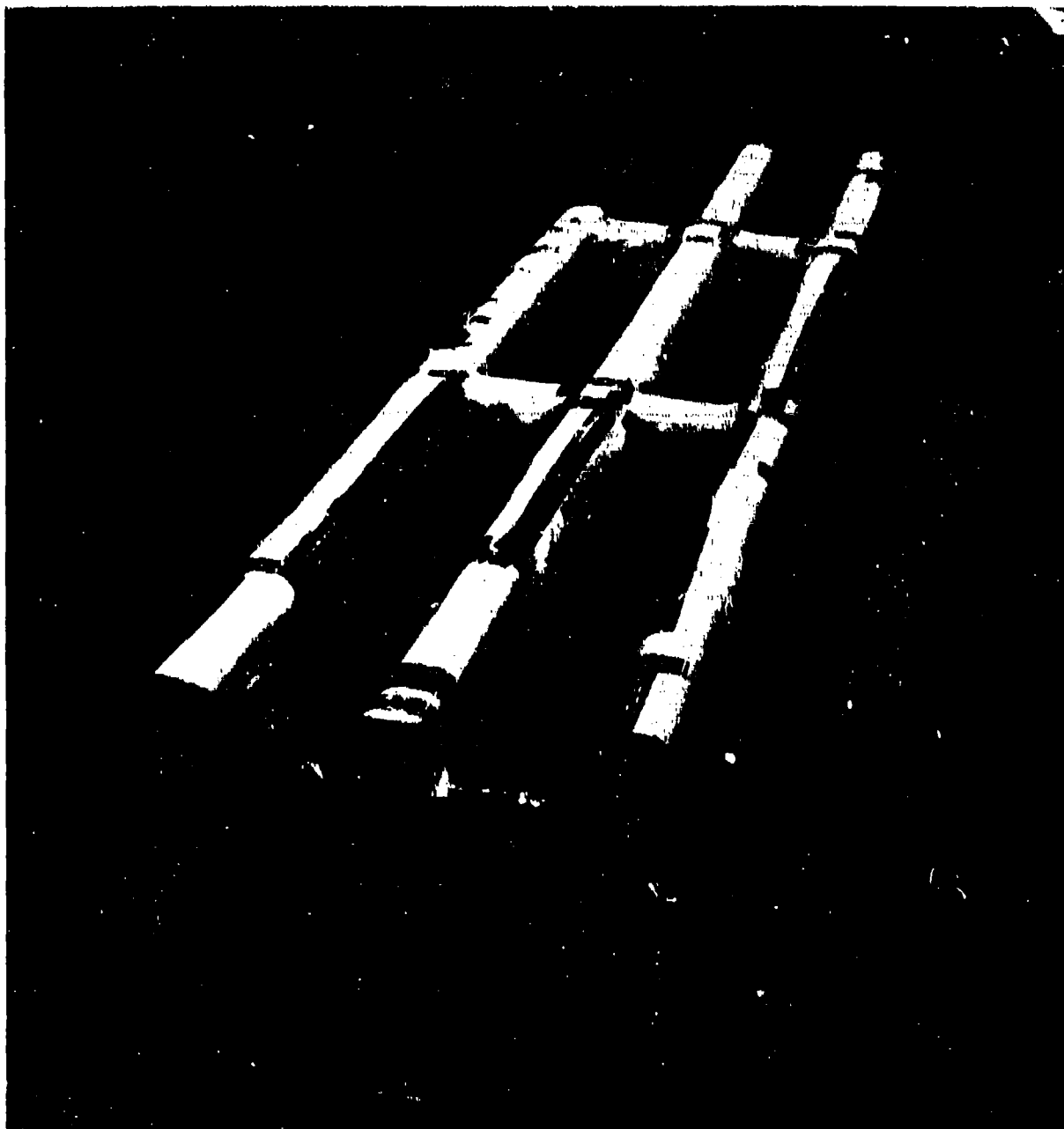
Figure 92. Prefit of Stub Box R1b - Close-Up View



Figure 93. Placing Rib and Spar Caps on Stub-Box Assembly



Figure 94. Fiberglass Wedges Placed on Ribs; Stub-Box Assembly



**Figure 95. Cocure Stub-Box Assembly; Upper Manifold in Place**



Figure 96. Cured Stub Box - Adequate Pressure During Cocure as shown by Adhesive Flow on Bondline

Prior to postcure, the stub box was visually inspected which revealed several small areas on the cover outside of the cocured section (near the root attachment zone) with delamination of the outer one-to-two plies. The resulting disbonds were filled with Shell 828 resin. This was accomplished by drilling two small (0.0312-inch) diameter holes at either end of each void area: one for the insertion of a hypodermic syringe and the other to act as a vent.

The delamination occurred in the boron/graphite/epoxy section of the laminate. The structural integrity of the part was not impaired since the aluminum ribs and spars which comprise the load introduction structure were mechanically attached to the box through the thickness of the skin and the cocured spars. This provided sufficient support to ensure the structural integrity of the part. No other defects were evident from the visual inspection and the box was postcured at 177°C (350°F) for 3 hours.

After postcure the stub box was inspected using hand-held pulse echo equipment in selected areas, as outlined in the inspection plan of Task 2. These areas comprised the critical load introduction areas of the cover and spars. The part thickness and the height of the spars and ribs were also measured.

During assembly of the aluminum loading hardware to the graphite/epoxy assembly and the drilling of the close-out covers for installation, several manufacturing defects occurred. These defects were eight figure-eight holes and four mislocated pilot holes drilled in the cocure cover side. Shimming of the aluminum load introduction spars at the root end of the stub box was also required. The front and rear spars were mislocated outboard 0.61 cm (0.24 inch) on each side during fitting into the cocure assembly. This occurred from locating the spars to the cover rough trim dimension rather than to the net trim dimension. No movement of the details was evident during cure and the discrepancy was corrected by bonding aluminum shims to the aluminum spars. The figure-eight holes were corrected by filling with chopped graphite fiber and epoxy resin, then redrilling and filling the misdrilled holes with Hilok fasteners. Spacematic drills with a drilling template were used for the cover hole installation (figure 97). The reworked items were ultrasonically inspected and the assembly proceeded with mating, final assembly, instrumentation of the stub-box details (as shown in figure 98 without the mechanically fastened cover in place).

Prior to placing the stub box into the fixture for testing, the 2024 aluminum load introduction blades, which attach through mechanical fasteners to the subcomponent at the base or root, were match machined for the required close tolerance fit into the vertical stabilizer root spindle. This close tolerance fit is required to ensure that the joint is capable of transferring the 2294 lb/in. shear flow at the critical load case.

The scale-up demonstration component box was statically tested. The applied loads for the stub-box resulted in simulation of the cover loadings at the root splice of the full-scale vertical stabilizer. Based on the (1) RPA gust condition.

The RPA gust condition is the maximum bending moment condition for the stabilizer.



Figure 97. Drilling Closeout Cover of Subcomponent



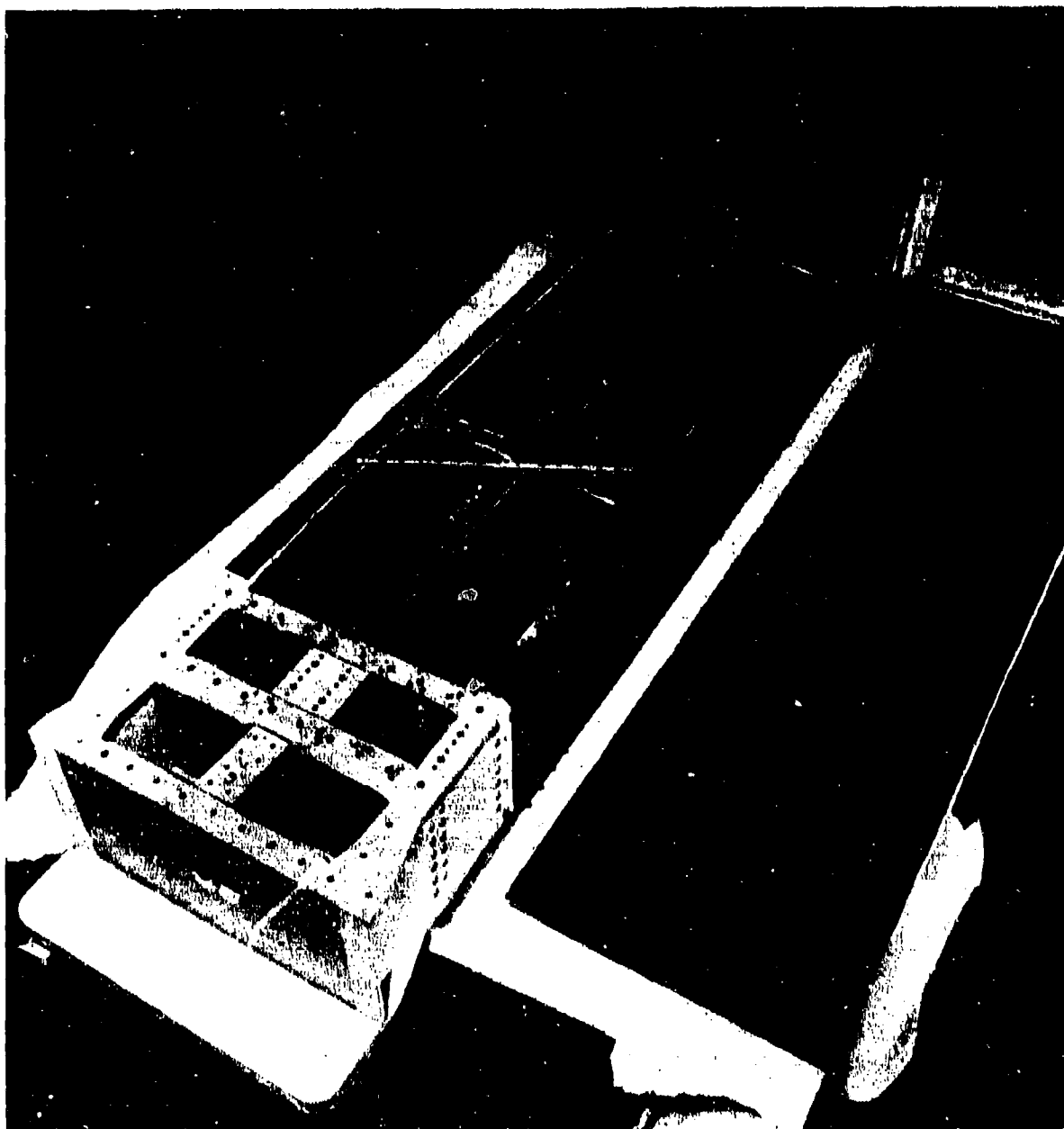


Figure 98. Stub Box Prior to Installation of Strain Gages

#### 4.2.2 TASK 2 - QUALITY ASSESSMENT

Quality assessment of the subcomponent was conducted in two areas; nondestructive inspection and static test of subcomponent. Nondestructive inspection consisted of ultrasonic C-scan and contact pulse echo of the various staged details and cocured structure and dimensional mapping of the part including thickness, length and height measurements, and flatness measurements. The static test of the subcomponent was conducted at ambient conditions and included failure and comparative analyses with the baseline subcomponent.

##### 4.2.2.1 Nondestructive Inspection

Nondestructive inspection standards were designed and fabricated to simulate both graphite/epoxy and graphite/boron-epoxy staged details. The two standards were 23-by 15-cm (9.0-by 6.0-inches) with varying ply thicknesses to represent the variety of thicknesses found in the subcomponent details. As shown in figure 99, three ply thicknesses were used: 64 plies, 30 plies, and 8 plies. The standard included both interlaminar defects, lead tape surface references, and pull outs. The standard developed for the cover (see figure 100) contained three areas of varying percentages of boron to represent the root attachment area. As with the previous standard, defects were included in the cover standard.

Utilizing these standards, all twelve staged details were ultrasonically inspected using C-scan. All details were scanned normal-to-planar surface under 1 MHz at 20 and 26 Db. Areas of attenuation loss were reinspected using hand-held contact pulse echo techniques to further resolve the anomaly.

A C-scan of the front spar, conducted at 1 MHz, 20 dB and shown in figure 101, showed no porosity except for a localized delamination at the end of the part (caused by the trimming operation which frayed the plies).

Other details such as the rib (figure 102) were also porosity-free, although the C-scan (as with the front spar) showed some delamination at the edge because of trimming the staged part. Also evident in this C-scan are the radius areas of the web-to-cap transition area. Changes in part thickness and contour appear to be anomalies. The inflection points of the sine-waves also

appear to have attenuation. A check with hand-held pulse echo confirmed that there were no anomalies in that area. The covers, which taper from a total of 72 plies at the root, contained 30 plies of boron to 32 plies at the tip, and were also porosity-free as shown in figure 103.

The results of the C-scan and contact pulse echo interrogation of the 12 staged details indicated that only the rear spar C-channel did not meet the acceptance standards. The part was remanufactured and subsequent inspection indicated that it was acceptable.

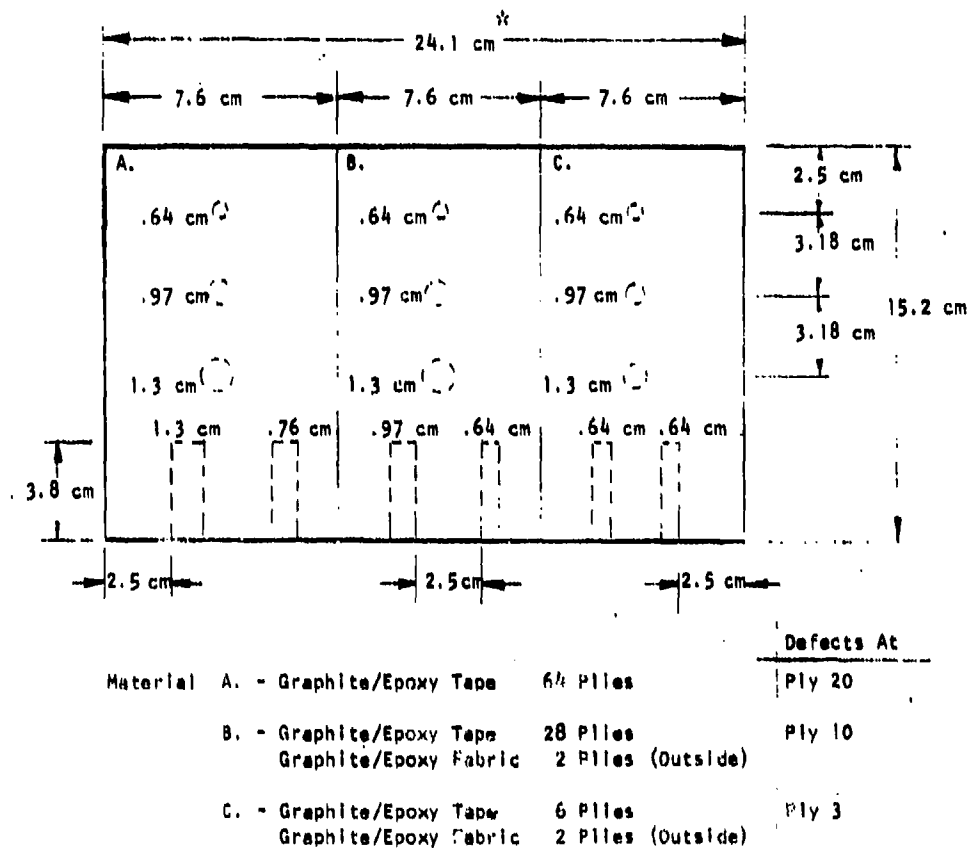
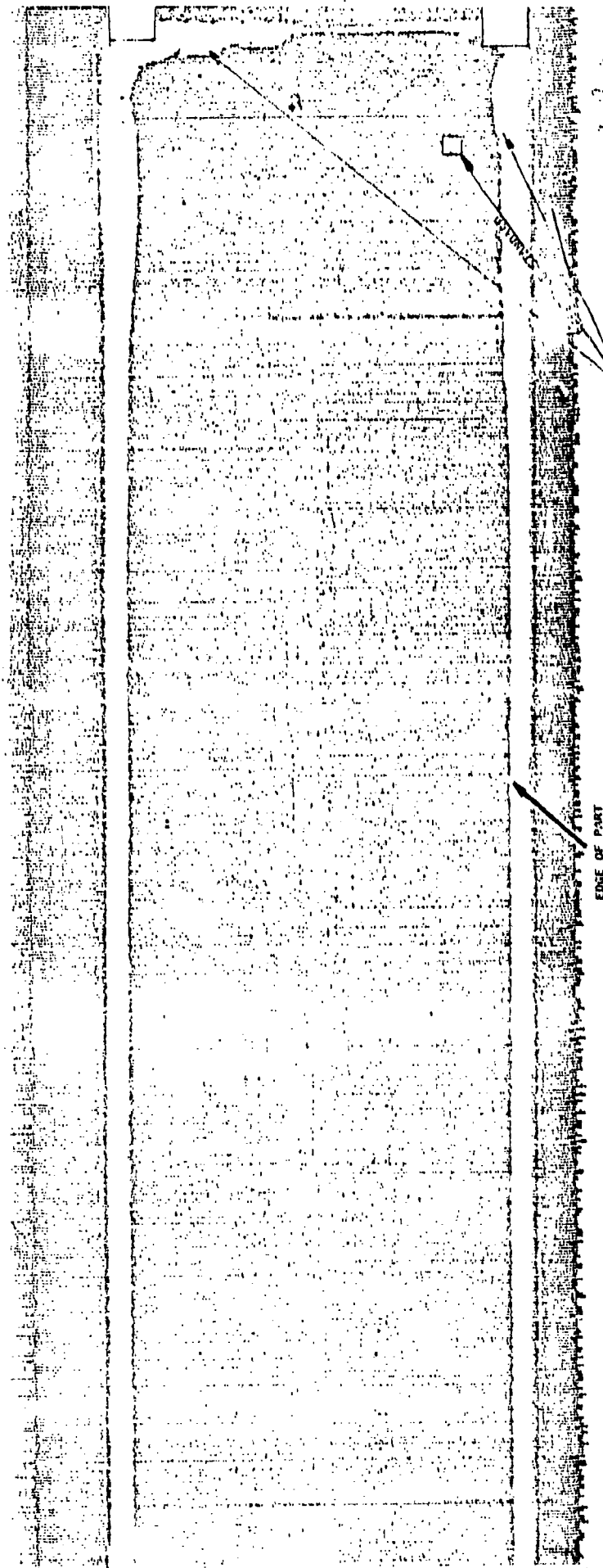


Figure 99. Nondestructive Inspection Standard to Simulate Graphite/Epoxy Staged Details



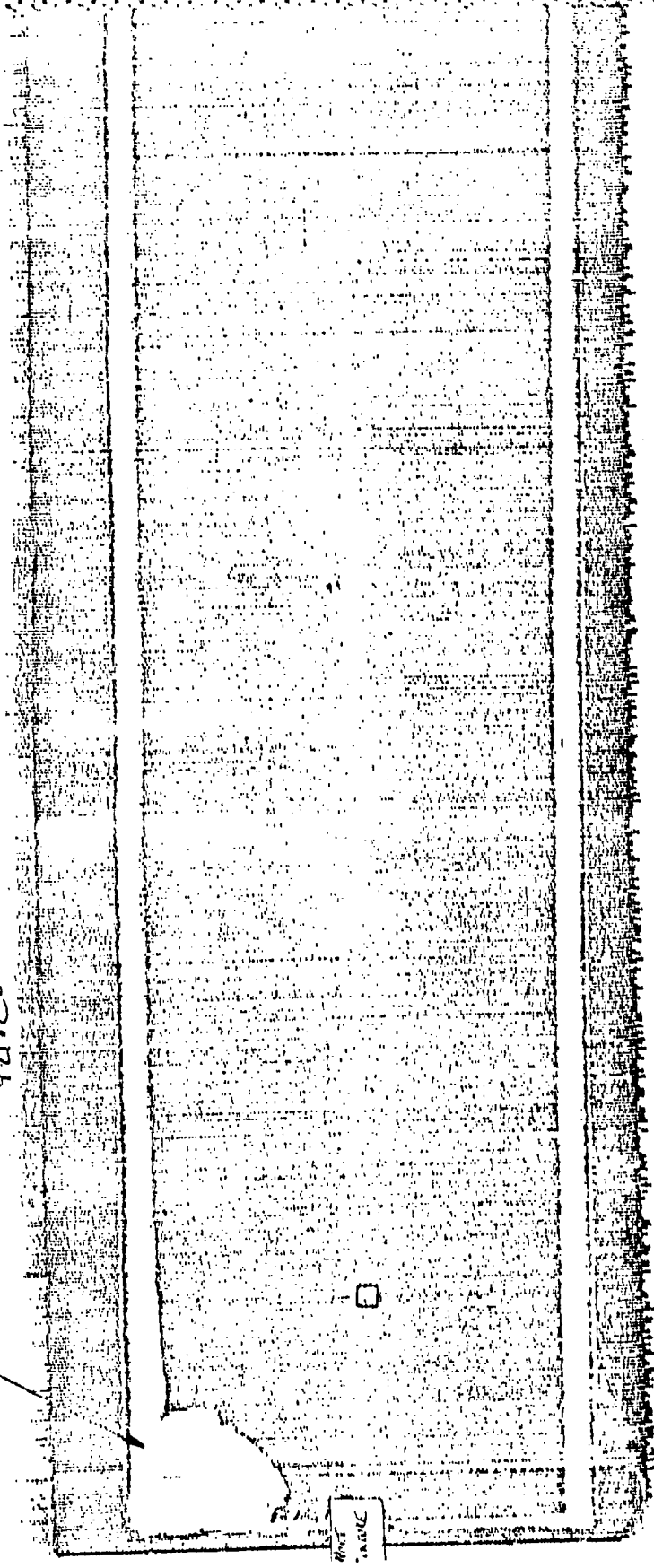


EDGE OF PART

DEFINITIONS & MULTIPLE USES  
 FOR THE PROJECT ENLIGHTENED Q.L.A.L. &

Figure 101. Ultrasonic C-Scan (1 MHz, 20 dB) of Stub-Box Front Spar - Porosity-Free

DEVELOPERS & VIKING PUBLISHERS  
REV. CONCEPT RISE EMBROIDERED  
92112



WINE  
TASTE

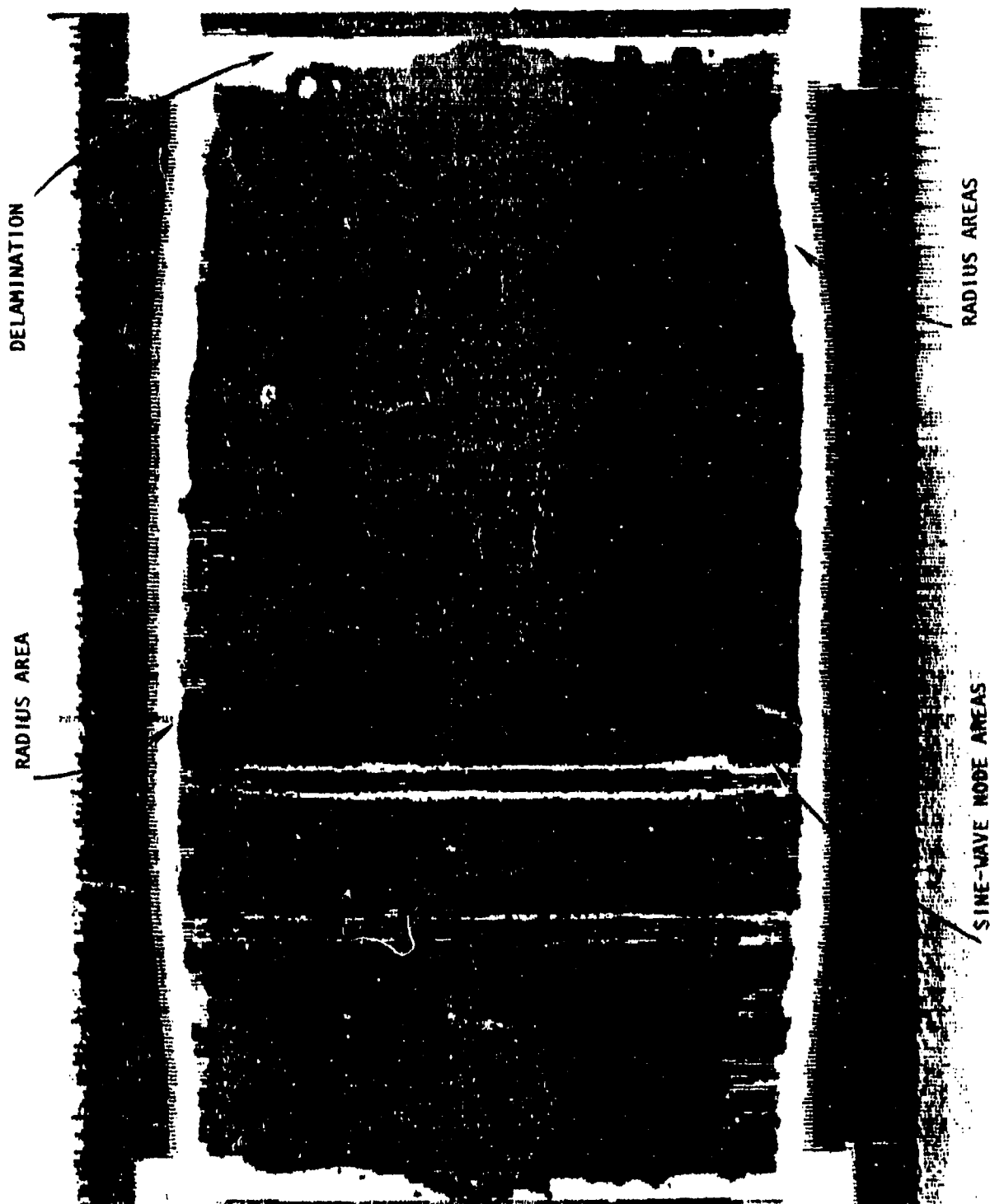


Figure 102. C-Scan (2.25 MHz, 20 dB) of Stub-Box R1b - Porosity-Free

Figure 103. Typical Section of Porosity-Free C-Scan (225 MHz 20



osity-Free C-Scan (225 MHz 20 dB) of Stub Box Covers (AC18100-008 004)

010-004

Hand held contact pulse echo inspection of the cured subcomponent was conducted as described below.

<u>Part No.</u>		<u>Description</u>
AC18100-010	Covers	Lower 13 inches of cover (boron areas) where accessible.
AC18100-003, -004	Ribs	Spot check web, especially where areas of anomalies appear in the C-scan of the staged detail.
AC18100-005, -006, -007	Intermediate Spars	Same as for AC18100-003, -004
AC18100-008	Front and Rear	Inspect areas indicated in figure 105 and areas of anomalies as indicated by C-scan.
AC18100-009	Spar and Rib	Same as for AC18100-003, -004

A map of the anomalies found is shown in figure 104. A total of nine anomalous conditions were found noted as items A through I on the injection report (figure 104). The nonbonds of items C, G and H were corrected through injection of shell 928 resin into the void. Item F was the outer ply nonbond discovered in the staged part and corrected by resin injection. The remaining indications were marked on the part and monitored during and after test.

The critical load carrying members (which are the front and rear spars and intermediate spars of the assembly) were dimensionally inspected according to figures 105 through 108. Height and thickness measurements were taken at various locations along the caps and webs of the details. The results are shown in table XXIII.

It is evident that, generally, thickness were 0.02 greater than calculated and the heights of the spar varied  $\pm .02$  inch. Thickness of the sinewave rib and spar caps were greater than drawing dimensions because of the folding of the web plies during the fabrication.

#### 4.2.2.2 Subcomponent Test

The purpose of this test was to validate the structural integrity of the subcomponent. This was achieved by comparing the structural response (failure modes, strain levels, ultimate strengths and stiffnesses, load introduction and distribution within the beam) of the nonautoclave-fabricated subcomponent with the structural responses of an autoclave-fabricated subcomponent, which was tested during the B-1 composite vertical stabilizer program (refer to AFFDL-TR-78-5). In addition, the subcomponent tests evaluated the strength of the integral cover to substructure joints.

The applied loads simulated the cover loading at the root splice of the full-scale vertical stabilizer. These loads were based on the following aircraft conditions:

<u>Conditions</u>	<u>Test Temperature</u>
1. RPA gust	RT (limit load)
2. RPA gust	RT (ultimate)



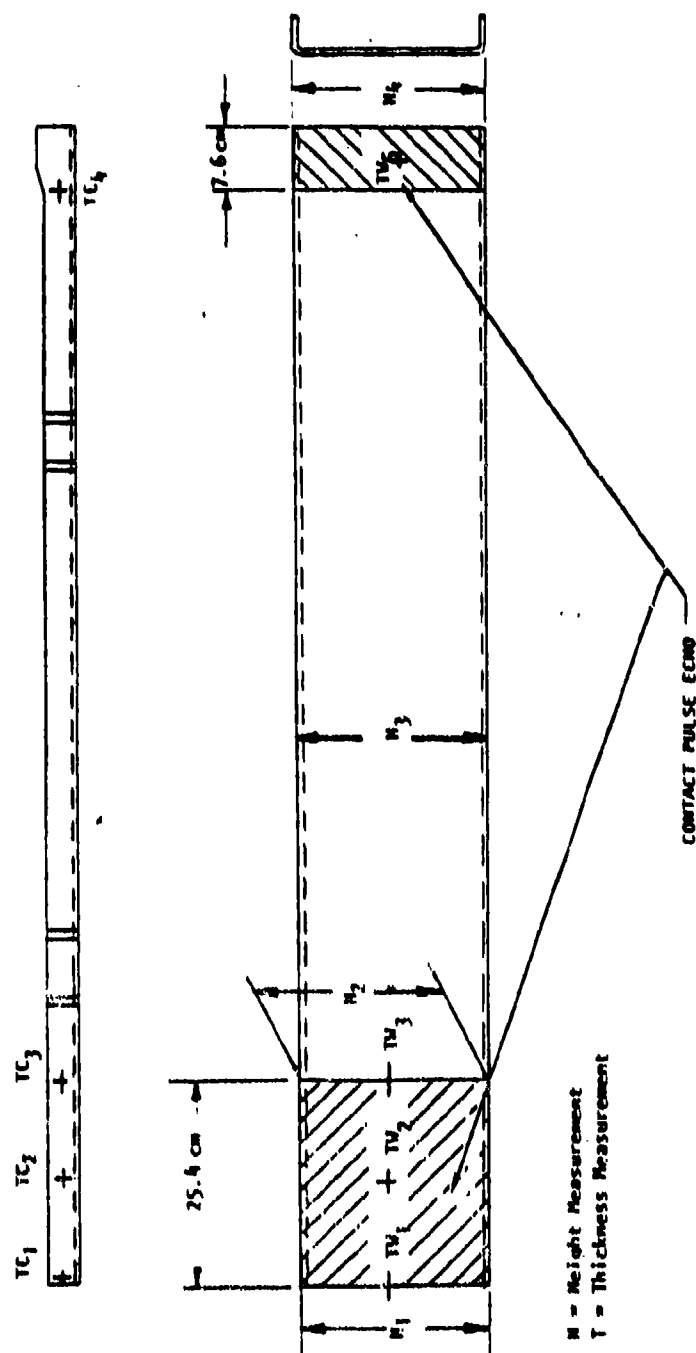


Figure 105. Dimensional Inspection - Rear Spar

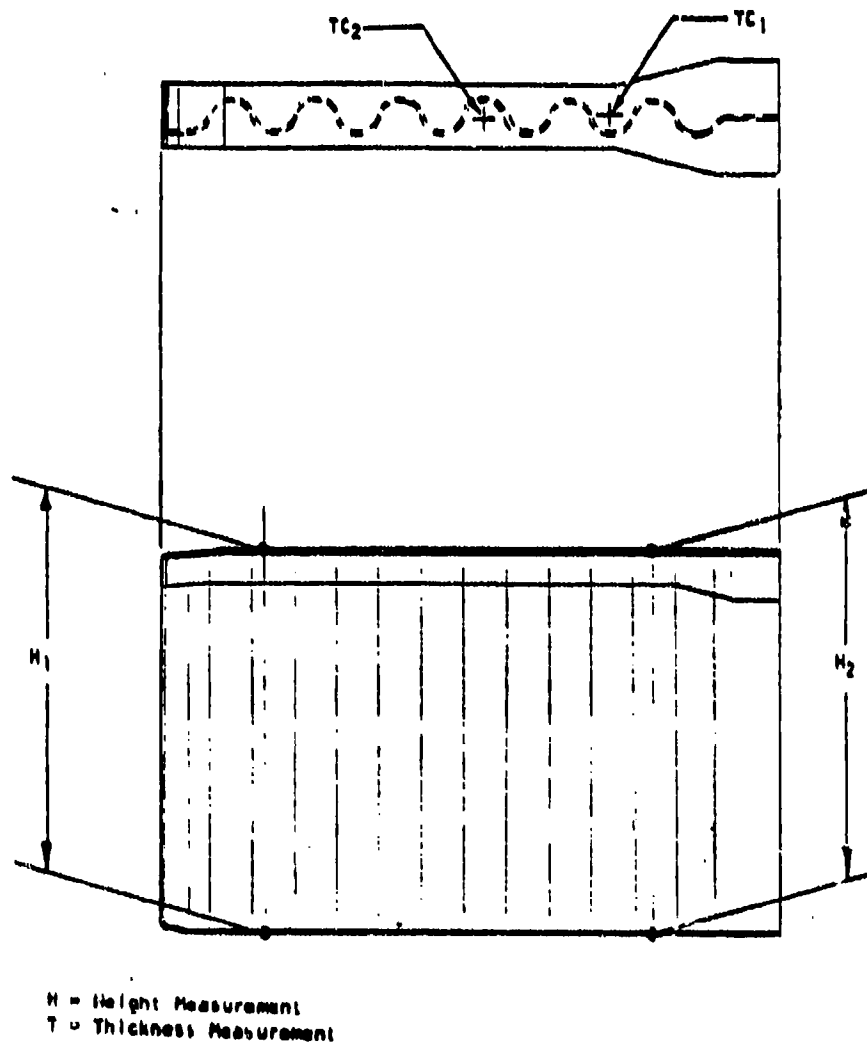


Figure 106. Dimensional Inspection - Intermediate Spar

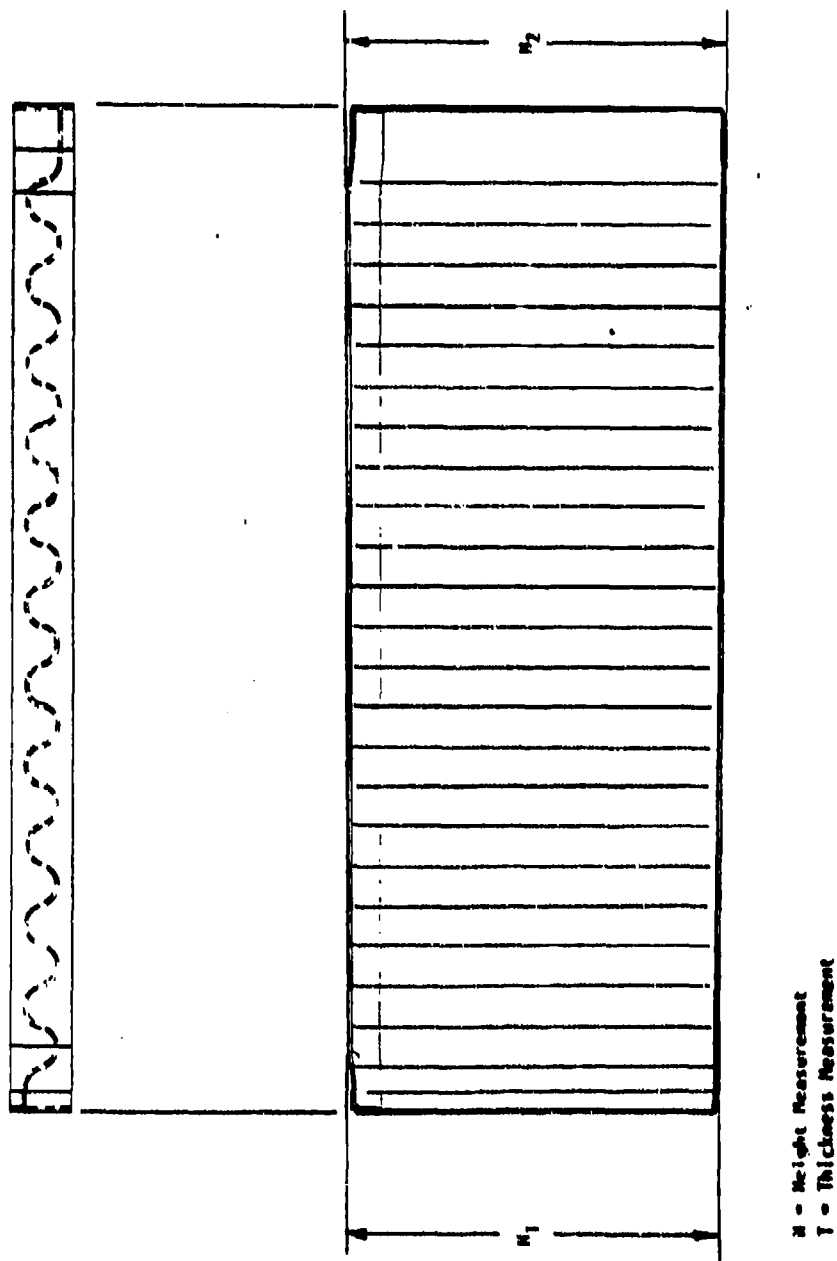


Figure 107. Dimensional Inspection - Intermediate Spar

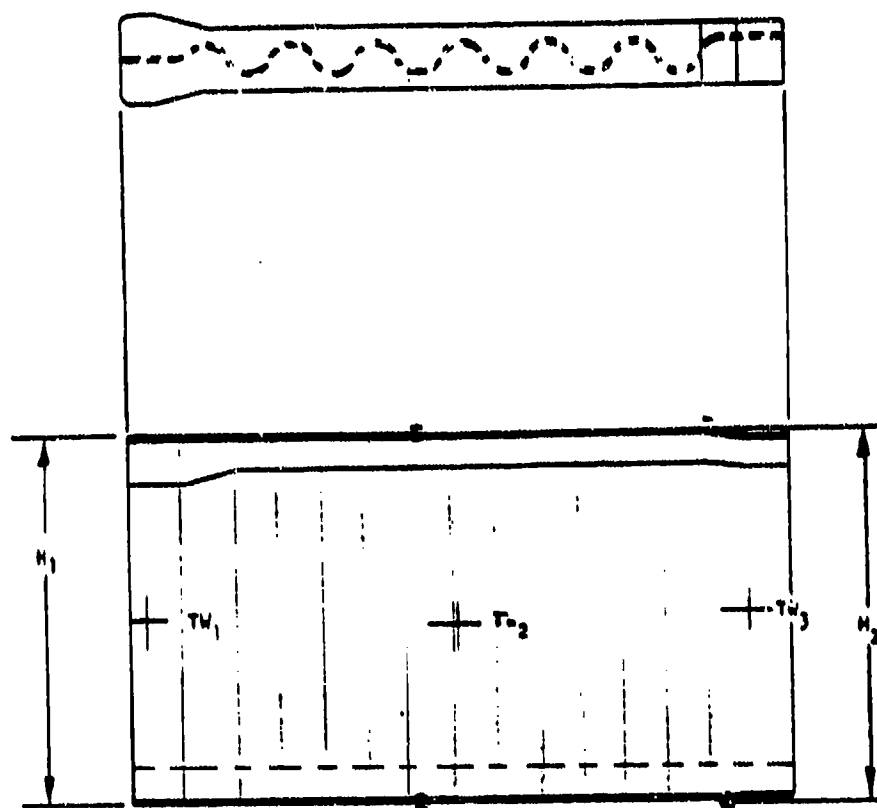


Figure 108. Dimensional Inspection - Intermediate Spar

TABLE XXIII

## DIMENSIONAL MEASUREMENTS OF SUBCOMPONENT

DESCRIPTIONS	MEASUREMENTS	REQ'D	ACTUAL	DELTA
Front spar	TC	.262 inch	.289 inch	.027 inch
	TC2	.262	.285	.027
	TC3	.262	.286	.027
	TC4	.262	.285	.027
	TW1	.231	.280	.049
	TW2	.231	.276	.045
	TW3	.231	.266	.045
	TW4	.231	.270	.039
Upper intermediate spar	TC1	.078	.130	*due to folding material
	TC2	.078	.125	*due to folding material
	H1	9.221	9.197	.024
	H2	9.215	9.197	.018
Lower intermediate spar	TW1	.078	.079	.001
	TW2	.078	.080	.002
	TW3	.078	.080	.002
	H1	8.969	9.010	.041
	H2	9.073	9.091	.018



The RPA gust condition was the maximum bending moment condition for the stabilizer. The subcomponent was attached to an existing test fixture (figure 109) and loads were applied through the end-loading rib at the free end in order to meet the required cover loads at the composite to aluminum root splice (figure 109). The test fixture simulates the methods of attachment and stiffnesses of the B-1 structural assembly. The bending moment and torque applied to the subcomponent are reacted in the form of couples applied to the subcomponent with the shear reacted as an axial load along the steel tube.

The critical load condition for the structural tests is the RPA gust (conditions of the B-1 vertical stabilizer) during which the bolted splice joint has an axial loading of  $N = 1838.2 \text{ kN/m}$  (10,500 lb/in.) and a shear loading of  $N_{xy} = 175.1 \text{ kN/m}$  (1,000 lb/in.). The single cantilever P-load offset 27.63 cm (10.88 inch) from the centerline of the beam provide these load intensities for the RPA gust condition. Table XXIV summarizes the load conditions for the stub box.

For test load condition (1), the load was applied in 10-percent increments (of limit) until the P-load has been reached. For condition (2), the load-to-failure would be in increments of 20-percent of ultimate until P-load (ULT), then in 10-percent increments (of ultimate) to failure.

Instrumentation of the subcomponent comprised 23 strain gages (rosette and axial) and deflectionometers. The majority of the instrumentation (shown in figure 110) was concentrated at the root attachment where failure was predicted to occur as a tension type failure of the cover. Strain gages were included on the front and rear spars as well as on the intermediate spar. Gages were also included at the load introduction end of the box to monitor box for accurate load introduction.

Figure 111 shows the subcomponent installed in the test fixture prior to loading. After an initial loading to 30 percent of limit load and unloading, the subcomponent was loaded and strain gage and deflection data were recorded at increments of 10 percent of ultimate load. At 70-percent design limit load (DLL) (46.9 percent DUL) the rear spar flange-to-cover integral joint completely debonded the length of the beam with a secondary debonding failure of the cover-to-first-rib flange integral bondline as shown in figure 112. An initial visual evaluation of the failure area indicated that very little or no bond was present between the rear spar flange and the cover. This was confirmed by the following calculations at the failure load.

$$q_{MAX} @ 160\% \text{ DUL} = 642.6 \text{ kN/m} (3670 \text{ lb/in}) \text{ (RPA gust condition at } 160\% \text{ DUL)}$$

$$\text{(Failure point of original stub box)}$$

thus

$$f_s \text{ (Rear Spar flange bondline at failure)} = \frac{3670}{1.4 \text{ (width of bondline)}} \times 4.69$$

$$f_s = 5.3 \text{ MPa (768 psi) @ failure}$$

which is far below the allowable utilized

$$f_s = 17.2 \text{ MPa (2500 psi) in the beam design.}$$

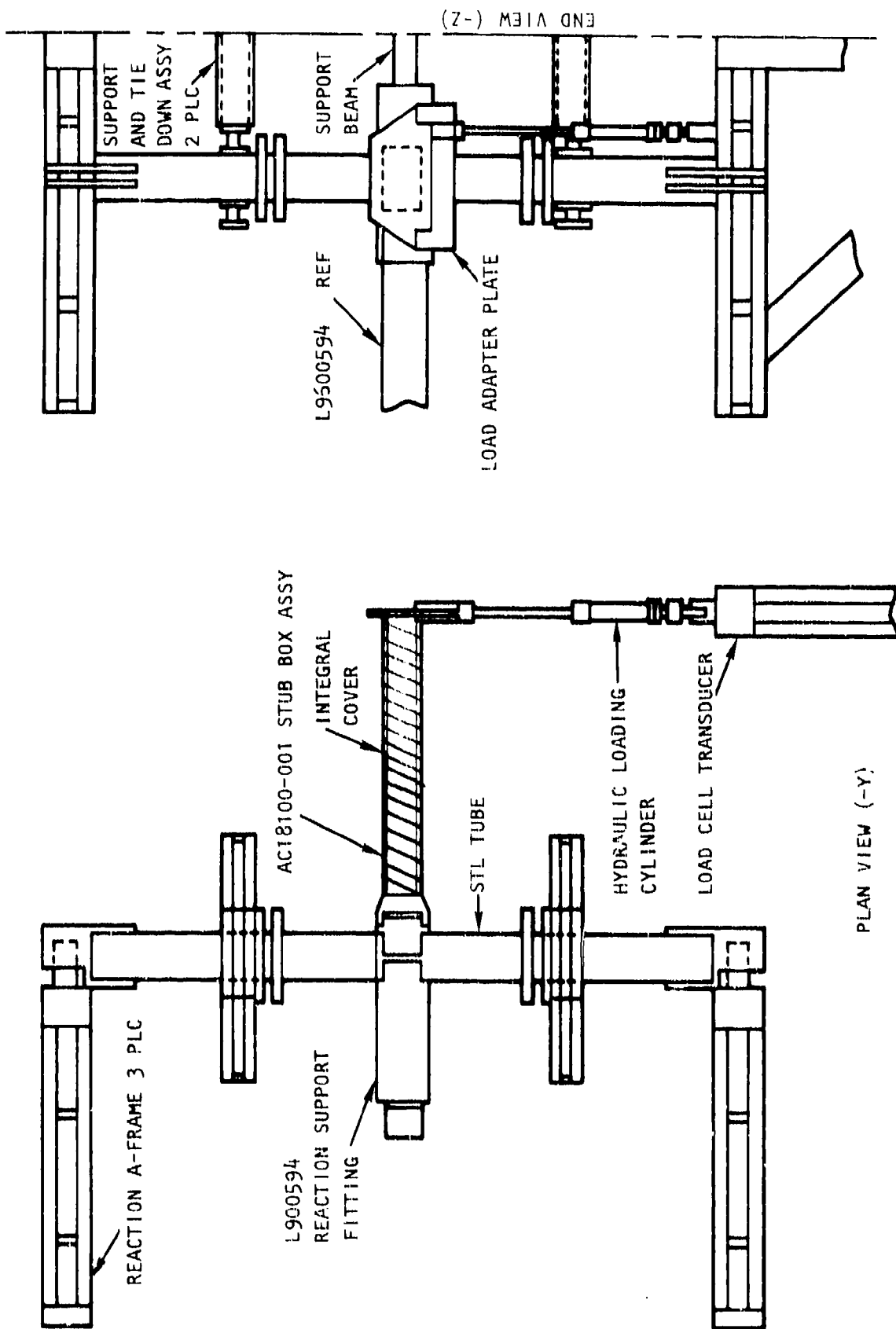


Figure 109. Subcomponent Box Test Setup

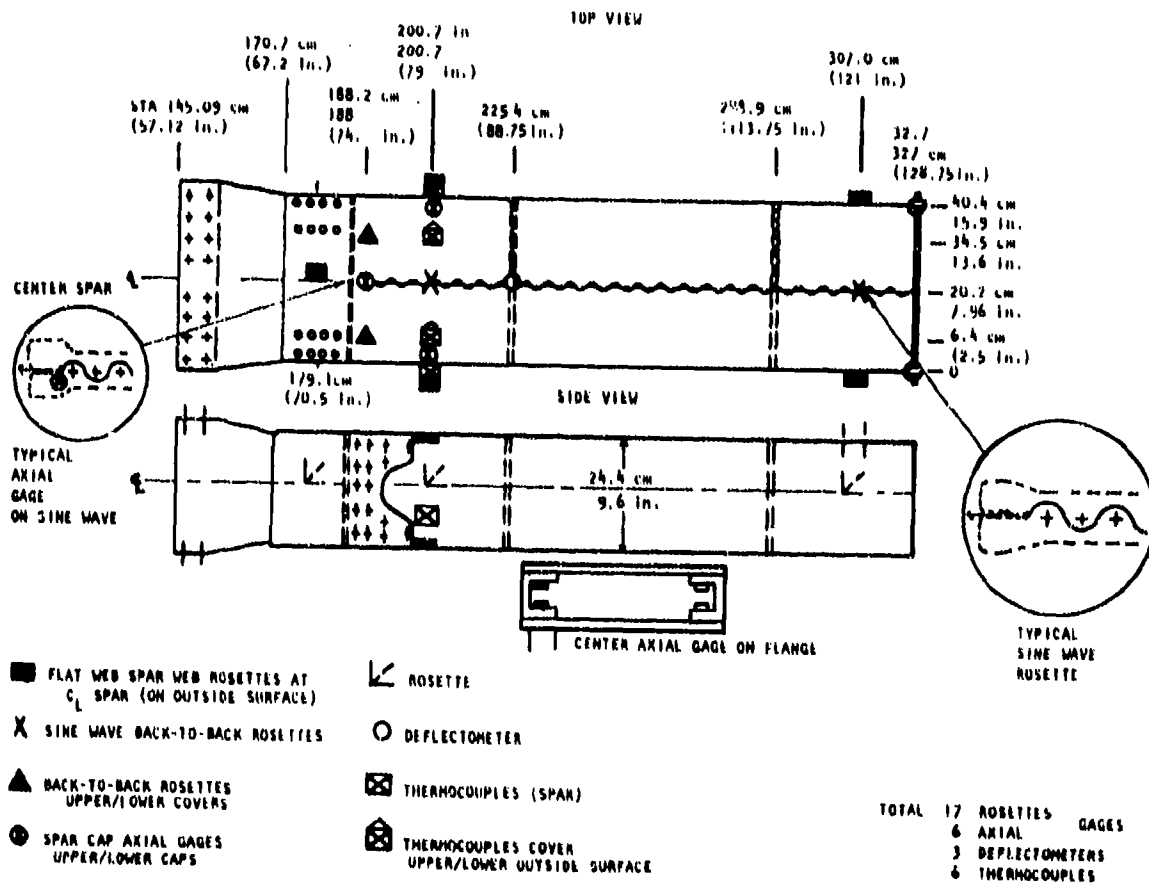


Figure 110. Location of Stub Box Instrumentation

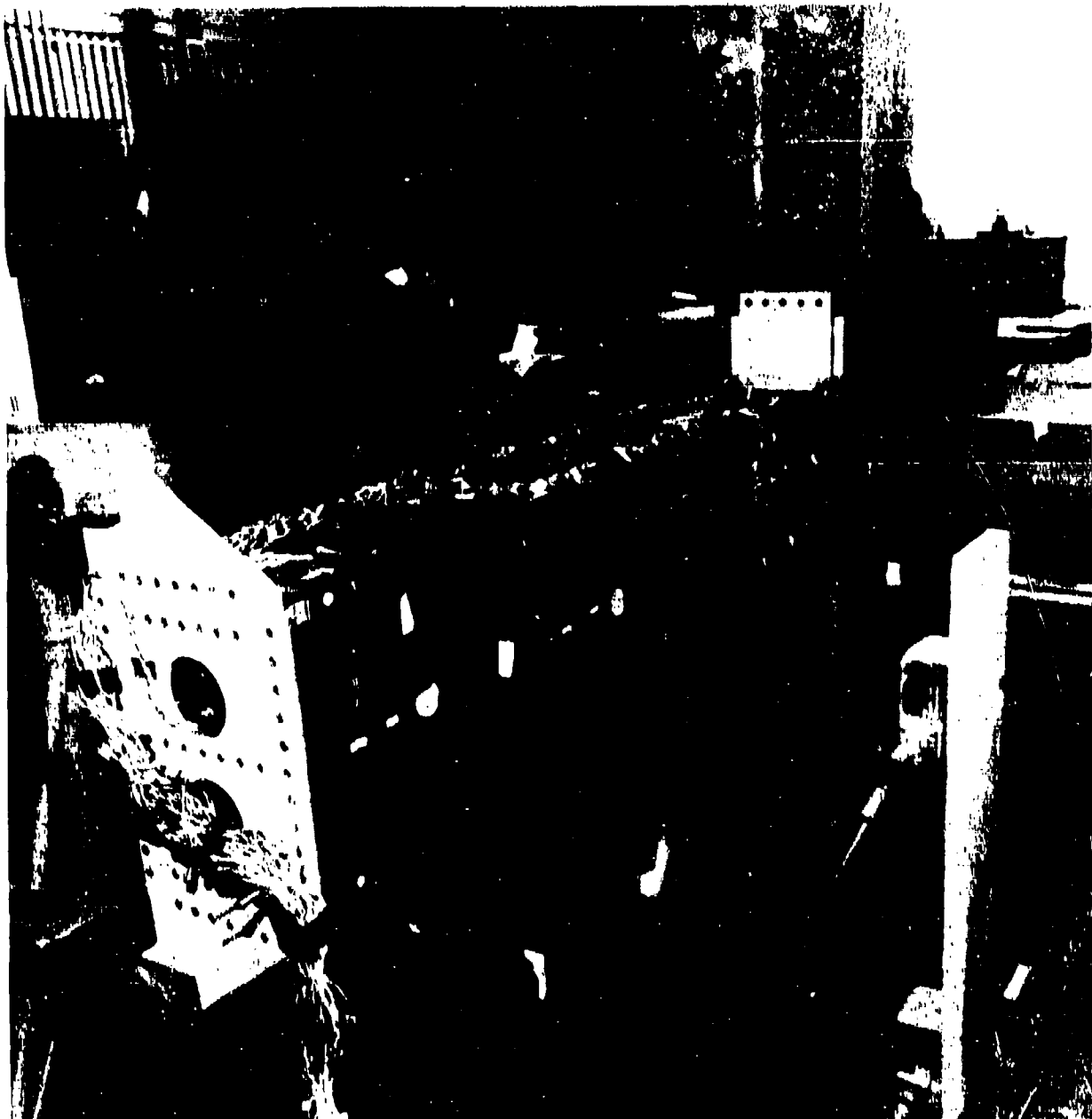


Figure 111. Subcomponent in Test Fixture

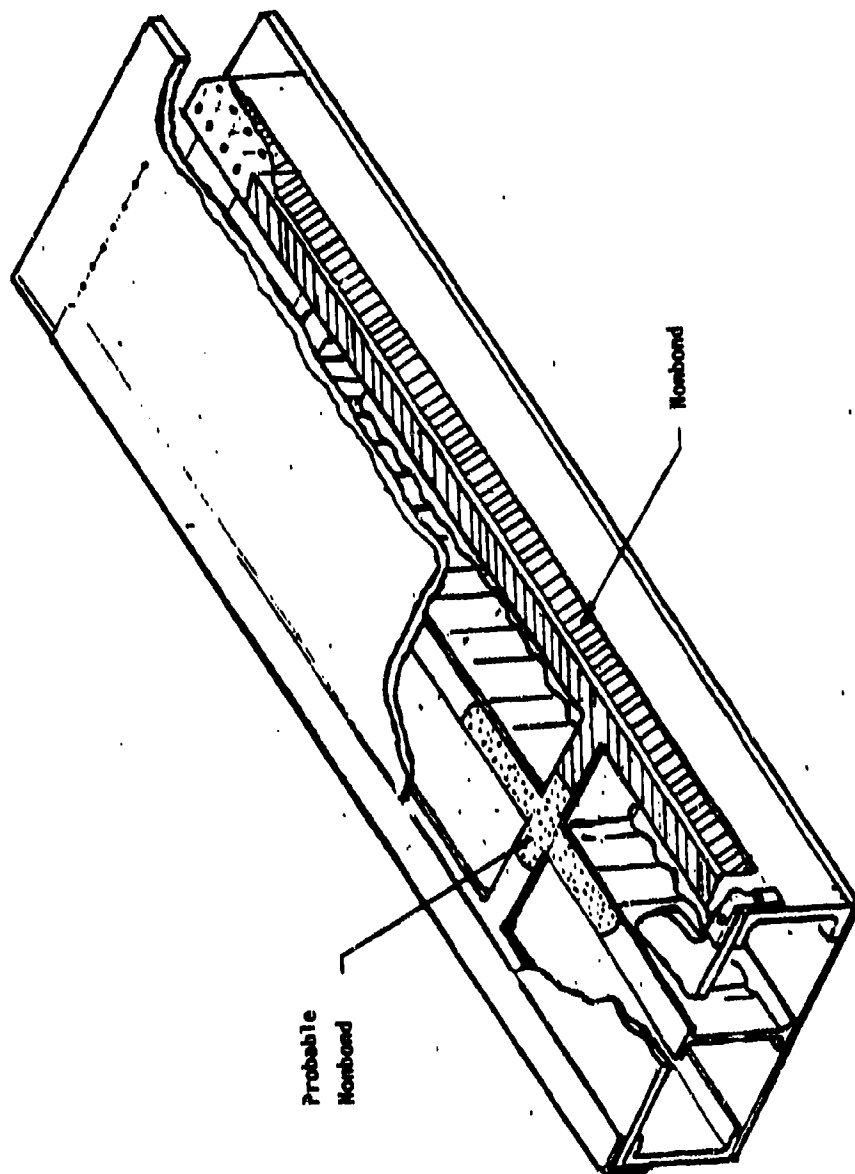


Figure 112. Contact Pulse Echo Results at Bondline Failure

TABLE XXIV

## SUMMARY OF LOAD CONDITIONS FOR STUB BOX COMPONENT

Test Load Condition	Loading Condition	Moisturization	Temp OC (OF)	P Load KN (lb)	Remarks
1	RPA Gust	Dry	RT	78.9(17,770)	Limit
2	RPA Gust	Dry	RT	118.5(26,655)	ULT*

\* Predicted failure load of beam

The next step was to compare the predicted strain levels in the beam with those measured. The comparisons of these strain levels for the cover, spars, and spar flanges (see figures 113 to 115) show very close predicted-versus-measured strain levels which indicate that the failure mode was not the result of any high strain levels within the overall design. A further comparison was made with the tip deflections of the original box and the nonautoclave specimen shown in figure 116. As evident in this figure, the nonautoclave box appears stiffer than the original. This can be explained by noting that the original box had a "strong back" boiler plate test support fixture whereas the nonautoclave box utilized the test fixture simulating the B-1A fuselage support to static test the B-1A vertical stabilizer.

To further evaluate the cause of the failure a section of the box was removed and the cover to substructure bond line examined. The section is shown in figure 117. The area of delamination is visible as chalk marks on the box. Figure 118 shows the section as it was removed; from this photograph it is apparent that there was no bonding of the cover to the substructure despite the evidence of a good bond. This evidence indicated a contamination of the skin surface.

The possibility of lack of pressure as a cause for the nonbond was eliminated. Measurement of the bond line thickness indicated it was within tolerance. Additionally, studies were conducted to evaluate the bonding characteristics of the FM 300 (cured without any pressure other than the layup and assembly) indicated that although a very porous bondline would occur, there was adherence of the adhesive to the Gr/Ep. These facts also indicated a presence of a contaminant on the surface of the skin.

To further evaluate the surface, sections of the skin were removed in the bond area and subjected to Auger analysis. The beam power was set at 2KV. Figure 119b shows the control or bare Gr/Ep sample with the peaks representing sulfur and carbon visible. In figure 119a a peak at 75 ev indicates the presence of silicone. This confirms the theory that even though the cover was sealed in a bag after staging, contamination of the surface occurred sometime during the assembly procedure.

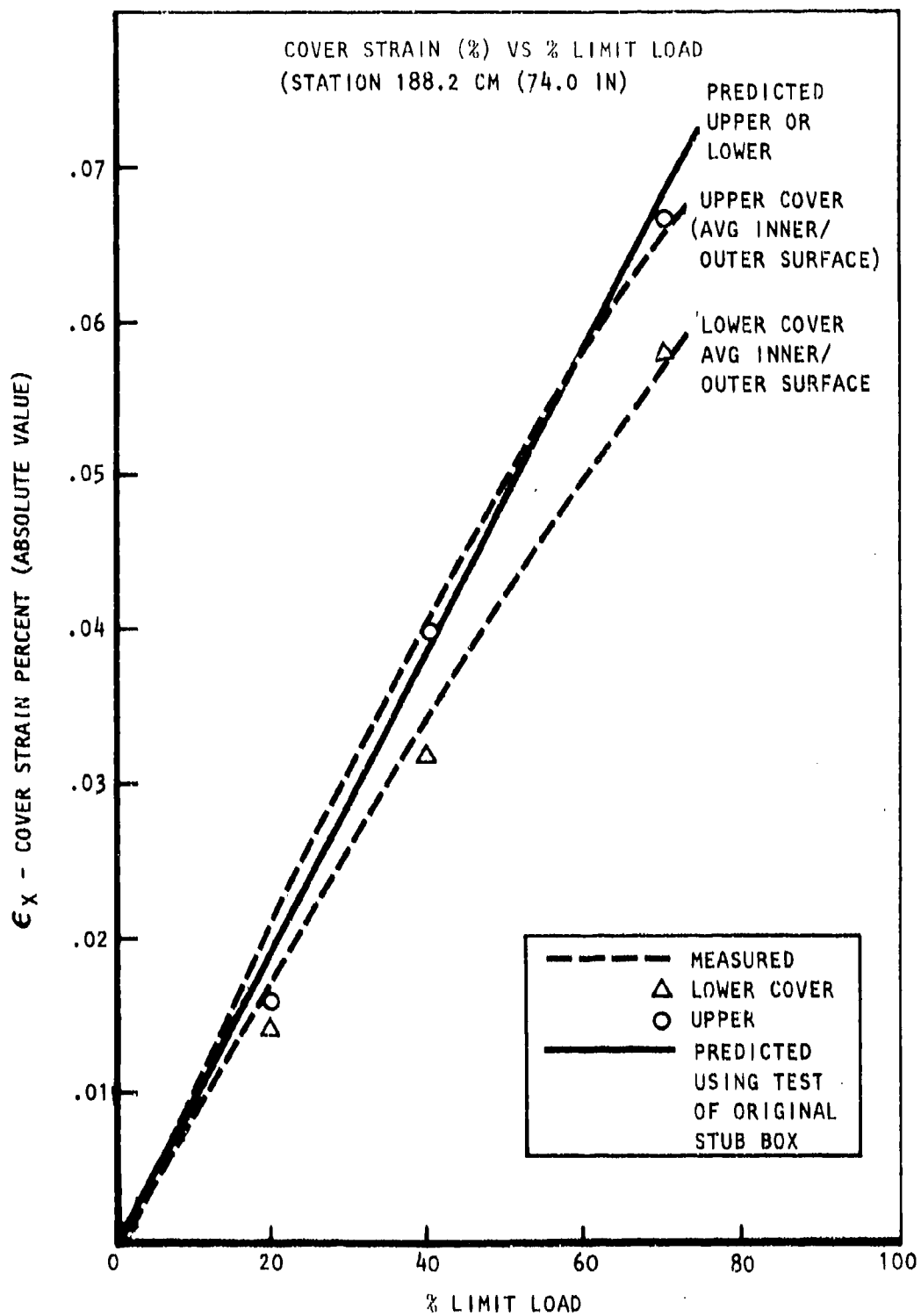


Figure 113. Comparison of Cover Predicted Maximum Axial Strains versus Measured

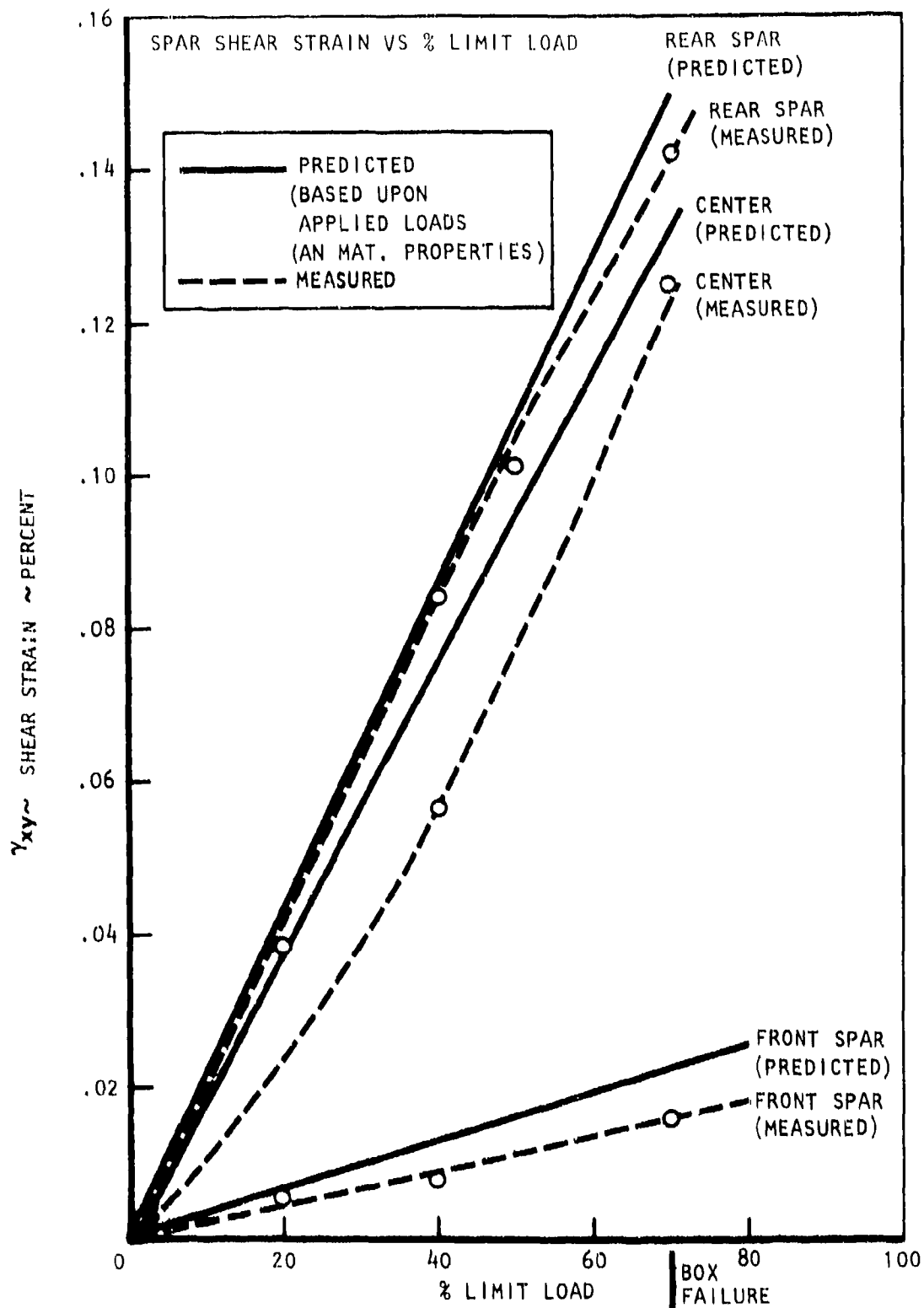


Figure 114. Comparison of Spar Predicted Shear Strains versus Measured



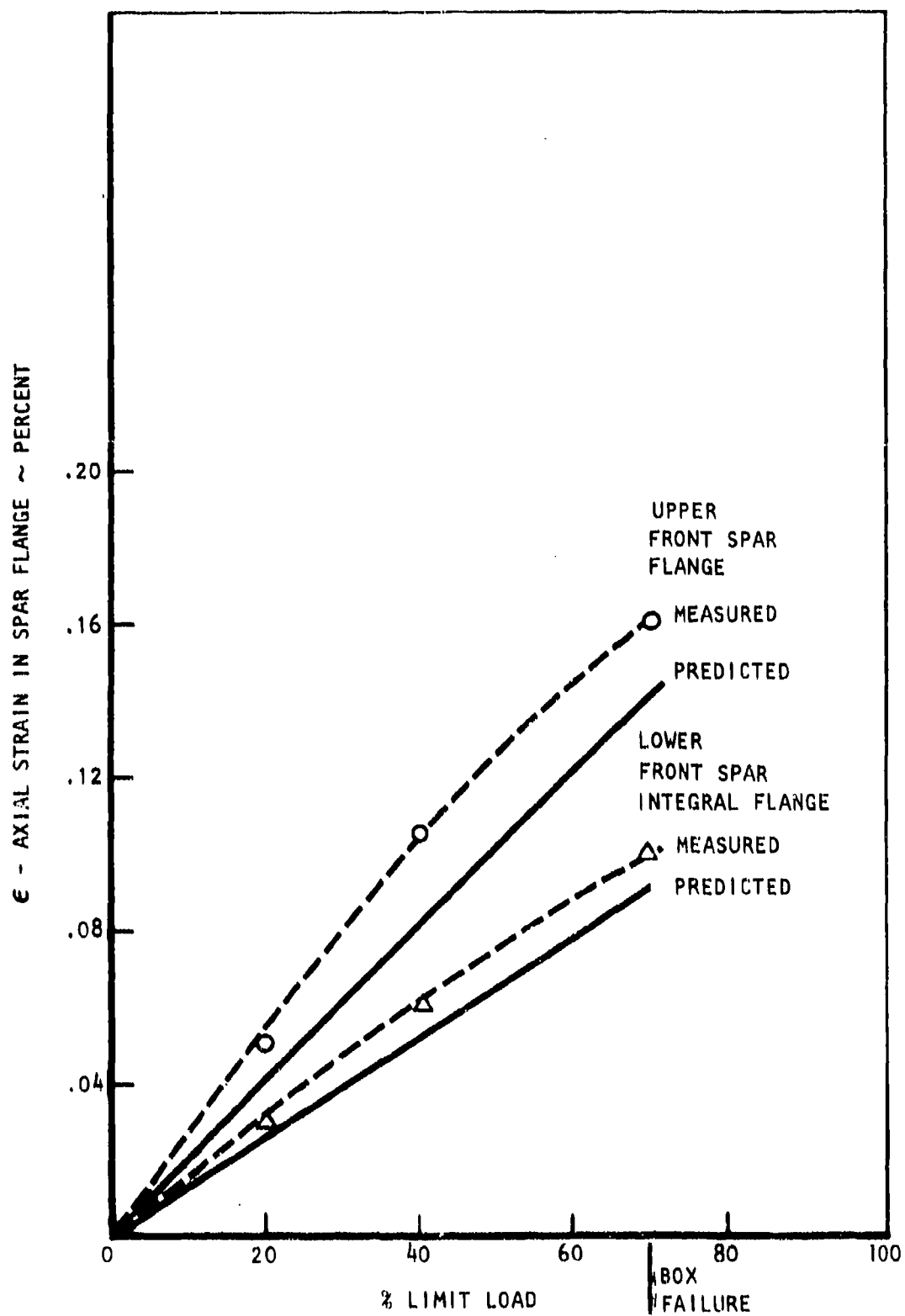


Figure 115. Comparison of Front Spar Flange Predicted Axial Strains versus Measured

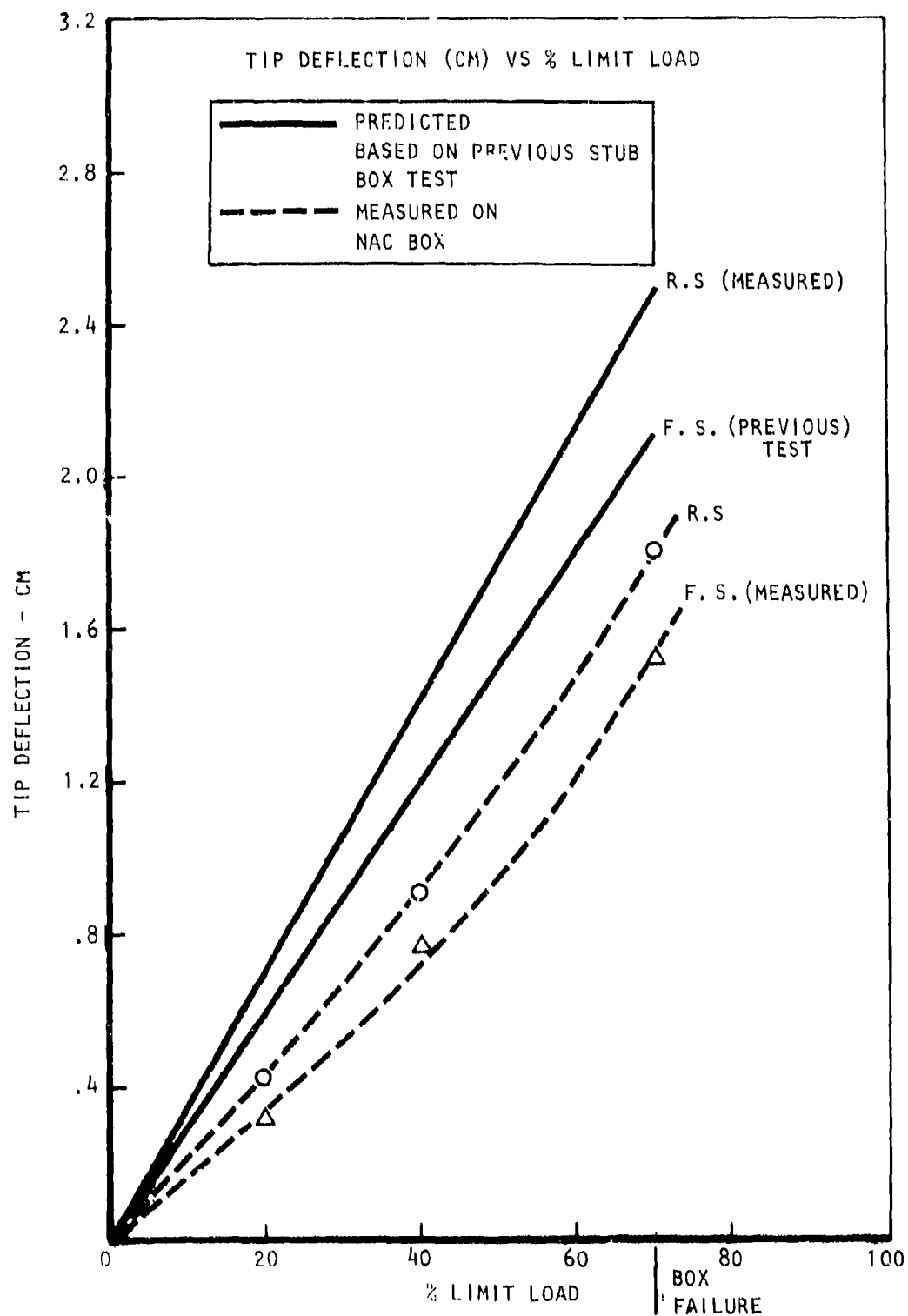


Figure 116. Comparison of Tip Deflections of Nonautoclave Subcomponent versus Baseline Subcomponent

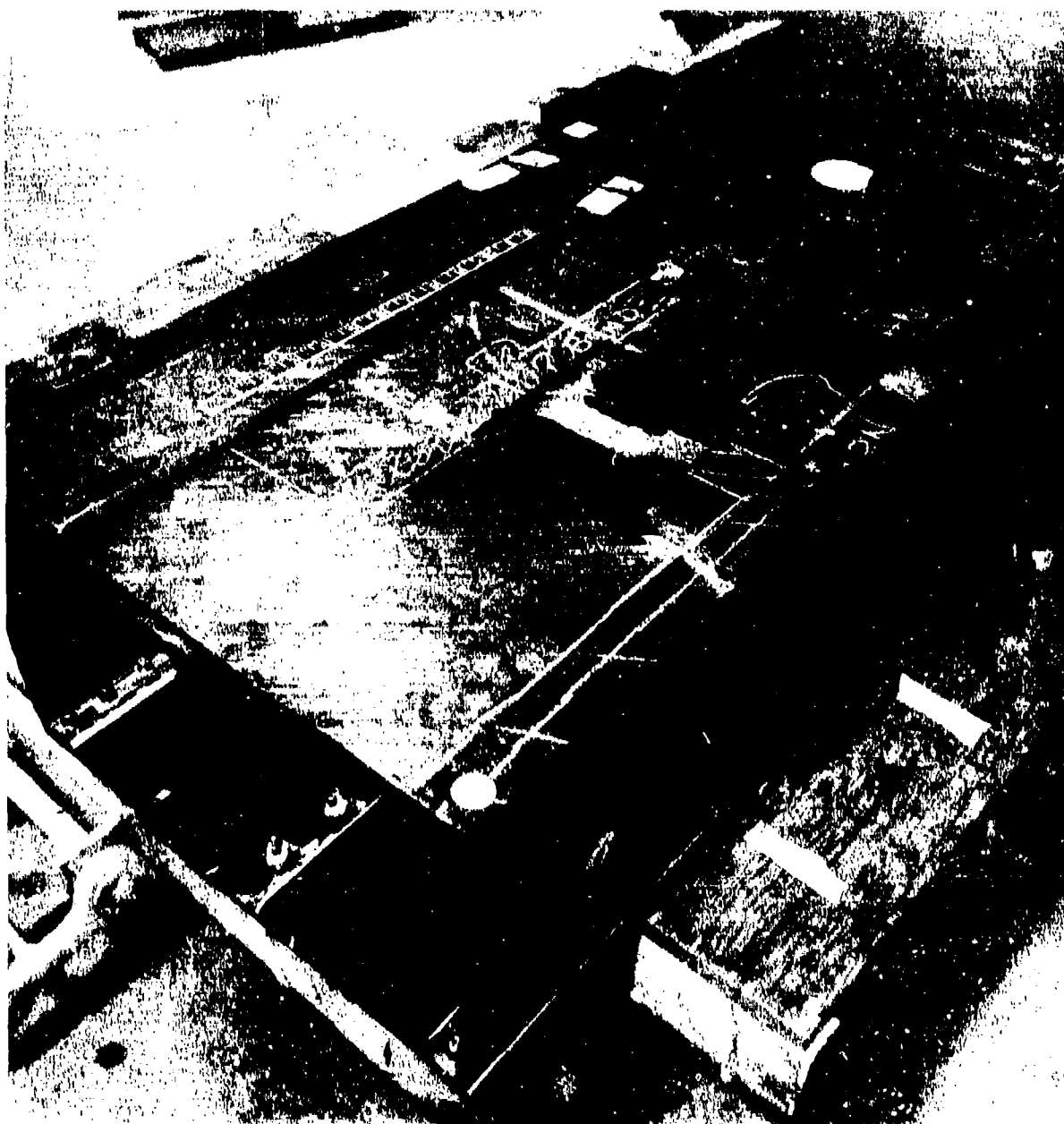


Figure 117. Section of Subcomponent Removed for Evaluation

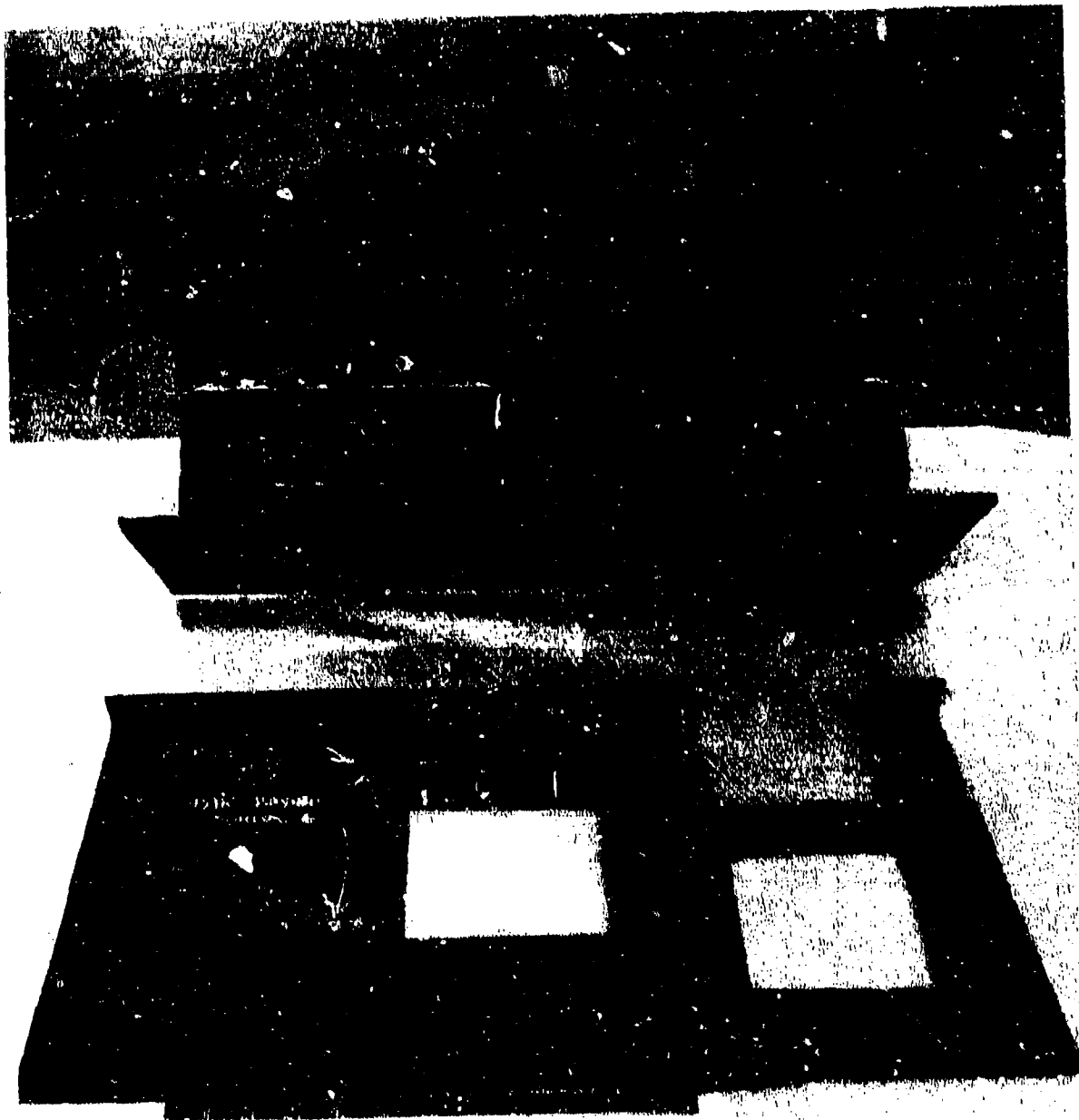
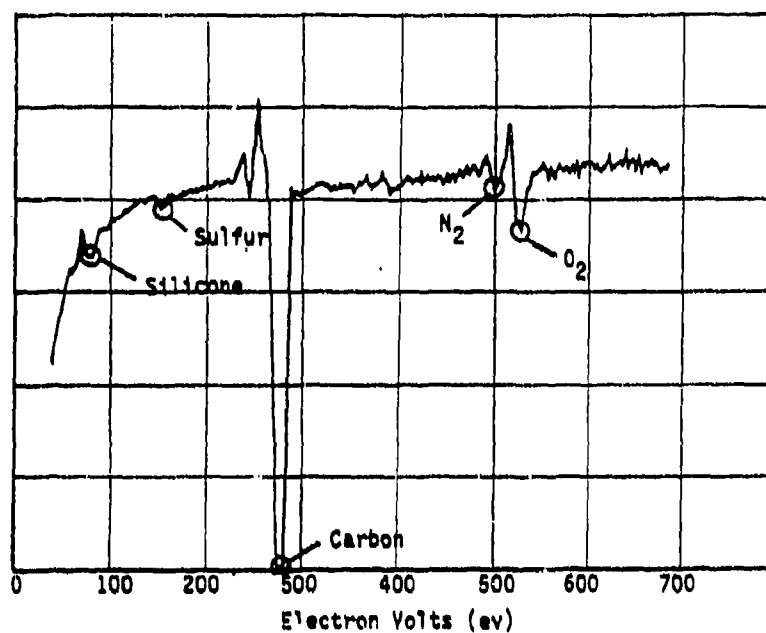
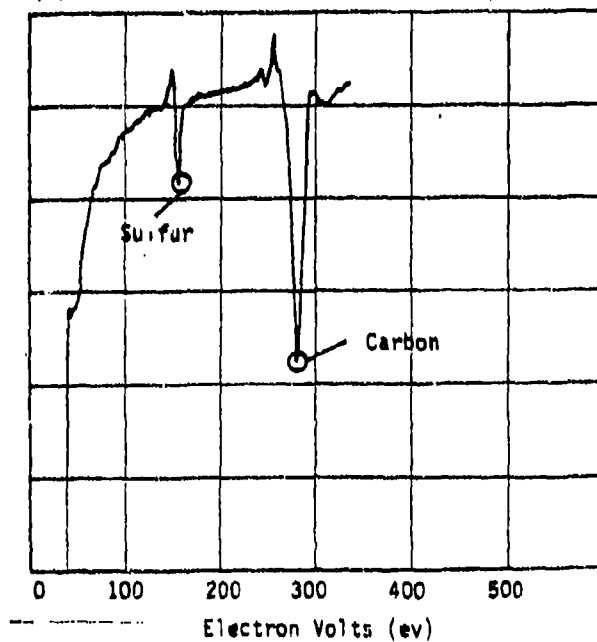


Figure 118. Section of Subcomponent Showing Lack of Bonding of Cover



(a) contaminated bondline - silicon peak visible at 75 ev



(b) Clean Sample - No Silicon Peak

Figure 119. Bondline Auger Analysis

#### 4.2.3 SUMMARY PHASE II - MANUFACTURING METHOD SCALE-UP

The ability of the nonautoclave process to fabricate larger subcomponent structures was proven during this phase. A subcomponent measuring 6 feet in length was fabricated using the methods and procedures developed during the previous phase.

A cocure bag which eliminated much of the tedious sealing required was demonstrated. The design utilized a one-piece construction which helped to reduce fabrication costs. This design was carried forward into phase three and made fabrication of the larger full scale component possible.

The development of a ultrasonic cutting knife to trim the staged details prior to placing them in the cocure assembly also resulted in cost savings.

Through the structural test of the subcomponent, a critical problem was brought to light. The subcomponent failed at 46.9 percent of ultimate load due to a disbond of the integral structure joint along the cover to spar bondline. Although state-of-the-art ultrasonic methods were used to evaluate the bond, they did not detect the disbond which was caused by silicone contamination of the faying surface of the cover. The success of the numerous articles fabricated previously conclusively proves that it was not the result of a problem inherent in the materials or processes used on the nonautoclave process. This instance clearly points out the need for strigent controls in the shop area to avoid silicone contamination and improved inspection methods for bonded structure. Despite this occurrence, the effort conducted during phase II reinforced the fact that gr/ep structure could be economically fabricated using the nonautoclave process.

During Phase III a full-scale demonstration component representative of the lower three-quarters of the B-1A vertical stabilizer (figure 120) was fabricated, inspected, and nondestructively evaluated. This component was fabricated, using the innovative methods verified in Phase I and validated in Phase II. The component, produced by nonautoclave manufacturing methods on tooling suitable for production, used production personnel to perform the manufacturing operations and production facilities in a production environment. Figure 121 depicts the manufacturing features and processes addressed during this phase of the program.

This full-scale composite vertical stabilizer component exercised aspects of the vacuum cure, nonautoclave process, and integral structure fabrication and, furthermore, demonstrated its generic application to aircraft wing structures. Thin laminates with complicated sine wave web configurations using woven cloth and unidirectional tape were processed for intermediate spar and rib assemblies. Full-length, contoured airfoil covers with thicknesses up to 103 plies demonstrated the processes used for thick laminates. The covers further demonstrated the processes and generic application of the process because the mechanically attached cover was degassed and cured completely as a detail, and the integral cover was staged first and cocured with the substructure.

The component was subjected to nondestructive evaluation (NDE) to verify its integrity. Final material and process specifications were prepared. Cost tracking was conducted on the Phase III component and at the completion of Phase III, a complete cost benefits analysis was conducted, reflecting the impact of optimized nonautoclave curing manufacturing methods. Figure 122 presents the activity flow of this phase.

#### 4.3.1 TASK 1 - FULL-SCALE PART FABRICATION

##### 4.3.1.1 Component Design

The full-scale component represented the main torque box of the vertical stabilizer with a surface area of over 55-square feet. The design of the three-quarter section of the vertical stabilizer (used in this program) was based on the composite vertical stabilizer design developed in 1974 for an earlier Air Force program, Low-Cost Composite Vertical Stabilizer program F33615-74-C-5164, AFFDL-TR-78-5.

The baseline or original Gr/Ep box component used advanced composite materials to provide cost and weight savings of approximately 15 percent when compared with its metal counterpart; the advanced composite torque box retained the identical form, fit, and function of its metal counterpart. The main box was designed using the stiffness requirements for flutter and aeroelastic stability and control (torsional stiffness GJ and bending stiffness EI). However, strength requirements (both static and fatigue) governed the area near the root splice as well as at fastener and

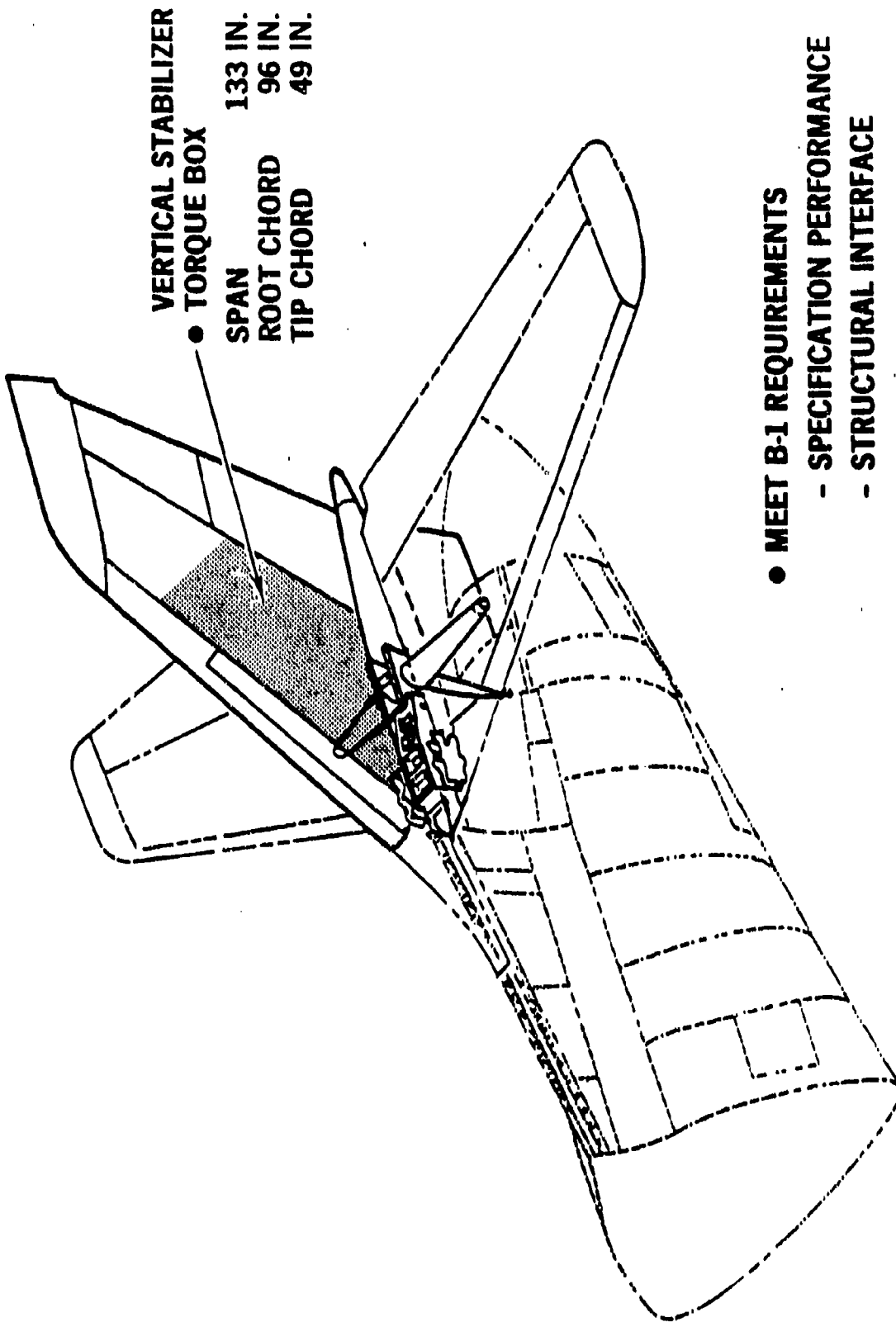
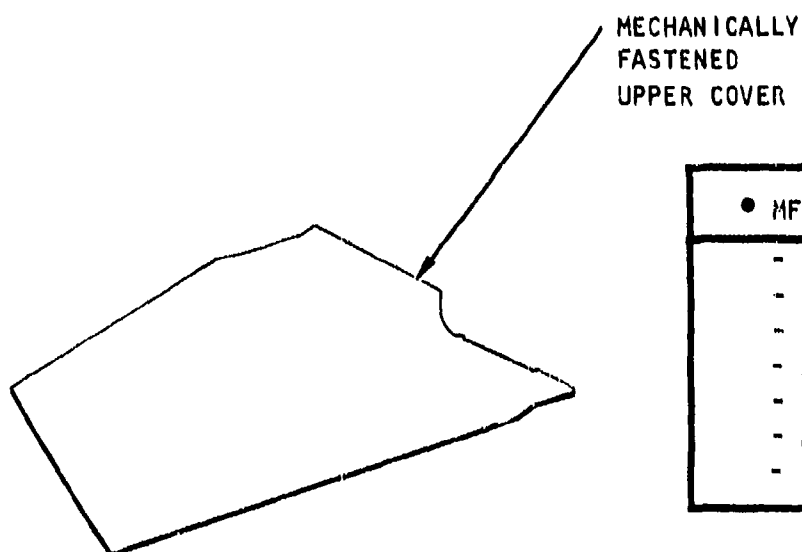


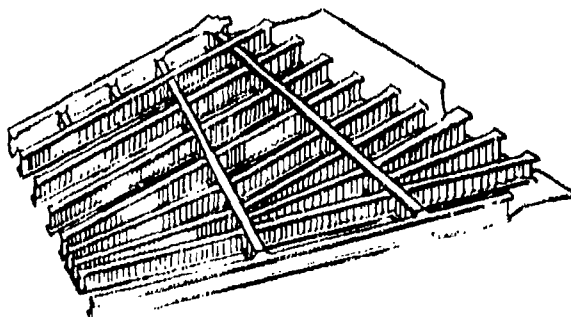
Figure 120. Phase III Full-Scale Component





• MFG FEATURES ADDRESS

- CANTED RIB
- MOLDLINE CONTOUR
- INTEGRAL STRUCTURE
- ACCESS PROVISIONS
- FIT-UP PROBLEMS
- ASSEMBLY OPERATIONS
- DIMENSIONAL STABILITY



• FABRICATION PROCESSES

- NON-AUTOCLAVE CURING
- ADVANCED TOOLING CONCEPT
- CAP/CAM
- NO-BLEED MATERIALS
- NET MOLDED EDGES
- FABRIC/BROADGOOD/TAPE  
MATERIAL FORMS

Figure 121. Manufacturing Features and Fabrication Processes

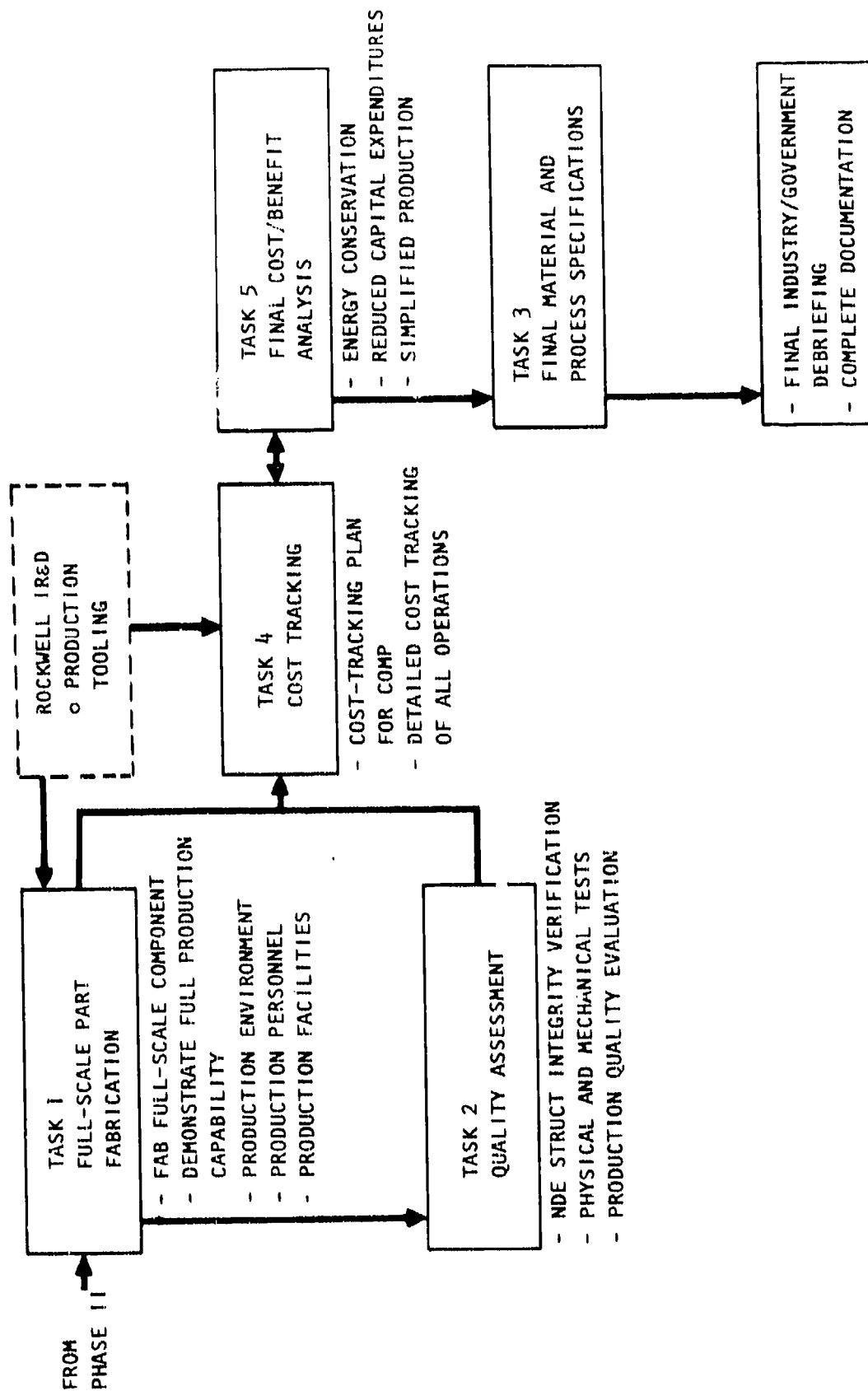


Figure 122. Phase III Flow Diagram

joint locations. Interface requirements governing hard-point locations and loading distribution were in the areas where the torque box attached to the fuselage.

The configuration of the nonautoclave design (figure 123) was similar to the composite vertical stabilizer component except that an integral structural concept was utilized in which the entire substructure was cocured together and to one cover. By changing to an integral structure design an additional 5-percent weight saving was possible as summarized in table XXV.

The integral design utilized the same Gr/Ep unidirectional tape ply orientation for both the mechanically attached and integral covers. The cover designs utilized boron/epoxy for the 0-degree plies in the root attachment area. The maximum thickness in this area was 103 plies of which 34 were 5.6 mil boron/epoxy. The cover taped from the root area (103 plies) to the tip which contained 40 plies.

The substructure was composed of 8 spars and 2 ribs. The spars were discontinuous at the ribs resulting in three sections. The 8 ply spar and rib caps on the mechanically fastened cover side were continuous over the intersection points to provide continuity of the load transition from the cover to the substructure. The higher loading at the root end required use of sine wave webs for the spars below  $Z_{VS67}$  111.594 (figure 124). Typical thicknesses of the spars in this area were 12 plies (0.068 inch) for the lower bay and 6 plies (0.036 inch) for the intermediate bays. The web was built up to 74 plies (0.110 inch) and 12 plies, respectively, as it transitioned into the cap area. All of the sine wave spars contained an outer ply of fabric. The upper bay of spars were flat web with an average web thickness of 16 plies (0.090 inch). The first spar was a constant section I-beam with a web thickness of 56 plies, the rear spar (no. 8) incorporated a combination of sine wave and flat web. This configuration of sine wave and flat web was used in the two ribs also. The 24-ply flat-web portion extended from the front spar to spar No. 5 then it transitioned to a 6-ply sine wave web for the remainder of the rib. These members, with integral shear clips and attach angles, were cocured with the right-hand cover under vacuum pressure and heat. Because of the change to an integral structure design the use of load couplers identical to those used in the Phase I and II designs were incorporated in the lower spar nos 4, 5, 6, and 7 as shown in figure 124.

#### 4.3.1.2 Tool Design and Fabrication

All tooling required for the fabrication of the full-scale demonstration component was provided to the contract through government property or from NAAO in-house efforts. The tooling represented as closely as practical production type tooling, although some concessions to tool longevity were made.

The two steel lay-up tools for the covers (figure 125) were furnished to the program from the previous vertical stabilizer program. The drawing numbers for the various details are listed in table XXVI.

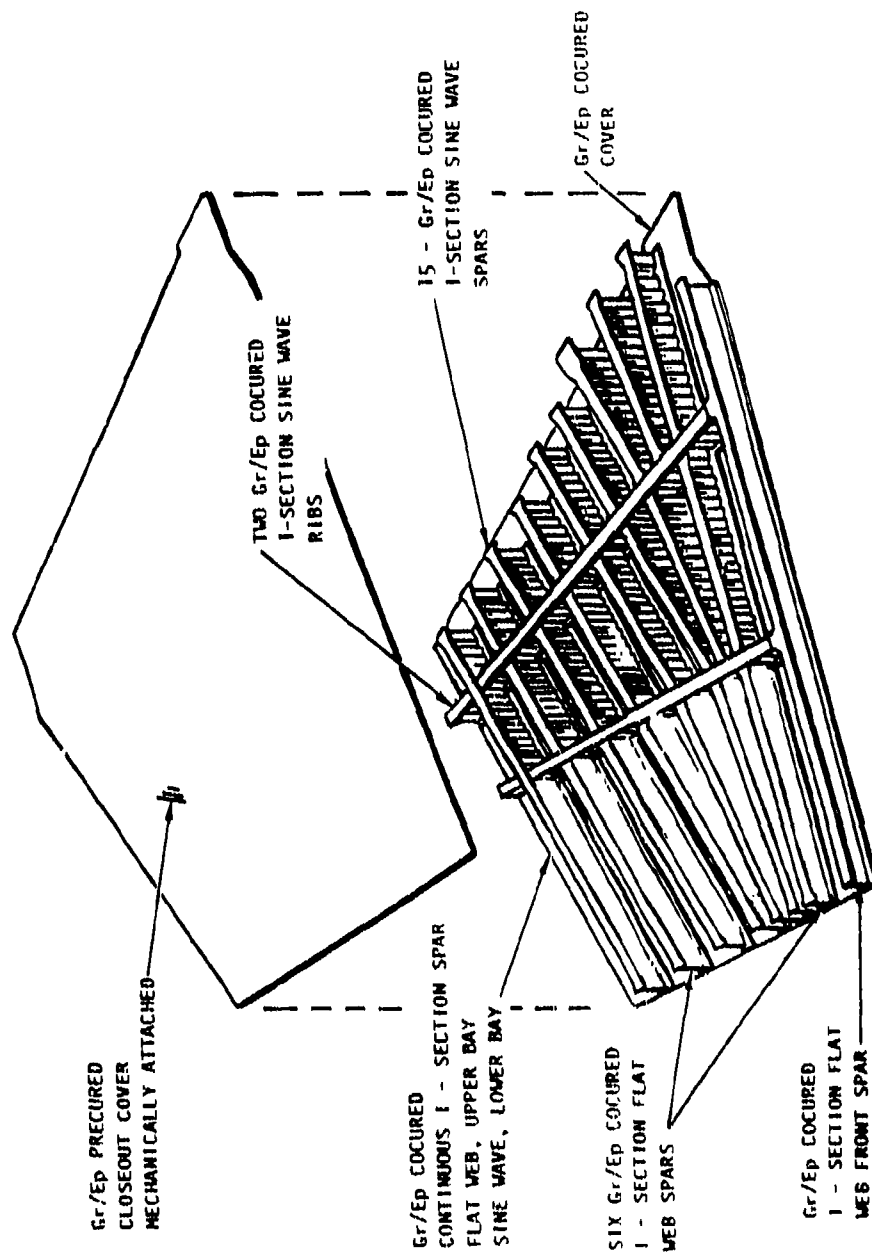
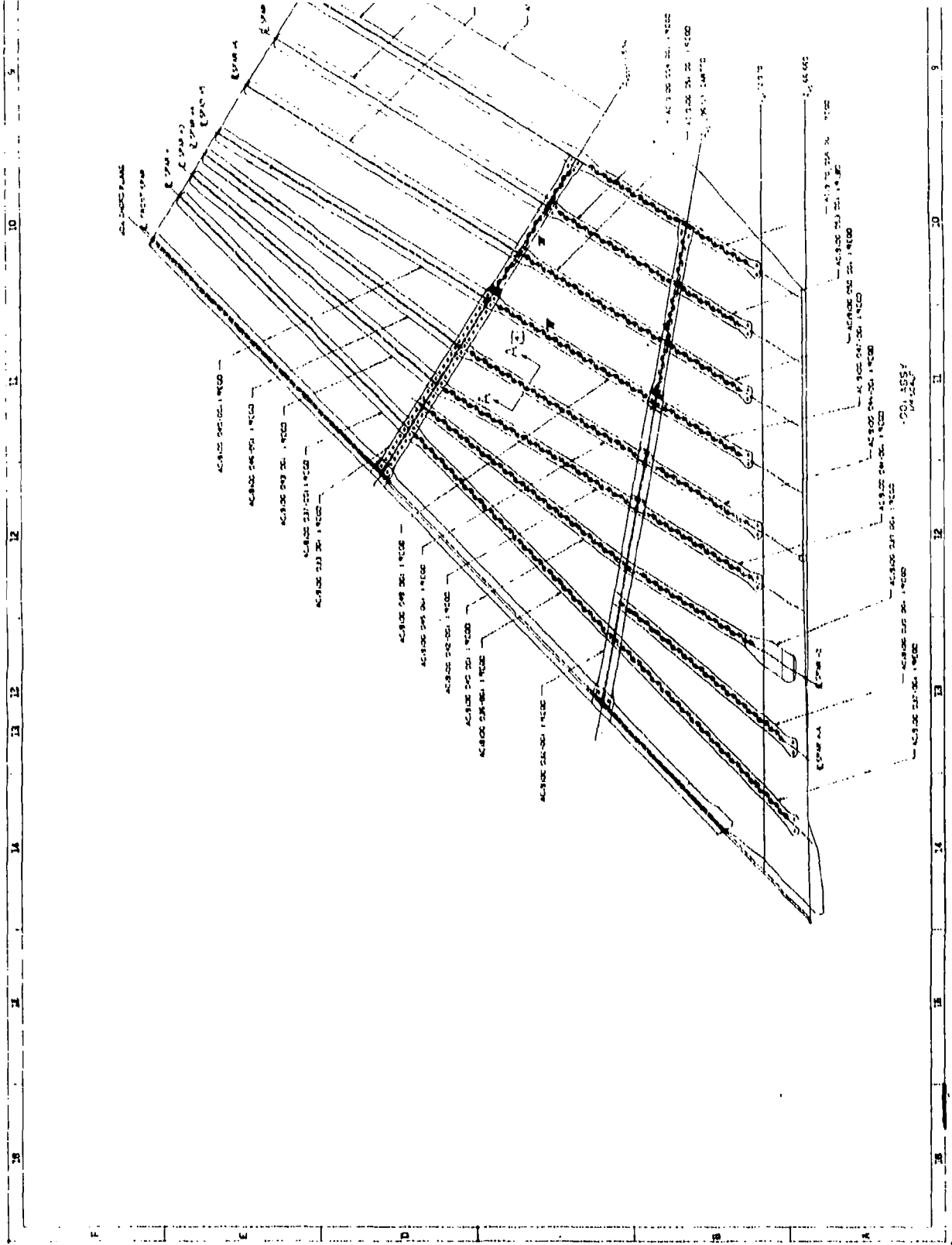
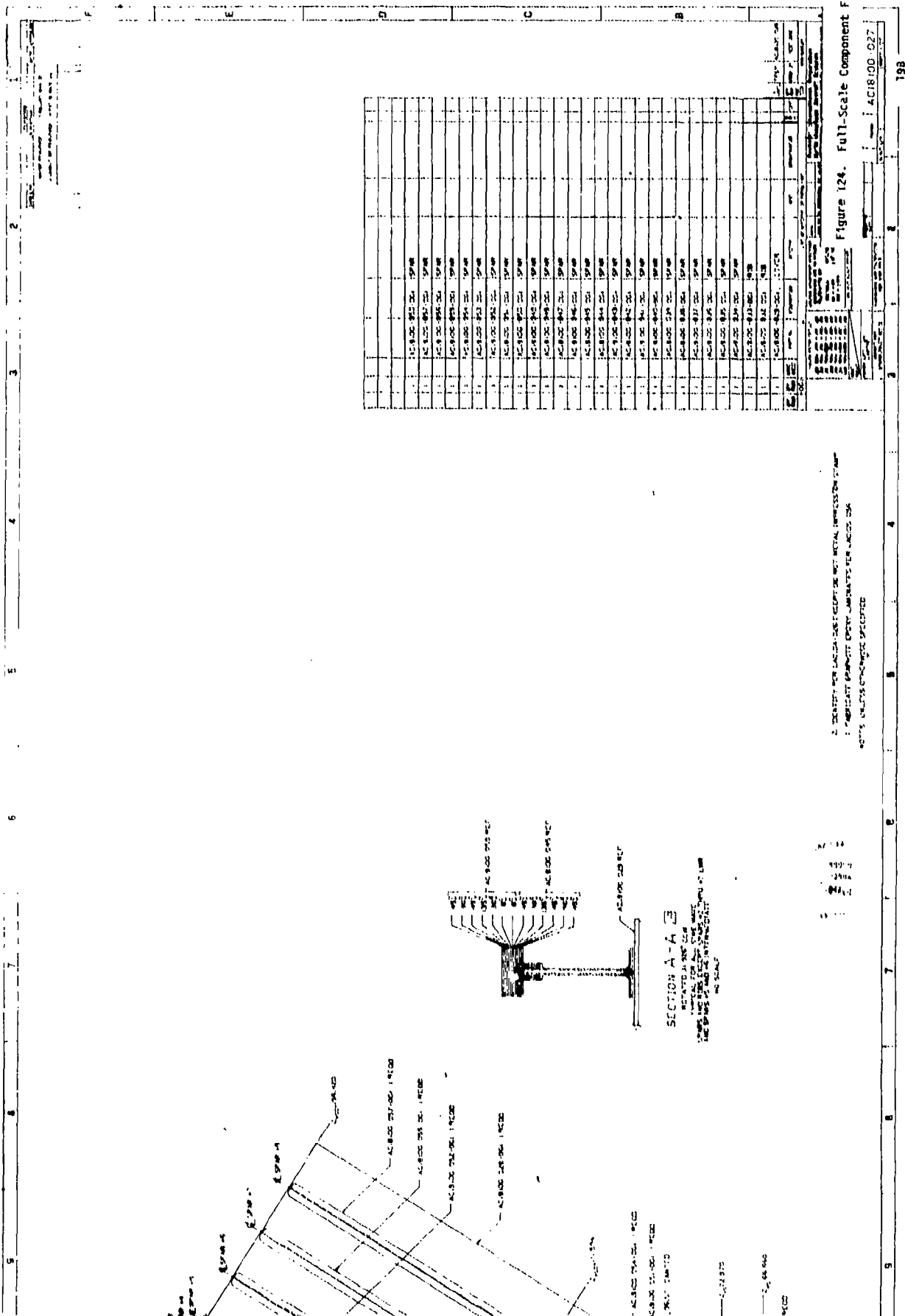


Figure 123. Integral Composite Structure Demonstration Article

TABLE XXV  
B-1 COMPOSITE VERTICAL STABILIZER  
WEIGHT SAVINGS SUMMARY

COMPONENT	METAL	COMPOSITE		
		CONVENTIONAL CONSTRUCTION	WT	INTEGRAL (NONAUTOCLAVE)
COVERS	( 414.4)	( 328.6)	( - )	( 328.6)
COMPOSITE PANELS		250.0		250.0
ALUMINUM SKIN	412.6	62.0		62.0
LIGHTING STRIKE PROTECT		13.9		13.9
DOORS	1.8	2.7		2.7
FRONT SPAR	( 31.6)	( 24.3)	( -0.10)	( 24.2)
INTERMEDIATE SPARS	( 55.1)	( 53.9)	( +5.0 )	( 58.9)
REAR SPAR	( 30.1)	( 31.2)	( - )	( 31.2)
TIP RIB	( 3.9)	( 5.6)	( - )	( 5.6)
TRAILING EDGE RIGS	( 5.6)	( 3.4)	( -0.2)	( 3.2)
INTERMEDIATE RIBS	( 26.1)	( 24.6)	( +0.7)	( 25.3)
Z <sub>vs</sub> 72.87		9.6		9.6
Z <sub>vs</sub> 6796.591		7.4	+0.7	8.1
Z <sub>vs</sub> 67111.59		4.7		4.7
Z <sub>vs</sub> 67156.42		2.9		2.9
ROOT RIB AREA	( 36.6)	( 35.7)		( 35.7)
Z <sub>vs</sub> 66.85	12.6	18.3		18.3)
Z <sub>vs</sub> 61.56	24.0	12.0		12.0
Fwd Transition Closeout		1.7		1.7
Transition Intercostals		3.7		3.7
FASTERNERS	( 27.2)	( 46.5)	( -10.1)	( 36.4)
CLIPS	( 2.6)	( 3.5)		( 3.5)
SHIMS AND MISC.	( 7.1)	( 2.3)		( 2.8)
<u>SUBTOTAL</u>	<u>640.3</u>	<u>560.1</u>	<u>( - 4.7)</u>	<u>555.4</u>
AVIONICS CONDUITS	( 7.7)	( 0.0)		( 4.0)
INTERIOR FINISH	( 6.9)	( 4.0)		( 4.0)
TOTAL TORQUE BOX(16)	654.9	564.1		559.4
PERCENT SAVING		13.9		14.6





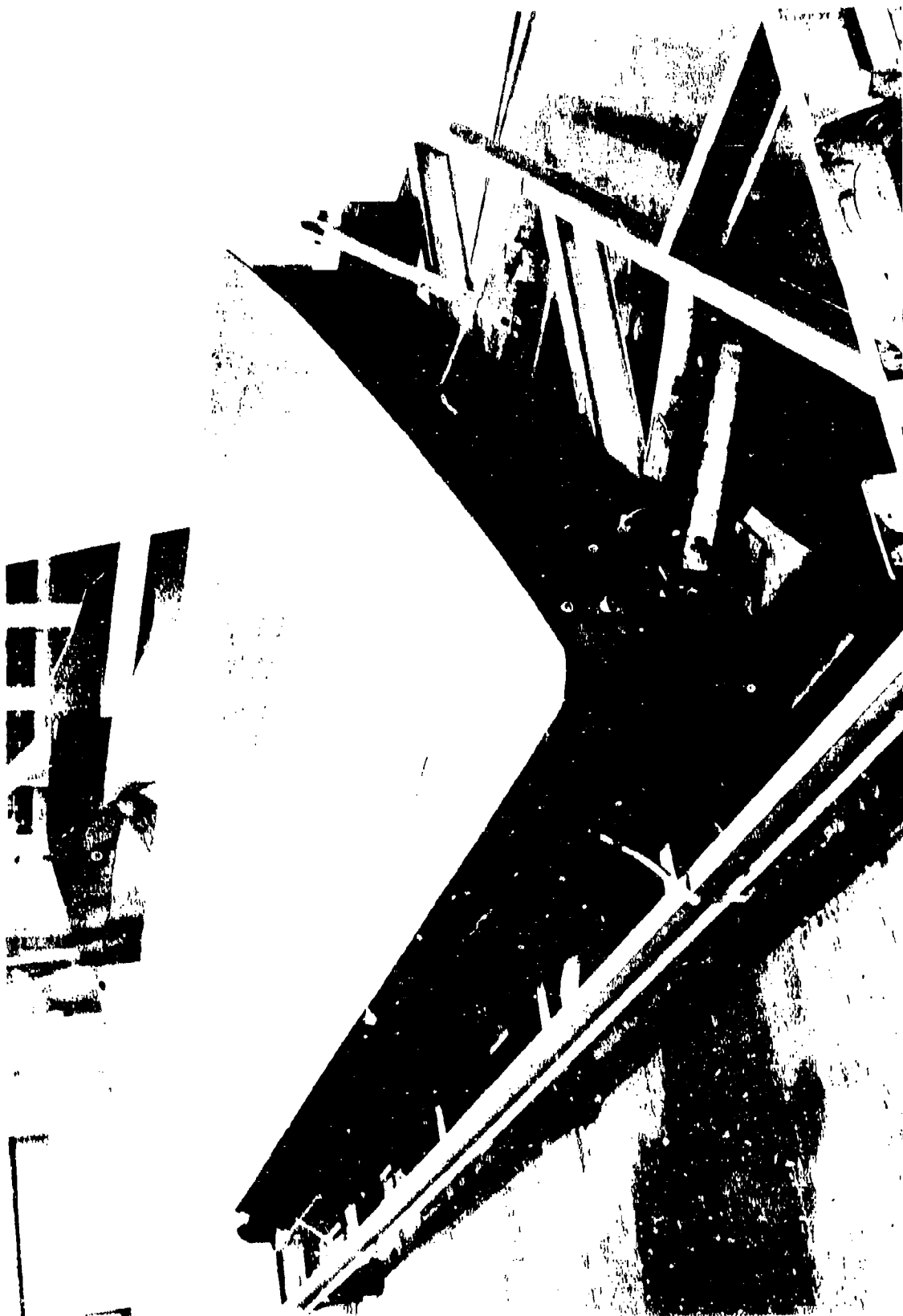


Figure 125. Vertical Stabilizer Skin Cover Tool



TABLE XXVI. FULL-SCALE COMPONENT DRAWINGS LIST

Drawing No.	Description
AC18100-026	Cap Box Assembly
AC28200-027	Substructure Assembly
AC18100-028	Cover Installation
AC18100-029	Cover
AC18100-030	Riblet - ZVS 6/ 96.591
AC18100-031	Riblet - ZVS 67 111.594
AC18100-032	Rib - ZVS 67 96.591
AC18100-033	Rib - ZVS 67 111.594
AC18100-034	Spar Assembly - Front
4448100-035	Spar Assembly - No. 1 Lower
AC18100-036	Spar Assembly - No. 1 Intermediate
AC18100-037	Spar Assembly - No. 1 Upper
AC18100-038	Spar Assembly - No. 1 A Lower
AC18100-039	Spar Assembly - No. 2 Lower
AC18100-040	Spar Assembly - No. 2 Intermediate
AC18100-041	Spar Assembly - No. 3 Lower
AC18100-042	Spar Assembly - No. 3 Intermediate
AC18100-043	Spar Assembly - No. 3 Upper
AC18100-044	Spar Assembly - No. 4 Lower
AC18100-045	Spar Assembly - No. 4 Intermediate
AC18100-046	Spar Assembly - No. 4 Upper
AC18100-047	Spar Assembly - No. 5 Lower
AC18100-048	Spar Assembly - No. 5 Intermediate
AC18100-049	Spar Assembly - No. 5 Upper
AC18100-050	Spar Assembly - No. 6 Lower
AC18100-051	Spar Assembly - No. 6 Intermediate
AC18100-052	Spar Assembly - No. 6 Upper
AC18100-053	Spar Assembly - No. 7 Lower
AC18100-054	Spar Assembly - No. 7 Intermediate
AC18100-055	Spar Assembly - No. 7 Upper
AC18100-056	Spar Assembly - No. 8 Lower
AC18100-057	Spar Assembly - No. 8 Upper
AC18100-058	Caps, Spars, and Ribs
AC18100-059	Spar Assembly - Rear

An upper chamber was fabricated from steel plate and 10-inch high I-beams. The beams were placed at 14-inch centers to provide the required stability to the tool cover to prevent warping when vacuum is applied (figure 126). To position the cavity above the tool surface, 2-inch thick solid Gr/Ep laminates matching the moldline of the tool were attached to the upper tool cover (figure 127). The upper and lower tools were clamped together using C-clamps with a piece of compressible rubber at the interface to act as a seal. While this system was not elaborate, it was proven satisfactory in the 15 runs that the tool was exposed to during the course of the program. The 1-inch diameter vacuum lines on the upper cover are visible in figure 128. A total of 12 0.25-inch vacuum outlets were provided in the upper tool cover and 8 in the lower lay-up die located around the periphery of the tool.

The substructure staging tools used the same design philosophy developed during Phases I and II. Plaster master tools (figure 129), fabricated from templates drawn from Computer Vision drawings, formed the basis for laying up the strongbacks, which were fabricated from Gr/Ep. The correct gap between the tool halves was maintained by steel channels (figure 130) and rubber shims on the bags. The strongbacks again were used as tools to spray the silicone rubber staging bags. D-aircraft compound No. 62 was used. The bag thicknesses were increased from the Phase II bags of 0.062 inch to 0.100 inch to make them more durable. Figure 131 shows the rib tool with only the bags in place. One modification to the substructure tools was the elimination of a C-channel at the end of the tool to reduce number of detail parts in the tool. In the Phase III staging tools a seal strip was added to the end of the bag so that when the two halves of the tool were mated, the bags would seal against each other. Bolts through the hardback and bag prevented the bag from slipping during the staging operation. Figure 132 shows some of the 24 substructure staging tools fabricated during the program.

The cure tool manifold system, which provided rib and spar height control as well as vacuum within the bag during the cocure operation, is shown in figure 133. This structure was fabricated from low-carbon steel rectangular tubing welded at all joints. The manifold was positioned above the cover tool surface at the correct height with 14 graphite/epoxy angles attached to the manifold using titanium bolts. Use of Gr/Ep for the standoffs reduced the thermal expansion during cure. Figure 134 shows the standoffs prior to installation on the manifold.

To ensure that the manifold structure would be adequate to maintain the correct chordal height of the substructure details, the square steel tube structure was analyzed using a NASTRAN finite element model. Loading on the manifold was primarily the result of the 257 pounds of manifold and the weight of the rubber bag which was 189 pounds. This combined weight was distributed at the node locations, as shown in figure 135. The maximum deflection observed in the analysis was 0.035 cm (0.014 inch) which is well below the 0.08 cm (0.03 inch) allowed for fitup discrepancies.

The various substructure tools were used to fabricate fiberglass tool proof parts which checked the dimensional accuracy of the tools and, in turn, those tool-proof parts were used as tooling for fabrication of the cocure bag. The 24 fiberglass parts assembled on the skin tool are shown in figure 136.

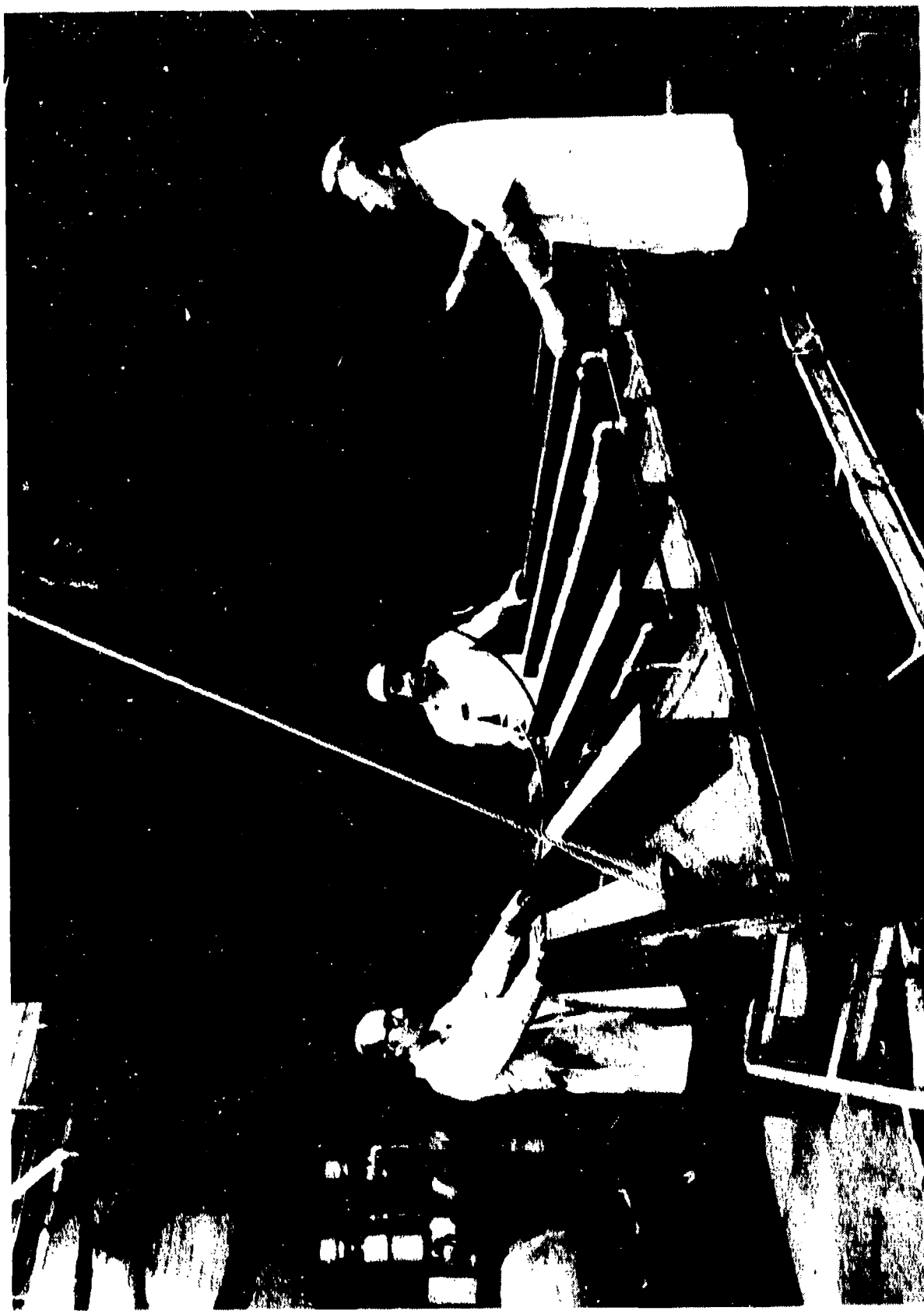


Figure 126. Skin Tool (Upper Chamber Placed on Lower Chamber)



Figure 127. Upper Cover Tool Assembly

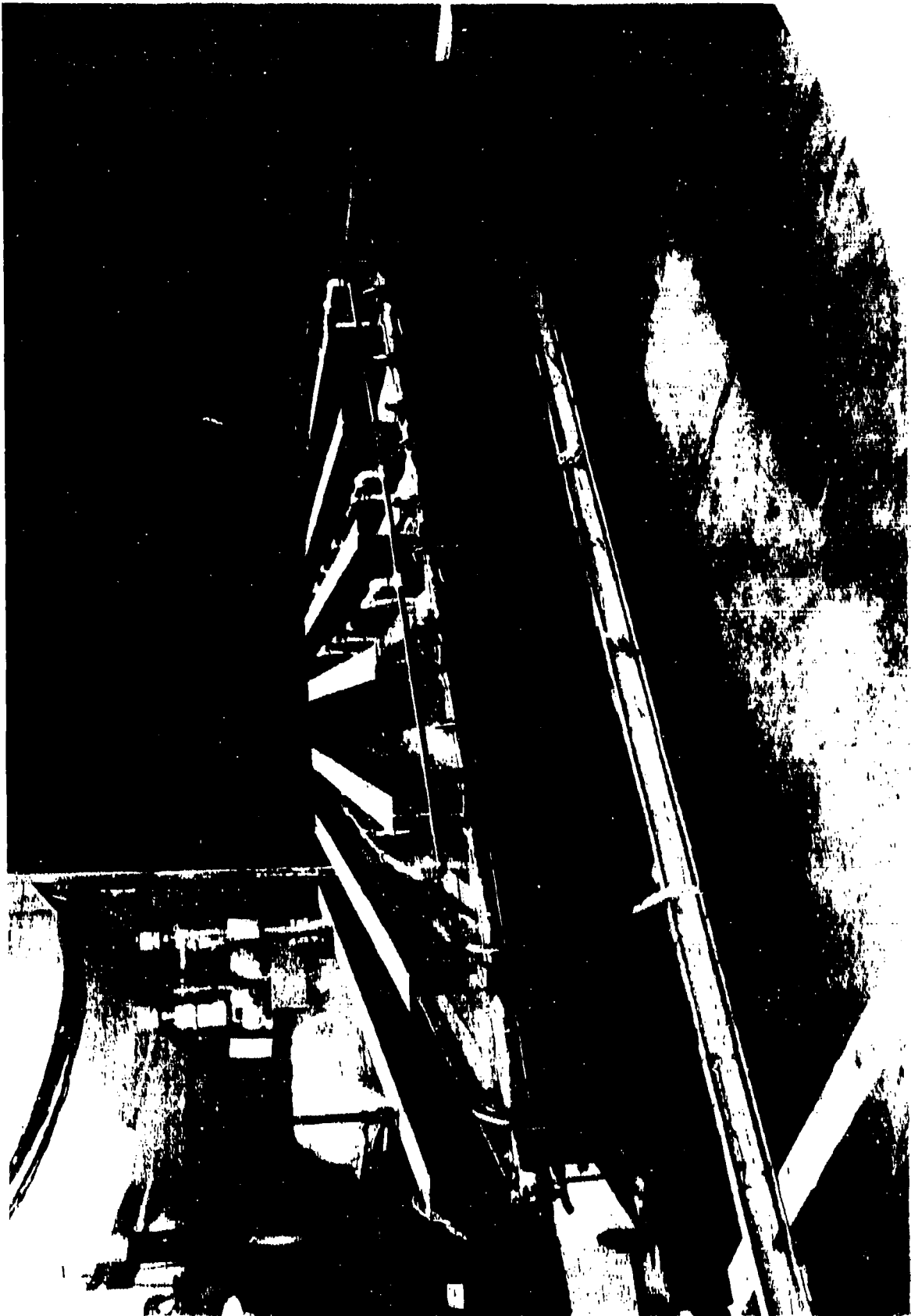


Figure 128. Composite Vertical Stabilizer (CAP Box) Skin Tool Assembly



Figure 129. Typical Plaster Tool Master for CAP Box Intermediate Rib at  
Station Z<sub>VS</sub> 111.594



Figure 130. CAP Box Intermediate Rib Tool (Strongbacks and Bag Not Included)



Figure 131. CAP Box Intermediate Rib Tool with Bag in Place - No Strongbacks





Figure 132. Completed Hardback Tooling for CAP Box

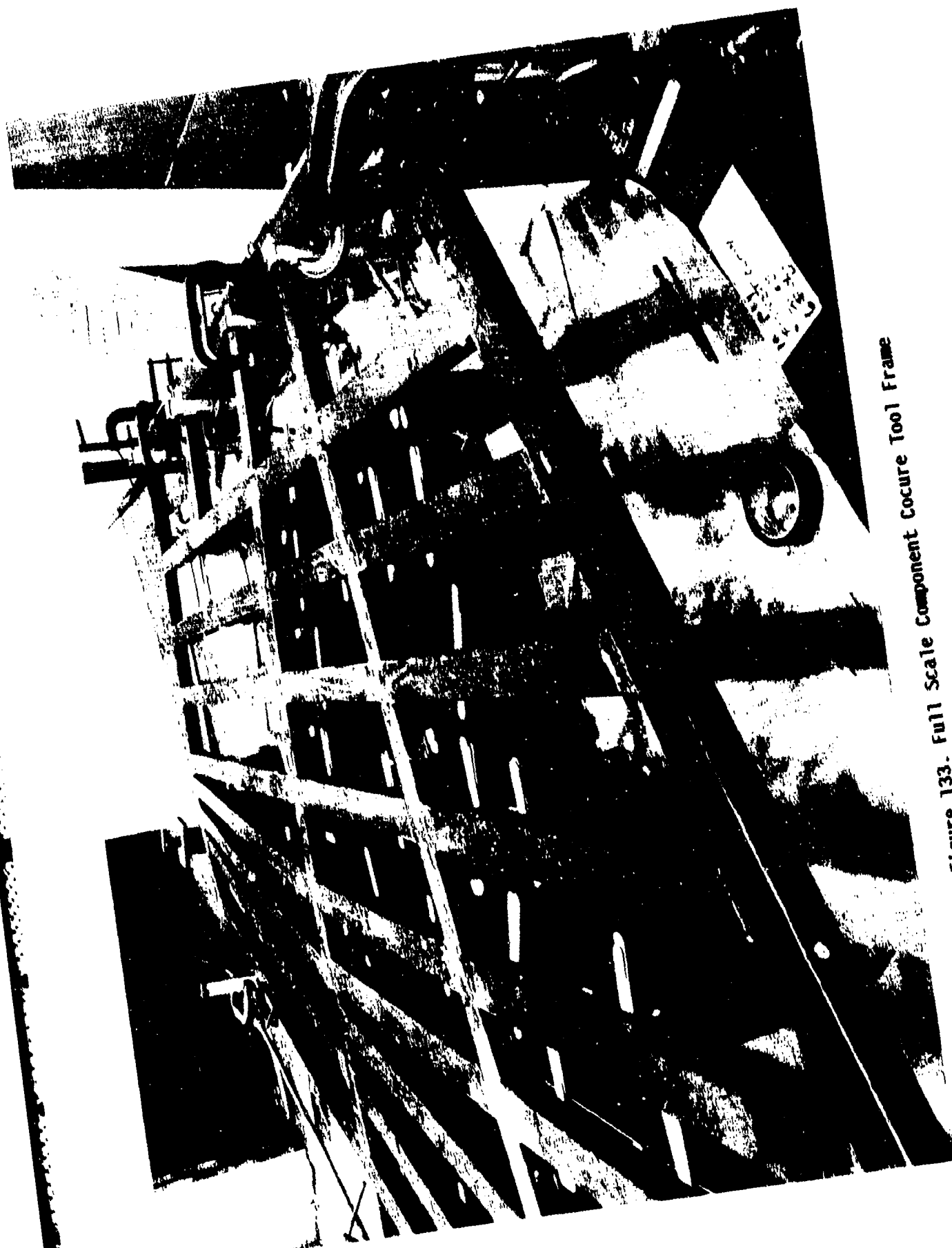


Figure 133. Full Scale Component Cocure Tool Frame



Figure 134. Closeup of Fitup Between Manifold and Part

# 14 Gr/Ep Vertical Supports

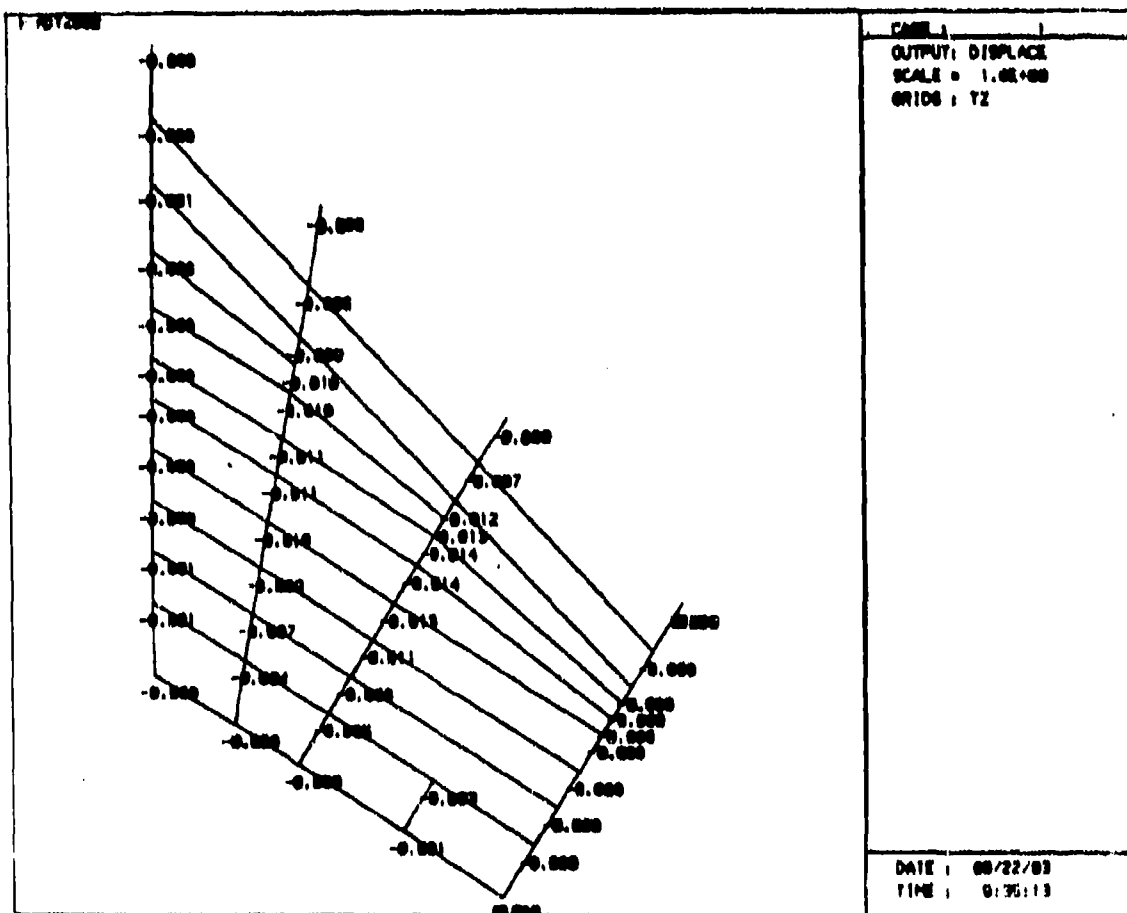
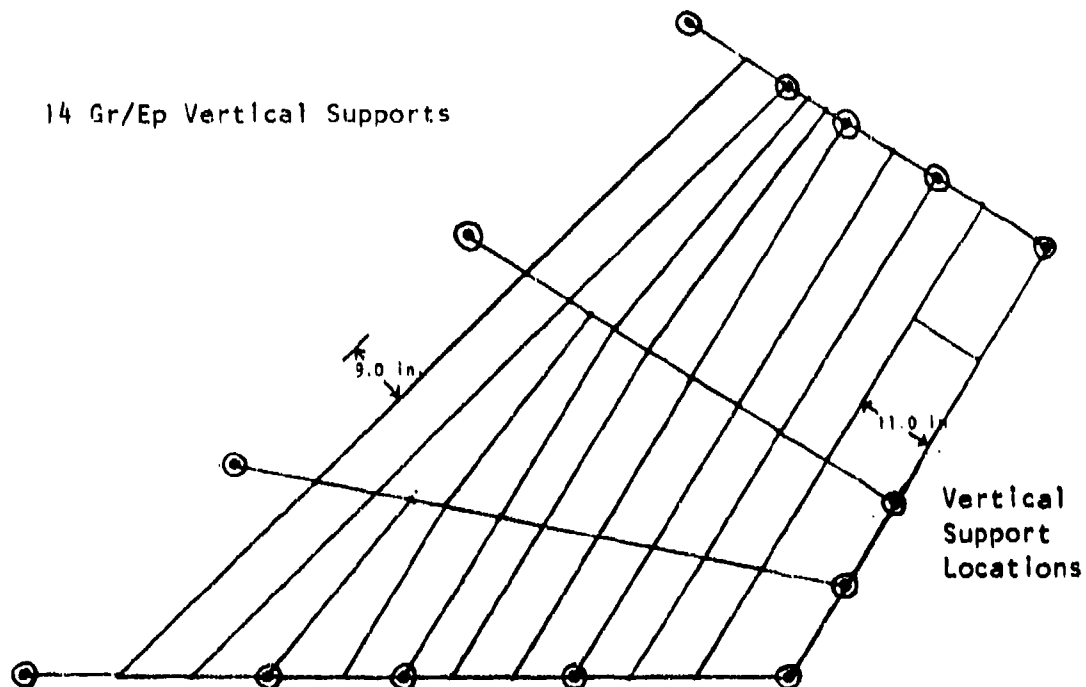


Figure 135. Vertical Displacements for Maximum (450 pound) Load

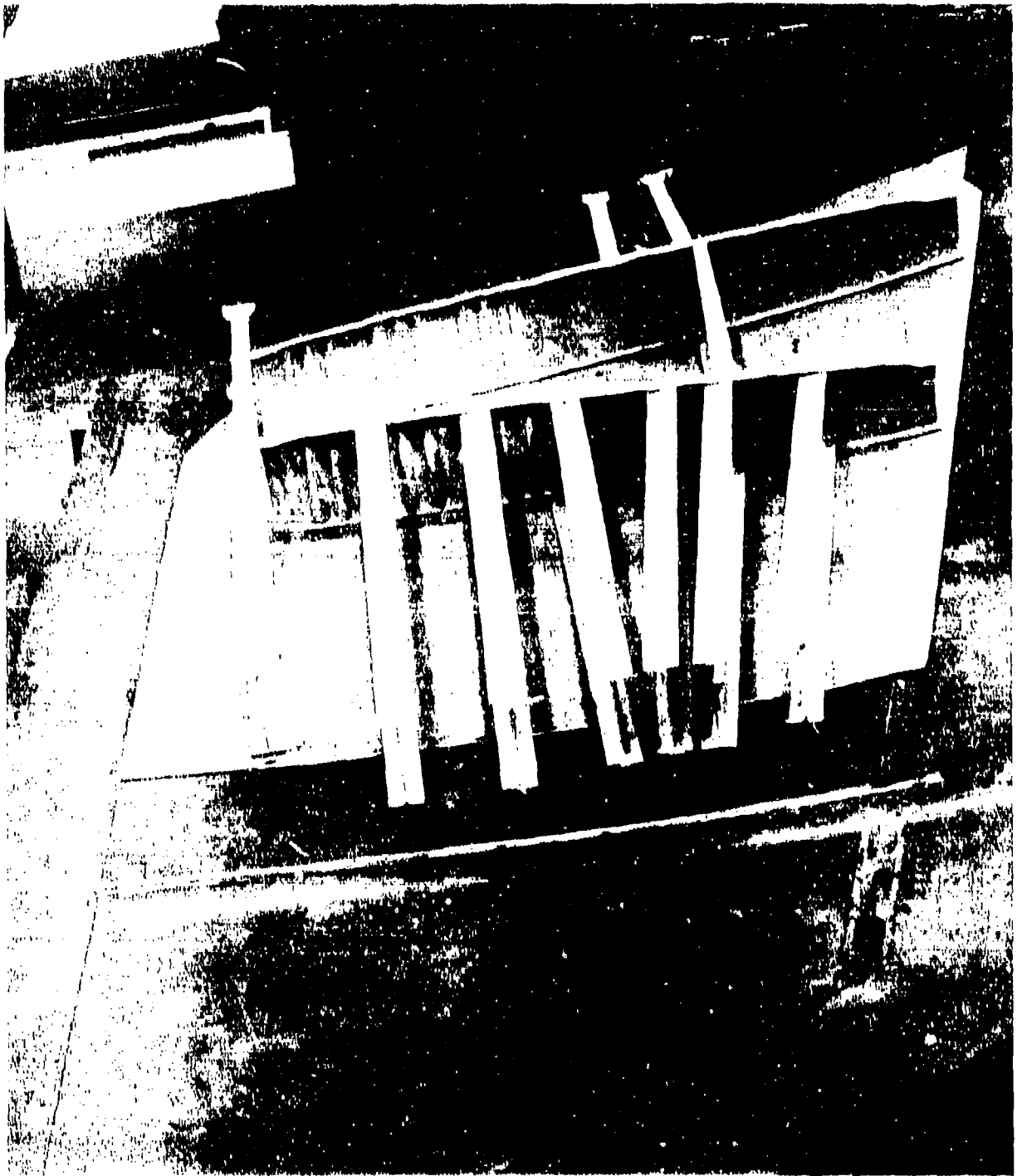


Figure 136. Fiberglass Tool Proof Details Prior to Fabrication of Cure Bag

The 189-pound cocure bag was fabricated from the D-Aircraft Compound-62 rubber (used for the stub-box cure bag). Because of the size of the bag required for the component and the location of the spars at the upper end of the box, which meet at very close angles making application of the rubber in this area virtually impossible, it was decided to fabricate the bag in separate sections, unlike the stub box which was sprayed as one entire unit. A system of spraying the bag involved spraying a section of the bag over each spar then assembling the sections into three larger bags. The fiberglass tool-proof parts were fitted with a wood block at the top to simulate the manifold and a section of the bag was sprayed over each detail, as shown in figure 137 and 138. Once all 26 sections were sprayed to a minimum thickness of 0.10 inch, the 26 individual sections were assembled on the tool and glued together using the Compound 62 rubber. Figures 139 show the assembly process. After all joints were sealed the bag was leak-checked, using a sonic leak detector, prior to installation over the graphite/epoxy details.

#### 4.3.1.3 Component Detail Fabrication and Assembly

##### 4.3.1.3.1 Scale-Up Evaluation

Prior to fabrication of the actual full-scale component details the ability of the nonautoclave process to fabricate large skins was verified through company funded efforts. A series of scale-up panels was fabricated on the full-scale production skin tools using the process specification (MPP 05L023-01) prepared during Phases I and II. Table XXVII summarizes the panels fabricated during this effort.

As a first step toward scaling-up the panel size parameters (thickness and area) of laminates a test laminate, 61 by 61-cm (24 by 24-inches), of 103-ply AS4/976 graphite/epoxy tape, was fabricated in the skin tool using a plain nylon bag. The normal stage cycle was used, 30 minutes at 121°C- 125°C (250°F-260°F) with full vacuum, 26-inches Hg. After removing the part from the tool, a 2.54- by 2.54-cm (1.0-inch by 1.0-inch) section was extracted, examined under the microscope, and found to be acceptable. The part was then bagged and cured under vacuum pressure at 177°C (350°F). The part was sectioned and found to be void free.

Having established that the maximum thickness of the part could be obtained, the tool contour and stability was checked. A fiberglass laminate, simulating the graphite/epoxy cover, was laid up on the cover tool and cured using vacuum only. Although this was a tool check to verify finished part thickness and tool contours, total variation in the laminate was less than 0.10-inch. The glass laminate was then used to fabricate the glass/epoxy tool proof article and to fabricate the cocure bag. The silicone rubber bag for cover laminate staging and curing was fabricated using calendered rubber sheet. The bag was approximately 0.17-inch thick with a 0.50-inch thick land area around the periphery for sealing. In latter cycles a conventional nylon bag was found to give satisfactory results and was ultimately used for the actual full scale covers.

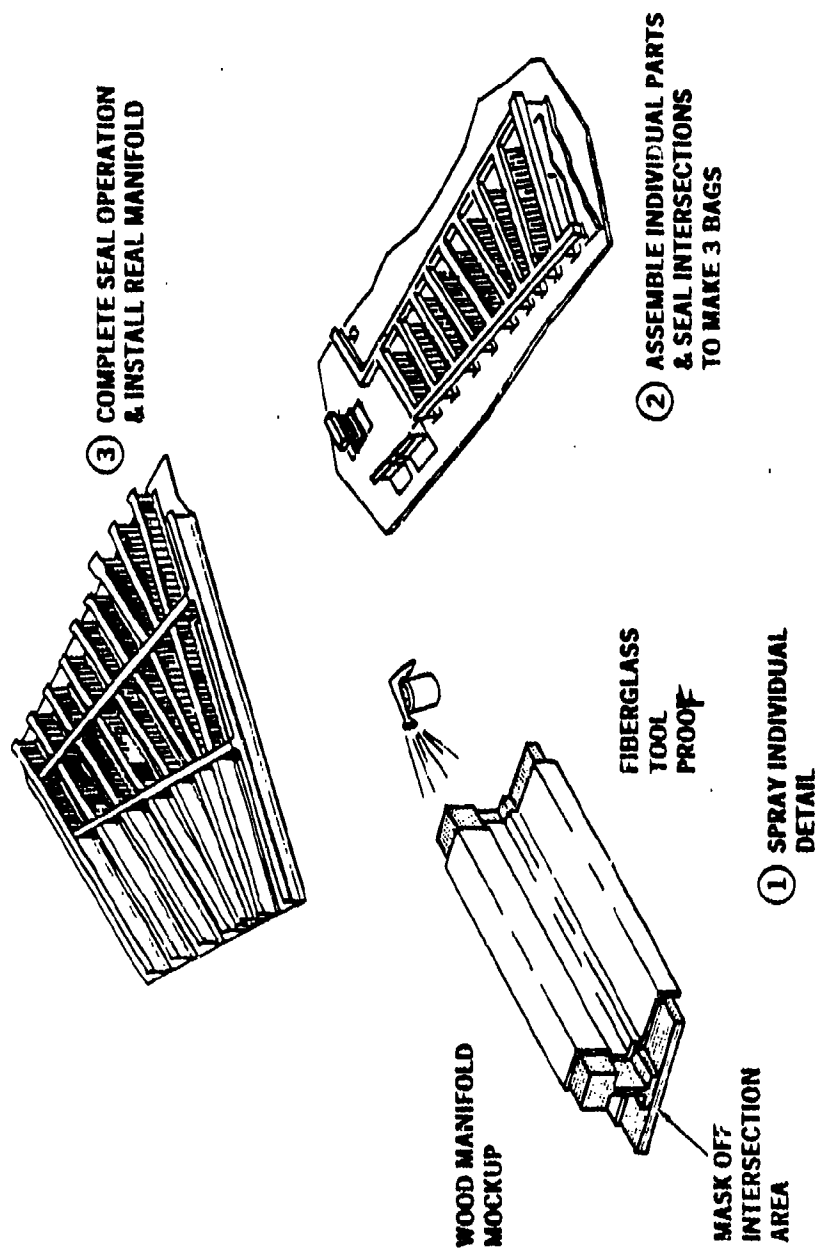


Figure 137. Full-Scale Component Cure Bag Fabrication Sequence



Figure 138. Spraying Process for Individual Sections of CAP Box



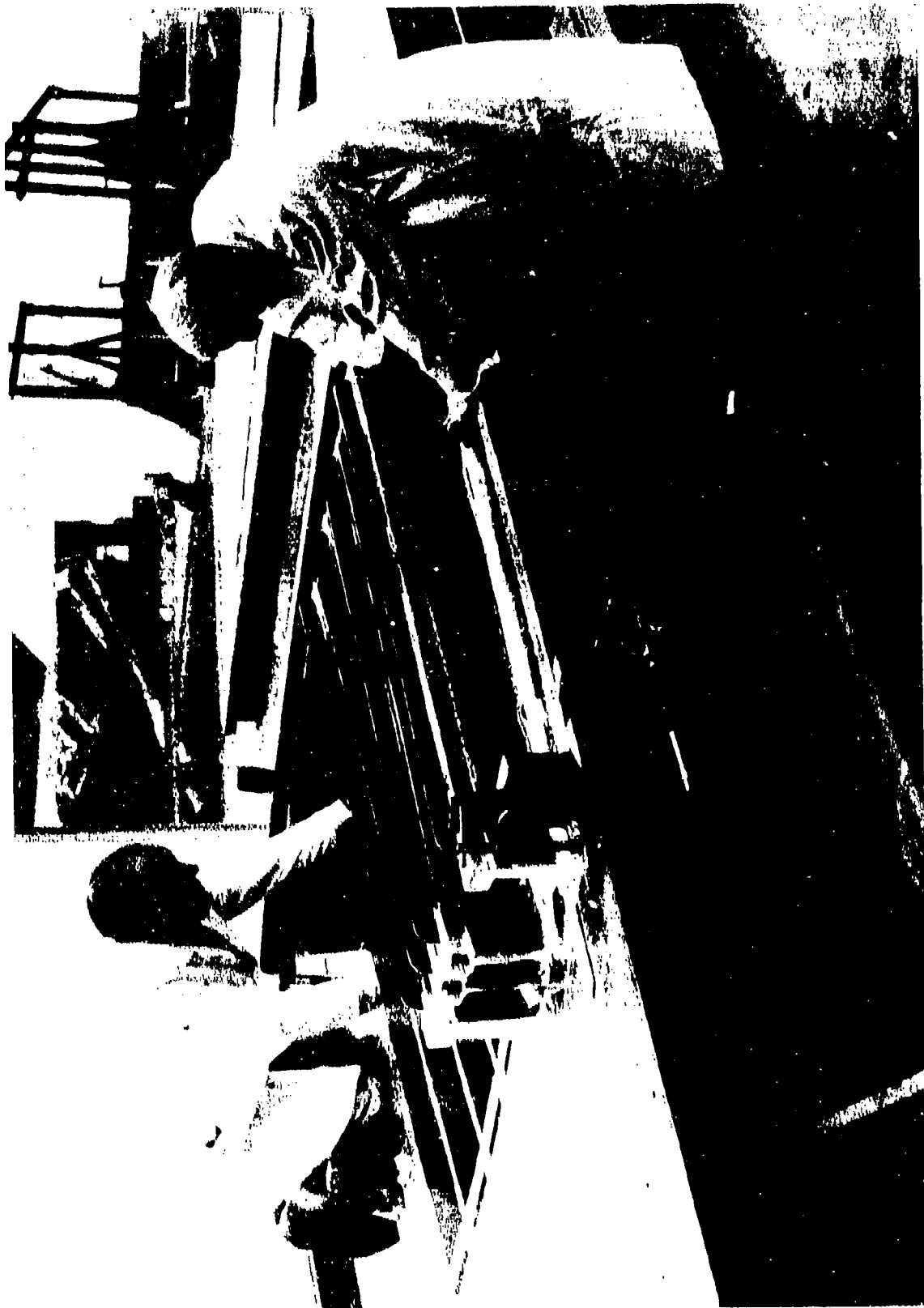


Figure 139. Assembly of Individual Sections of CAP Box Cocure Bag

TABLE XXVII  
NONAUTOCLAVE PANEL SCALE-UP SUMMARY

PANEL NO.	MATERIAL	NO PLYS (MAX-MIN)	SURFACE AREA (Ft <sup>2</sup> )	C-SCAN	QUALITY SURFACE FINISH	MICRO	MECHANICAL
1	AS4/976	103	4	N/A	GOOD	NO POROSITY	N/A
2,3	CE9000	103-40	55	N/A	GOOD	N/A	N/A
4	AS4/976	20	55	N/A	WRINKLES	N/A	N/A
5	AS4/976	20	55	N/A	WRINKLES	POROSITY	N/A
6	AS4/976	20	55	ACCEPTABLE	WRINKLES	ACCEPTABLE	MEET SPECIFICATION
7	AS4/976	20	50	ACCEPTABLE	MINOR WRINKLES	ACCEPTABLE	N/A
8	AS4/3501-SA	20	50	ACCEPTABLE	GOOD	NO POROSITY	N/A
9	AS4/3501-BA	60	16	NO POROSITY	GOOD	NO POROSITY	N/A
10	AS4/3501-5A	100-40	20	NO POROSITY	GOOD	NO POROSITY	N/A
11	AS4/976	376	2	NO POROSITY	GOOD	NO POROSITY	N/A

To evaluate the plan area parameter, a 20-ply graphite/epoxy laminate was staged, cured (utilizing the right side skin tool), and examined using ultrasonic and micrographic inspection.

The first test panel, full-envelope size (55-square feet), 20-ply thick, was staged according to the normal cycle and removed from the tool. Numerous large wrinkles, some of which went through to the bottom surface were evident. To prevent this from recurring, it was determined that a cured graphite/epoxy slip sheet would be used under the skin layup to counteract the differential thermal expansion between the Gr/Ep laminate and the steel tool.

A second 20-ply laminate was staged in the tool with a reduced upper cavity size and using a 4-ply, precured Gr/Ep slip sheet. Three additional vacuum ports were installed in the tool for more even distribution of pressure. Some wrinkles were still evident, but they were much less severe and were attributed to wrinkling of the 181 fiberglass cloth breather material.

A third panel was fabricated with similar results. After removing the part from the tool, a 2.54- by 2.54-cm (1.0- by 1.0-inch) section was extracted, examined under the microscope, and found to be acceptable. The part was then bagged and cured under vacuum pressure at 177°C (350°F) only. The part was sectioned and found to be void free.

To evaluate the mechanical properties of this third cover laminate, edgewise (90 degree) coupons were taken from the same area as for the photomicrograph. Results of these room temperature tests (refer to table XXVIII) showed very good correlation with the analytic predictions based on autoclave-cured lamina data. The average compressive test strength, 522.6 MPa (75.8 ksi), was within 4-percent of the predicted value of 543.3 MPa (78.8 ksi) indicating that the nonautoclave process produced laminates of autoclave strength.

A fourth panel was fabricated utilizing adhesive-backed teflon placed on the slip sheet and cover laminate. This technique virtually eliminated the wrinkling. A final laminate was fabricated using a heavy 1010 mat breather which eliminated the wrinkling.

Data from the 20-ply panels were evaluated and demonstrated on a 4.0- by 4.0-foot, 60-ply (0/±45/90) test panel of AS4/3501-5A material. The panel was staged, cured, and ultrasonically tested. Photomicrographs of the panel disclosed no porosity after either the staging or curing cycle and, in addition, the panel had excellent surface and dimensional quality. This panel reinforced the capability of the nonautoclave process to produce acceptable large full-scale parts.

As a final step before committing to fabrication of the actual covers, the effect of ply dropoffs was evaluated. The previous panels had constant thickness, and while demonstrating the capability of the process to fabricate large structures, still did not represent applicability to actual structures. Other research had indicated that the interstices at the edge of a ply dropoff were habitual sites of void formation when using 85 psi autoclave techniques. This phenomenon was evaluated using a 4.0- by 5.0-foot

TABLE XXVIII

## ROOM TEMPERATURE MECHANICAL PROPERTY COMPARISON

20-PLY AS4/976 CAP BOX TOOL PROOF LAMINATE

 $[0_2/45_8/90_2]$ 

	EDGEWISE (90°)		COMPRESSION		
COUPON NO.	FAILURE STRESS		AC-50 PREDICTED		<u>TEST/PREDICTED</u>
	MPa	(ksi)	MPa	(ksi)	
1-1	519.2	(75.3)	543.3	(78.8)	
1-2	512.3	(74.3)			
1-3	528.1	(76.6)			
1-4	487.5	(70.7)			
1-5	548.8	(79.6)			
3-1	529.5	(76.8)			
3-2	488.8	(70.9)			
3-3	537.7	(78.0)			
3-4	528.1	(76.6)			
3-5	<u>545.4</u>	<u>(79.1)</u>			
AVG.	522.6	(75.8)	543.3	(78.8)	0.96

panel which varied in thickness from 100 to 40 plies in 20-ply increments. The panel, shown in figure 140, contained sections of dropoffs which were not exposed to free edges, as would be the case in actual structure. Six inches of constant thickness panel were allowed between dropoff areas with 0.20-inch between individual plies.

After staging and curing the panel, it was C-scanned and sections were removed from various locations within the panel. Figure 141 is typical of the photomicrographs of the sections at the ply dropoff locations. It is evident that there was complete resin fill at all of the ply dropoff locations. Through the development of these full-scale panels, the capability of the nonautoclave process to fabricate large panels was demonstrated.

#### 4.3.1.3.2 Skin Fabrication

During fabrication of the five full-scale panels it was observed that the heat-up rates were below specification of 60°F/min. Concern for the sensitivity of the nonautoclave process to heatup rate prompted an evaluation of the effect of heat-up on the viscosity of AS4/3501-5A graphite/epoxy. Large tools may adversely affect the heat-up rate and be detrimental to the cure or staging of the part. Three heat-up rates were examined: 1.80°C/min (3.20°F/min.), 0.90°C/min (1.60°F/min.), and 0.56°C/min (1.00°F/min). The heat-up rates were from room temperature to 121°C (250°F) then 30-minute dwell time. The rheology experiments were carried out using the dynamic parallel-plate technique with the Rheometrics Dynamic Spectrometer at a measurement frequency of 10 rad/sec.

The viscosity of Hercules 3501-5A resin during a cure cycle having a heating ramp of 1.80°C/min. (3.20°F/min) to 250°F is shown in figure 142. The viscosity of the resin after the 30-minute dwell at 121°C (250°F) or with a total processing time of 80 minutes was about 30 poise. The same experiment was conducted with a heating rate of 0.90°C/min (1.60°F/min.) (figure 143). The viscosity in this case was about 47 poise after a 30-minute dwell at 121°C (250°F) or with a total of 135 minutes processing time. This difference was very small and almost within the experimental error of the technique. The reason for the small effect was that the Hercules 3501-5A resin was quite slow to react at 121°C (250°F) and therefore insensitive to minor changes in the heat-up rate used to reach this temperature. In conclusion, it appeared that small differences in heat-up did not require that an adjustment in the dwell condition used in the nonautoclave processing of Hercules 3501-5A cover laminates.

To decrease the heat-up time as much as possible, the oven was preheated to 300°F prior to placing the cover laminates into the oven. The cover was fabricated from net resin (31 ± 2) percent AS4/3501-5A Gr/Ep prepreg tape.

Using over 300 location mylars for each cover, the layup took approximately 80 hours per cover to complete. After layup of the AS4/3501-5A Gr/Ep tape and 4 mil boron/epoxy material, the cover laminates were bagged using a standard nylon bagging material and staged. The left hand close out cover was then cured and the right hand cover was bagged and stored until required for installation into the cocure assembly.

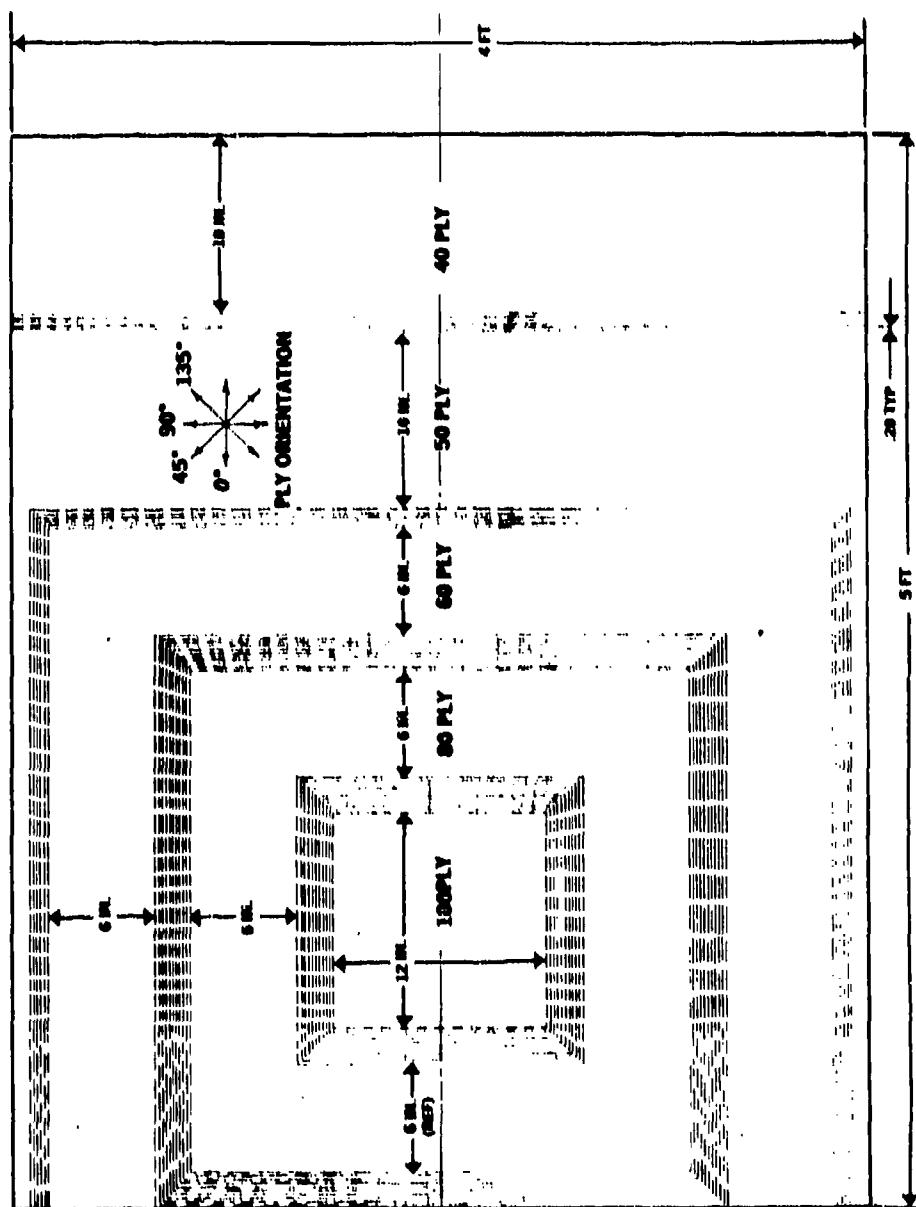


Figure 140. Ply Drop-Off Evaluation Panel

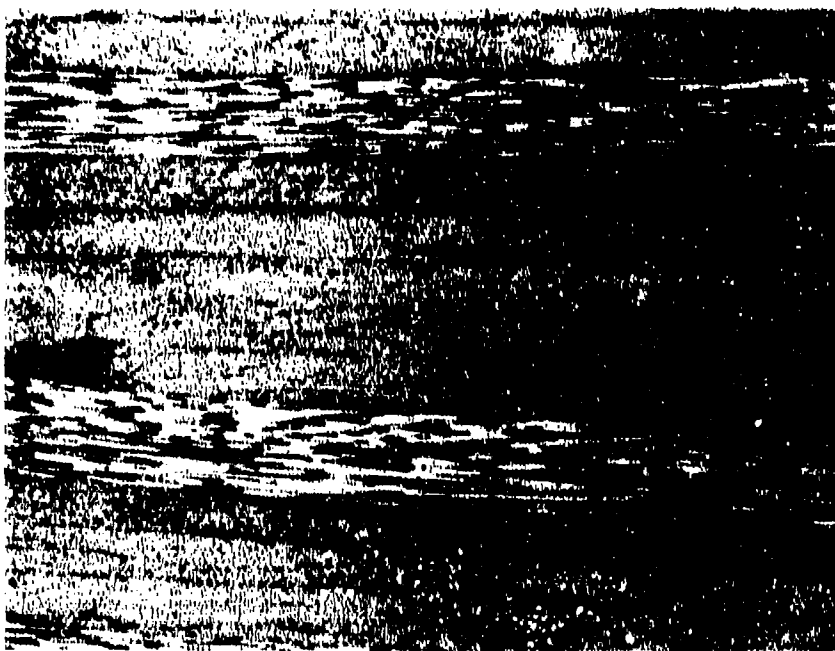
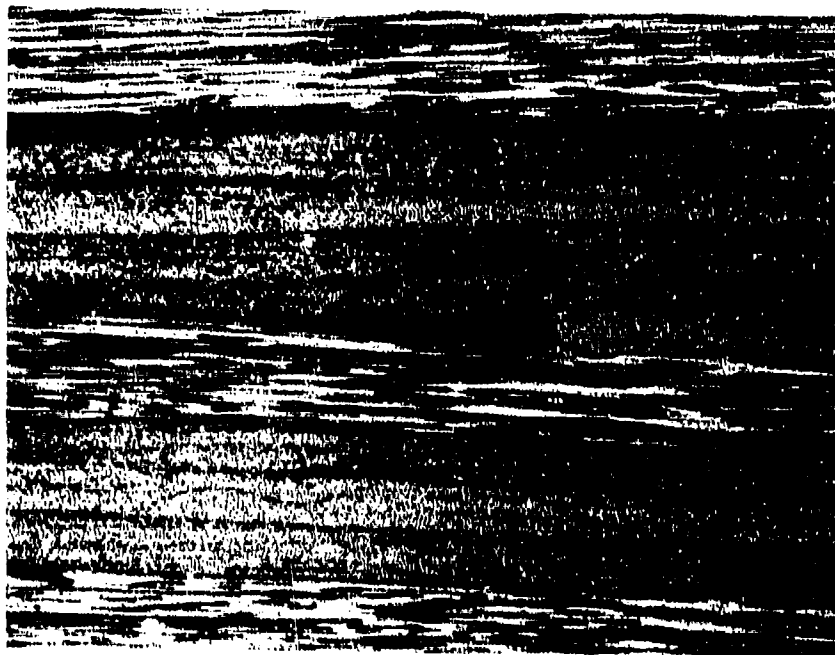


Figure 141. Typical Photomicrographs of 100-Ply Laminate Test Panel

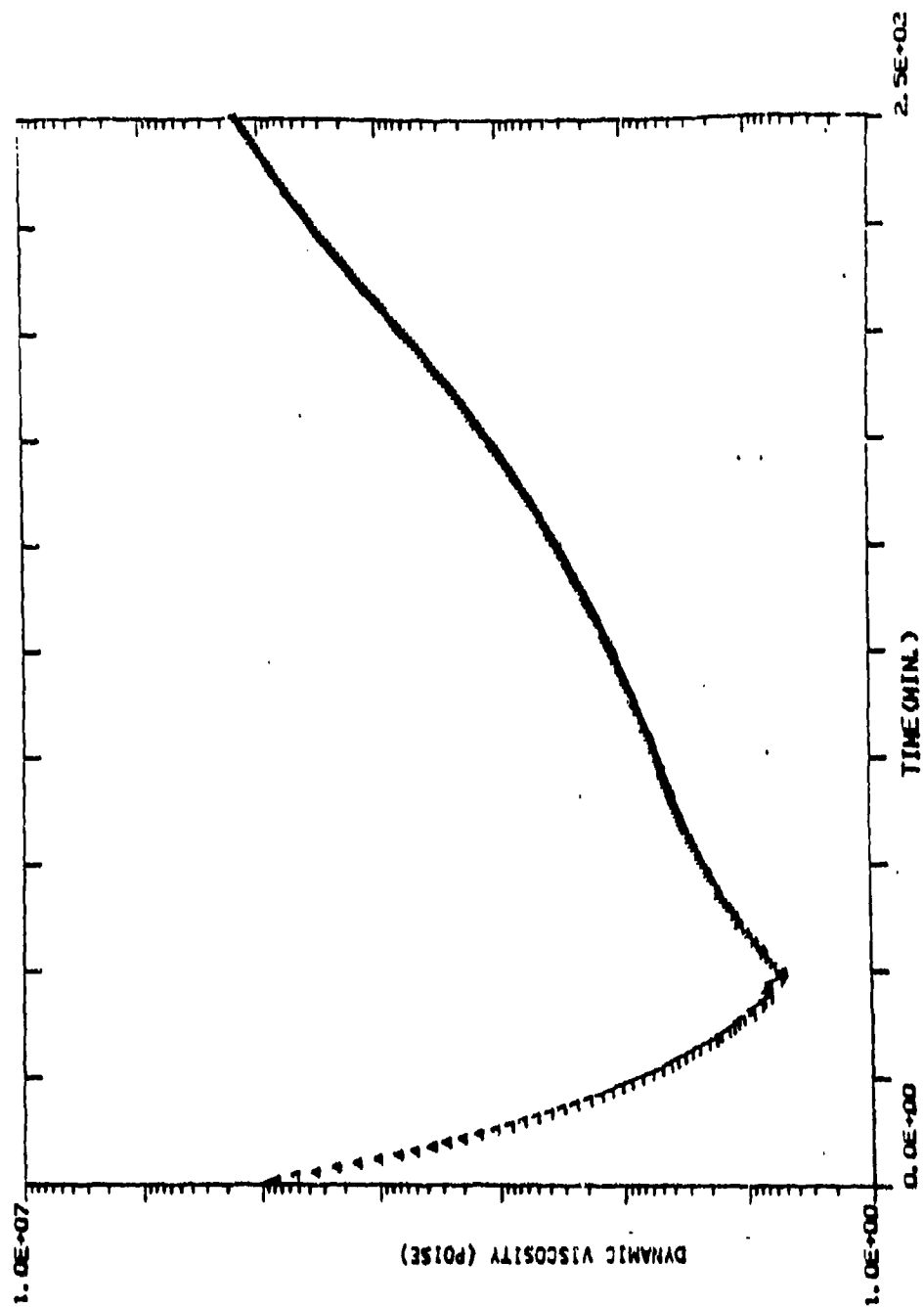


Figure 142. Viscosity of Hercules 3501-5A Resin During Cure Cycle - RT to 250°F at 3.2°F/min. and Held



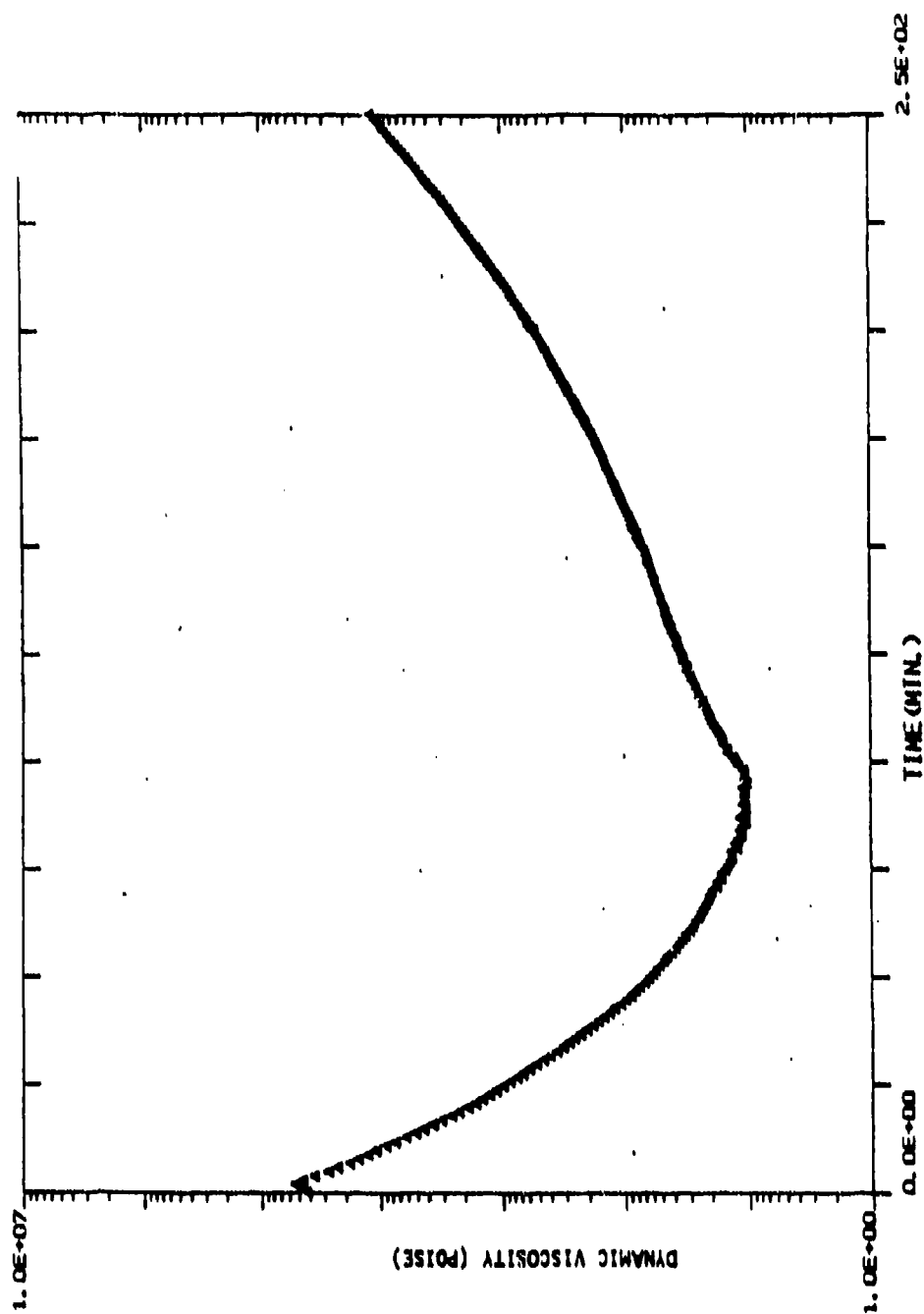


Figure 143. Viscosity of Hercules 3501-5A Resin During Curing Cycle - RT to 250°F at 1.6°F/Min. and Held

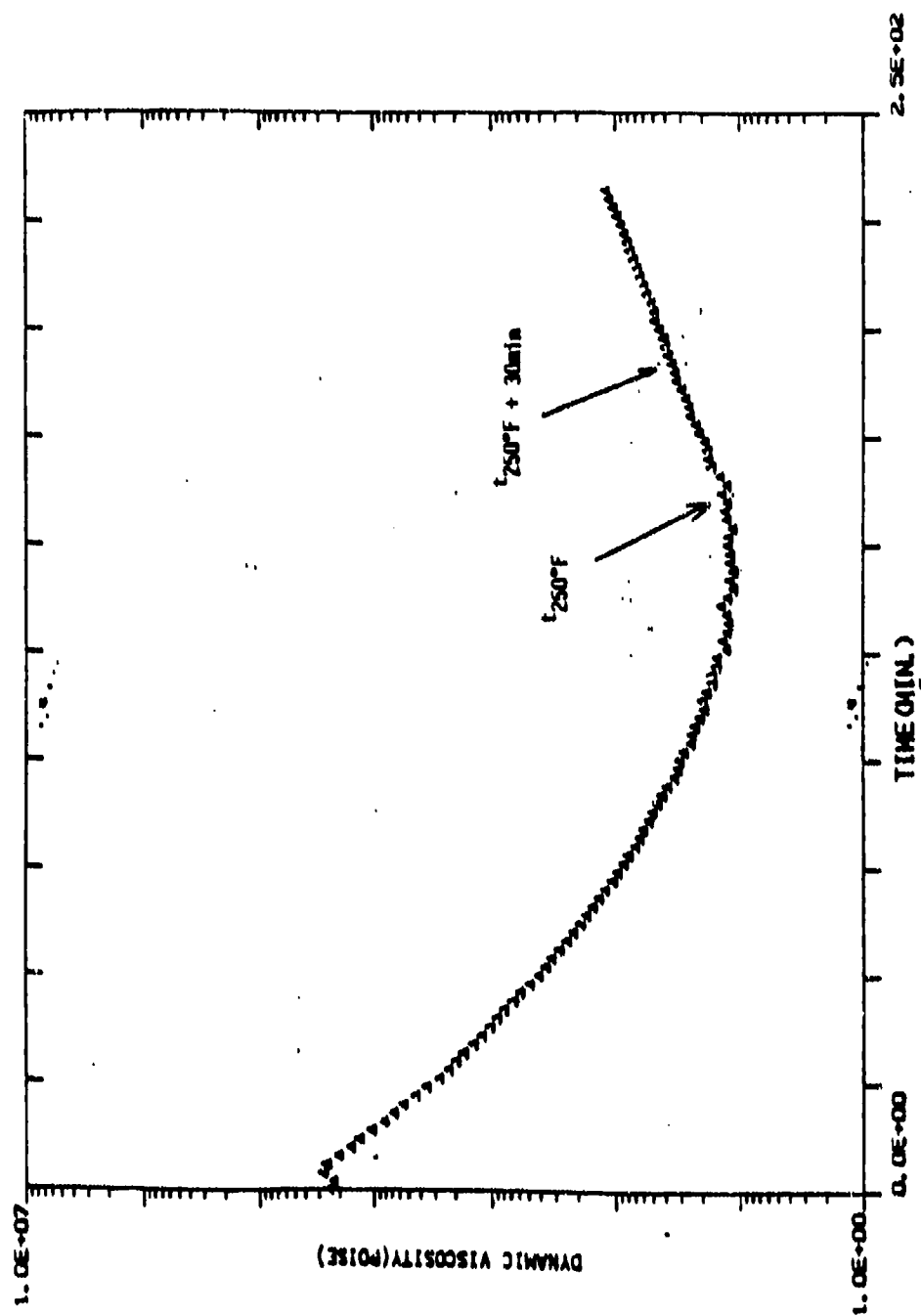


Figure 144. Viscosity of Hercules 3501-5A Resin During Cure Cycle - RT to 250°F at 1.0°F/min. and Held

Staging of the two covers was conducted using MPP05L023-01 which was the standard nonautoclave cycle used throughout the program. Heat-up rates of the two covers were 1.8 and 1.6°F/min, as shown in table XXIX which lists some of the in-house and rib parts also. Although the specification called for a heat-up rate of 5 to 6°F/min, the size of the cover tools prevented this from occurring. However, as described in the previous paragraphs, this longer than optimum staging time did not adversely affect the minimum viscosity that the resin reaches or the quality of the finished part.

The cocure skin had several wrinkles located in the top two plies of the laminate in the lower, forward section near the root attachment area. Additionally, the C-scan (2.25 MHz, 18dB) of the staged cover showed several areas indicating porosity. By placing the skin through a second staging cycle the wrinkles were reduced and the porosity eliminated.

The question arises on the effect of repeated staging of the material on the physical properties, in particular the resin rheology (i.e., minimum viscosity). It is assumed that there is an upper limit to the number of times a resin can be subjected to 250°F without adversely affecting the minimum viscosity of the material and, consequently, the ability to obtain adequate resin flow during final cure to allow cocuring of the structure. By experimentally measuring the dynamic viscosity of neat resin 3501-5A subjected to varying lengths of time at 250°F, a measure of the number of staging cycles that the material can be subjected to can be obtained. Figure 145 displays these data for unstaged material staged for 60 minutes or essentially two staging operations and 100 minutes or three staging cycles. It is evident that the minimum viscosity of the unstaged and the material subjected to three staging cycles (about 100 minutes) varies between 80 poise and 120 poise. While no upper bound of acceptability was established, it was determined that only two staging cycles would be allowed.

The ability to interrogate parts using C-scan while in the staged condition and then resubmit them to another staging cycle to correct any deficiencies proved to be a significant advantage in the program by reducing scrap during the fabrication of the substructure.

The close-out cover was staged and inspected and found to be acceptable. After curing the C-scan confirmed the quality of the part.

#### 4.3.1.3.3 Substructure Fabrication

The substructure was comprised 38 detail parts including the ribs, spars, and caps and 64 clips joining the ribs and spars at their intersection. The lower and intermediate section of the structure contained sine-wave web spars while the upper bay was flat web. The ribs and rear spar contained both sine wave and flat web sections and the 120-inch long front spar contained flat web only.

The ten 8-ply caps were flat layups which were laid up and staged in a single sheet then trimmed to final dimension using the ultrasonic cutter. The 64 clips were fabricated in the same manner; laid up as a single

TABLE XXIX

## Staging Heat-Up Rate

IR&D Panel No	Max No Piles	Area (ft <sup>2</sup> )	Heat Rate (°F/Min)	DELTA T Max (°F)
1	20	55	2.29	20
2	20	55	2.50	7
3	20	55	3.03	25
4	20	55	1.60	10
5	20	55	1.20	7
6	100/40	20	1.23	8
Cocure Cover (-029-1)	103/40	55	1.80	25
Closeout Cover (-029-2)	103/30	55	1.6	20
-032 R1b	20		3.4	N/A
-033 R1b			3.93	N/A
-037 R1b			3.84	N/A
-043 R1b			2.97	N/A
-049 R1b			2.72	N/A
-052 R1b			3.84	N/A
-056 R1b			2.49	N/A

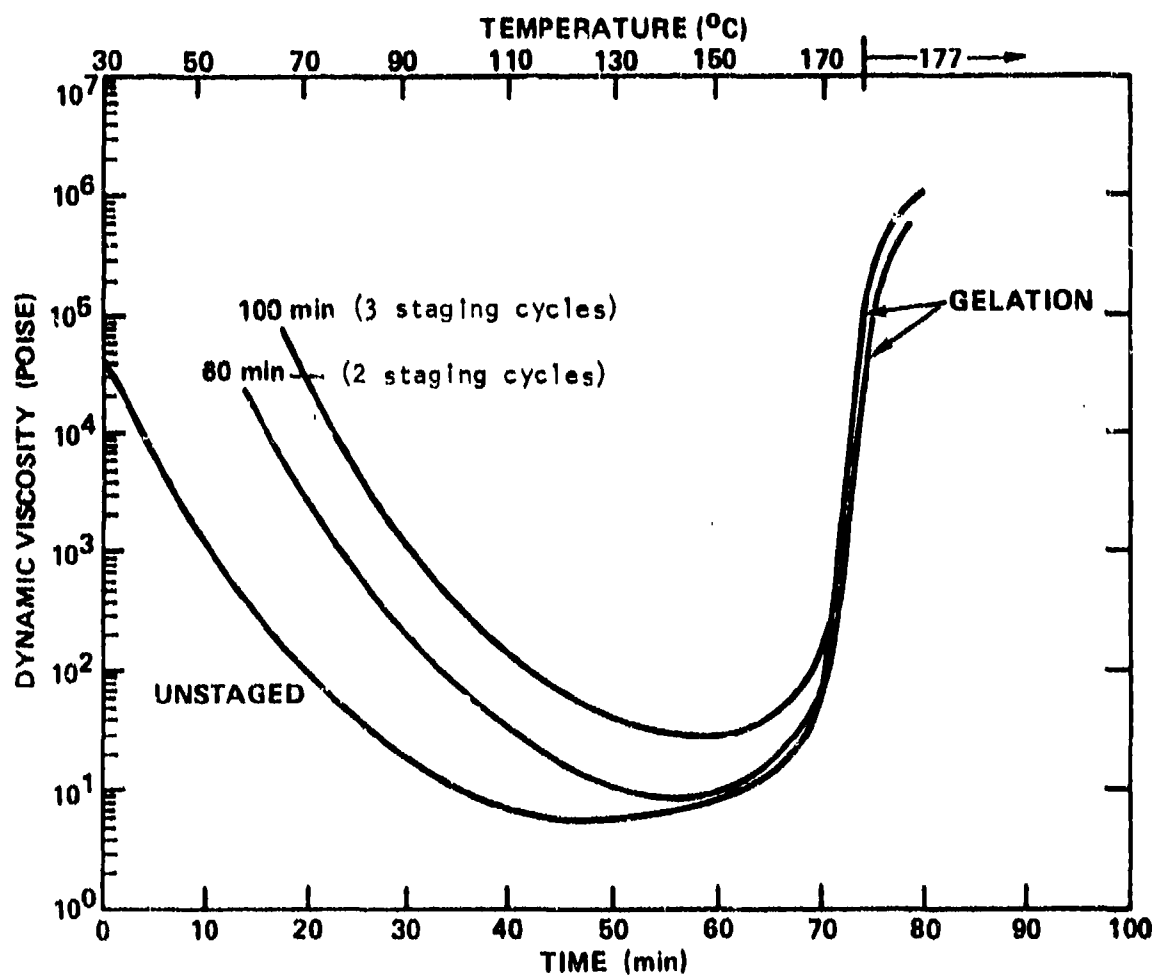


Figure 145. Cure Rheology of 225°F-Staged 3501-5A Resin

sheet, staged, then trimmed to final dimensions. The 90 degree bend in the clip was produced after staging by heating the laminate with a heat-gun then bending the laminate over a tool.

The 38 major substructure details were fabricated using the layup and staging tools described in section 4.3.1.2. During staging of the first batch of sine-wave parts which included the two ribs (-32 and -33) and three spars (-56, -35, and -39) the parts exhibited extremely large wrinkles in the sine-wave sections often extending across the length of the part and to a depth of 0.2 inch.

It was discovered that wrinkles were the result of two problems which were associated with the tools. The first resulted from the layup procedure. In the first run the two halves of the I-beam were laid up on each half of the tool then mated when the tool was assembled. Because of the change in tooling design the seals at the ends of the bag which provided the seal instead of the steel C-channels as in the Phase I and II tools, prevented the two halves of the laminate to come into intimate contact when the tool was assembled. Consequently, during the staging operation when the two halves of the laminates were brought together during the consolidation part of the cycle, the two halves would not nest. Bringing the two halves of the laminate together before completing the assembly of the tool eliminated this problem.

The second problem was related to both the tooling and the design of the ribs and spars. When the tools were designed, the rule-of-thumb for the gap between the laminate and the tool (as described in section 4.1) was used. The gap was based on the thickest part of the web as was the case in the element and subcomponent parts fabricated earlier. However, in the ribs and spars for the full-scale component the window ply reinforcements were thicker than those used in the stub box. The typical ply buildup for the ribs was 12 plies or a 6 ply increase from the subcomponent details. Because of the extra window ply buildups, the gap between the tool and the web was greater than the one-half times the web thickness guideline (illustrated in figure 146). Evidently, this excessive gap was the cause of the wrinkles. By placing a 4-ply precured fiberglass caul-plate between the bag and the part to reduce the gap, the wrinkles were eliminated during a restaging operation. The resultant surface quality of the restaged parts was excellent as shown in figure 147. The effect of placing the caul between the bag and the tool was also tried with improved results. By placing the caul behind the bag, the sharp markoff in the part caused by the end of the caul was reduced.

Rather than remanufacture the remaining 13 tools to correct the gap problem, the precured caul plate placed behind the bag was used during the remaining staging operation. The resultant parts exhibited none of the wrinkling evident in the first batch. It is of interest to note that the wrinkling was not evident in the flat-web spars or the front spar. It appears that the added complexity of the sine-wave (which requires matching sine-wave nodes and valleys in the bag with the part) and the extra material involved in the sine wave compounded the problem. The 120 inch long front spar was staged without incident and exhibited no wrinkles or twisting (figure 148).

As in all previous work, each of the substructure details were

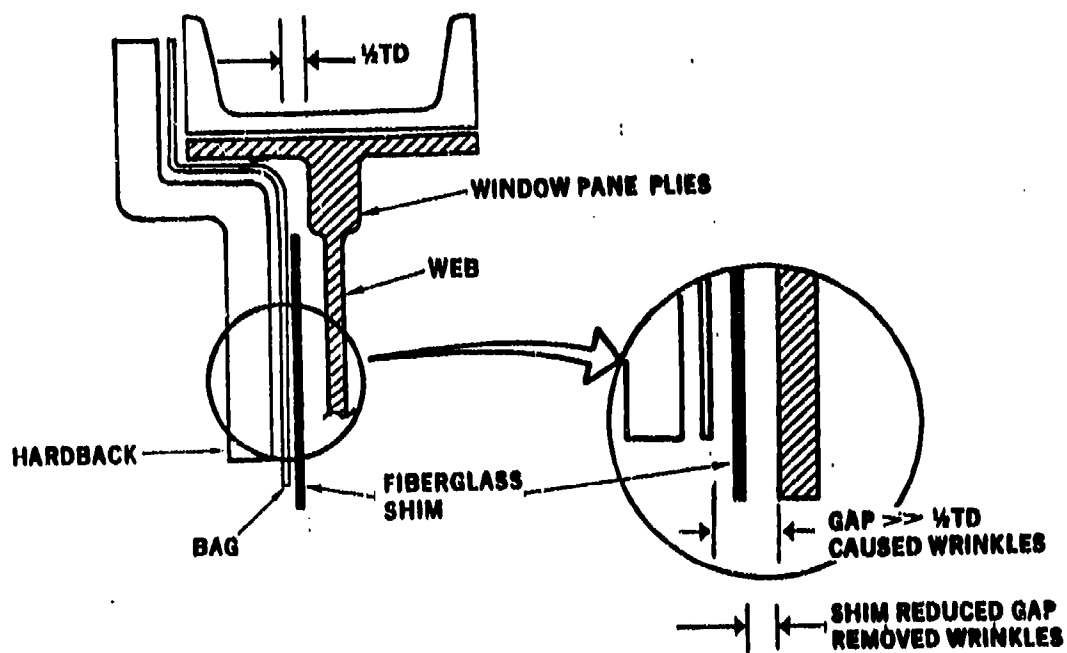


Figure 146. CAP Box Stage Tool Detail

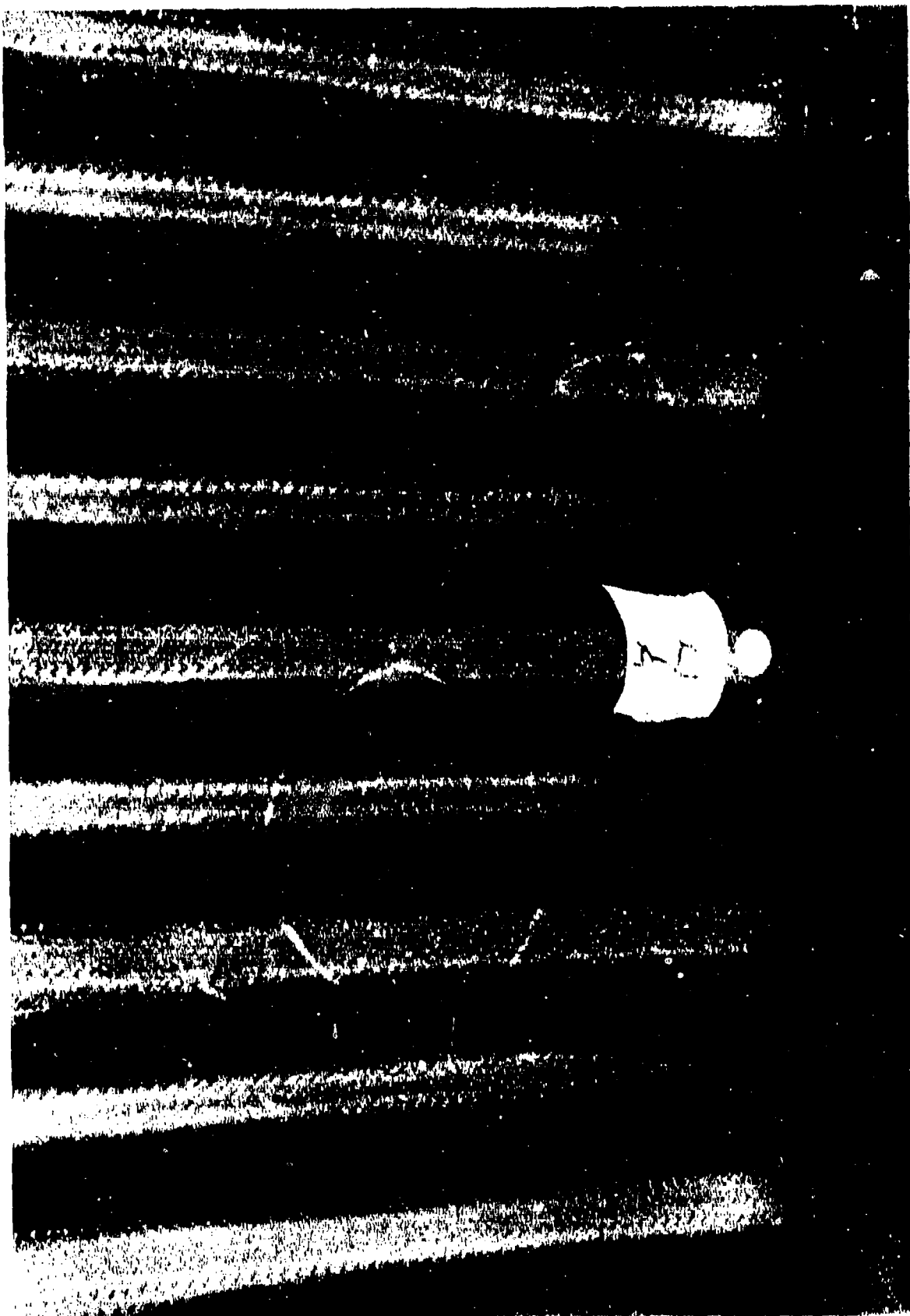


Figure 147. Surface Quality of Restaged Rib



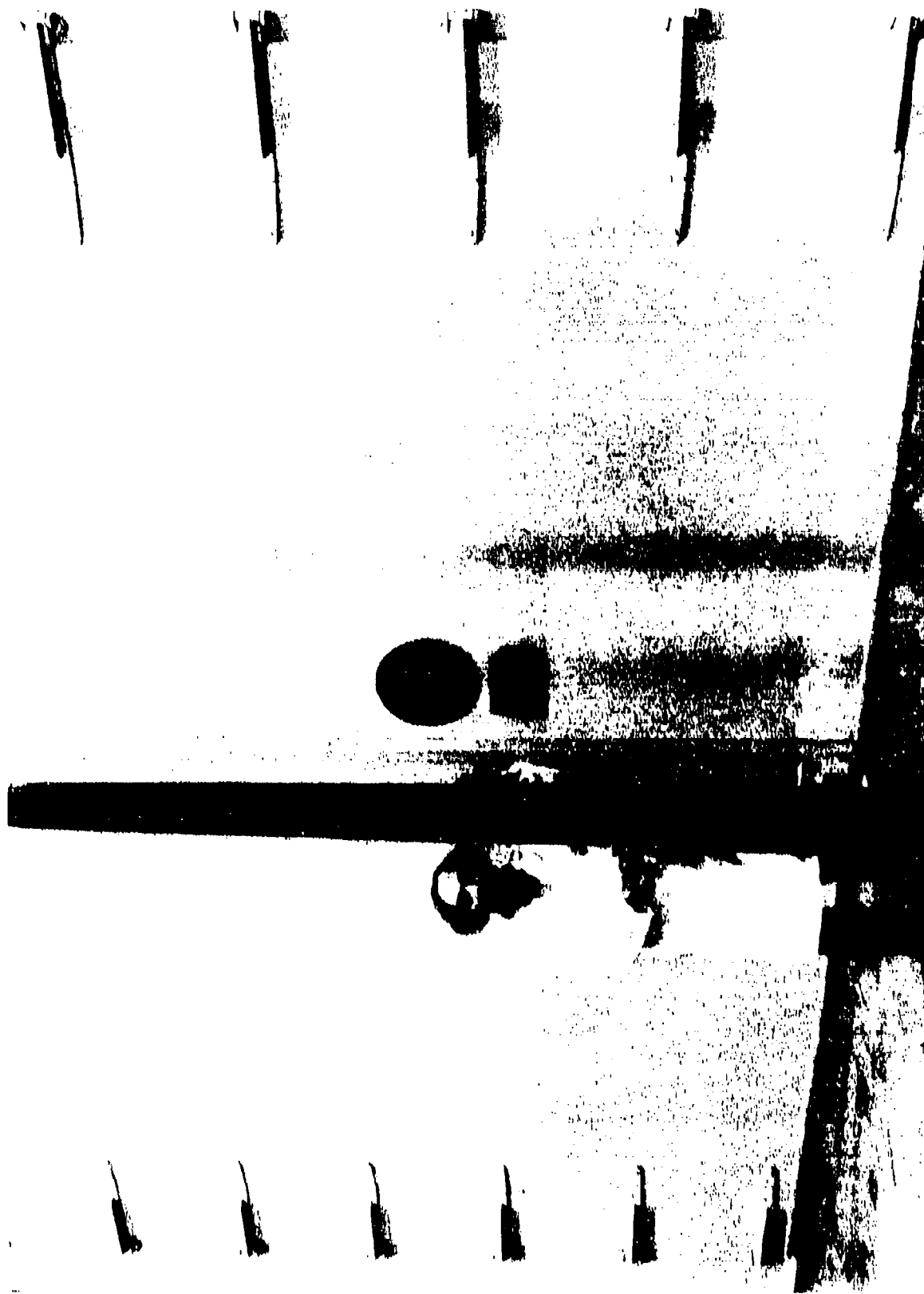


Figure 148. Full-Scale Component Front Spar

evaluated after staging using ultrasonic C-scan at 2.25 Mz, with lead tape standards.

#### 4.3.1.3.4 Assembly and Cocure

All 26 graphite/epoxy detail sections of the full-scale box were trimmed using the ultrasonic cutter, prefitted, and assembled into the cocure structure. Location of the details on the skin was accomplished by the use of layouts from mylars directly onto the skin. By placing 0.125 inch diameter, 0.25-inch long titanium pins through the caps of the ribs and spars into the cover, the details were prevented from moving during the assembly operations. The use of the titanium pins were not detrimental to structure because of their limited number, one at each end of the part, and their small size.

The individual graphite/epoxy details were next fitted and assembled with FM300 film adhesive at the faying surfaces (between the cover spars, ribs, and clips). Figure 149 shows the graphite/epoxy details after assembly. Note that the rib and spar caps which were assembled last maintained continuity at the rib and spar intersection.

The steel tube manifold structure (which provided the chordal height control of the box and vacuum path between the bag and the part) was then fitted over the assembled graphite/epoxy details (figure 134). Fitup between the manifold and the part was noted and gaps greater than 0.10 inch were corrected by adding plies of graphite/epoxy prepreg tape on the spar or rib cap thereby forming a structural shim.

With one ply of TX1040 teflon breather placed on the Gr/Ep details and with the manifold positioned over the details, glass breather cloth was placed over the manifold to prevent trapoff of the bag to the manifold. (See figure 150.) Next, the three sections of the cocure bag were placed over the assembly. Figure 151 shows the middle section of the bag after installation. The three sections were sealed, as shown in figure 152, and a vacuum checkout of the system performed. The part was placed in the 12,000-square foot gas oven for final cure cycle.

Heat-up rate was monitored by a network of over 30 thermocouples which were placed under the bag, on the part, on the tool, on the manifold, and in the open oven air. Early sensor reading showed a trend toward a 10°C (50°F) variation in thermal couple readings. The maximum oven temperature setting was lowered from the 149°C (300°F) to 121°C (250°F) range to narrow the temperature gradient. At about 104°C (220°F), a nominal temperature differential of 14°C (25°F) was attained and a heat up rate of approximately 20°F/min was maintained.

Heating of the part tended to aggravate vacuum decay because of the expansion of any anomalies in the bag. At 104°C (220°F), vacuum decayed to 22-inches Hg. At 121°C to 132°C (250°F to 270°F), a significant leak developed in the seal approximately 10 inches from the lower end of the rear spar. Vacuum, however, was maintained at 18 inches Hg throughout the remainder of the cure cycle. Subsequent to cure, visual inspection of the part evidenced adequate flow which indicated that a good cocure was achieved at all bondlines. Figures 153 and 154 show the complete full-scale component.



Figure 149. Full-Scale Component Details After Assembly



Figure 150. Glass Breather Cloth in Place Over Manifold



Figure 151. Middle Section of Cure Bag After Installation

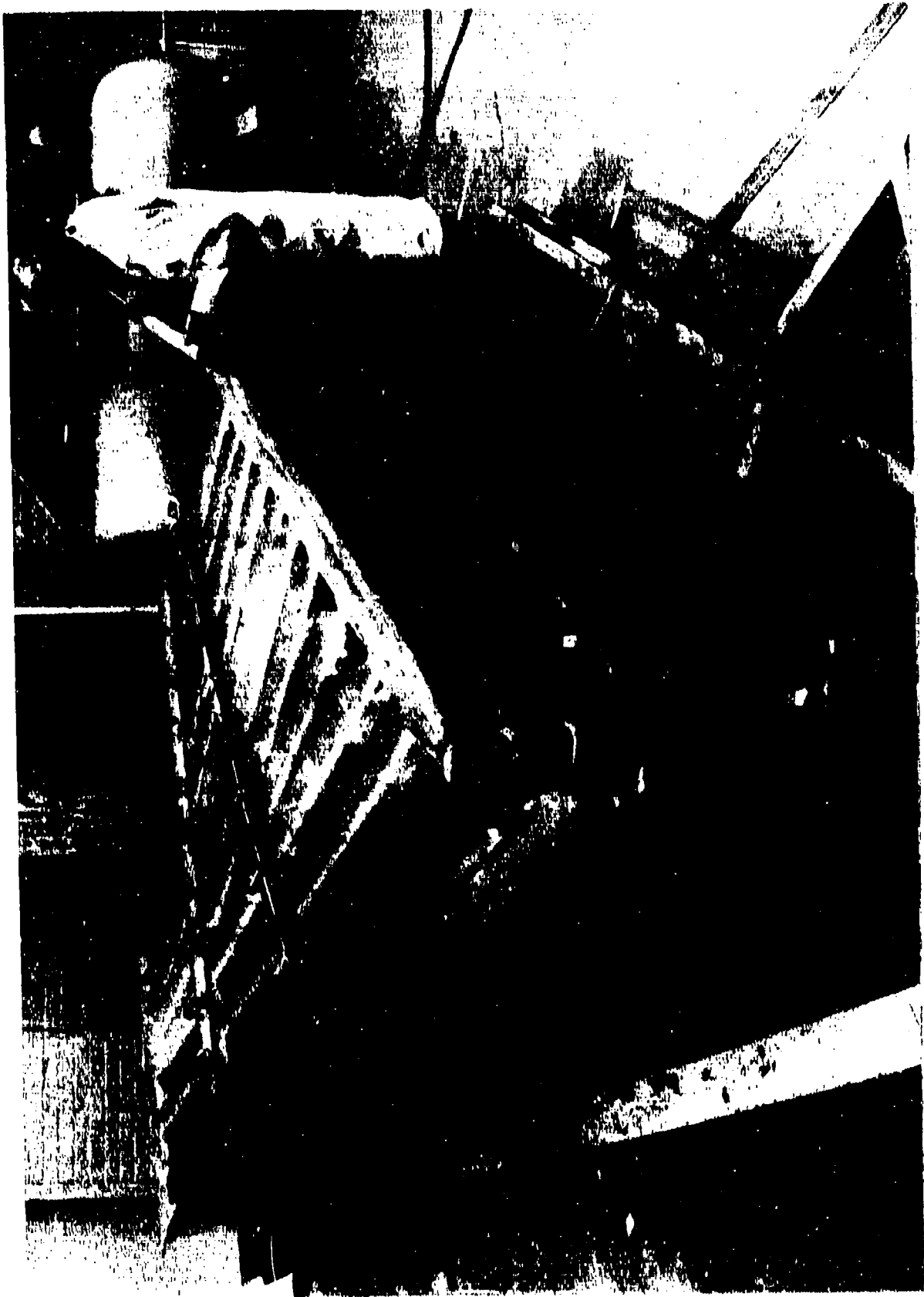


Figure 152. Cure Bag Sealed at All Joints

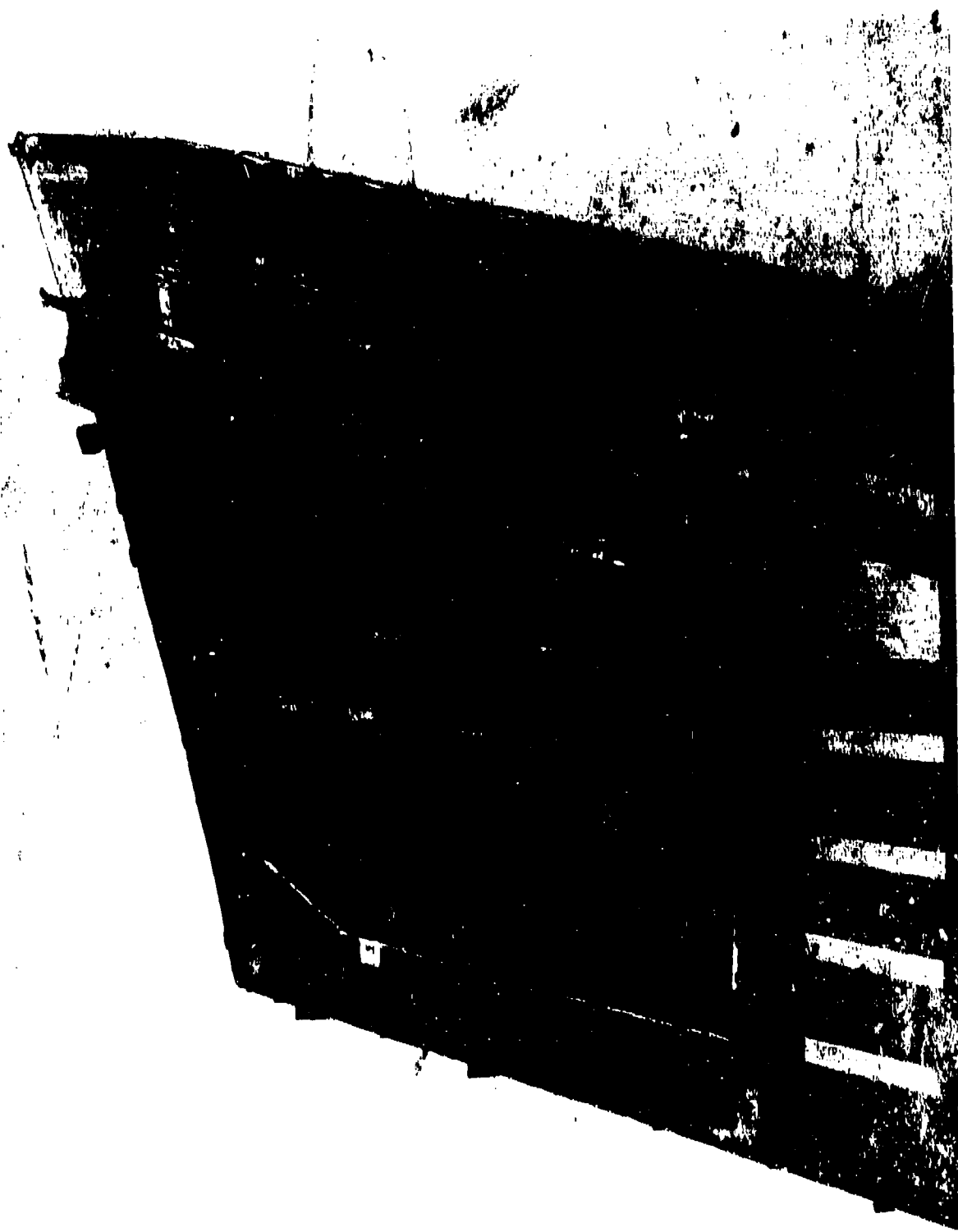


Figure 153. Completed Full-Scale Component

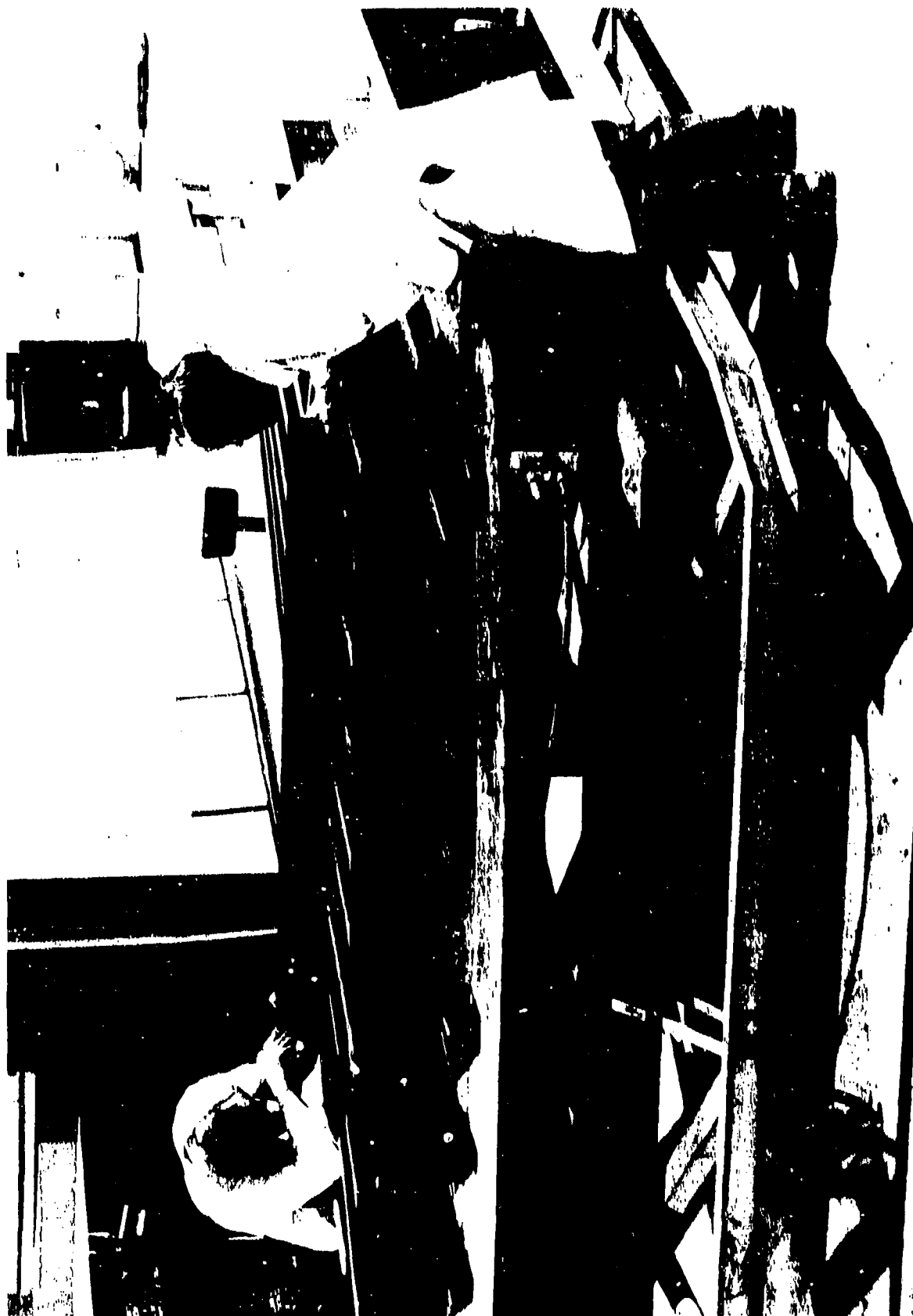


Figure 154. Full-Scale Component After Final Cure



#### 4.3.2 QUALITY ASSESSMENT

Although the bag provided adequate pressure throughout the cure cycle to ensure a good bond, there was some deformation of the sine-wave webs in the lower spars that occurred during the cure. An evaluation of the cause concluded that the sine-wave spar wrinkling was related to the method of bag fabrication. (The earlier bags were sprayed as one continuous piece, but the size of the component required sectional fabrication of the cure bag followed by assembly into one continuous bag.) Although this method was expedient, it caused some problems. For example, at the bondlines (especially at the intersection of the rib and spar webs) the rubber buildup was extensive, sometimes over 0.375-inch. It was possible that because the volume of rubber was greater at the bond lines than at the adjoining webs, a differential in expansion occurred causing the web on one side of the web to expand dissimilarly from the other side and thus cause a wrinkling or deformation of the part at that specific point. Additionally, it was discovered that four of the manifold standoffs at the tip and root of the component required to prevent the manifold from deflecting during cure were inadvertently left off.

It should be noted that no resin fills or surface gloss was found which indicated that the bags maintained contact (i.e., vacuum) throughout the cure. Of the 25 spars and ribs, seven flat-web spars (including the front spar) exhibited no deformation. Of the remaining 16 sine-wave spars and two ribs, the two ribs did not wrinkle nor was there any wrinkling in the lower spar Nos. 1, 14, and 3. Figure 155 is a close-up of a typical sine-wave deformation. A map of the spars having structural wrinkles or deformation is shown in figure 156. The moldline of the upper or close-out surface of the ribs and spars was checked using a template. Mold-line contours were held within prescribed tolerances of  $\pm 0.01$  inch.

While the article was successful as a manufacturing demonstration of the full-scale nonautoclave cocure feasibility, it was determined that it was prohibitive in cost to repair the wrinkles and thus make the part adequate for the full-scale structural testing within the scope of this program.

Ultrasonic C-scan of the component bondlines indicated that the loss in bag pressure caused less than satisfactory bond between the cover and the substructure. Figure 157 shows the location of the 24 areas of attenuation located in the C-scan. Table XXX lists the sizes of the anomalies. They appear to be grouped at the lower aft end of the component which would coincide with the development of the large leak in the bag during the cure.

#### 4.3.3 SUMMARY PHASE III -- FULL SCALE STRUCTURE COMPONENT

Fabrication of the full scale component represented one of the largest integral structure cocure assemblies to date. The 55 ft<sup>2</sup> structure contained over 38 separate structural details each of which was bonded together and to one cover. The component, which is comparable in size to a fighter wing, was a major accomplishment for the nonautoclave process and integral structure design.

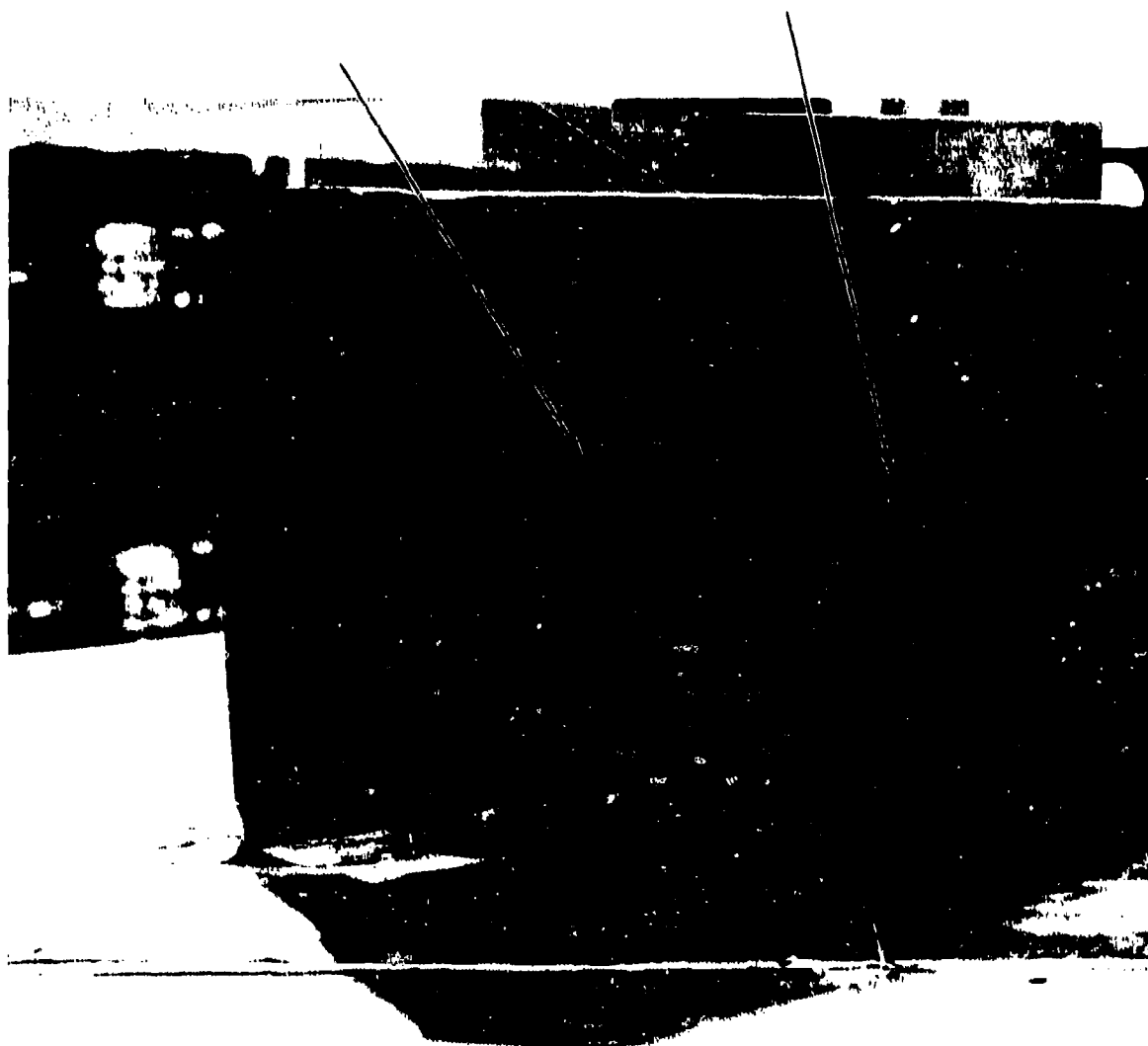
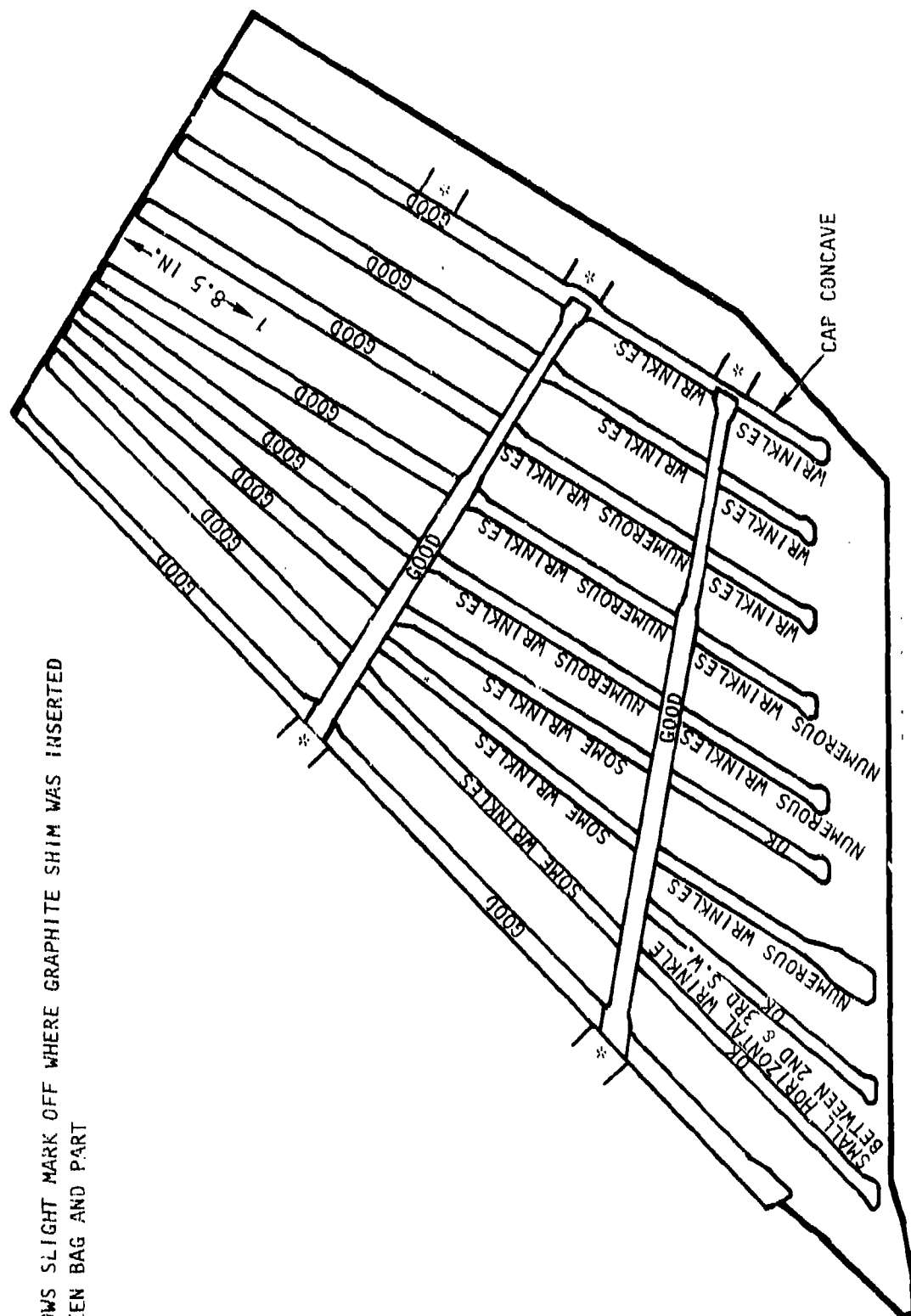


Figure 155. Typical Sine-wave Spar Wrinkles in Cured Component



\* SHOWS SLIGHT MARK OFF WHERE GRAPHITE SHIM WAS INSERTED  
BETWEEN BAG AND PART

Figure 156. Visual Quality Assessment of Cured Component

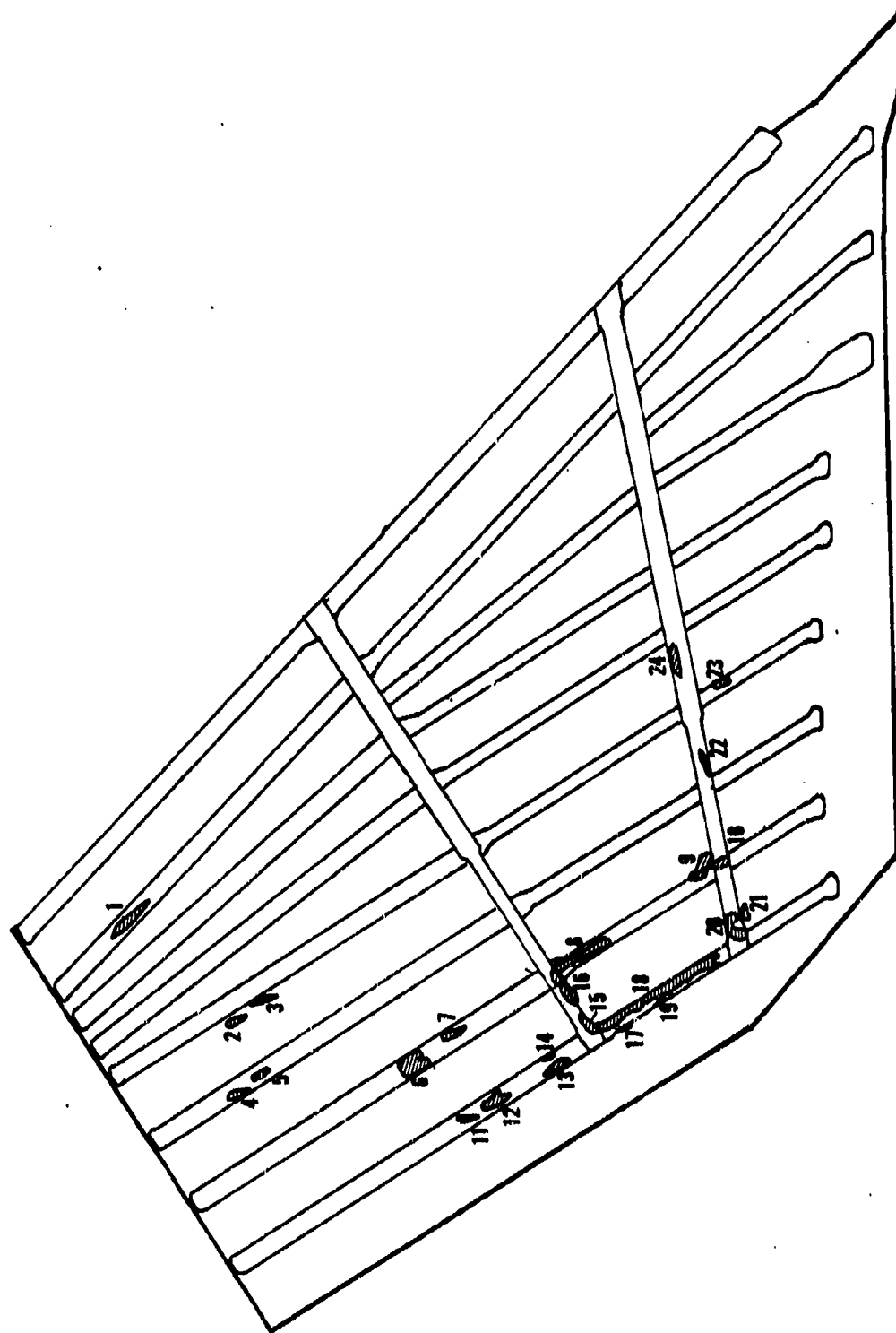


Figure 157. Summary of Ultrasonic C-Scan Nonbond Indications of Cocured Component

TABLE XXX

## COMPONENT NONBOND SIZE

DEFECT NO.	DIMENSIONS (INCHES) MAJOR AXIS X MINOR AXIS
1	2.75 X 0.5
2	1.625 X 0.5
3	4.75 X 0.5
4	0.625 X 0.875
5	3.75 X 0.5
6	2.5 X 1.625
7	1.25 X 0.25
8	7.75 X 1.625
9	2.25 X 1.615
10	1.25 X 0.25
11	2.0 X 0.5
12	3.0 X 1.25
13	2.0 X 0.5
14	1.375 X 0.25
15	2.0 X 0.225
16	3.250 X 0.375
17	1.750 X 0.5
18	15.625 X 2.875
19	2.125 X 0.5
20	2.0 X 0.5
21	1.5 X 0.375
22	1.0 X 0.375
23	1.0 X 0.375
24	2.25 X 0.50

It was demonstrated that large area Gr/Ep structures could be economically fabricated using the nonautoclave process. The application of the process to laminates up to 376 plies extends the potential use of the process to even larger structures such as a large wing cover.

The evaluation of heat-up rates on the cover laminates which showed that the specification requirement of 5-6°F/minute was not critical to part fabrication quality. It was found that heat-up rates, because of the size of the tooling mass, of 2°F/minute produced good quality laminates. This indicates the need for more indepth cure modeling prior to establishment of specifications.

The ability to stage a part then subject it to a second or third staging cycle without adversely affecting the minimum viscosity of the resin was found to be of enormous value in reducing scrap rate. Many of the substructure details were restaged after an error in the tooling was discovered which caused the sinewave details to wrinkle. By restaging the details in reworked tools, hundreds of hours of labor and thousands of dollars in material were saved.

Throughout the program the development of the nonautoclave process was coupled with demonstration of cocured integral structure. The key to fabricating integral structure is the co-cure bag. A significant amount of evaluation of silicone rubber bag materials and fabrication technique was

conducted. The bag durability was improved somewhat by changing rubber compounds and the use of sprayed co-cure bags reduced the co-cure bag fabrication time considerably from previous cast or calendered rubber bags. However, it is evident that there is still the need for more development in this area. The size and shape of the Phase III bag required a somewhat awkward approach for manufacturing the co-cure bag and there is still the need for rubber compounds that can withstand repeated usage at the 350°F cure temperatures.

In conclusion, the fabrication of the B-1 vertical stabilizer component was successful in demonstrating the manufacturing feasibility of the nonautoclave process.

At the completion of phase III, a cost-benefit analysis was conducted. Data from the three phases was analyzed to assess the success of the total effort, including cost and quality data on elements and subcomponents through production of the full-scale demonstration component.

The results of the analysis of cost and quality data was used to determine the impact of the nonautoclave curing and manufacturing methods for composite integral structure on projected production costs. Energy usage during full-scale fabrication of composite primary aircraft structural components was monitored and comparisons with predicted energy usage were made. The program data were combined and analyzed in order to establish the energy-saving benefits of this program, including a projection of energy saving for the nonautoclave cure process.

Cost savings through energy conservation, reduced capital expenditure, simplified processing procedures, and other pertinent factors were analyzed in order to establish projected cost savings for future production as well as calculated return on investment (ROI) from this program. The ROI was based on the proposed integral composite vertical stabilizer concept described herein. Since portions of the fabrication procedures were different for the parts fabricated in this program compared with baseline parts, the cost analysis included corrections for the following:

1. Cost of all aluminum parts as determined from the cost tracking data from the previous completed Low Cost Composite Vertical Stabilizer and in-house CAP Box programs.
2. The differences resulting from final assembly operations caused by utilization of integral structure techniques.
3. The cost data from the previous composite vertical stabilizer programs was revised utilizing cost information from the integral 15-foot box program to provide a baseline integral autoclave-cured structure concept for comparison with the data developed during this program for similar nonautoclave cured procedures.

This approach provided a sound method for determining the true cost saving associated with the advanced nonautoclave curing process.

#### 4.4.1 WEIGHT ANALYSIS

The parts fabricated during this program were compared with similar parts fabricated in previous programs to establish accurate baseline data which were used in the cost analysis. The 40-inch long box beam fabricated during phase I (figure 16) was virtually identical to those fabricated under the Low Cost Composite Wing/Fuselage Manufacturing program (F33615-77-C-5278) AFML-TR-79-4110. Geometrical configuration dimensions, web, cap, and cover thickness were the same. Table XXXI delineates the actual and predicted weights of the two 40-inch long elements fabricated during this program. One

TABLE XXXI

## WEIGHT ANALYSIS - PHASE I ELEMENTS

ELEMENT NUMBER	FASTENERS INCLUDED		FASTENERS NOT INCLUDED
	CALCULATED	ACTUAL	
Nonautoclave No. 1	23.0 LB	23.1* LB	20.89 ** LB
Nonautoclave No. 2	23.0 LB	23.2* LB	20.94 ** LB
IR&D Element	<u>23.0 LB</u> 23.0 LB	<u>22.9* LB</u> 23.06 LB	<u>20.90 ** LB</u> 20.91 LB
Wing Fuselage (1)	N/A	N/A	20.52 ** LB

\* Actual measured weight

\*\* Estimated

(1) Reference AFML-TR-79-4110



element was fabricated as part of NAAO's in-house efforts and the box was fabricated under the Wing/Fuselage program. The actual and predicted weights for the elements with and without the addition of mechanical fasteners used to attach the upper close-out cover are included in table XXXI.

The comparison of the average weight 20.91 lb for the three nonautoclave fabricated boxes with the baseline 20.52 lb from the Wing Fuselage program shows excellent correlation with only a 2-percent variation between the two elements. This was expected since the only difference was the way in which the various details were staged and cured. Both elements were integrally bonded.

A comparison of the subcomponent fabricated in phase II which weighed 78.1 lb (figure 78) with the baseline is shown in table XXXII. The baseline was the stub-box built during the Low Cost Composite Vertical Stabilizer program (F33615- 74-C-5164) weighed 81.26 lb. A similar wing box component, weighing 101.6 lb fabricated during 1975 under NAAO in-house funding, is also shown. The stub-box was the baseline for the cost evaluation because it maintained a geometrical configuration nearly identical to the Phase II subcomponent, except that it was assembled using mechanical fasteners rather than cocuring as was the case during this program. The in-house part was fabricated using integral structure but was 1.0-foot longer, 3.0-inches thinner, and 8.0-inches wider than either the stub-box or the subcomponent fabricated during the program. The in-house part did contain the same number of details and provided an opportunity to evaluate larger subcomponents fabricated in different manners. Both the stub-box and the in-house box were fabricated using autoclave manufacturing procedures.

Weight of the Phase III, full-scale component (presented in table XXXIII) is compared to the baseline component fabricated during the Low Cost Composite Vertical Stabilizer contract. As with the Phase II subcomponent, the nonautoclave component was designed for integral structure whereas the baseline, which maintained the same form, fit, and function, was conventionally assembled using mechanical fasteners. All of the baseline Gr/Ep details were fabricated using an autoclave. Adjustments were made in the baseline weight to remove all metallic details and fasteners. With this adjustment the calculated nonautoclave weight was 283.4 pounds versus 270.0 pounds, while the actual measured weight of 278.5 pounds for the baseline.

#### 4.4.2 ENERGY EVALUATION

The staging and curing processes for advanced composites are highly "energy intensive" because they take place at high pressure and temperature for long periods of time. As a result, any improvements in the process which can reduce the required time of operation or minimize the heat losses which result for the operation will result in large savings in energy. The nonautoclave process which utilizes ovens to perform the required staging and curing of advanced composites demonstrated savings which resulted from this change.

TABLE XXXII

## WEIGHT ANALYSIS PHASE II SUBCOMPONENT

	Gr/Ep ONLY		INCLUDING ASSEMBLY AND A1 DETAILS
	CALCULATED	ACTUAL	
Nonautoclave Subcomponent	58.50 lb (2)	78.1 lb	164.56 (1) lb
Vertical Stabilizer Stub Box		81.26 lb	70.0 (1) lb
IR&D Component		101.6 lb	
NOTES: (1) Includes -017 aluminum attachment blade, test hardware and angles.			
(2)			
	AC18100-003	R1b	0.88
	AC18100-004	R1b	0.88
	AC18100-005	Int Lwr Spar	0.71
	AC18100-006	Int Mid Spar	0.98
	AC18100-007	Int Upr Spar	0.61
	AC18100-008 -011	Front Spar	9.17
	AC18100-008 -012	Rear Spar	9.17
	AC18100-009 -011	Spar Cap	0.22
	AC18100-009 -003	R1b Cap	0.18
	AC18100-010 -001	Upr Cover	17.6
	AC18100-010 -002	Lwr Cover	17.6
	Cover Ply		<u>0.5</u>
S/T			(58.5)
	Adhesive & Filler		0.20
	Fastener		9.11
Metallic Details			
	Attachment Hardware		90.20
	Angles		5.78
	Clips		0.28
	Shims		0.22
	Retainer		<u>0.27</u>
			(119.84)
TOTAL			164.56 lbs.

TABLE XXXIII

## WEIGHT ANALYSIS FULL SCALE COMPONENT

	NONAUTOCLAVE		AUTOCLAVE	
	CALCULATED (1b)	ACTUAL (1b)	CALCULATED (1b)	ACTUAL (1b)
<u>Composite</u> (1)				
Covers (2)	187.5		187.5	
Front Spar	24.2		24.3	
Intermediate	58.9		53.9	
Spars (22)				
Ribvs (2)	<u>12.9</u>		<u>12.9</u>	
S/T (ASSY)	(283.4)	(270.0)	278.5	N/A
<u>Fasteners</u>				
Cover(s)	21.3		42.6	
Substructure	0		12.0	
Metallic Details	9.1		9.1	
<u>Metallic</u>				
Rear Spar	31.2		31.2	
Rib Zvs 72.87	9.6		9.6	
Zvs 156.42	2.9		2.9	
Zvs 66.85	18.3		18.3	
Zvs 61.56	12.0		12.0	
Intercostals	3.2		3.4	
Clips	3.5		3.5	
Shims	2.3		2.3	
Root Attachment				
Blades (2)	<u>62.0</u>		<u>62.0</u>	
	464.8	N/A	487.9	470.0

NOTE: (i) Weights include adhesive.

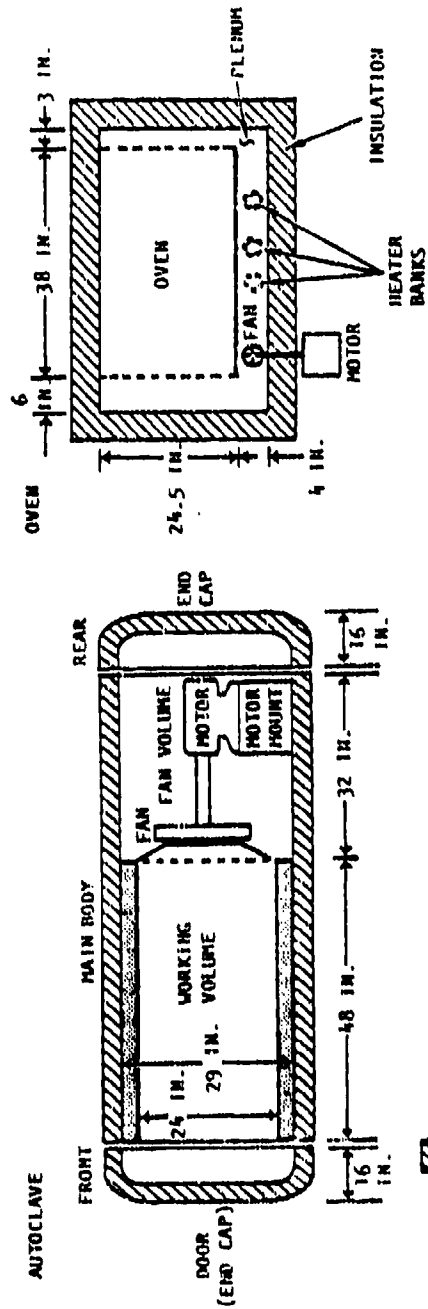
The capital cost benefits of ovens versus autoclaves are clear: due to the fact that they are not pressure vessels they are less expensive to manufacture and procure. Less apparent are the operating energy savings which occur from the change to ovens. Actually, these two factors cannot be totally divorced. The size of the oven or autoclave to be selected for use depends on the size, shape, weight, and material of the largest items to be processed. The capital cost savings derived from oven procurement in lieu of autoclave allows the user of large ovens excess capital available for smaller ovens to process smaller product items more efficiently from the energy standpoint. The autoclave user would be forced to process both small and large product items in the same large autoclave, with resultant inefficiencies due to proportionately larger energy utilization per pound of product.

The energy requirements for the operation of ovens or autoclaves are based on (1) the heat required to raise the product item and auxiliaries (trays, conveyors, etc) to the required process temperature (2) the heat required to raise the oven/autoclave ventilating air temperature to the required levels (3) the heat required to raise oven/autoclave structural mass temperatures (4) the energy needed to compensate for heat loss through the oven or autoclave walls and openings, and (5) the necessity for additional energy required when pressurizing autoclaves. In determining the benefits to be derived from use of a nonautoclave system for processing advanced composites, all the above factors were considered and analyzed from the standpoint of what is needed in an energy efficient, yet cost-effective process design.

To evaluate the energy usage of autoclaves and ovens, the energy usage of small laboratory units were measured. The units were both electrically heated and were of approximately the same working volume (see figure 158), 11-cubic feet. Thermocouples to measure internal atmosphere temperature, ambient atmosphere temperature, external surface temperature, internal part temperature (when used) and power usage (via a recording ammeter) were installed on both pieces of equipment. Additionally, the cooling lines to the autoclave were outfitted with flowmeters and thermocouples in order to determine the heat loss due to the circulation of cooling water through the autoclave.

Several cure cycle runs were made to determine the baseline (no part in unit) energy requirements for staging/curing cycles on the autoclave and the oven. After completion of the baseline measurements the cure cycle measurements were repeated with a tool (weighing approximately 8 kg) loaded into the units.

The results presented in table XXXIV are based on the staging/cure cycles presented in figure 159, with cure times of 60 minutes for each process. The energy required to run a complete autoclave cure cycle was approximately 11 times that needed to run the equivalent nonautoclave cycle,  $3.9 \times 10^6$  watts for the autoclave versus  $3.65 \times 10^5$  watts for the oven. As can be seen from table XXXIV, a majority of the energy used by the autoclave (approximately 55 percent) was spent heating water in the autoclave cooling coils. If this energy could be prevented from exiting the system the



SCALE 1/4 IN = 6 IN.

COMPARISON		OVEN	
WORKING VOLUME TOTAL VOLUME SURFACE AREA (INTERNAL)	WORKING VOLUME	12.57 CU FT	10.78 CU FT
	TOTAL VOLUME	60.40 CU FT	15.51 CU FT
	SURFACE AREA (INTERNAL)	150.9 SQ FT	39.6 SQ FT

Figure 158. Phase I Energy Assessment of Autoclave and Oven

TABLE XXXIV

## PRELIMINARY ENERGY SAVINGS

	TIME (MIN)	TOTAL ENERGY USED (WATTS)	ENERGY ABSORBED BY COOLING COILS (WATTS)	ENERGY ABSORBED BY TOOL (WATTS)
Autoclave w/o Tool	Heat Up	72	7.3 x 10 <sup>5</sup>	1.8 x 10 <sup>5</sup> watts (4.6% of total energy) 3.6 x 10 <sup>5</sup> watts inclusive of cooling coil losses
	60 min cure	60	1.24 x 10 <sup>6</sup>	
	Total time	132	1.97 x 10 <sup>6</sup>	
Autoclave w/Tool	Heat Up	92	2.15 x 10 <sup>6</sup> (55.1% of Total)	
	60 min cure	60		
	Total time	152		
Oven w/o Tool	Heat Up	11	1.91 x 10 <sup>5</sup>	9.3 x 10 <sup>4</sup> watts (25% of total energy)
	Bake/ik & Cure	105	8.12 x 10 <sup>5</sup>	
	Total	116	2.72 x 10 <sup>5</sup>	
Oven w/Tool	Heat Up	62	3.12 x 10 <sup>5</sup>	
	Bake/ik & Cure	105	5.26 x 10 <sup>4</sup>	
	Total	167	3.65 x 10 <sup>5</sup>	

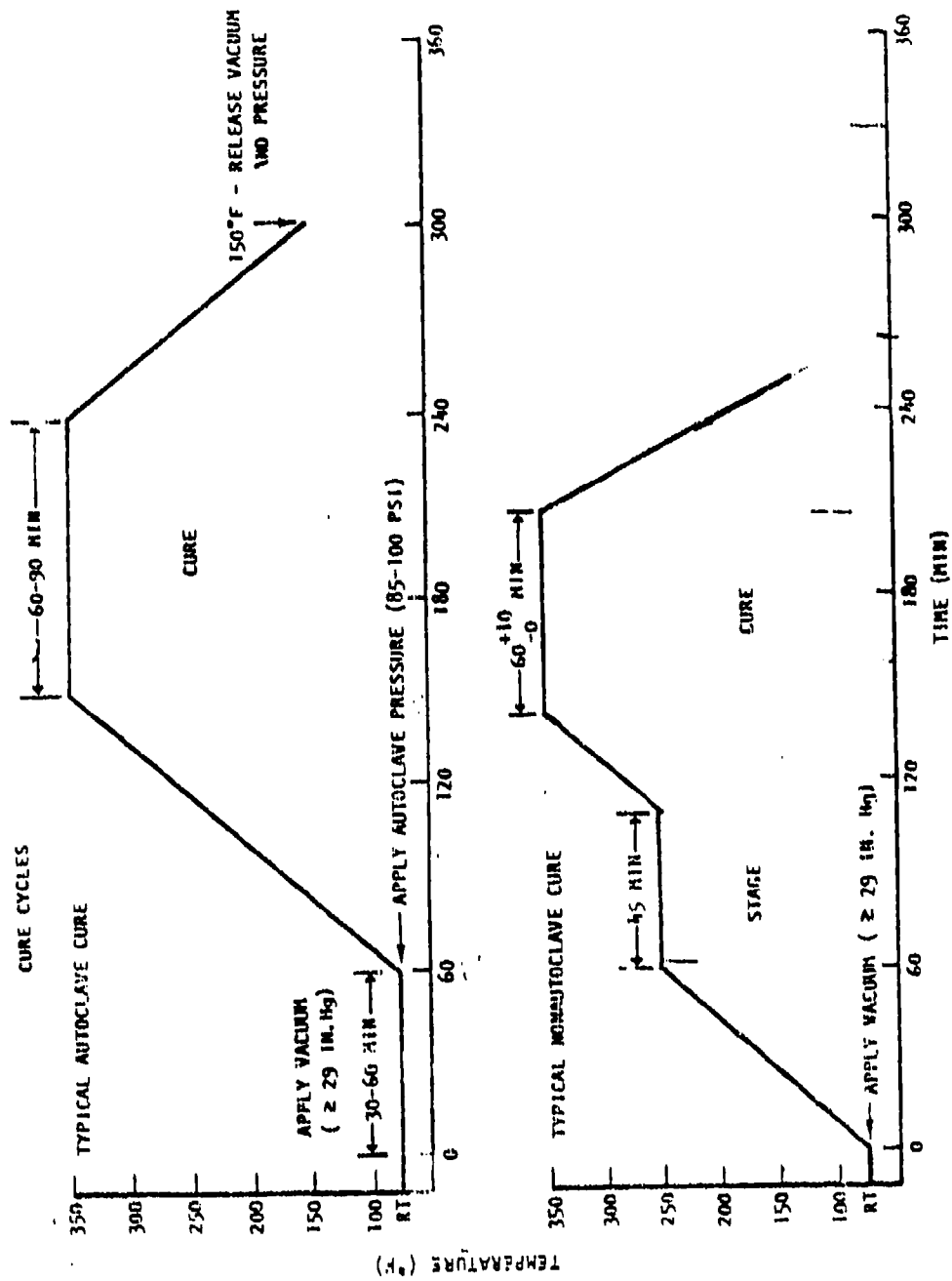


Figure 159. Cure Cycle Used in Phase I Energy Assessment

autoclave process efficiency would be improved (albeit at the expense of temperature control in the unit used). Energy delivered to the part (once corrected for the losses due to the autoclave cooling coils) is roughly equivalent between the two processes with the differences most probably due to the higher heat losses of the autoclave.

This initial study indicated that the nonautoclave process is more energy efficient than the comparable autoclave process. This is seen in that the nonautoclave process uses one-tenth the energy of the autoclave process while still delivering the required energy to the part. In terms of energy utilization, the autoclave processed part absorbs less than 5 percent of the total energy used in the cure cycle but this same amount of absorbed energy is more than 25 percent of the total energy used in the nonautoclave cure process. This energy savings was accomplished with no significant increase in process time. It can be seen, therefore, that for the equipment used, the nonautoclave cure process is from five to ten times more energy efficient than the equivalent autoclave cure process.

The study was continued during Phase III to evaluate production equipment. For the 10,000 ft<sup>3</sup> gas heated oven utilized in the staging and curing of all of the nonautoclave parts, the energy usage was determined by monitoring the gas usage and compared to historical data for the 12,000 ft<sup>3</sup> production autoclave used for the B-1B production hardware. Energy usage for the gas oven was monitored during the cure cycle of the phase III component. Table XXXV summarizes the energy usage data for the earlier lab experiment and this evaluation. Cost per pound of Gr/Ep structure is also included in the table based on Southern California area 1984 energy costs for gas and electricity.

Tooling weight was estimated at 4,000 pounds for all of the detail staging tools and the cocure tool of the phase III component. The Gr/Ep weight shown of 550 pounds includes staging and curing the 270 pound structure. In other words each detail would see two cycles; staging from room temperature to 250°F, then curing from room temperature to 350°F. This in effect creates the cycle used in Table XXXV. The total energy used by the autoclave is divided between electricity to run the vacuum pumps and natural gas to heat the autoclave. Energy usage for the autoclave was based on historic data for a 4 hour autoclave cycle was  $4.8 \times 10^7$  BTUs for gas and  $4.25 \times 10^7$  BTU for electricity. The energy cost then for eight hours of usage is  $9.05 \times 10^7$  BTU.

Based on these data a \$3.87/pound of Gr/Ep savings can be attributed to the use of the nonautoclave process which utilizes a gas heated oven in lieu of an autoclave. Extrapolating these savings to a production quantity is discussed in the following paragraphs.

By adjusting these values for a full oven or autoclave run provides a more accurate evaluation of the costs in a production environment. To adjust the energy usage from one part to a full run it must be remembered that a portion of the total energy used in the cycle goes to heating only the source. The remainder is used to heat the part. Consequently doubling the number of parts in an autoclave run does not result in a doubling in the



TABLE XXXV

## AUTOCLAVE VS OVEN ENERGY SAVINGS SUMMARY

	ELECTRIC LAB AUTOCLAVE	ELECTRIC LAB OVEN	TULSA SHOP GAS OVEN	TULSA AUTOCLAVE
VOLUME (Ft <sup>3</sup> )	12.5	10.8	10,500	12,550
TOOLING WT (1b)	17.6	17.6	4,000(3)	4,000(3)
GR/EP WT (1b)	9	9	550	550
BTU/8 HR CYCLE (1)	2.2 x 10 <sup>7</sup>	1.66 x 10 <sup>6</sup>	1.2 x 10 <sup>6</sup> (5)	2.80 x 10 <sup>8</sup>
BTU/LB	2.45 x 10 <sup>6</sup>	1.84 x 10 <sup>5</sup>	2.18 x 10 <sup>3</sup>	3.88 x 10 <sup>5</sup>
COST PER LB (2) GR/EP (\$/LB)	\$36.02/LB	\$2.71/LB	\$0.016/LB	\$3.89/LB
SAVINGS (\$/LB)		23.31		3.87
NOTES:	1. RT - 250°F; 2. Hold @ 250°F - 1 hr; 3. 250°F - 330°F; 4. Hold 350°F - 1 hr; 5. 350°F - RT. (2) Electricity = \$1.47/10 <sup>5</sup> BTU (5¢ kw-hr) Gas = \$.75/10 <sup>5</sup> BTU. (3) Includes detail and cocure tooling estimate. (4) Typical 4 hour cycle 4.8 x 10 <sup>7</sup> BTU Gas, 4.25 x 10 <sup>7</sup> BTU Elect. (5) Includes detail staging and cocure			

energy usage. Based on the Phase I studies these relationships were established as:

For the Autoclave:

Total Energy = 0.95 energy source + 0.05 energy part

For the Oven:

Total Energy = 0.75 energy source + 0.25 energy part

A total of four cocure assemblies or 1,080 pounds of Gr/Ep structure could be positioned in the oven at one time, for purposes of comparing similar processes and equipment this was assumed to be a full load for either the oven or the autoclave. Plotting the energy usage versus pounds of Gr/Ep is shown in figure 160. The graph is extended to 5,000 pounds of structures which is roughly equivalent to the total structural weight per aircraft of the composite material on the B-1B. The total savings then on the production of 100 B-1B aircraft would be:

$4989 \text{ lb/AC} \times 100 \text{ A/C} \times \$3.87/\text{lb} = \$1,930,733$

The savings on the vertical stabilizer alone would be

$270 \text{ lb/AC} \times 100 \text{ A/C} \times \$3.87 = \$105,000$

#### 4.4.3 Cost Analysis

Detailed cost tracking was conducted to the manufacturing operations level of the data abstraction form of the DOD/NASA Structural Fabrication Guide, figure 161 and table XXXVI for all elements fabricated during the contract. Corrections to the actual recorded hours were made for scrapped or reworked parts. These cost data provided the basis for the cost analysis required to evaluate the comparison between nonautoclave- and autoclave-processed composite structural elements.

The hours recorded in each of the three phases and the baseline parts included recurring fabrication hours only and did not include support functions which were considered equivalent.

Tables XXXVII through XXXIX summarize the cost tracking data for the Phase I, II and III parts. Also, included in these tables are the baseline data. In some instances to provide an accurate comparison between the nonautoclave fabricated components and the baseline components estimates were made to adjust the hours to add or delete operations that were not recorded separately from the total recorded separately from the total recorded hours. In this way, an accurate analysis of components that have the same level of complexity was possible.

In comparing the Phase I, 40-inch-long element, (table XXXVIII) the comparison is between virtually identical assemblies. Both the nonautoclave elements and the baseline were fabricated utilizing integral structure. The 25 percent savings from the baseline of 399.5 hours to the nonautoclave elements with a total of 299.0 hours is attributed to three improvements developed during the contract: (1) The bagging techniques used; the baseline

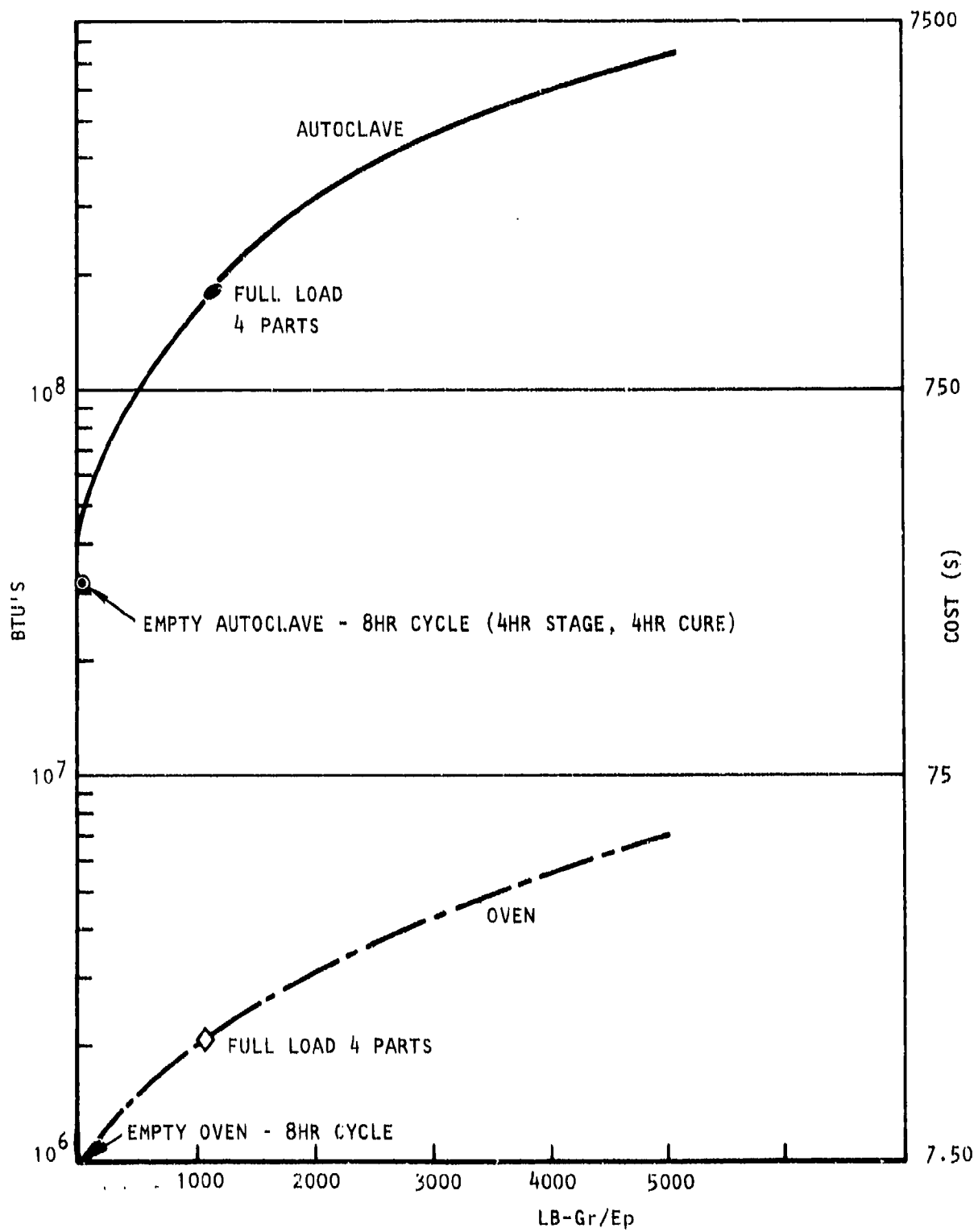


Figure 160. Energy Saving - Nonautoclave versus Autoclave



## TABLE XXXVI

## GLOSSARY OF FABRAICATION COST OPERATIONS

1. Tool Preparation - preparation of tool surface for layup, Mylar templates, bonded assembly tooling, trim and/or drill fixtures for application to part, assembly tooling, etc.
2. Composite Orientation - layup of advanced composite material to orientation required, includes trim to template, prebleed and debulk operations, identification, protective packaging, and direct layup of composite material to a tool or part subassembly surface.
3. Pattern Cutting - cutting bleeder material stock and preimpregnated glass fabric for subsequent layup.
4. Layup - positioning of bleeders, ply-oriented composite sheets, impregnated glass fabric patterns, and honeycomb core on a mold surface and cured solid laminate detail, assembly bonding, and cocure assembly.
5. Honeycomb Preparation - expanding from the HOBE, machining, cleaning, and joining H/C segments, includes all operations to produce a honeycomb subassembly.
6. Instrumentation - installation and checkout of thermocouples for cure temperature monitoring.
7. Bagging - preparation of bag material if not reusable, installation of bag, and vacuum check.
8. Cure - positioning of tool or fixture in autoclave (oven), hookup of thermocouples and vacuum hoses, monitoring of cure cycle, and removal of tool after cure.
9. Postcure - any curing accomplished after the initial cure cycle.
10. Part Removal - strip bag, remove part, and ;minor part cleanup (flash removed, etc).
11. Machining - edge trim, hole drilling, etc of cured composite.
12. Finishing - all operations associated with preparing surfaces and application of final finish systems.
13. Assembly - Mechanical assembly of details and subassemblies to final assembly configuration.

TABLE XXXVII

## NONAUTOCLAVE COST ANALYSIS PHASE I ELEMENT

OPERATION	NONAUTOCLAVE			BASELINE			DELTA HOURS	% SAVINGS TOTAL HOURS
	RECORDED HOURS	HRS S/T	% TOTAL FAB HRS	RECORDED HOURS	% TOTAL FAB HRS	HOURS S/T		
1 TOOL PREP	6.00	6.00	2.01	3.00	0.75	3.00	3.00	-0.75
2 ORIENTATION(DEBULK)	0.00		0.00	104.50	26.16		-104.50	26.16
3 CUTTING BLEEDER/BREA	31.00		10.37	5.00	1.25		26.00	-6.51
4 LAYUP GR/EP	143.00	174.00	47.83	61.00	15.27	170.50	82.00	-20.53
5 HONEYCOMB PREP	N/A		0.00	N/A	0.00		0.00	0.00
6 INSTRUMENTATION	2.50	2.50	0.84	2.00	0.50	2.00	0.50	-0.13
7 BAGGING(FAB&INSTALL)	14.00	14.00	4.68	52.00	13.02	52.00	-38.00	9.51
8 STAGE & (CO)CURE	5.50	13.50	1.84	8.00	2.00		-2.50	0.63
9 POSTCURE	8.00		2.68	4.00	1.00	12.00	4.00	-1.00
10 PART REMOVAL	5.50		1.84	16.00	4.01		-10.50	2.63
11 MACHINE AND TRIM	14.50		4.85	76.00	19.02		-61.50	15.39
12 ASSEMBLE FOR COCURE	29.00		9.70	28.00	7.01		1.00	-0.25
13 MECHANICAL ASSY.	40.00	89.00	13.38	40.00	10.01	160.00	0.00	0.00
TOTAL	299.00	299.00	100.00	399.50	100.00	399.50	-100.50	25.16
WEIGHT HRS/LB	20.89 14.31			20.52 19.47				

NOTES: 1. Graphite/epoxy detail fabrication and assembly of cocure structure and mechanical fastening of covers only. Does not include fabrication or assembly of test hardware.

2. Reference AFML-TR-79-4110

3. All hours for fabrication. No support or inspection hours are included.

TABLE XXXVIII

## NONAUTOCLAVE COST ANALYSIS PHASE II SUBCOMPONENT

S/T	OPERATION	NONAUTOCLAVE			BASELINE (2)			DELTA S/T	% SAVINGS HOURS	6-FT IRAD INTEGRAL STRUCTURE SUBCOMPONENT	
		RECORDED HOURS	% TOTAL S/T	ESTIMATED FAB HRS	% TOTAL	HOURS	RECORDED TOTAL			HOURS	
1	TOOL PREP	160.00	9.11	1.00	29.50	29.50	130.50	-4.42	76.00	76.00	
2	ORIENTATION (DEBULK)	0	0.00	5.00	147.49	147.49	-147.49	5.00	300.00	300.00	
3	INSTALL BLEEDER/BREA	290.00	16.51	15.00	442.46	442.46	-152.46	5.17	250.00	250.00	
4	LAYUP GR/EP	506.00	28.82	30.00	884.91	1474.85	-378.91	12.85	586.00	1136.00	
5	HC/STYRENE PREP	N/A		0.00		N/A		N/A	0.00	N/A	
6	INSTUMENTATION	67.00	3.82	0.50	14.75	14.75	52.25	-1.77	67.00	-67.00	
7	BAGGING (FAB/INSTALL)	264.00	15.03	10.00	294.97	294.97	-30.97	1.05	275.00	275.00	
8	STAGE & (CO)CURE	8.00	0.46	0.50	14.75	22.75	0.00	0.23	8.00	8.00	
9	POSTCURE	8.00	0.46		8.00		0.00	0.00	8.00	16.00	
10	PART REMOVAL	87.00	4.95	2.00	58.99		28.01	-0.95	45.00		
11	MACHINE AND TRIM	41.00	2.33	2.00	58.99		-17.99	0.61	42.00		
12	ASSEMBLE FOR COCURE	125.00	7.12			0.00	125.00	-4.24	N/A		
13	MECHANICAL ASSY.	200.00	11.39	34.00	1002.90	1120.89	-802.90	27.22	N/A	607.00	
	TOTAL	1756.00		100.00	2957.70	2957.70	-1194.95	40.74	2177.00	2177.00	
	WEIGHT MDS/LB	78.11 22.48			81.26 36.30				101.60 21.43		

NOTES: 1. Graphite/epoxy detail fabrication and assembly of cocure structure and mechanical fastening of covers only. Does not include fabrication or assembly of test hardware.  
2. Reference F33615-74-C-5164 "Low Cost Composite Vertical Stabilizer" program.  
3. All hours for fabrication, no support are included.  
4. Baseline hours calculation:  
1. TOTAL HOURS 4999.00  
2. LESS SUPPORT @30% -1497.30  
3. LESS FAB & ASSY. -544.00  
TOTAL 2957.70

NOTES: 1. Graphite/epoxy detail fabrication and assembly of cocure structure and mechanical fastening of covers only. Does not include fabrication or assembly of test hardware.  
 2. Reference F33615-74-C-5164 "Low Cost Composite Vertical Stabilizer" program.  
 3. All hours for fabrication, no support are included.  
 4. Baseline hours calculation:

1. TOTAL HOURS 4999.00  
 2. LESS SUPPORT @30% -1497.30  
 3. LESS FAB & ASSY. OF METAL -544.00

TOTAL 2957.70

TABLE XXXIX

## NONAUTOCLAVE COST ANALYSIS PHASE III COMPONENT

OPERATION	NONAUTOCLAVE			ESTIMATED % TOTAL FAB HRS	BASELINE		DELTA HOURS	% SAVINGS TOTAL HOURS
	RECORDED HOURS	S/T	% TOTAL FAB HRS		HOURS	S/T		
1 TOTAL PREP	204.00	204.00	3.07	1.00	122.55	122.55	81.46	-0.66
2 ORIENTATION (OF BULK)	4.00		0.06	5.00	612.73		-608.73	4.96
3 INSTALL BLEEDER/BREA	403.00		6.06	10.00	1225.45		-822.45	6.71
4 LAYUP GR/EP	785.00	1192.00	11.80	20.00	2450.90	4289.08	-1665.90	13.59
5 HONEYCOMB PREP	N/A		0.00		N/A		N/A	0.00
6 INSTRUMENTATION	16.00	16.00	0.24	0.50	61.27	61.27	-45.27	0.37
7 BAGGING (FAB/INSTALL)	661.00	661.00	9.93	10.00	1225.45	1225.45	-564.45	4.60
8 STAGE & (CO)CURE	223.00		3.50	0.50	61.27			-1.40
9 POSTCURE	8.00	241.00	0.12		8.00	69.27	0.00	0.00
10 PART REMOVAL	104.00		1.56	2.00	245.09		-141.09	1.15
11 MACHINE AND TRIM	279.00		4.19	2.00	245.09		33.91	-0.28
12 ASSEMBLE FOR COCURE	1143.00		17.18		0.00		1143.00	-9.32
13 MECHANICAL ASSY.	2815.00	4341.00	42.30	49.00	6004.71	6494.89	-3189.71	26.01
TOTAL	6655.00	6655.00	100.00	100.00	12262.50	12262.50	-5779.23	45.73
WEIGHT HRS/LBS	306.40 21.72				315.00 38.90			

NOTES: 1. Graphite/epoxy detail fabrication and assembly of cocure structure and mechanical fastening of covers only. Does not include fabrication or assembly of test hardware.

2. Reference MAAG IR20 composite application program.

3. All hours for fabrication no support or inspection hours are included.

4. Baseline hours calculation:

1. TOTAL HOURS	26321.00
2. LESS SUPPORT @30%	-7294.50
3. LESS REMOVAL OF HOBLES	-271.00
4. LESS FAB & ASSY. OF METAL DETAILS @ 29 HRS/LB (REF METAL VERT. STAB)	-4495.00
TOTAL	12262.50



element utilized cast rubber bags that were more complex to fabricate and more difficult to seal, (2) the machining and trimming operation which provided for trimming of the trimming of the details to the final dimension while in the staged condition in the nonautoclave process, while the baseline component details were trimmed after cure. Assembly house included assembling the mechanically fastened cover but not the loading hardware required for testing of the individual I-beams, (3) the elimination of the debulking operation also added to the overall savings. These hours are illustrated in figure 162.

The Phase II subcomponent hours are shown in table XXXVIII and figure 163. Detail tracking to the operational level utilized during this contract was not conducted for the baseline component. To provide a comparison of the nonautoclave and baseline subcomponents at the operations level, detail operation estimates were made for the baseline costs based on percentages of total fabrication costs which were obtained from historical cost data. The 6-foot long IR&D box (figure 164) is also included for information purposes although it was not used as a baseline point because of the difference in geometry. The baseline subcomponent was fabricated in 2,957 hours compared to 1,756 hours for the nonautoclave subcomponent. Major contributors to the cost savings were the incorporation of integral structure which accounted for 694 hours of the total savings. This is reflected in the reduction in the machine and trim and assembly operations. Additional savings were realized by deleting the debulking and bleeder installation as was the case for the Phase I elements. The nonautoclave parts which did not require bleeder installation resulted in 152 hours savings because net resin (31 percent) material was utilized. The cutting operation included debulking which was not required for the nonautoclave process. This resulted in a 147 hour savings. Other savings such as seen in the layup operation must be attributed to changes in other factors such as factory improvements and may be discounted for a direct cost comparison.

Savings in the bagging operations were not fully realized partially due to the experimental scale-up of the fabrication of the cocure bags which required some additional fabrication hours (these would not be seen in a production environment). However, the scale-up conducted during Phase II resulted in savings during Phase III. Higher than expected tool preparation hours for the nonautoclave tools was due in part to scaling up the tooling from the 40-inch long elements to the larger subcomponent.

As in the case of the Phase II baseline detail operation costs for the Phase III full-scale components were not available. Therefore, estimates were utilized based on the total recorded fabrication hours. Adjustments to the baseline hours were made to remove fabrication and installation of the metal details. Support functions and additional hours for rework of the fastener holes.

Analysis of the full-scale component hours tracking (table XXXIX and figure 165) substantiated the previous two Phases work. A five percent savings was realized due to elimination of the debulking operations, a 6.7 percent savings due to the use of net resin material and a 17.6 percent savings due to incorporation of integral structure. An additional 4.6 percent savings was realized due to bagging operations. As with the previous phases

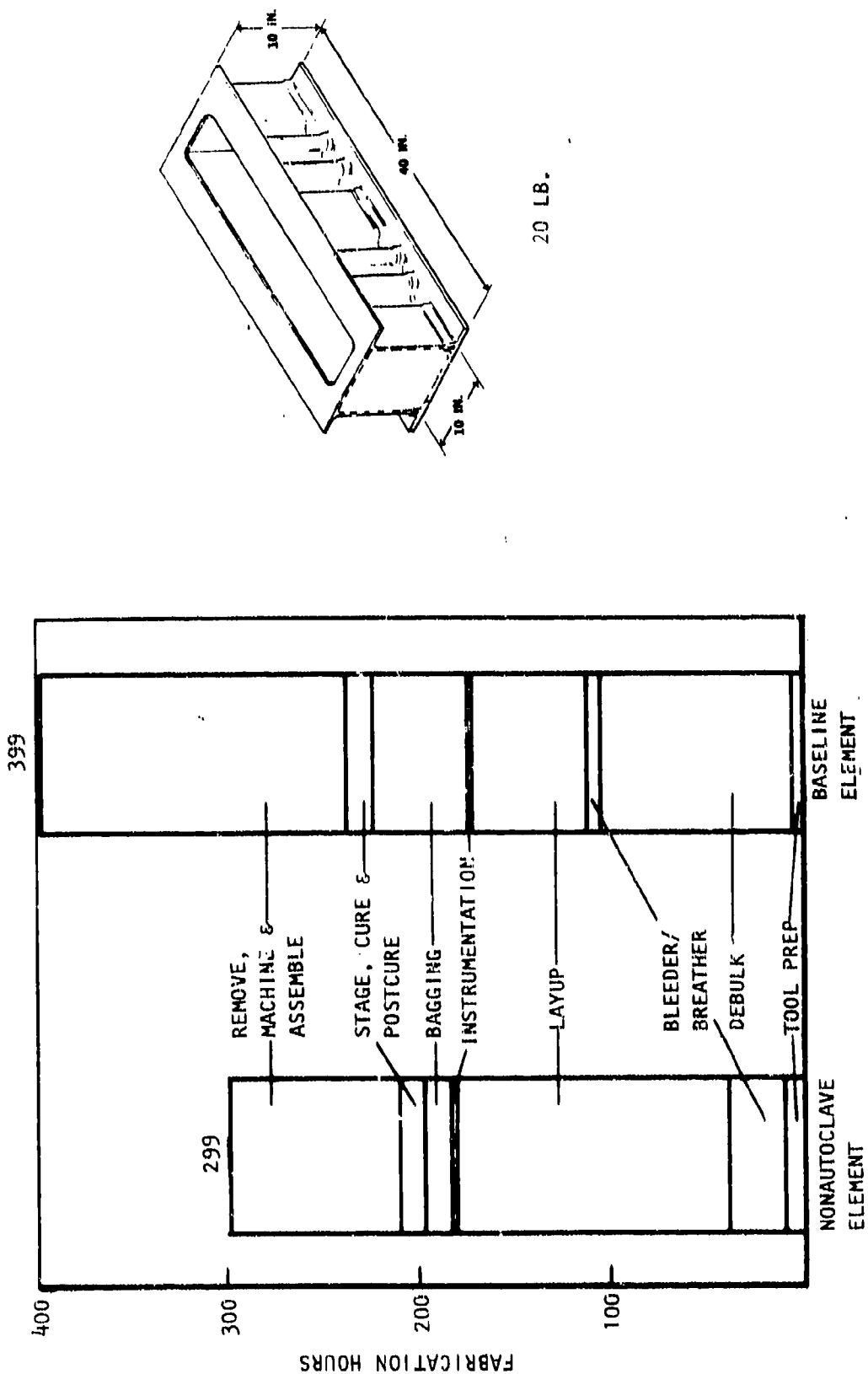
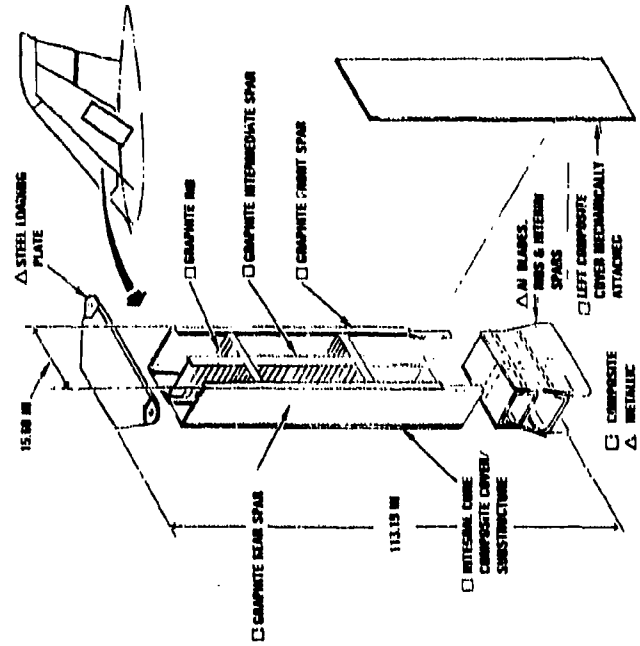
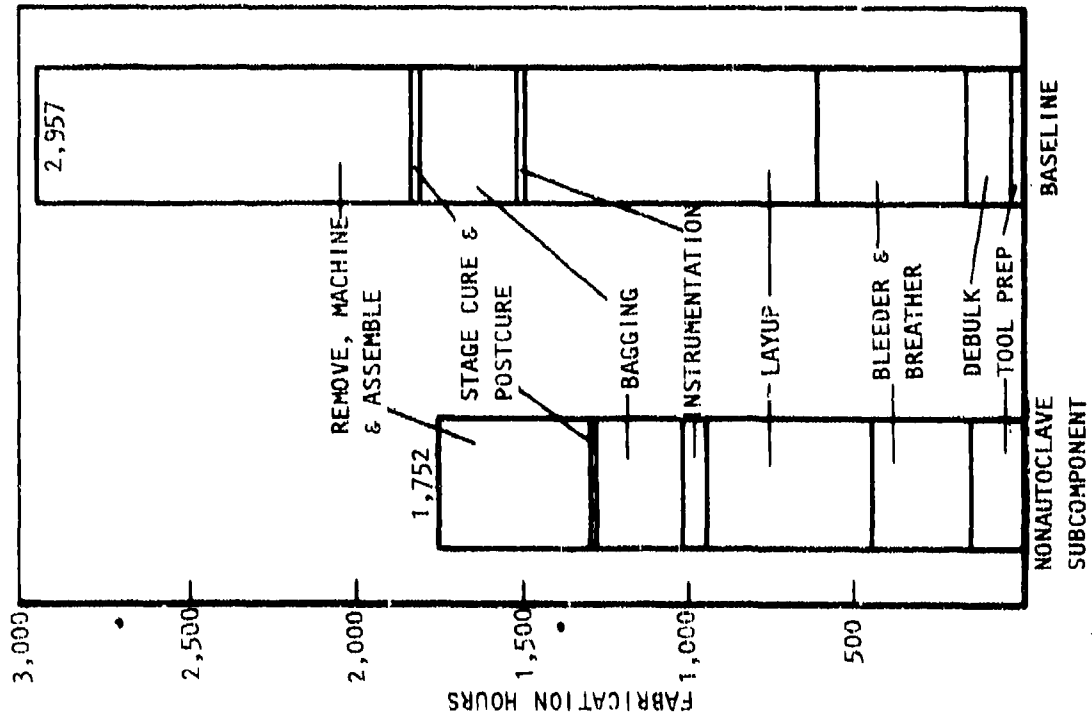


Figure 162. Phase I Cost Data Comparison



DS-80-6975A

Figure 163. Phase II Cost Data Comparison

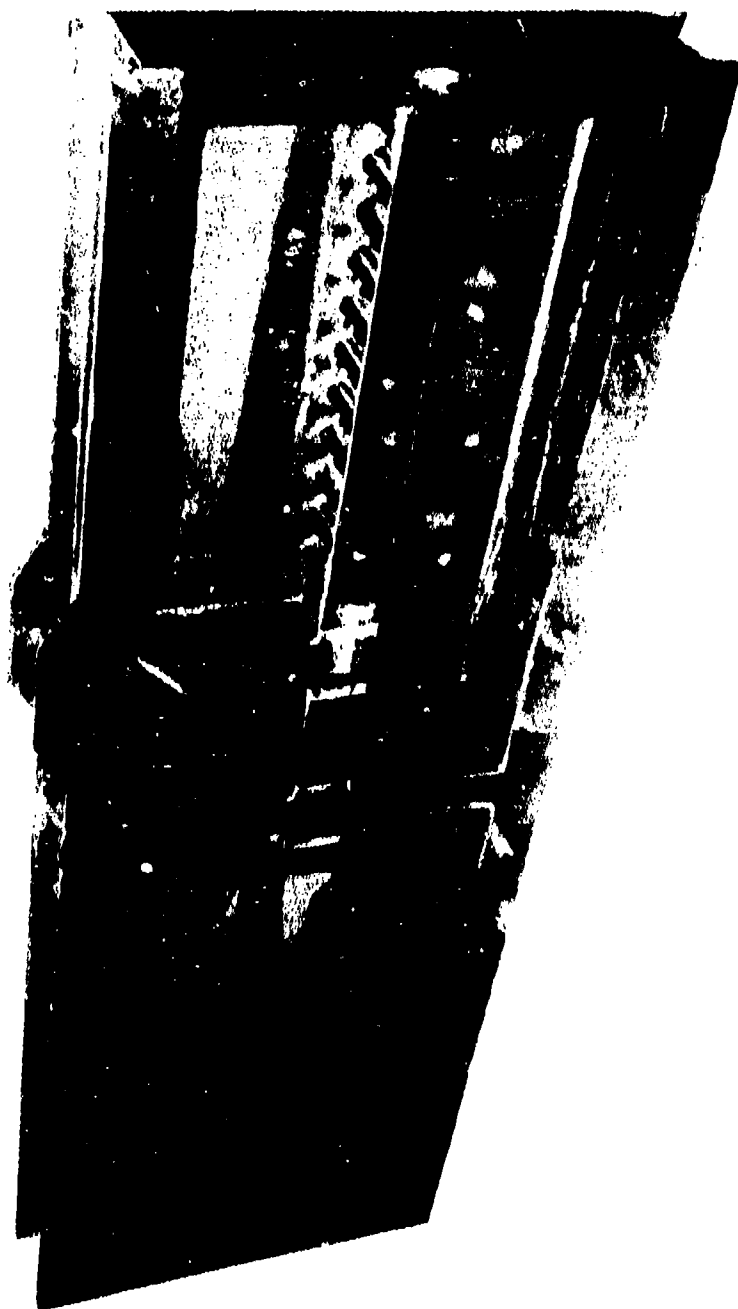


Figure 164. 6-Foot IR&D Subcomponent

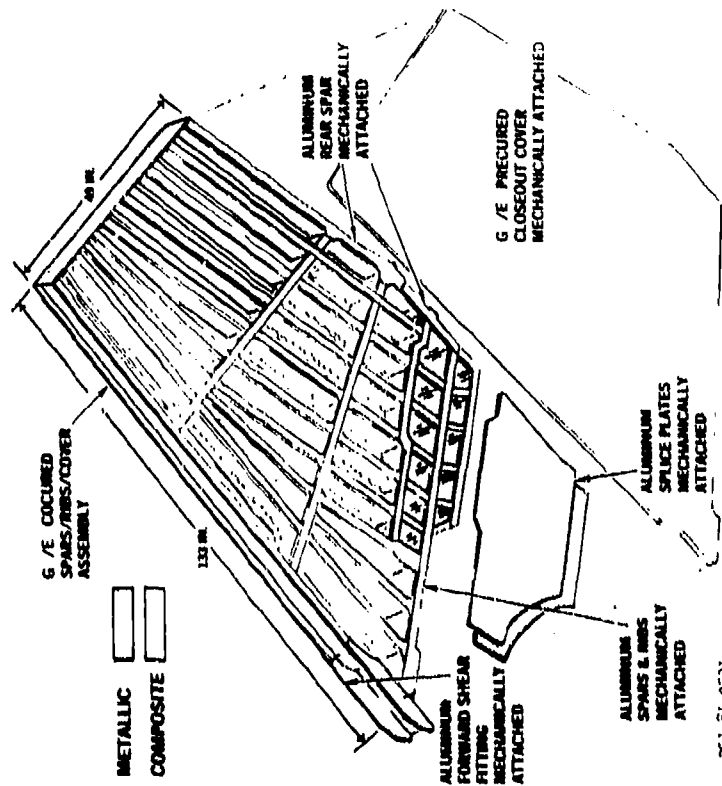
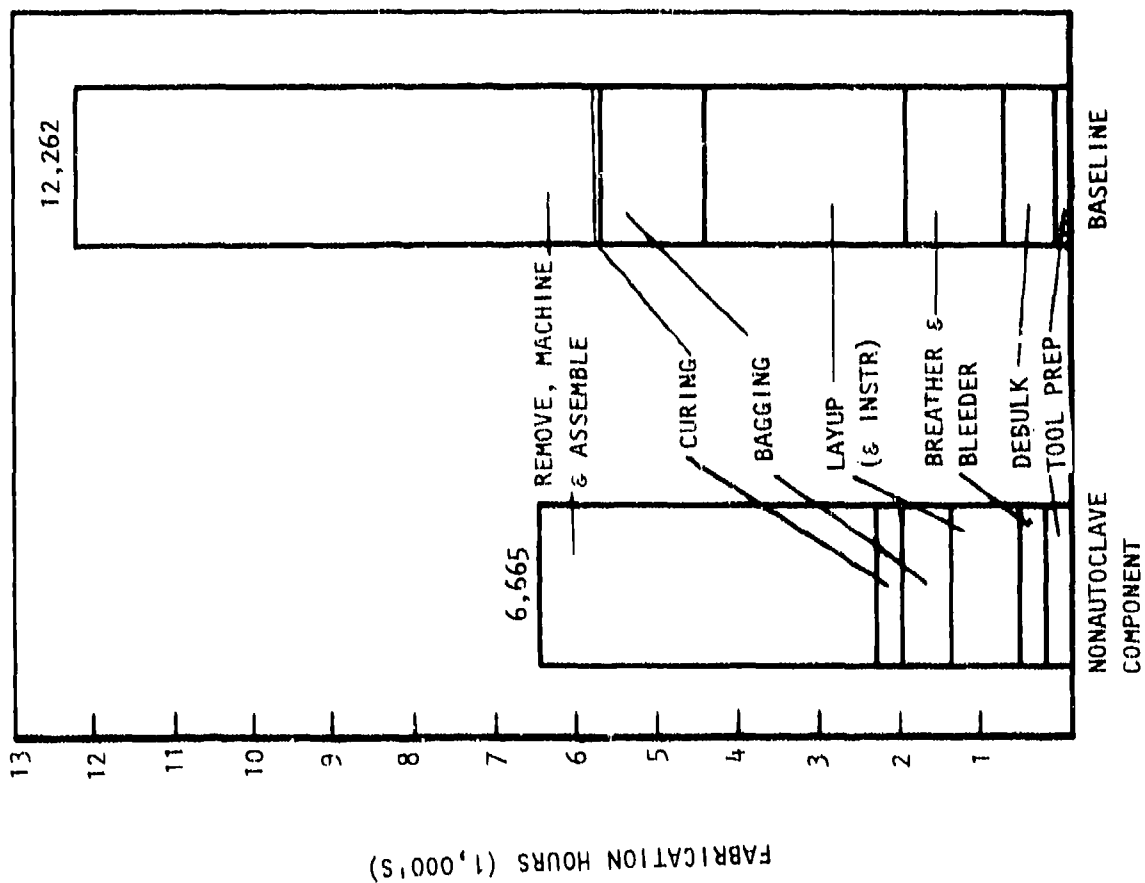


Figure 165. Phase III Cost Data Comparison

the analyses savings in the layup operation must be attributed to improvements in experience of the personnel and layup operations and should not be associated with developments in this contract. Figure 166 summarizes the hours per pound data for the baseline and nonautoclave components.

Averaging the detail operation level hours of tables XXXVII, XXXVIII and XXXIX a 44 percent savings was realized. The greatest savings are attributable to utilization of integral structure. On the average about 22 percent of the total savings is shown in table XL are the result of elimination of fastener installation as a result of integral structure (Item 12 and 13). There appears to be some savings (5.2 percent) attributable to the machining and trimming operations which could be associated to trimming details in the staged condition or could include some hole drilling operation not included in the mechanical assembly operation. Improved bagging techniques which utilized sprayed form fitting bags that reduced the labor intensive operation of fitting nylon sheet material around complex geometries such as the sine wave webs resulted in a 5 percent savings. There was a 12 percent savings in the debulk operation. Each debulking operation requires (1) application of a vacuum bag and numerous supplemental materials (i.e., separator, breather, vacuum valves, etc.), and (2) return to the layup area for debagging and subsequent layup and/or assembly operations. Obviously, these debulking iterations in general precipitate substantial labor and autoclave usage costs but also negatively influence on-station component flow which strongly affects the production rate.

A comparison of the tooling hours between the baseline autoclave tooling and the nonautoclave tooling is shown in table XLI. As can be seen in the table there is a 779 hour increase in the nonautoclave tooling as compared to the baseline tooling. The impact of this increase, however, is small when considering the overall production cost of the vertical stabilizer component.

Utilizing the cost data recorded for the full-scale Phase III component and the associated baseline cost data for that component a projection of the fabrication cost savings which would be realized by placing the integral structure nonautoclave B-1 vertical stabilizer into production was conducted. The assumptions used in this analysis are listed in table XLII.

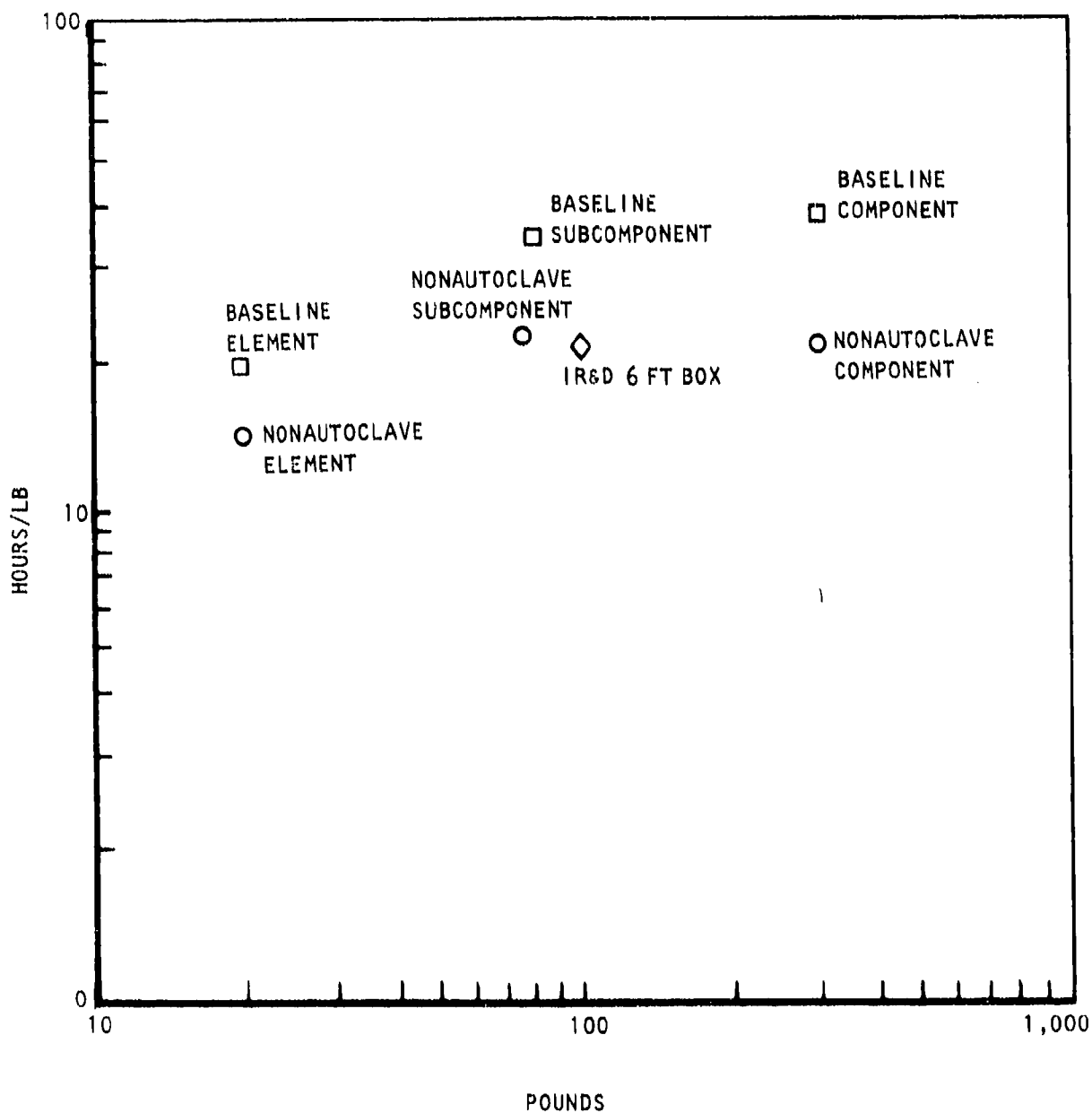


Figure 166. Nonautoclave versus Autoclave Hours/Pound

TABLE XL  
NONAUTOCLAVE COST ANALYSIS  
AVERAGE DETAIL HOUR SAVINGS

		AVG % HOUR SAVING
1.	Tool Prep	- 1.94
2.	Orientation (Debulk)	12.00
3.	Cutting (Bleeder/Breather)	1.79
4.	Layup	1.97
5.	Honeycomb Prep	N/A
6.	Instrumentation	- 0.51
7.	Bagging	5.05
8.	Stage & Cure	- 0.18
9.	Post Cure	0.0
10.	Part Removal	0.94
11.	Machine & Trim	5.24
12.	Assemble for Cocure	- 4.61
13.	Mechanical Assembly	26.61
		46.36

Notes: Average of Phase I, II and III parts



TABLE XLI  
TOOL FABRICATION COST ANALYSIS

COMPONENT	COMPONENT WEIGHT (LB)	HOURS	HR/LB
Nonautoclave Phase III Component (Staging * Cocure Tools)	306.40	15,000	N/A
Baseline B-1A Composite Vertical Stabilizer	315.00	14,221	N/A
B-1A Metallic Vertical Stabilizer	N/A	N/A	114.9

TABLE XLII

## B-1 Vertical Stabilizer Cost analysis Assumption

1. 85 percent Crawford Learning Curve utilized for all composite fabrication efforts.
2. Capital costs for the curing source are included based on 1983 quotes from manufacturers.
3. Only touch labor fabrication hours are included, support hours are assumed to equivalent for both components.
4. Inspection hours are assumed to equivalent for both components.
5. For the nonautoclave component staging and cocure bags will be replaced after five years.

It should be noted that these assumptions are conservative. For example inspection hours for the integral structure component would, in all likelihood,, be less than for a mechanically attached structure in which each of the approximately 2000 fasteners holes would have to be individually inspected. A rough estimate for this alone would be 1000 hours.

The assumption that the nonautoclave bags would need to be replaced every 5 units is based on the current bag material and techniques. Development of more durable bagging materials is continuing and there is every reason to believe that a 20 run life for bags is feasible. Additionally, it was assumed that the autoclave bags would require only a token amount of maintenance throughout the 100 unit run. This was not borne out by actual experience and more maintenance of the autoclave bags could in fact be required.

The result of this analysis delineated in table XLIII indicates that a \$13 million savings for 100 aircraft could be realized by implementing the nonautoclave components into production.

One major factor that cannot be easily quantified in the cost analysis is the fact that smaller subcontractors which, due to their size, cannot afford the very large capital investment for autoclaves and consequently have been unable to participate in expanding composite industry. By demonstrating that quality primary Gr/Ep structure can be fabricated using much lower cost ovens and entire second tier of subcontracting sources can be drawn upon to produce aircraft structures. The advantage to this for the government and prime contractors are the lower overhead costs found in these small subcontractors. The result is lower cost structure.

In fact applications of this nature are today being exploited in the repair of composite structure. By providing a means to repair composites without an autoclave ALC's, can now repair and manufacture composite structures without the need for expensive facilities. The payoff is even greater for the Navy when on-board space in ships precludes the use of an autoclave.

TABLE XLIII

COST ANALYSIS  
8-1 VERTICAL STABILIZER COMPONENT

WEIGHT (lb)	NONAUTOCLAVE 306.4	BASELINE AUTOCLAVE 315.0
Non Recurring Cost 10,000 ft <sup>2</sup> Curing Chamber Tooling S/T	\$ 700,000 (Oven) <u>750,000</u> \$ 1,450,000	\$ 2,000,000 (Autoclave) <u>711,050</u> \$ 2,711,050
Recurring Cost Fabrication Tool Maintenance Tool Material	\$ 145,591 ( $T_1=21.72\text{Hr/lb}$ ) <u>4,000</u> <u>1,500</u> \$ 151,091	\$ 268,069 ( $T_1=38.90\text{Hr/lb}$ ) <u>1,000</u> <u>50</u> \$ 269,119
Cum Total Recurring Fab. @100 Units Energy Cost (5)(7) 100 Units	\$15,109,100 <u>375</u> \$15,109,475	\$26,911,900 <u>37,500</u> \$26,949,400
Total Cum Avg Cost	\$16,559,475	\$29,660,450
Notes: 1. 50 \$/Hr 2. 85% Crawford Learning Curve 3. Nonautoclave Bag Replacement @ 5 units (400 hour/1 set state & cure bag) 4. Nonautoclave bags 300 lb/1 set of stage & cure bag x \$25/lb 5. 4 Parts/run, 25 runs/100 A/C 6. Cum Avg Factor 85% Crawford = 0.437539 @ 100 units 7. Autoclave energy cost include \$175/run for nitrogen		

Bonded repairs can also be conducted on-site resulting in tremendous time and cost savings by pre-staging the patch then using a heating blanket as a heat source to cure the bonded repair using a vacuum only.

The \$13 million savings demonstrated is only a small part of the value of the nonautoclave process in composite fabrication savings.

Based on a total savings of \$13 million by utilizing the nonautoclave fabricated integral structure vertical stabilizer instead of the autoclave fabricated baseline a return on investment (ROI) of 9 can be realized based on the following formula.

$$ROI = \frac{\text{Savings/aircraft} \times \text{number of aircraft} - \text{implementation cost}}{\text{Implementation Cost}}$$

Implementation Cost

Where the savings/aircraft is obtained from table XLIII and the implementation cost is the procurement cost difference between an oven and an autoclave. The ROI is then:

$$\frac{13,006,852 - (2,000,000 - 700,000)}{(2,000,000 - 700,000)} = 9$$

## 5.0 SUMMARY & RECOMMENDATIONS

### 5.1 Summary

Through the successful execution of this 42 month - 3 phase technical effort, a generic curing technique for 177°C (350°F) organic matrix graphite/epoxy primary structures has been demonstrated which does not require the use of an autoclave.

This objective was accomplished by demonstrating the tooling and processing procedures needed to fabricate a series of elements, a test subcomponent, a full scale component (representative of a typical wing or empennage primary structure) and by tracking production costs, assessing the quality of all fabricated hardware, and preparing the material and process specification.

A summary of those accomplishments significant to Phase I and the validation of nonautoclave processing in general is outlined below. Included are accomplishments from NAAO's in-house activities which were vital to the successful Manufacturing Technology demonstration.

PHASE I - MANUFACTURING METHOD VERIFICATION, provided a definition of the fabrication and tooling methods for the nonautoclave cure of the composite parts and included fabrication of elements of typical Gr/Ep structures, quality assessment, cost tracking and analysis of those elements, the preparation of the preliminary material and process specifications and a production plan for the manufacturing methods validated by the construction of the critical root attachment area (or stub box) of a large aircraft vertical stabilizer.

#### PHASE I ACCOMPLISHMENTS:

1. Characterized the process as generic to graphite/epoxy tape and fabric.
2. Conducted extensive characterization of fabric and tape to establish gel times and processing cycles, (4 hours versus 80 minutes, respectively), for 350°F cure systems.
3. Established resin content criteria for net-resin tape and fabric prepreg.
4. Determined sensitivity of volatile migration to exterior pressure during staging versus.
5. Established a hardware fabrication approach.
6. Established tooling parameters and established that 95% of outgassing is through the edge of the laminate.
7. Feasibility of boron/graphite/epoxy and glass/graphite/epoxy hybrid demonstrated.

8. Determined need for low-cost, one-piece, cocure bag approach (i.e., eliminated vacuum leaking due to multiple bags).
9. Eliminated need for bleeder plys (i.e., net resin fabrication).
10. Use of outer fabric ply for supportability, handlability, and molding of complex shapes demonstrated.
11. Assessed out-time of staged material to 360 days without property degradation.
12. Demonstrated viability of ultrasonic trimming.
13. Fabricated net molded cocured hardware.
14. Conducted structural validation under hot/wet conditions.

A summary of those accomplishments significant to Phase II and the validation of nonautoclave processing in general is outlined below. Included are accomplishments from NAAO's in-house activities which were vital to the successful Manufacturing Technology demonstration.

PHASE II - MANUFACTURING METHOD SCALE-UP, extended and optimized the manufacturing methods validated in Phase I by the construction of the subcomponent representing the critical root attachment area of a large aircraft vertical stabilizer.

#### PHASE II ACCOMPLISHMENTS:

1. Scaled-up of process to six foot long, six-cell, cocured box-beam comprised of 38 detail parts. These included:
  - Clips
  - 76 ply gr/boron/epoxy hybrid tapered covers
  - Cap strips
  - Sine-wave I-Beam elements
  - Tapered/Reinforced Flat web I-beams and C-channel elements
  - Local reinforcements (fuel flow holes)
2. Improved bag durability with D-Aircraft compound 62 rubber
3. "Bladder", one-piece cocure sprayed bag demonstrated
4. Cocure tool containing manifold to eliminate bag perforations and maintain height demonstrated
5. First useage of ultrasonic trimming
6. Ultrasonic standards for staged parts established
7. Out-time extended to 360 days without property degradation
8. Ambient storage of details for 6 months without property degradation

A summary of those accomplishments significant to Phase III and the validation of nonautoclave processing in general is outlined below. Included are accomplishments from NAAO's in-house activities which were vital to the successful Manufacturing Technology demonstration.

PHASE III - FULL SCALE DEMONSTRATION, fabricated a 3/4 section of the full scale vertical stabilizer of the B-1 aircraft. Cost tracking, quality assessment, preparation of final cost benefit analysis of the nonautoclave cure process was also completed during this phase.

#### PHASE III ACCOMPLISHMENTS:

1. Scale-up to 55 sq. ft., largest known cocured primary structure to date, accomplished
2. Use of precured Gr/Ep slip sheet utilized to preclude tool/part thermal mismatch wrinkling of skins
3. Evaluated poured, painted, sheet and sprayed bags
4. Cocure assembly locating methods, (i.e., pins, stitching, wires) utilized successfully
5. Restaged details to compact radii and correct anomalies
6. Heat-up-rate sensitivity studies conducted showed that the required 5 to 6 degrees per minute could be degraded to 2 to 3 degrees per-minute without sacrificing part quality
7. Demonstrated method of tooling to OML with good fit up. Splash tooling from cover IML can accommodate significant geometry interfaces with substructure "OML" (i.e., rib and spar caps). Combined with ability of staged substructure details to "move" or "conform" during cocure, minimized or eliminated needs for shimming of OML designed structures

#### 5.2 Recommendations

Through the course of this Man Tech demonstration program, numerous advancements in advanced composite processing, fabrication, tooling, assembly and related technologies were identified and demonstrated.

Not the least of these advancements was the development of self-contained, one-piece cocure bag tooling; ambient storage of staged composites; net-molded-edge hardware fabrication; ultrasonic enhanced trimming and assembly and, of course, the use of staged materials for repair. Based on the summary accomplishments of the preceding paragraphs, 16 items which warrant further research, development and/or demonstration have been identified and are listed

below. A number of these are already being addressed through the Air Force Material Laboratories Large Aircraft Man Tech program and some have been the subject of recent industry research. All are considered to be important to the continued advancement in the state-of-the-art of advanced composites fabrication and to the enhancement of the industrial base for future Government and Aerospace industry fabrication needs.

**Recommendations:**

1. Develop production type "reinforced" bags, spray-on one piece bags or vacuum formed bagging to minimize recurring costs.
2. Evaluate robotics for cocure bag spraying.
3. Assess chemical, thermal, ultrasonic or mechanical enhancement of volatile migration in large area and/or thick composite laminates.
4. Validate use of ultrasonic trimming and other ultrasonic enhanced processing methods (such as "tack-joining" of staged composites).
5. Evaluate locating methods, (i.e., stitching, pins, etc.) for cocuring and "caul-plating" for attachment surface accuracy.
6. Establish industry/government porosity standards.
7. Improve NDE techniques and procedures for co-cured and/or bonded structures
  - Develop automated sine wave inspection techniques
  - Develop radii inspection techniques
  - Improve wet/staged surface contaminane detection techniques
  - Develop "staged standards"
8. Evaluate rework potential of staged parts (i.e., wrinkle removal, radii compaction, etc).
9. Validate repair applicability of nonautoclave processing. Make use of ambient storage times of staged materials and "reworkability" to develop repair techniques which meet field, "shipboard" and ALC level requirements. Investigate:
  - Ship-board, high moisture environment
  - Reduced capitalization of ALCs
  - Field repair
10. Extend vacuum cure principles and tooling to BMI and thermoplastics materials
11. Extend "stage/advancement" to lower-temperature matrices (i.e., less than 350°F)



12. Assess production long-term storage, under ambient conditions (i.e., ability to use "sheet metal cell" inventory, material handling techniques and learning-curve data for composite assembly "cost effectiveness" analysis)
  - Rate and inventory costs
  - Storage handling costs
  - Energy savings
13. Validate transfer of nonautoclave process to small business and university sector of composites/aerospace community
14. Demonstrate flow-through-oven automation concept for nonautoclave cocuring